Signal Processing for Early Warning Arrhythmia Detection and Survival Prediction for Clinical Decision

Amit Walinjkar

A thesis presented for the degree of
Doctor of Philosophy
(Ph.D)

School of Computer Science & Electronic Engineering
University of Essex
Date of submission August 2019

Abstract

According to the British Heart Foundation, UK, there is a population of around 7 million living in the UK with heart and circulatory diseases; about 25% of all the deaths in the UK are caused by cardiovascular diseases and more than 30,000 people a year suffer cardiac arrest out-of-hospital. As people all over the world, continue to live busy and stressful lives, a vast majority of people start showing cardiac arrhythmia-related symptoms which, if not treated in time may lead to a serious heart condition or even sudden cardiac death. To identify the early-warning signs in cardiac arrhythmia, methods to identify the precursors to fatal arrhythmia were developed in this research study, using a wearable kit. To enable accurate classification between arrhythmic beats, novel feature extraction algorithms using spectral components were developed. Often a fatal cardiac arrhythmia, or a serious injury, may lead to trauma and in such situations, it becomes imperative that the critical care teams have adequate information about the patient's health status at remote location following an ambulatory response. A real-time trauma scoring algorithm was developed, and correlation and regression analyses were performed to arrive at these scores using the physiological parameters and vital signs. It was found that with appropriate feature extraction algorithms, supervised learning classifiers could identify the precursors to arrhythmia in real time and on a resource-constrained device, regardless of time and location. The trauma scoring algorithm, implemented using ICU patients' dataset, produced values that agreed with the patients' status and events could be logged to electronic health records using standard clinical coding systems. It could, therefore, be concluded that regardless of situation and location of an individual, fatal arrhythmia and trauma events could be identified ahead of time before reaching a state of emergency.

Publications

- ➤ Walinjkar, A. & Woods, J. (2017a) ECG classification and prognostic approach towards personalized healthcare, 2017 International Conference On Social Media, Wearable And Web Analytics (Social Media). 19-20 June 2017.

- ➤ Walinjkar, A. & Woods, J. (2017b) Personalized wearable systems for real-time ECG classification and healthcare interoperability: Real-time ECG classification and FHIR interoperability, 2017 Internet Technologies and Applications (ITA). 12-15 Sept. 2017.

- ➤ Walinjkar, A. (2018a) A Composite and Wearable Sensor Kit for Location-Aware Healthcare Monitoring and Real-Time Trauma Scoring for Survival Prediction. Applied System Innovation, 1(3), 35. ISSN 2571-5577
DOI:10.3390/asi1030035

- ➤ Walinjkar, A. & Woods, J. (2018b) FHIR Tools for Healthcare Interoperability. Biomed J Sci&Tech Res 9(5)-2018. BJSTR. MS.ID.001863.
DOI:10.26717/BJSTR.2018.09.001863.4

Acknowledgements

The research study began as a parallel project to a Knowledge Transfer Partnership grant (9562) year 2014-2016 and I would like to thank my supervisor, Dr John Woods (Director of Education and Senior Lecturer, School of CSEE, University of Essex), Jan Stringer (KTP Adviser, Innovate UK) and Mr Roy Lawrence (Chairman, Raytel Security Systems Ltd) to present me with this opportunity to research novel methods for early signs arrhythmia detection and classification, which we think can bring practical benefits to health services world wide. It has been a pleasure to research under the supervision of Dr John Woods, who has also been a mentor for the past ten years. The supervision not only included guidance in subject area of the research study but also approach to research novel methods developing innovative projects and funding. I would like to especially thank Jan Stringer, who supported the research study and funding claims, right from the beginning during my tenure as a KTP Associate. I would like to specially thank Mr Roy Lawrence for supporting a parallel project along with an ongoing project in security systems over the entire duration of the research.

I would like to thank the School of CSEE and the University of Essex for funding the research for the first 2 years of the project and everybody involved in the emails to support the claims.

I would like to thank my supervisory panel Dr Nikolaos Thomos and Professor Kun Yang for being supportive during the supervisory meetings.

I would like to thank all my colleagues at Raytel Security Systems Ltd., who have been supportive during the ongoing efforts.

I would like to thank my family, my wife while balancing work and family commitments. Last but not the least and more importantly, I would like to thank my parents for providing all the support, they could, throughout the duration of the project.

Thank you.

Contents

List of Tables

List of Figures

Chapter 1

Introduction

1.1 Background

'Keeping your heart healthy, whatever your age, is the most important thing you can do to help prevent and manage heart disease. There are many different heart conditions and problems. Together, we call them heart disease ... Heart conditions include angina, heart attack, heart failure and abnormal heart rhythms - as well as many other conditions including congenital heart disease and inherited heart conditions.'

- *The British Heart Foundation*

'From 1st April 2015 to 31st March 2016, the London Ambulance Service NHS Trust (LAS) attended 10,116 patients who had suffered an out-of-hospital cardiac arrest. LAS clinicians attempted to resuscitate 4,389 (43.4%) patients. Resuscitation efforts were not undertaken on 5,727 (56.6%) patients, the vast majority of whom (n=4,687) were recognised as deceased on arrival of the LAS. 1,040 patients had a Do Not Attempt CPR (DNA-CPR) order, advanced directive or similar equivalent in place, or the patient's death was expected.' - Cardiac Arrest Annual Report, 2015/16.

- *The London Ambulance Service, NHS Trust, UK*

1.1.1 Arrhythmia Problems and Current Clinical Pathways

In this section current status of problems related to arrhythmia have been discussed, with current clinical pathways that exist within a national health framework; these, however, could be extended to healthcare services worldwide. An introduction to problems related to arrhythmia detection and a proposed solution which later became the foundation for the research study has also been provided.

The prevalence of cardiac arrhythmia problems and clinical pathways : An abnormal heart rhythm – also called an arrhythmia – means that the heart is beating too fast, too slow, and/or with an irregular pattern (NHS 2018). This happens due to the disturbance in the heart's electrical system.(NHS 2018) The most common symptoms abnormal heart rhythm are palpitations in the chest region, dizziness, breathlessness, tiredness and loss of consciousness. According to the British Heart Foundation, a UK based charity supporting researches aimed at cures and treatment of cardiovascular diseases, there is a population of around 7 million living in the UK with the burden of cardiovascular diseases. About 25% of all the deaths in the UK are caused by heart and circulatory diseases each year and about 175,000 people are admitted to the hospitals with a heart attack each year. The British Heart Foundation also states that about 150,000 deaths due to heart and circulatory diseases over each year with an average of 420 people each day. (BHF 2014). From 2014 to 2016 it has been estimated that about 750 people per 100,000 population have premature death rate due to cardiovascular diseases. Atrial fibrillation (AFib)is a heart condition that causes an irregular and often abnormally fast heart rate. In particular, about 30% of people with atrial fibrillation remain undiagnosed and therefore not being offered treatment, which increases their risk of stroke. It is a known fact that atrial fibrillation can lead to stroke and it is estimated that 5000 strokes could be prevented each year, according to National Institute of Health and Care Excellence (NICE) Surveillance Report 2017 (NICE 2017), if everyone diagnosed with atrial fibrillation could be provided with treatment in time. More than 30,000 people suffer cardiac arrest and a possible sudden cardiac death out of hospital.

A heart rhythm is measured as the bio-potential on human body surface over a period of time as an *Electrocardiogram* (ECG). Individuals or patients suffering from arrhythmia show abnormal patterns of ECG charts. Abnormally fast and random heart rhythms also called Atrial Fibrillation and heart blocks, which are the heart beats that occur very slowly and with an abnormal rhythm, are usually monitored using an ECG device. Once the patients approach a General Practice (GP), a healthcare entity managed by National Health Service (NHS) in the UK, with complaints related to palpitations, chest pain and unconsciousness, then depending on the severity of the case, they are either subject to cardiac arrest protocol at Accidents and Emergencies (A&E) or further referred to bedside cardiac examination with 12 lead ECG tests. If the high-risk factors are present, they are referred to a cardiologist. If the ECG findings are suggestive of paroxysmal atrial fibrillation, which are episodes of abnormal and fast heart rhythms that come and go intermittently and usually stop within 48 hours without any treatment, then atrial-fibrillation management pathway is adopted. This pathway requires patient monitoring for longer duration using Holter monitor (Hughes et al. 2015); (Bansal and Joshi 2018) or the AliveCor device (NICE 2015) (Halcox et al. 2017). The Holter monitors are portable devices that can record ECG for as long as 48 hours and AliveCor device can record ECG for even longer duration and can also detect AFib. If the heartbeats are irregular and the heart-rate exceeds 120 bpm, then medical admission is called for. If there are recurrent episodes of symptoms, even if the ECG was normal, longer duration of monitoring using Holter monitor is offered to initiate a diagnosis.

Currently, the NHS runs Rapid Access Chest Pain Clinic (RACPC) (UCLH-RACPC 2018) for patients with new onset of chest pain for rapid and effective assessment of symptoms and investigations for arrhythmia. All patients are offered an appointment RACPC within two weeks, and the referral letters are sent out within 24 hours. Patients normally approach a GP with symptoms like chest pain or blackout, also called transient loss of consciousness. Based on the symptoms the GP normally decides whether the patient should be referred further for a thorough examination at RACPC or a consultant cardiologist. The

British Heart Foundation state a spending of about £9 billion each year by NHS in treating heart and circulatory diseases. The average cost of care per stroke patient is currently £23,315.

Currently, there are no monitoring devices at primary care GP level, which could automatically detect frequently occurring premature arrhythmia or heart blocks. These can only be monitored, currently, at an RACPC or in a hospitalised environment where an expert cardiologist could investigate the ECG readings. Current pathways in diagnosis and treatment of cardiac arrhythmia in NHS, according to the National Institute for Health and Care Excellence (NICE) MedTech Innovation Briefing [MIB101] (NICE-Medtech-Zio 2017) the current methods of arrhythmia detection are:

1. 12 lead ECG,
2. 24- to 48 hour or 7-day continuous ambulatory monitoring, including using Holter monitors,
3. Long-term continuous monitoring for up to 30 days,
4. External loop recorders,
5. Insertable loop recorders, which can record events for up to 3 years for arrhythmia that sometimes occur months apart.

The Holter (Katritsis, Siontis, and A. J. Camm 2013) (Hughes et al. 2015) monitor is the method most commonly used in the NHS for detecting atrial fibrillation. Holter monitors continuously record the heart rhythm using several electrode patches, which are stuck on the user's chest. These electrodes detect and record electrical signals produced by each heartbeat. The signals are recorded in a portable machine. The user can press a button on the recording device when they think they are showing any symptoms related to abnormal heart rhythm, or before going to bed or taking medication. These points can then be easily found in the continuous monitoring data. The Holter monitoring is used for 24 to 48 hours for people who have regular symptoms or can be extended for seven days or more for people with symptoms that happen less often. An expert cardiologist then analyses the results during an appointment. For long duration monitoring the Zio

Service (NICE-Medtech-Zio 2017) provides a continuous recording of ambulatory cardiac monitoring for up to 14 days. The wearer can go about their normal daily activities during monitoring, including showering or bathing. An expert cardiologist then analyses the results.

Atrial Fibrillation Prevalence: According to the NICE guidelines MIB35 (NICE 2015) the prevalence of Atrial Fibrillation (E. Burns 2018) was likely to be close to 2% of total population and the prevalence of AFib is reported to be greater in men than in women. Atrial Fibrillation can cause morbidity and mortality and can lead to stroke. The AliveCor Heart Monitor, though effective, focuses only on Atrial Fibrillation. The Surveillance report 2017 on Atrial fibrillation: management (2014) and the NICE guideline CG180 (German et al. 2016) (NICE 2017) make recommendations that 12 lead ECGs should be a preferred method of AFib diagnosis at primary care, due to the sensitivity of the interpreting software. As the devices like AliveCor make impact due to their portability, identification and detection of other high-risk arrhythmia is possible along with AFib.

According to NICE Guidelines (NICE-Medtech-MIB152 2018), a referral to an NHS consultant cardiologist or electrophysiologist can take between 2 and 18 weeks and the patient must travel to hospital. The NICE guidelines state there are some automated ECG interpretation services as presented in table 1.1 and related technologies that use algorithms to interpret ECGs that are automatically uploaded to cloud networks or virtual private networks (VPNs).

The currently available ECG monitoring kits like AliveCor are only focused on atrial fibrillation while frequently occurring premature ventricular complexes leading to cardiomyopathy and second-degree branch bundle block cannot be detected automatically. There are approximately 750 people per 100,000 population suffering premature deaths due to undiagnosed cases of arrhythmia. Advanced stages of AFib can cause permanent damage to heart muscle and can lead to stroke. It is estimated that 5000 strokes could be prevented each year if everyone diagnosed with atrial fibrillation could be provided with early treatment. The average cost of care per stroke patient in NHS is currently £ 23, 315.

Atrial arrhythmia such as the permanent AFib may lead to stroke if not treated in time (E. Burns 2018). Frequent occurrences of some premature

Examples of some automated ECG diagnostic services according to NICE MIB152 guidelines					
Company	**Transmission**	**Interpretation**	**Proposed reporting time**	**Devices**	**Modality**
MEOMED	NHS email, dedicated software upload.	Instant report or consultant cardiologist's or electrophysiologist's written patient care plan with level of urgency.	Under 24 hours; average 2 hours.	None.	12-lead, Holter, loop/ event.
Primary Diagnostics	NHS email, dedicated software upload.	Technician's written report – if a consultant cardiologist's expertise is needed, the ECG can be passed on to a service such as MEOMED.	Under 24 hours.	None.	12-lead, Holter, loop/ event.
Express Diagnostics	NHS email.	An accredited data analyst's report with pathway recommendation.	Same day; up to 10 days.	Supplies/ leases third-party devices.	12-lead, Holter.
Smart Tele cardiology	Webpage upload or dedicated online platform.	Technician's or the cardiologist's downloadable report.	4 to 48 hours, depending on geographical location and depth of interpretation.	None.	12-lead, Holter, loop/ event.
ECG On-Demand	Automatic – digitally with NHS email or webpage upload.	SCST-accredited cardiac physiologist's written report with level of urgency. Quality control performed by consultant cardiac electrophysiologists.	Within 24 hours or immediately on request. Average turnaround 2 hours.	Supplies/ leases third-party devices	12-lead, Holter/ event.

Table 1.1: Comparison of ECG Diagnostic services in NHS UK pathways according to NICE MIB152 guidelines

arrhythmia, though not fatal in the beginning, may lead to conditions such as Cardiomyopathy if not treated in time. (Moses 2018; Baman et al. 2010). In such cases in order to avoid deterioration, regular monitoring would be necessary. (Moses 2018)

1.2 Motivation

A significant number of patients admitted to the Accidents & Emergencies (A&E) are first time admits with fatal arrhythmia, as their arrhythmia had remained undiagnosed and had occurred while they were at work or during a commute. Premature Atrial Contractions (PAC) which are sinus rhythms that occur earlier than the following sinus rhythms of the heartbeat and Premature Ventricular Contractions (PVC) which are electrical impulses when ventricular walls contract prematurely, are types or premature arrhythmia and there is a strong evidence that these can be observed in seemingly healthy individuals (Baman et al. 2010; Moses 2018; Krasteva et al. 2015; Gomes et al. 2010) , detailed in section 2.2. The premature arrhythmia if not treated in time may manifest as fatal arrhythmia, especially the ventricular flutter or the ventricular fibrillation and may lead to cardiac arrest or sudden cardiac death if not treated in time. In such emergent situations, where the patient has undergone a traumatic experience, in addition to identifying the type of arrhythmia, additional trauma-related information related to the patient's health condition is normally required by the triage or critical care team that would be attending the patient on admission (Cooke et al. 2006). A significant number of patients also suffer from cardiac arrests if they were injured or may have met with an accident. In such situations, the patient's health condition has to be assessed, while the patient is being carried to the hospital. Traditionally, trauma scores have been used to assess patient's health and vital signs have been used to calculate trauma scores (Holcomb et al. 2005), though these are calculated only in hospitalised or ambulatory settings. The incident response teams, sometimes, carry a portable vital signs monitor, though this becomes available only after the ambulatory service has reached the site. The vital signs monitors could be portable but are not wearable.

With the large number of Internet of Things (IoT) health monitoring kits becoming available it has become increasingly difficult to log the real-time patient monitoring information to healthcare repositories. E.g. With Holter monitors, although these are wearable, the patients have to wear the device for at least 48 hours and then submit the device to their clinics before they could obtain any diagnosis on their submitted ECG. Despite the availability of devices like AliveCor, that can perform AFib detection, the device cannot upload the AFib episodes to their respective healthcare servers when these actually occur. patients continue being monitored in real-time, it has become essential that the trauma events information such as stroke or cardiac arrhythmia be uploaded to the Electronic Health Records (EHR) in real-time, so that the health care services can provide effective incidence response and decision support . Health monitoring devices (e.g. AliveCor) can monitor and analyse an abnormal condition but cannot upload these events to EHR in real-time, due to absence of telecommunication or internet link and software interfaces to update the EHR. In case of emergencies related to injury, cardiac failure and trauma, patient's health status should raise alerts and alarms for critical care response.

The key solution to the current problems mentioned in the section 1.1.1 is a wearable health monitoring device which can perform real-time arrhythmia detection and classification. Along with real-time arrhythmia detection and classification it could also gather vital signs information and upload the patient health status information to the EHR when these episodes occur. The kit should deliver at GP primary care without needing sophisticated hardware or monitoring equipment at the GP clinic. The primary aim of this research study, therefore, was to produce a wearable health monitoring kit, that can detect the early warning arrhythmia such as the premature atrial complexes and the premature ventricular complexes by carrying out data analysis and compare a patient's (or an individual being monitored) heart rhythm with the typically known composite waveforms of previously diagnosed forms of heart arrhythmia. The proposed kit would detect arrhythmia in its *early stages* and could alert medical professionals of a potential risk as *early warning* that the patient could be in danger, thereby providing an alerting mechanism to the critical care staff. The proposed kit would be able to detect these undiagnosed cases of arrhythmia and would thereby save several hundred lives and thousands of NHS funds per patient. Besides, the kit would also be able to identify and detect the intermittent cardiac arrhythmia if a patient is monitored for longer duration.

With the advances in micro-fabrication of bio-medical analogue front-end devices, embedded system technology, data acquisition and signal processing, it has now become possible to devise a monitoring kit that can perform heart monitoring and cardiac arrhythmia detection in real time (Duking et al. 2016; Lerma and Glass 2016; Gradl et al. 2012). Early detection of any form of arrhythmia will enable monitoring and/or treatment to begin before any aberration in heart performance leads to a critical condition. The composite, wearable healthcare monitoring kit can perform arrhythmia detection and classification in real-time. Such a system can facilitate an emergency response and can enable the critical healthcare teams to prepare for medical emergencies ahead of time. Such a system due to its ease of use and ability to detect such early warning cardiac arrhythmia can enable auxiliary medical staff to draw the attention of doctors and cardiac specialists to potentially dangerous conditions.

The research study presented in this thesis, at an outset, focused on the classification and prediction problems whereby an arrhythmia could be electronically detected *before* the heart condition would start to deteriorate. The research focused on identifying patterns of heart rhythms, and on classifying heartbeats into a categories of ECG abnormalities. MITDB (MIT-BIH Database) records dataset, discussed in section 3.3 of chapter 3, was used to generate learning and prediction models using WFDB (Waveform Database) software package (Ary L Goldberger et al. 2000; Luz et al. 2016; Silva and G. B. Moody 2014). Initially, a review on current state of the research and examples of existing smart systems for ECG monitoring was conducted. These systems, however, do not have a predictive analysis component to detect or alert individuals of ECG abnormalities well in time and before it's too late for treatment.

Moreover, some of these devices have been implemented on hardware that restrict mobility, so cannot be used by patients while engaged in their day to day activities, which is when they are most likely to suffer a cardiac arrest or a heart attack. The research study involved developing hardware and software tools and techniques along with efficient methods to train early warning ECG arrhythmia classifiers and their predictive aspect. For a case study, a real-time smart IoT (Internet of Things) health monitoring kit was developed, to perform ECG signal acquisition and arrhythmia classification tasks. As the proposed wearable kit was aimed at monitoring individuals regardless of location, it would present additional benefits if integrated with the Electronic Health Records (EHR) systems, so that the arrhythmia events could be updated to the EHR and if required the critical care teams could be alerted of any fatal cardiac arrhythmia related emergencies. To achieve this task, the monitoring kit had to be integrated with using widely accepted Health Level 7 (HL7) based Fast Healthcare Interoperability Resources (FHIR) standard (Raths 2014; Mandel et al. 2016), discussed in section 6.3 of chapter 6. Such infrastructure is now also becoming available in many countries across the globe, and the proposed system could be easily integrated with such infrastructure as it could communicate with the electronic health records systems using standard protocols and clinical coding systems. The research study involved using vital signs and other physiological parameters, to calculate trauma scores (Alam et al. 2014) such as the National Early Warning Score (NEWS), Revised Trauma Score (RTS), Trauma Score - Injury Severity Score (TRISS) and Probability of Survival (Ps), presented in chapter 5 and to log the trauma event to electronic health records using standard coding schemes such as the Systematized Nomenclature of Medicine-Clinical Terms (SNOMED-CT) coding system (Richesson, Andrews, and Krischer 2006), and the trauma information was logged to electronic health records using Fast Health Interoperability Resources (FHIR) servers. The FHIR servers provided interoperable web services to log the trauma event information in real time and to prepare for medical emergencies.

1.3 Aims and Objectives

1.3.1 Objectives in real-time arrhythmia classification

Although current literature in arrhythmia classification illustrates methods and technologies of arrhythmia detection and classification, these remained confined to equipment used in hospitalised and ambulatory settings as compared to restricted and wearable hardware devices. Also, some arrhythmia types require monitoring for longer duration as mentioned in section 1.1.1. To overcome the problem of long-term monitoring, the main aim of research study presented in this thesis was to focus on real-time methods of arrhythmia classification and trauma analysis algorithms on restricted hardware. The important tasks were: real-time ECG signal acquisition, conditioning and conversion into a digitally encoded format that could be used by the machine learning algorithms already trained on and arrhythmia dataset with a specific digital format. The data acquisition filtering and conditioning along with arrhythmia classification tasks had soft real-time constraints. This problem was solved by training the arrhythmia classifiers on a widely accepted MITDB MIT-BIH arrhythmia dataset .

The classifiers that were trained on the training dataset in a desktop environment were ported to the restricted device that could perform real-time arrhythmia classification. The most important problem solved in arrhythmia classification was the development of a real-time classifier that could take as an input raw ECG samples and by using the WFDB routines and a novel feature extraction algorithm based on spectral components, could detect the locations of abnormal arrhythmia types within the ECG signals.

To determine whether a real-time arrhythmia annotator based on machine learning algorithms could be effective in arrhythmia classification, the classifier had to be trained on the abnormal annotation types found in the MITDB database. An ECG waveform related to a particular arrhythmia type exhibits a specific pattern which could be used in the classification task. Using the feature extraction algorithm and classification models developed in this research study it was possible to classify abnormal annotation types with an overall accuracy of

97.8% presented in section 4.2.2.2 chapter 4.

If the fatal arrhythmia such as atrial fibrillation or ventricular fibrillation are detected at very late stages the patient could be at a risk of having a cardiac arrest or similar emergency related situation. Although arrhythmia such as atrial fibrillation have been detected in past research studies using inter-heartbeat intervals (Shouldice, Heneghan, and Chazal 2007) and techniques such as Heart Rate Variability Analysis (HRV) (Ebrahimzadeh, Pooyan, and Bijar 2014) which are influenced by age and gender (Voss et al. 2015), delays in detection may put patient at risk as some of these fatal arrhythmia do not show any symptoms in early stages. To prevent these problems, data mining tasks had to be performed to detect those arrhythmia types that were a precursor (Gomes et al. 2010) (Katritsis, Siontis, and A. J. Camm 2013) to fatal arrhythmia. In order to solve this problem, the precursors to fatal arrhythmia, Premature Atrial Beats (PAB) (also called Premature Atrial Contractions (PAC)) and Premature Ventricular Complexes (PVC) had to be detected and classified using a classifier model presented in chapter 4. A novel feature extraction algorithm was required that could extract features related to these early signs arrhythmia, as no two heartbeat signals belonging to the same arrhythmia type or normal heartbeat had exactly the same morphology, which made it more difficult to extract meaningful features which could be used to differentiate between the arrhythmia types. A detailed study of ECG signal was conducted, considering spectral components of the entire ECG waveform in a heartbeat and its sub-portions i.e. the P-wave, the QRS complex and the T-wave. A novel feature extraction algorithm based on these spectral features was proposed which then increased the overall accuracy of classification to 97% as presented in section 4.4 of chapter 4.

Having developed a successful classification algorithm to classify between abnormal arrhythmia types, another problem that was required to be solved was that the fresh ECG samples may contain a mixture of normal heartbeat samples and abnormal heartbeat samples and the normal samples exceeds the abnormal samples in large quantities, e.g. the abnormal to normal samples ratio was approximately 81: 100,000. Even within the abnormal annotation types, the most represented annotation type is almost ten times the underrepresented annotation type, which created a large imbalance in the dataset, and these problems related to dataset imbalance and classification between normal and abnormal type annotations were solved using dataset balancing techniques presented in 4.3.3 of chapter 4. The least represented arrhythmia type could then be classified with an accuracy of 100%. The classifier models had to be ported from the desktop environment to the IoT device by using persistence package in Scikit-Learn.

The ECG signal acquisition, filtering and signal smoothing had to be performed in real time under noisy conditions and in real time, as the bio-potential measurement in a wearable device is susceptible to a great degree of noise and electrical interference and contains motion artefacts. The raw ECG signal was filtered using a combination of suitable filters to obtain a denoised signal that could be digitised according to the MITDB format.An extended feature extraction algorithm had to be developed for a restricted device that could perform signal conditioning and MITDB format conversion, section 4.5.

1.3.2 Objectives in trauma analysis and EHR interoperability

Cardiac arrhythmia can lead to emergencies and trauma situations, which need to be monitored and the events related to trauma had to be logged to EHR, if required, while the individual being monitored remains engaged in day-to-day activities. A trauma scoring mechanism was required that was widely used and acceptable in clinical and hospitalised environment and the scoring measures had to be reliable and variables used to calculate the trauma scores should be easily acquired. The vital signs and certain physiological parameters were used to calculate reliable trauma scores in real-time which could ascertain the extent of trauma and if required could produce prediction of survival scores, sections 5.2 and 5.3 of chapter 5. Several problems had to be solved to achieve this task – the most important being acquiring the physiological parameters that could enable calculations for vital signs measures in real-time. In a hospitalised environment vital signs are measured using bedside monitors and such equipment is not wearable. Some vital signs such as the respiratory rate and the blood pressure were traditionally obtained using clinical devices such as the spirometer and the sphygmomanometer, and in the absence of a wearable device to directly measure these vital signs, these had to be calculated and approximated. Technically speaking, the problem was reduced to calculating the respiratory rate and the blood pressure from the ECG and the PPG signals acquired using the IoT device. A potential solution had to be tested using the Pulse Transit Time (PTT), which is the time difference between an QRS wave peak and the PPG wave peak in the same heartbeat, could approximate the systolic blood pressure which was one of the vital signs used in trauma scoring algorithm. To extract other vital signs the unique feature extraction algorithm along with WFDB routines were used. Even for trauma analysis, the raw signals from the ECG and the PPG sensor had to be denoised using similar techniques.

The most commonly used trauma scores such as the Revised Trauma Score (RTS) (Champion et al. 1989), the National Early Warning Signs - NEWS, the TRauma Injury Severity Score TRISS (Champion 2018; Gary B Smith et al. 2013; Nedea 2017; Boyd, Tolson, and Copes 1987) were calculated from the physiological parameters and vital signs acquired from the IoT health monitoring kit in real-time. The severity levels associated with each of these, scores were also calculated along with the prediction of survival scores.

For the IoT health monitoring device to be useful for individuals wearing it during their day to day activities, if arrhythmia event or a traumatic event occurred, the events should have to be logged to EHR automatically for further referrals and analysis. To enable such a provision standard telemetry protocols to encapsulate the arrhythmia and trauma event according to standard coding schemes were adopted. It could be argued that such a provision could trigger a critical care response in emergent situations. The critical care team would also have the arrhythmia and the trauma-related information to decide on a course of treatment enabling real-time decision support. The Fast Healthcare Interoperability Resources (FHIR) Web services protocol was adopted, and a FHIR client-side web service was implemented that could transmit the arrhythmia event and the trauma event related information to the FHIR server to illustrate the real-time operation of the composite health monitoring kit, section 6.5 chapter 6. The problem was solved by encapsulating the trauma-related information, vital signs and physiological parameters along with the location information, according to the FHIR specification and transmitting the payload to the FHIR server using appropriate telemetry protocols.

1.4 Thesis Structure

In order to achieve the goal of real-time ECG arrhythmia classification and trauma analysis, beginning with the steps involved in signal acquisition up to machine learning classification tasks, followed by the integration with electronic health records, the problems that were solved as discussed earlier and have been presented in the subsequent chapters. Each problem solved, with proposed and developed solutions, along with the discussions that led to the choice of methods involved in arriving at the respective solutions, have been discussed.

The *Literature Review* chapter, presents the state-of-the-art and current research efforts in similar directions in solving the combined problem of cardiac arrhythmia classification and trauma analysis in real time implemented on an IoT device. Several past and present research studies have been cited to discuss and to bring about the importance of the concepts involved in ECG arrhythmia study and the characteristics of the ECG signals about the normal and abnormal types section 2.1.1. A primer on ECG cardiology related concepts has been provided to understand the components of an ECG signal and the structural variations in the ECG signal due to arrhythmia. Spectral analysis overview has also been provided as a conceptual framework in early signs arrhythmia detection, section 2.2. The traditional methods such as the Heart Rate Variability (HRV) and their drawbacks for an IoT-based solution have been discussed in section 2.6 which largely relate to the inadequate information in the morphological structure of an ECG signal to be used as features that could be used for arrhythmia classification. The important concepts related to signal denoising and filtering tasks used to obtain a denoised signal from the raw ECG samples have been described 2.5. An overview of current practices for training arrhythmia classifiers has also been presented, section 2.4 . The*Literature Review*chapter also provides information on a widely used trauma scoring mechanisms, triage and use of trauma and injury severity scores along with assumptions and the calculations involved, section 2.7 sections 2.8.1 and 2.8.2. An introductory section on FHIR interoperable services to model and integrate patient health status information using a client/server model has also been provided, section 2.9.

The chapter on *Materials* provides information on the hardware and the software used to conduct the experiments in the ECG analysis and Trauma analysis chapters, section 3.1. An implementation of embedding location awareness capability has been described in section 3.1.1. A sample code implementation for encapsulating and modelling a trauma observation is provided in 3.1.3 As the arrhythmia classification was implemented on a resource constrained device, the chapter provides information MITDB arrhythmia dataset used in ECG analysis, section 3.3 and the MIMIC Numerics dataset, section 3.4, used in trauma analysis.

The chapter on *ECG Analysis and Arrhythmia Detection* provides detailed information about the structure of the MITDB dataset and the WFDB routines that were used for extracting features from the ECG records contained in the MITDB dataset. The steps involved in developing classification models, section 4.2.2 to classify the abnormal annotation types have been presented along with the discussions related to the choice of the methods and routines in the WFDB library. The rationale behind the use of spectral analysis to extract features from the ECG heartbeat signal that could be used to adequately differentiate between normal and abnormal types has been presented, section 4.2.3. The novel consolidated feature extraction algorithm that considered spectral energy components, section 4.3, within the sub-portions of the ECG heartbeat signal has been presented in section 4.3.2. The problems related to dataset imbalance and regularisation and classification models have been presented along with discussions related to hyper-parameters tuning, section 4.3.3. In the signal acquisition section, the methods of real-time ECG signal processing have been discussed. The design of filters and the parameters associated with the filter design and signal smoothing and an algorithm for real-time extraction of features from an ECG signal acquired from human subject and processing using the WFDB routines and spectral analysis has also been presented in section 4.5

The *Trauma Analysis* chapter presents methods of obtaining trauma scores from vital signs in real-time trauma scoring from within the IoT device. In the absence of equipment traditionally used in hospitalised settings certain vital signs had to be approximated and the calculations related to these approximations have been presented in this chapter. The MIMIC Numerics dataset 3.4 was used for trauma analysis. As the dataset contains the same set of vital signs that could be calculated from a real human subject it was considered to be an ideal choice to model the trauma scoring algorithms. A novel trauma scoring algorithm 5.3 that was developed during the research study, is presented in this chapter that could extract and approximate, physiological parameters and vital signs involved in trauma scoring. Discussions related to the interrelationships between the trauma scores, the physiological parameters and their co-relationships have been presented using statistical measures, section 5.5. The calculations related to obtaining systolic blood pressure and respiratory rate that were calculated from the ECG and the PPG signals are presented in section 5.2.1. As location awareness had to be included in the composite health monitoring kit with location-aware implementation has also been illustrated. A regression model for prediction of survival based on trauma scores as a feature vector is also presented, section 5.6.

In the *Electronic Health Records Interoperability* chapter the current in the state-of-the-art standards in implementing software solutions for public health data management and retrieval have been discussed. An overview of FHIR standard with clinical and enviable perspective has been provided, section 6.3. The essential task of encapsulating the cardiac arrhythmia related event and the trauma related event using relevant coding systems and the interoperability standards and their implementations in software have been presented and illustrated in section 6.5. Before encapsulating the arrhythmia and trauma event data according to FHIR specifications, their information had to be modelled in an appropriate format and according to a specific architecture and semantic structure to enable a client/server application to exchange information payload, section 6.5.1. An implementation of FHIR client/server system has also been developed and demonstrated. The tool used to model the arrhythmia and trauma-related information according to FHIR Resource specifications and to illustrate inter-relationships between the resources for effective organisation of entire resource bundle has also been presented in section 6.6. The modelling resulted in a novel structure involving Patient, Arrhythmia type, Trauma information and Device FHIR resources which could be used as a template for real-time arrhythmia classification and trauma analysis applications implemented on IoT devices.

The chapter on *Conclusions* presents overall discussion on key novelties and knowledge generated from the experimental results from ECG analysis, trauma analysis and the healthcare interoperability chapters. The advantages of using the novel feature extraction algorithm in real-time on a wearable resource constrained device are discussed. The advantages and disadvantages of various classification models used in the ECG analysis chapter and trauma analysis chapter are discussed. In terms of overall aims and objectives related to real-time arrhythmia detection, classification, discussion on whether the problems discussed in literature review were solved and to the extent they were solved, are presented.

Chapter 2

Literature Review

With an aim to research the problems mentioned in the introduction chapter, a broad literature review was conducted to research problems associated with real time early warning arrhythmia detection, trauma analysis and electronics health records interoperability using clinical standards and using standard tools widely accepted in clinical and biomedical engineering. In this chapter, initially background information on ECG interpretation has been provided followed by the clinical conceptual framework to identify characteristics of premature arrhythmia which could be detected algorithmically and by extracting features that could identify the premature arrhythmias. An introduction to the MITDB MIT-BIH arrhythmia database has also been provided. Comparisons of various methods and techniques used in the past and in recent research studies have been presented along with the discussions related to the advantages and disadvantages of these techniques in arrhythmia classification, in order to achieve near real-time arrhythmia annotator using novel feature extraction algorithms. Advantages and disadvantages of using heart rate variability analysis and its comparison with machine learning alternatives have been presented. In the literature review for trauma analysis, the means and methods of measuring physiological parameters in order to calculate vital signs from human subjects have been presented. Various trauma scores and measures to calculate these trauma scores have been compared along their comparisons and their effectiveness in calculating the prediction of survival scores. Problems associated with real-time trauma scoring on an IoT device and integrating the results with the electronic health records along with location awareness have been discussed.

2.1 Background theory on ECG and arrhythmia types

The human heart is essentially twin pumps operating side by side and in perfect synchronisation. The upper chamber (atrium) of the right hand pump receives de-oxygenated blood from all parts of the body via the superior and inferior vena cava veins and this blood flows down through a non-return valve (tricuspid valve) into the right lower chamber during the 'resting phase' (diastole) of each heartbeat. Meanwhile, freshly oxygenated blood flows from the lungs via the pulmonary vein into the left hand upper chamber (atrium) and down into the left lower chamber (ventricle) via the non-return mitral valve during the same rest period. In the second phase (atrial systole) of the heartbeat, a small node (sino-atrial node) on the inner surface of the right atrium triggers a compression of both upper chambers, forcing any remaining blood still in the atria down into their respective lower chambers (ventricles). In the third phase (ventricular systole), a second node(atrioventricular node) triggers a compression of the two lower chambers forcing de-oxygenated blood from the right hand ventricle via the pulmonary valve into the pulmonary artery and thereafter to the lungs. At the same time, oxygenated blood from the left ventricle is forced via the aortic valve into the aorta, the main artery of the body and thereafter to all parts of the body. It should be noted that the sino-atrial node is the heart's natural pacemaker with a natural beat of circa 100 beats per minute but this is controlled by the hypothalamus in the brain via the cardiac centre in the medulla (a part of the brain stem concerned with automatic vital functions) and the vagus nerve. This slows the heartbeat to approximately 70 beats per minute when a person is at rest but quicker during exercise or when adrenaline is released during the 'fight or flight' mode.

Background theory ECG interpretation The heart comprises of a muscle called myocardium that is rhythmically driven to contract and drives the circulation of blood throughout the body. Before every normal heartbeat, also called systole, a wave of electrical current passes through the entire heart and triggers a myocardial contraction. The pattern of this electrical current and its propagation is not random, but spreads over the entire structure of the heart in a coordinated pattern and leads to an effective, coordinated systole and flow of blood in and out of the heart. This results in a measurable change in potential difference (voltage) on the body surface of human beings. The resultant amplified (and filtered) signal is known as an *electrocardiogram* (ECG, or EKG). (Clifford, Azuaje, McSharry, et al. 2006) A broad number of factors affect the ECG which are, but not limited to: abnormalities in cardiac muscles, metabolic abnormalities (lack of oxygen, or ischemia) of the myocardium, and macroscopic abnormalities of the geometry of the heart. ECG analysis is a routine part of a complete medical check-up, due to the heart's essential role in human health and disease, and the recording and analysis of the ECG in a noninvasive manner can be done relatively easily.

It is a well-known fact that the heartbeat rhythms vary depending on the health of a person, their state of activity and their age. However, it is known that once the heartbeats exceed or if they fall below a certain count then the person concerned is in danger of several heart related ailments. The common one being a cardiac arrest or a heart-attack and other conditions which could be fatal to humans. The term tachycardia is used to describe a heart rate greater than 100 beats/min. A bradycardia is defined as a rate less than 60 beats/ min (or $<$ 50 beats/min during sleep). (Clifford, Azuaje, McSharry, et al. 2006; Meek and Morris 2002; Morris, Brady, and J. Camm 2009). The ECG measurements show that the heart rhythms follow a distinctive pattern and these can be identified as the P, QRS and the T sub-waves and each of these have a time duration in humans with minor relative variation. Usually the ECG strip that presents the charts of the ECG waveform, is 10 seconds long.

As a result of the electrical activity of the heart cells, the current flows within the body and potential differences are established on the surface of the skin, which can be measured using suitable equipment, which is the ECG kit. As in a normal electrochemistry, "when the metal of an electrode comes into contact with an electrolyte an exchange of ions and electrons takes place, the ions from the metal electrode enter the electrolyte and ions from the electrolyte combine with the metal electrode at the electrolyte–electrode interface. At the skin–electrolyte interface a similar process occurs with an exchange of ions taking place between the body and the electrolyte. The graphical recording of these body surface potentials measured and across a radial multi-polar axis as a function of time produces the *Electrocardiogram* (Kocheril and Sovari 2009). A The atrial flow of blood due to the heart muscles followed by the ventricular activation follows the progression of the depolarisation occur in some sequence and this sequence keeps repeating. It starts at the mid portion of the left side of the septum, then progress to the right and forward: the resulting vector has the same orientation. (Goy et al. 2013; Morris, Brady, and J. Camm 2009). The distinctive sub-waves are as shown in table 2.1

2.1.1 Phases in ECG measurement and interpretation

Phase I:

The 12-lead ECG tracing is standard method of measuring an ECG with leads shown in table 2.2. Six leads are recorded by placing wires on each limb. The other six leads are recorded by placing wires on the chest in six specific positions. In total 6 views are obtained due to the leads placement according to Einthoven's triangle (Crawford and Doherty 2012; Kocheril and Sovari 2009) as shown in table 2.2 The first three views called Standard Leads I, II and III, also called "bipolar leads" due to the two sensors placement on the skin surface (a positive and a negative similar to a battery) to complete the circuit. The other 3 views called the inferior views are obtained due to augmented leads aVL, aVR and aVF.

The abnormal pattern of heart beats resulting from an abnormal rhythms in atrial and ventricular muscles is called Arrhythmia. For diagnosis of most arrhythmias, lead II is most commonly used. Lead II (and the chest leads) most consistently show the clearest P Wave which can be diagnostic of many common arrhythmias. (Crawford and Doherty 2012).

Phase II: In order to examine and interpret the ECG signal following steps are usually carried out:

Step One: Identity the QRS complex.

Components of an ECG waveform	
P wave	Represents depolarisation of the right and left atria.
QRS Complex	Represents depolarisation of the right and left ventricles
T Wave	Represents ventricular depolarisation
U Wave	Represents depolarisation of a small segment of the ventricular muscles or ventricular septum and this wave occurs after most of the right and left ventricles have been repolarized
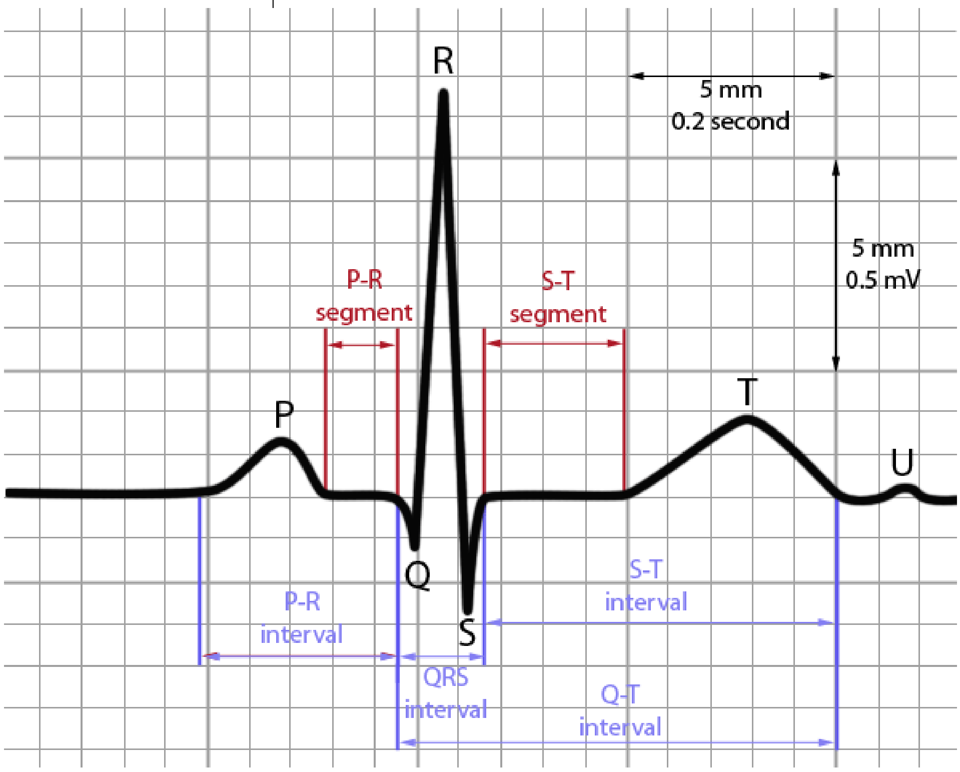	
Source: https://www.medicine.mcgill.ca/physio/vlab/cardio/introECG.htm	

Table 2.1: Components of an ECG wave

Step Two: Determine the heart rate.

Step Three: Determine the ventricular rhythm.

Step Four: Identify the P. Waves.

Step Five: Determine the P-R or R-P interval.

Step Six: Determine the pacemaker rate.

Phase III: Determine the Arrhythmia depending on whether the atrium or the ventricles are affected the arrhythmia could be either Atrial arrhythmia or Ventricular arrhythmia.

Some types of arrhythmia which depend on the heart rate in beats per

ECG leads and their placement	
Limb Leads are: I, II, III, IV, V and VI where: Lead IV also called AVR, Lead V also called AVL, Lead VI also called AVF Chest leads are: V1, V2, V3, V4, V5 and V6	
The leads and their relationship to areas of the heart muscle are as follows	
V1, aVR Right side of the heart. V2, V3, V4 Transition between right and left sides of the heart. V5, V6, I, aVL Left side of the heart. II, III, aVF Inferior aspect of the heart.	
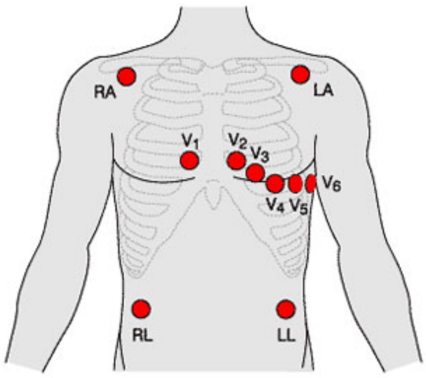 	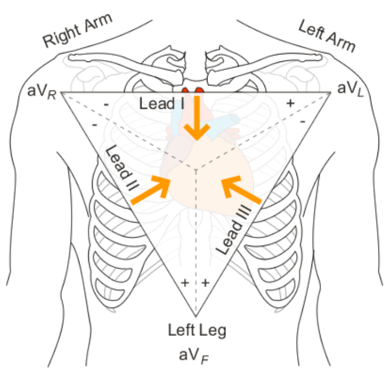
Source: https://www.wikilectures.eu/w/Unipolar_and_bipolar_connection	

Table 2.2: ECG Leads and their placements

minute (bpm) can be broadly classified as bradycardia or tachycardia as shown in table 2.3

A generalised arrhythmia description for bradycardia or tachycardia	
sinus tachycardia	Heart-rate 105 bpm, regular, wide complex, P-waves with normal morphology, P precedes each QRS
polymorphic ventricular tachycardia	Heart-rate 200 to 250 bpm, irregularly irregular beats, wide complex, disassociated P-waves are abrupt and have an onset that is long and RR intervals are short.
ventricular tachycardia	Rate 180 bpm, regular beats, QRS wide complex, disassociated P-waves

Table 2.3: Types of generalised arrhythmia based on heart-rate

Once the abnormal component of the ECG is identified from the sub-waves that are showing abnormal patterns then name the arrhythmia can be identified. If the abnormality is in the atria (P wave), then identify the atrial arrhythmia and if the abnormality is in the ventricles, then identify the ventricular arrhythmia. (Kocheril and Sovari 2009)

The classification or arrhythmia type is made first, according to the site of the arrhythmia and secondly by the type of mechanism responsible for arrhythmia shown in table 2.4.

Arrhythmia classification based on sites affected	
Sites	**Mechanisms**
Sinoatrial Node (sinus rhythms)	Tachycardia (rate over 100 bpm)
Atrial (atrial rhythms)	Bradycardia (rate under 60 bpm) Atrial Flutter or Fibrillation showing defects in conduction when the electrical activity originates from several points in the atria.
Atrioventricular junction node (nodal rhythms)	Premature beats
Ventricles (ventricular rhythms)	Ventricular Fibrillation showing defects in conduction due to disorganised electrical activity in the ventricles leading to serious cardiac arrest, unconsciousness and no pulse.

Table 2.4: Arrhythmia classification based on sites affected

The ECG measurements show that the heart rhythms follow a distinctive pattern and these can be identified as the P, QRS and the T sub-waves and each of these have a time duration in humans with minor relative variation.

The classification is made first, according to the site of the arrhythmia and secondly by the type of mechanism responsible for arrhythmia. Arrhythmia can be of following kinds (Stroobandt, Barold, and Sinnaeve 2015):

Atrial Arrhythmia:

It is recognised by a rate of over 140 per minute and shows normal QRS complexes and abnormally shaped P waves when they are visible and not hidden by the preceding T wave.

Atrial Flutter: This arrhythmia is similar to Atrial Arrhythmia in origin and located usually in the lower atrium near the AV node. The rate for flutter, however, could be 250-350 per minute. Another difference with flutter is that not all of the P-waves show in individual heartbeats.

Atrial Fibrillation: This arrhythmia occurs due to multiple electrical impulses leaving the atrium and can cause scarring of the atrium. This scar tissue becomes “irritable” and begins to send out many impulses across the atria. The ECG tracing rate is extremely rapid (350-600 bpm). The patient’s pulse is irregular and since the P waves are so rapid and at irregular intervals, even the ventricular response is irregular and so is the pulse.
Premature Atrial Contractions (PAC): PAC’s are discharges from the atrium causing contraction of the atrium, however these are not followed by ventricular contraction. The focus of the discharge may be either the right or left atrium. These could be identified by abnormally shaped P waves due to overlap between the current P wave and the preceding T wave. This type of arrhythmia is an early signs arrhythmia, which if untreated and if it remains undiagnosed for longer periods may result into atrial fibrillation.
Ventricular Arrhythmia:

Defects in conduction due to disorganised electrical activity in the ventricles result into ventricular arrhythmia.
Premature Ventricular Contractions (PVC): PVC’s are extra beats which occur from the ventricular walls. There is an irritable spot on the myocardium that may send out a powerful electrical impulse which spreads across the ventricles, causing them to contract out of proportion and in random sequence. The ventricles contract before they have had a chance to completely fill with blood from the contraction of the atria. The PVC are also an early signs arrhythmia, a highly frequent occurrence of these contractions over a longer period of time may result into cardiomyopathy, if a permanent structural damage has been caused to the ventricular muscles.
Ventricular Tachycardia (V-Tach): This is a very serious arrhythmia. Whenever three or more consecutive PVS’s are seen, at a rate of 100 bpm or more. Ventricular Tachycardia (V-Tach) occurs. The ventricles do not have sufficient time to fill and thus, cardiac output is greatly reduced. This arrhythmia may also lead to Ventricular Fibrillation (V-Fib) (cardiac arrest) and sudden death. The blood pressure drops immediately to zero and so does the cardiac output. The heart is merely quivering due to the rapid multiple electrical discharges in

the myocardium. V-Fib is one of the most common causes of cardiac arrest. It usually occurs in the presence of significant cardiac disease. The literature points the following conditions that may lead to V. Fib., coronary artery disease, myocardial ischemia, acute myocardial infarction, and third degree AV Block with a slow ventricular response. (Cohen 2010; Crawford and Doherty 2012; Kocheril and Sovari 2009; Stroobandt, Barold, and Sinnaeve 2015)

2.2 Conceptual framework for early signs arrhythmia detection

The normal sinus rhythm waveform shows all the sub-waves in an ECG signal as shown in table 2.1. The P-wave, the QRS complex, and the T-wave show prominent morphological structure in the waveform and it repeats regularly producing normal heartbeats as could be seen in in a healthy individual. The research study presented in this thesis however, focuses on early signs arrhythmia that should be detected before the arrhythmia results into a more complex and serious cardiac arrhythmia such as the atrial fibrillation or ventricular fibrillation. *The two most common types of early arrhythmia are the Premature Atrial Contractions (PAC) and Premature Ventricular Contractions (PVC) (Cohen 2010; Stroobandt, Barold, and Sinnaeve 2015). There is a strong evidence that these two types of arrhythmias also occur in seemingly healthy individuals and may go unnoticed during an ECG recording due to their intermittent occurrences. (Baman et al. 2010; Moses 2018; Krasteva et al. 2015; Gomes et al. 2010) It could therefore be hypothesised that if these two early arrhythmia types could be identified, serious heart conditions due to arrhythmia could be avoided by medical interventions ahead of time.*

2.2.1 Clinical basis early signs arrhythmia

Premature Atrial Contractions (PAC):

In Premature Atrial Contraction (PAC) as shown in table 2.5, a single sinus rhythm occurs earlier than the next expected sinus rhythm of the heartbeat. The pulse originates prematurely and outside of the sinoatrial node. After the

Premature Atrial Contractions and their characteristics
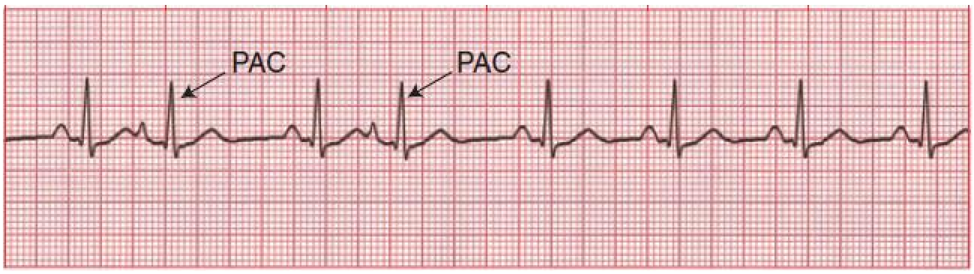
Heart Rate: Depends on the rate of underlying heartbeat rhythm over a period of time. Rhythm: Irregular whenever a PAC occurs. P waves: Present, though in the PAC these may have different shape as it overlaps with the next sinus rhythm beat. PR interval: Varies whenever the PAC occurs, otherwise it is normal (0.12 to 0. 20 seconds) QRS interval: Normal (0.06 to 0.10 second)

Table 2.5: ECG wave with Premature Atrial Contractions (PAC) characteristics

PAC has passed, sinus rhythm usually resumes as normal. If PACs are not treated in time, they may lead to atrial fibrillation or even a stroke.

Premature Ventricular Contractions (PVC):

In Premature Ventricular Contractions as shown in table 2.6are extra beats which occur from the ventricular walls. There is an irritable spot on the myocardium (heart muscle) that sends out powerful electrical impulses which spread across the ventricles, causing excessive contractions that may originate in random sequence. The ventricles, therefore contract before they have had a chance to completely fill with blood from the contraction of the atria.

Branch Bundle Blocks:

Although only the PACs and the PVCs have been considered in this research study as early warning arrhythmias, the branch bundle blocks related arrhythmia may also result into a fatal and serious heart conditions. Although the research study focuses on identifying the PVCs and the PACs, similar machine learning models and signal processing tasks could be performed to identify branch bundle blocks (Ary L. Goldberger, Z. D. Goldberger, and Shvilkin 2018). The branch bundle blocks however, require monitoring different ECG lead views in the Einthoven triangle. The branch bundle blocks have been considered

Premature Ventricular Contractions and their characteristics

Heart Rate: The overall heartrate depends on the rate of underlying sinus rhythm over a period of time. Rhythm: Premature ectopic (random) are not really the beat from the myocardium causes slight irregularity in the ventricular rhythm. P waves: The ectopic (random) beat is not preceded by a P-wave, i.e. atrial contraction). QRS interval: wide and bizarre, different from underlying QRS complexes. The T-wave is frequently in the opposite direction from the QRS complex.

Table 2.6: ECG wave with Premature Ventricular Contractions (PVC) characteristics

for arrhythmia classification task in ECG analysis chapter to determine the effectiveness of classification models to classify between the arrhythmia types. Branch bundle blocks however, have not been considered for real-time arrhythmia classification due to their very low frequency and intermittent nature of occurrence and due to the monitoring requirements through different ECG lead views. The ventricles of the heart (either left or right) contain a sufficient bundle of muscle-cell mass to cause effective compression of the ventricles. The bundle branches (left and right) carry the signal from the atrioventricular node via the 'Bundle of His' conducting fibre. Conduction blocks can occur in either of the two bundle branches. These can occur as the result of infarction of the tissue, although a number of otherwise normal people have a bundle branch block due to the invasion of the conduction pathway with fibrous tissue. It could be observed in rather healthy looking individuals. Despite the condition, the ventricles will continue to depolarise (contract), but via a cell-to-cell interaction which is quite a bit slower than the normal pathway.

The ECG monitoring is normally done when the person in question has shown symptoms of any of the degenerative heart conditions. However, historically *as evident from the hospital admissions for heart related ailments and ICU records; most of the patients, almost 30,000 a year according to BHF, suffer from a cardiac arrest or failure any time of the day or night outside hospitals and without showing significant signs of deterioration in heart condition just before they enter a state of trauma. (BHF 2014; Townsend et al. 2015) Constant monitoring to detect arrhythmias seem to be the most appropriate solution to heart related treatments. (Gradl et al. 2012; Leutheuser et al. 2014). With advent of modern System-on-Chip devices, advanced electrode designs, accurate ECG readings can be obtained even using wearable ECG kits.*

2.3 Wearable ECG kits

There are commercially available wearable 3-Lead ECG kits which can take ECG sample readings while the person under observation is engaged in day to day activities (NICE 2015; Tu et al. 2017; Hernandez et al. 2001). However, many of these kits focus only on data-acquisition and monitoring and provide no analysis or prognosis information in real-time. Furthermore, with these kits intelligent aspect of prediction and raising appropriate alarms, before a fatal arrhythmia and trauma occurs, has not been adequately addressed. Some Internet-of-Things (IoT) devices (Nguyen et al. 2017) are known of having the capability to encapsulate health status events in a standard clinical coding system (Richesson, Andrews, and Krischer 2006) and could transmit the information to the electronic health records (Bowman 2005) in real-time. Similar efforts have been made for electronic health records integration (Franz, Schuler, and Krauss 2015; Mandel et al. 2016) and novel standards such as Fast Healthcare Interoperable Resources (FHIR) have emerged and are currently being adopted by the healthcare services worldwide. Ageing populations and working population due to unbalanced work lifestyles has seen an increase in chronic diseases all over the world have raised the requirement for efficient healthcare monitoring. There has been a focus on remote health monitoring systems based on IoT technology and the concept is being accepted and adopted by hospital monitoring systems and private healthcare providers and has turned out to be effective in, reducing healthcare costs, and at the same time improve healthcare for ageing patients and patients with chronic diseases. The IoT based healthcare assists in real-time monitoring resulting in continuous monitoring at the same time remote monitoring reducing the accommodation requirements in the hospitals and private health care providers. The system results in an architecture with sensing devices, sensing network, data distribution, ubiquitous sensor networks, data analysis servers and computing farms and feedback systems. This approach considers a range of aspects including sensing, data processing, mining and machine learning mechanisms. Using this approach will help to develop effective solutions for pursuing systems development in IoT healthcare applications.

The maturity of Internet of Things (IoT) has led to the rapid development of connected transport, smart cities, connected homes and healthcare. IoT is a technology that connects "things" that are embedded with sensors/actuators and network connectivity to collect and exchange the data over the internet and cloud systems. The enhanced capabilities of resource-constrained embedded devices due to advances in microelectronic fabrication have enabled these devices to collect sensor readings and deliver messages across internet and telecommunication and ubiquitous networks leaves several avenues. Use of standard IoT protocols like Message Queuing Telemetry Transport (MQTT) and Constrained Application Protocol (CoAP) has become common in IoT environment (Oryema et al. 2017). The problems with these devices mentioned in this literature is that a complete workflow of real-time signal acquisition, arrhythmia classification and EHR integration is not available as a single kit. The functions and services provided by the examples cited here are restricted only to monitoring, and no real-time arrhythmia classification functions have been provided on the devices themselves to be used in-situ. With a complete IoT solution, these devices would be able to monitor patients on a 24/7 basis.

2.4 Training classifiers on arrhythmia datasets

In the absence of a specific algorithm that could extract characteristics of abnormal arrhythmia types, especially the PVCs and the PACs, machine learning models could be used to train the classification models on these pre-existing arrhythmia type ECG signals and could be used to perform classification of fresh ECG samples obtained from a real human subject in-situ and in real-time. Similar efforts have been conducted in the past where non-invasive abnormal heartbeat classification tasks were performed and Support Vector Machines (Li, Rajagopalan, and Clifford 2014; Luz et al. 2016) were trained to perform classification based on the MITDB MIT-BIH arrhythmia database (G. B. Moody and Mark 2001). Other techniques that were used involved discrete wavelet transforms (Banerjee and Mitra 2010) and auto assistive and feed-forward neural networks (Chakroborty 2013; Chakroborty and Patil 2014; R. G. Kumar and Kumaraswamy 2013). Although these techniques could perform accurate classification tasks these could not be implemented on an IoT device with processor and memory constraints. In order to implement arrhythmia classification models, these had to be trained on the physiological parameters extracted using the WFDB library provided and maintained by PhysioNet (Ary L Goldberger et al. 2000; Silva and G. B. Moody 2014) and later port the models to the IoT device. For the analyses presented in this research, MIT-BIH Arrhythmia database, described in section 3.3 has been used for data analysis. MITDB has been used in several research studies to derive feature sets based on ECG morphology and heartbeat intervals, and have developed supervised algorithms for detection and classification of arrhythmia (De Chazal, O'Dwyer, and Reilly 2004). The database consists of ECG recordings that has wide range and variety of waveforms that could possibly cover most of the abnormal beat waveforms and which can be used to build a machine learning model and test it. The MIT-BIH Arrhythmia Database contains 48 half-hour two-channel ambulatory ECG recordings, obtained from 47 subjects studied by the BIH Arrhythmia Laboratory. The recordings were digitised at 360 samples per second per channel with 11-bit resolution over a 10 mV range (G. B. Moody and Mark 2001). Two or more cardiologists independently annotated each record to obtain the computerised reference annotations for each beat (approximately 110,000 annotations in all). The database also happens to be widely used, referenced and cited, and is considered to be a gold standard for ECG data analysis. MITDB WFDB also provide ECG analysers that could be used to test trained models (Silva and G. B. Moody 2014). The trained models were then used on acquired data samples in real-time to classify arrhythmia. Despite the availability of ECG WFDB routines to extract information such as heart rate, respiratory rate and ECG signal characteristics, the library doesn't contain methods to annotate and classify the test ECG signal captured from a human subject in real-time. The research study aims at developing real-time classifier using machine learning models and novel feature extraction algorithms.

Hidden Markov Model's (HMM) and Discrete Wavelet Transform (DWT) have been successfully used in the past to identify N-type and V-type annotations from MITDB, to detect supra-ventricular arrhythmia and atrial fibrillation (Gomes et al. 2010). The techniques involved linear segmentation and wavelet spaced feature extraction. Although the algorithm was successful in identifying V-type annotations related transitions, the DWT along with HMM state transitions may not be able to identify abnormalities like the A-type arrhythmia, as the structure of A-type and the N-type signals is very similar with very subtle differences in morphology. Furthermore, important features like the RR interval, heart-rate and PR intervals, which are very important features in arrhythmia detection, have not been considered in this study. An ECG QRS detection is an important aspect in ECG analysis and techniques such as K-Means, PCA (Principal Component Analysis), K-Nearest Neighbours (K-NN) and Probabilistic Neural Network (PNN) have been successfully in the past yielding over 99% classification accuracy (Merino, Gomez, and Molina 2015; Rodriguez et al. 2015; Zadeh, Khazaee, and Ranaee 2010). These techniques can detect the QRS peaks, though cannot identify abnormal regions within an ECG waveform to classify these abnormalities into appropriate arrhythmia types. Another drawback is that these models tend to accept test data in large samples and perform analysis on entire dataset in a single execution cycle instead of beat-by-beat samples in real-time. Also, the physiological parameters extracted using the WFDB library alone may not be adequate to differentiate between the two types of early signs arrhythmia, as there is only subtle difference, especially between normal heartbeats and premature atrial contractions. A novel feature extraction algorithm was required to extract relevant features to identify these subtle differences. In ECG analysis chapter such a feature extraction algorithm has been proposed which uses spectral analysis for a consolidated feature extraction.

2.5 ECG signal conditioning

An ECG signal is a very noisy signal, especially when captured from human subject during various motion states (F. Adochiei, Edu, and N. Adochiei 2011; Ebrahimzadeh, Pooyan, Jahani, et al. 2015). In hospitalised settings the patients are made to lay down in a supine position for ECG recordings, however for a wearable kit signal acquisition has to contain with lies related to electrical interference, muscle movement and errors such as baseline wandering in used to motion artefacts. Several efforts have been made in the past to denoise the freshly acquired ECG signal using linear, nonlinear and adaptive filters (F. Adochiei, Edu, and N. Adochiei 2011; AlMahamdy and Riley 2014; Taouli and Bereksi-Reguig 2010; Taouli and Bereksi-Reguig 2010) to obtain a signal that could be used for further analysis. These techniques relied on signal processing toolboxes which required a high compute power and memory requirements; for a wearable health monitoring kit however, the filters had to be implemented on a resource-constrained IoT device.

So far Fourier transform based techniques were used in signal processing of ECG signals. The Fourier transforms are combination of sine and cosine wave representation of a signal with the decomposed signal functions localised in Fourier space, however, in real world and real-time signal processing, it is the non-localised sudden changes in the signal properties that require identification. These sudden changes in the waveforms can also characterise a signal in time and frequency domain. For example, in an ECG signal it was the QRS complex, i.e. the QRS peaks that characterised the signal along with the P-wave and the T-wave. So, in order to correct the noisy ECG signal, the wavelets which appeared as non-localised sudden changes in QRS, P-wave, and T-wave had to be identified. There are two types of wavelet transforms, the Discrete Wavelet Transform (DWT)(Banerjee and Mitra 2010) and the Continuous Wavelet Transform (CWT). It is the orthogonality that differentiates between these two wavelet transforms. The DWT decomposes the signal into wavelets that are orthogonal in translations and scaling such that the orthonormal transformation preserves lengths of vectors and angles between vectors. The CWT is based on arbitrary scales and arbitrary wavelets that are not orthogonal and is based on computing a convolution of a given signal with the scaled arbitrary wavelet. Considering the orthogonality whereby the scales and angles between the vectors could be preserved, DWT was chosen as preferred choice for further signal processing. In MATLAB the MODWT (Maximal Overlap Discrete Wavelet Transform) was used, because the MODWT was an energy-preserving transform that computed the energy of the signal and compared it with the sum of the energies over all scales of the signal. A Multivariate Wavelet Denoising step was then performed using *'wmulden'* in MATLAB on the filtered ECG signal with a 'sym4' level 5 wavelet, which completely detrended the ECG signal along with baseline correction while still preserving the properties of the ECG signal, figure 2.1.

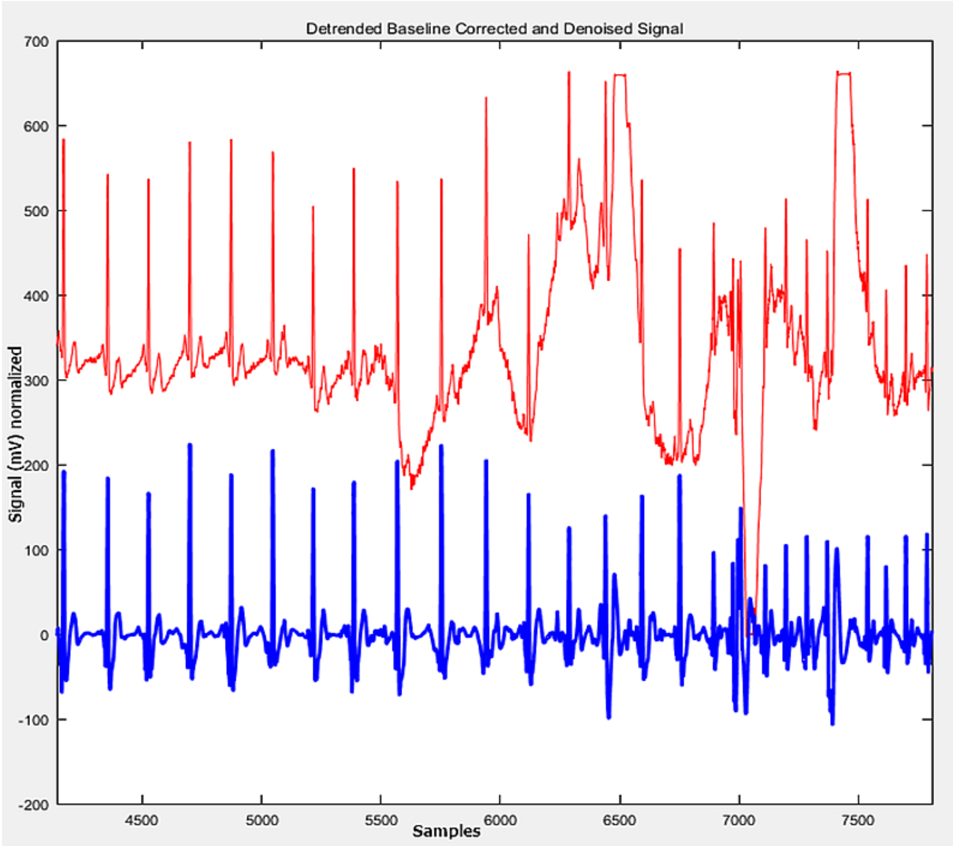

Figure 2.1: A denoised and baseline corrected ECG signal obtained after using multivariate wavelet denoising filter

2.6 Heart Rate Variability (HRV) analysis advantages and disadvantages.

The commonly used techniques in arrhythmia detection using WFDB and PhysioBank tools, relied on frequency domain measures which were calculated by resampling the original RR-interval (Peltola 2012) or NN interval series, i.e. distance between two consecutive QRS peaks, and then applying the fast Fourier transform or auto-regressive spectral estimation (the maximum entropy method), which caused attenuation in the high frequency components of the ECG signal. If discontinuities existed, either because of the presence of abnormal beats or because of extreme noise in the original ECG signal, traditional approaches require approximation of QRS peak locations which induced approximation errors. The frequency-domain spectra can be calculated using the Lomb periodogram for unevenly sampled data, to eliminate the approximation and interpolation errors (Krafty et al. 2014).

Heartrate variability (HRV) (Ebrahimzadeh, Pooyan, and Bijar 2014; Hart 2013) has been widely applied in basic and clinical research studies. The clinical application of HRV analysis and effectiveness in its adoption are still a matter of research as the results tend to vary across age, gender, medications, health status, and physiological variations, among others ((Voss et al. 2015). Furthermore, outliers due to spurious ectopy and motion artefact can have major effects on computed HRV values, especially as seen in elderly population with varying supraventricular rhythm. In order to reduce the effects due to the approximations, several techniques such as Detrended Fluctuation Analysis, Multiscale Entropy Analysis, and Information-Based Similarity, among others has been used to improve on HRV analysis techniques in arrhythmia classification (Cornforth, Jelinek, and Tarvainen 2015).

There also exists a high degree of correlation between Heart Rate Variability (HRV) and arrhythmia. The problem, however, is that HRV analysis depends on the morphology of the ECG waveform and QRS detection, which depends on the accuracy of the ECG equipment and accurate 12-lead ECG equipment may not be portable and certainly not wearable. HRV analysis is also influenced by age and gender-specific information (Voss et al. 2015). The same feature extraction algorithm and machine learning models developed in methods section could be used with other databases from Physionet e.g. the Creighton University ventricular tachycardia database, MIT-BIH atrial fibrillation database and Holter database which are records of patients who suffered sudden cardiac death during recordings and can be used for ECG pattern recognition of extreme conditions and quite a few efforts have been made in the past. (Ebrahimzadeh, Pooyan, and Bijar 2014; Lerma and Glass 2016; Rajskina 1999). It is worth noting that an arrhythmia is non-linearly dependent on P, T, QRS waves and on individual features like RR interval, heart rate, signal strength and arterial blood pressure, or a combination of these, so a Principal Component Analysis was used to reduce the dimensionality in such a way that the variance of data in lower dimensions could be maximised to visualise the data in lower-dimensional space. Other techniques in identification of normal versus abnormal individual heartbeats, and their correct used deep convolutional neural network (CNN) to automatically identify 5 different categories of abnormalities in ECG signals with an accuracy of 94.03% (Acharya et al. 2017). Many of these and other techniques consider the morphological structure of the ECG waveform where RR interval values are commonly used for comparative analysis. However, the morphological structure of the QRS waveform and past pattern from the individual's waveform to use for a comparison to detect abnormal from normal waveform presented challenges, which were overcome using a unique feature extraction algorithm that relied on spectral features of the ECG signal and its sub-waves, rather than HRV analysis.subsectionLiterature review Trauma scoring

Commonly available health monitoring kits focus on a single physiological parameter e.g., Electrocardiogram (ECG) or Photoplethysmogram (PPG), and a comprehensive analysis comprising of all of the physiological parameters seems to be missing with these kits. Multi-parameter health monitoring is available only in hospitalised or ambulatory settings. An individual sensor module, e.g., an ECG module, can only measure the biopotential, as a composite sensor; however, with additional modules such as the Pulse Oximeter sensor, other physiological parameters from a human subject can be measured simultaneously. These readings, collectively, can be used to calculate trauma scores in real-time and they can be used to estimate the prediction of survival in patients. They can also be used to study correlations and regressions amongst themselves, and they can be used to develop other statistical models for further analysis. Several wearable health monitoring kits currently exist in the market that focus on individual physiological parameter monitoring, such as the Electrocardiograph (ECG), Electromyography (EMG), the Galvanic Skin Response (GSR), with very common ones being the 'AliveCor' and 'Shimmer' sensing kits (NICE 2015; Richer et al. 2014; A. Burns et al. 2010). These kits focus on individual physiological parameters e.g., ECG, and they do not consider trauma scores that are associated with an emergency that is related to cardiac arrest. Moreover, the vital signs (Lockwood, Conroy-Hiller, and Page 2004) and triage information is collected, and preparations are made after the patient has been carried to the hospital, which in cases like cardiac arrest, could be too late. These kits don't measure vital signs such as the blood pressure and respiratory rate, and these are measured after the patient is admitted to the ICU after the trauma episode has occurred, which could cause a delay in treating the patient. The composite devices in this research not only monitor individual physiological parameters, but they also calculates related physiological parameters and vital signs. The device uploads the trauma event information and triage information to the Electronic Health Records (EHR) in real-time, and it can raise alarms well in time. Moreover, location awareness is built into the device, which locates the nearest healthcare service provider and calculates the shortest path to reaching the healthcare provider.

2.7 Vital signs measurement problems and challenges

Vital signs (J. Smith and Roberts 2011) are useful in detecting or monitoring medical problems. Vital signs can be measured in a medical setting, at home, at the site of a medical emergency, or elsewhere. With more and more wearable kits that have become easily available, manual intervention in healthcare monitoring has been reduced in many hospital and pre-hospital settings. With an increasing number of miniaturised Internet of things (IoT) devices, Analogue Front-End (AFE) modules and digital signal processing (DSP) devices that have surfaced recently, vital signs and other physiological parameters can be easily measured non-invasively; and the readings can be analysed in a networked environment to provide a managed health monitoring system (Nguyen et al. 2017). Increasing the use of machine learning algorithms and neural networks on vital sign data can determine the deterioration of health in a patient, and can help to predict the health status ahead of time, to prepare for an emergency. Several hospitals and healthcare service providers use standard trauma scoring mechanisms to ascertain or at least estimate patient health, though these are restricted to hospital or ambulatory settings. Scoring measures such as the National Early Warning Score (NEWS), the Glasgow Coma Scale (GCS), the Injury Severity Score (ISS), the Trauma and Injury Severity Score (TRISS) and the Simplified Acute Physiologic Score (SAPS) II/III have been successfully used to identify high health risks and the extent of trauma in ICU settings (Aminiahidashti et al. 2017; Long, Bachulis, and Hynes 1986; Sbiti-Rohr et al. 2016). These scores, in turn, can estimate the probability of survival (Ps) in a patient and can help the critical care team to prepare for emergency procedures ahead of time, though due to limitations in the size of equipment, this has remained restricted to hospitalised settings. The research focuses on the development of a composite healthcare monitoring device that a patient can wear in case of emergency. The device would capture vital signs and other physiological information, and transmit this telemetry data to the electronic health records, and can raise alarms to prepare for medical emergency.

The problems and challenges related to measuring vital signs are such that these are commonly measured only in hospitalised settings or require manual intervention e.g. to measure blood pressure and respiratory rate. The readings taken from the human subjects are in a time-series format, and they have noise and motion artefacts. To perform an accurate waveform and statistical analysis, the data should be clean and accurate. In the trauma analysis section, the research subsequently illustrates the use of data acquisition, filtering, smoothing, and quantisation error removal techniques to extract the portion of the signal that is error-free. The MATLAB Digital Signal Processing toolbox was used to perform signal conditioning, and the MATLAB Coder tool was used to convert the MATLAB code to the corresponding C/C++ code, which could be compiled on the TI AM335x (Beaglebone Black, Texas Instruments). The MATLAB environment and SPSS statistical tools are largely been used for waveform and statistical analyses. Since the parameters being measured were medical in nature, a software library that is widely accepted by the biomedical research community was used. Physionet provides all of the software tools and dataset from real patients for data analysis research that was related to physiological parameters (Lockwood, Conroy-Hiller, and Page 2004; Saeed et al. 2011). The composite sensing device could measure vital signs in real-time; however, in order to perform data analysis, to calculate trauma scores based on vital signs and physiological parameters, the device would have to be tested on real trauma patient. In the absence of patient availability, a database of vital signs and physiological parameters of patients admitted to ICU under trauma conditions had to be considered. The Physionet MIMIC II Numerics database (Ary L Goldberger et al. 2000; Daniel J. Scott et al. 2013a) was used to develop the correlation and regression models to a establish relationship between the trauma scores and the prediction of survival. The NEWS, RTS and TRISS scores were found to be quite useful in estimating the probability of survival in the patients. There is enough evidence in more recent studies that these trauma scores have a direct correlation with the prediction of survival of the patient (Burnham, McKinley, and Vincent 2006; Long, Bachulis, and Hynes 1986). Following the trauma scores calculations, adding location awareness features to the sensor kit was illustrated by using Quantum GIS and Global Positioning System (GPS) tools and techniques, in order to calculate the shortest route from the subject's current position, to the nearest healthcare provider using GIS tools and techniques.

For a composite healthcare monitoring kit to be useful to patients, as well as the healthcare service providers, the readings and trauma scoring have to be transmitted to the healthcare service providers using a standard telemetry protocol. Furthermore, the readings and the trauma experience has to be encoded in a standard coding system that is widely accepted within the medical community. Health Level 7 (HL7) based Fast Health Interoperability Resources (FHIR) interoperable software components have been used to encode the events related to trauma as observations that can be logged to the electronic health record databases in real-time. The research demonstrates the use of the FHIR servers (HL7.org, 2018a), and the development and generation of the trauma event context and observation models for EHR interoperability. Due to the importance of trauma scoring in emergent situations and for the prediction of survival calculations, it became necessary to derive relationship between the trauma scores and physiological parameter. In the discussion and results section, the correlation and regression relationship between the vital signs and trauma scores has been discussed.

There has been a focus on remote health monitoring systems based on the Internet of things (IoT) technology, and this concept is being accepted and adopted by private and public healthcare service providers. This has resulted in the reduction of healthcare costs and at the same time an improvement in healthcare for ageing patients and patients with chronic diseases. It also assists in reducing accommodation requirements in hospitals and private healthcare providers. This continuously monitored information, however, would have limitations in terms of diagnosis if there were no emergency-related trauma scores available to the critical care team ahead of time. The research endeavours to bridge this gap between the monitoring, diagnosis, and timely treatment in trauma-related events. The IoT-based healthcare system results in an architecture with sensing and analytical IoT devices, ubiquitous sensor networks, standard coded data distribution, FHIR servers, and incident response systems

2.7.1 Obtaining blood pressure and respiratory rate as vital signs from the health monitoring kit

The most important aspect of any biomedical device is data acquisition and the techniques involved in signal filtering, smoothing, and signal processing whilst making sure that no information has been lost in acquiring the samples. In the section 4.5 of the chapter on ECG Analysis, the hardware and the software used to obtain vital sign readings from the human subjects is discussed. The parameters such as sampling frequency and the filtering (passbands) parameters, had to be set in order to ensure that the required amplitude peaks were captured while making sure that the outliers were detected and eliminated. Another important aspect in biomedical instrumentation is the removal of motion artefacts and noise due to muscular movements, and the effect of environmental conditions on the sensors.

The blood pressure and the respiratory rate can be calculated from the readings from the ECG and SpO2 sensors using the pulse transit time (PTT), the pulse arrival time (PAT), and the pulse delay time (PDT) (*Heartisans - How it works* 2017). These are estimated blood pressure values, which can be used in the absence of proper digital blood pressure kits. The external BP sensor kits can provide accurate blood pressure readings, though it may not be possible to integrate and synchronise these readings with the ECG and SpO2 sensor readings. Since the readings from the individual sensors have to be sampled in a single sweep and timestamped and importantly all the sensors must be synchronised. The RR and BP calculated using the PTT can be accurate, and they may serve as a good starting point. The RR and BP can then be used as features that are extracted from the waveforms, and they can be used for further statistical analysis and trauma value calculations (Ahmad et al. 2012; S. Kumar and Ayub 2015; Park et al. 2006).

2.8 Physiological parameters for health status determination

Vital signs have been widely used as performance indicators of a person's health. The four main vital signs that are routinely monitored by health care providers are body temperature, pulse rate/heart rate, respiration rate (rate of breathing), blood pressure (non-invasive systolic).(Lockwood, Conroy-Hiller, and Page 2004; J. Smith and Roberts 2011)

The pulse rate and heart-rate are correlated. As the heart pumps blood in and out of the body, this action puts pressure on the arteries, which could be felt as a pulse. Taking a pulse on the wrist measures the heart-rate and can indicate heart rhythm and health. The normal pulse for healthy adults ranges from 60 to 100 beats per minute. The pulse rate can fluctuate, and it may increase with exercise, illness, injury, and emotions. As it is the heartbeats that cause the pulse, the heart rate can be used just as effectively as the pulse rate. Pulse rate, however, can use used in heart rate variability measurement (Hart 2013). The respiration rate is the number of breaths taken by a person per minute. It is usually measured when a person is at rest, sometimes in a supine position, and it simply involves counting the number of breaths for one minute. Respiration rates also vary, and can it increase with fever, sickness, and with other medical conditions that influence respiration. The normal respiration rates for an adult person in resting position range from 12 to 20 breaths per minute, and may depend on age. Traditionally, in intensive care units and ambulatory settings, a spirometer has been used to measure the respiration rate; however, there has been a range of modern respiration rate sensing devices that have emerged, even in the consumer market, which are non-invasive in nature (Duking et al. 2016). This research uses the ECG signal to calculate the respiratory rate, also called the ECG-derived respiratory (EDR) rate. Thus, all of the sensors mentioned in this research are ubiquitous, wearable, and accurate, as compared to the traditionally used sensing devices and manual interventions (Holcomb et al. 2005). Blood pressure is the force of the blood pressurising the artery walls during the contraction and relaxation of the heart. Each time the heartbeats, it pumps blood into the arteries, resulting in an increase and peak in blood pressure as the heart contracts, and when the heart relaxes, the blood pressure falls. Two measures have been traditionally recorded when measuring blood pressure using an instrument called sphygmomanometer. The higher measure, called the systolic pressure, refers to the arterial pressure when the heart contracts and pumps blood through the body. The lower measure, called the diastolic pressure, refers to the arterial pressure due to the heart when it comes to rest and is filled with blood. Both the systolic and diastolic pressures are recorded as "mm Hg" (millimetres of mercury). The research revolves around using modern state-of-the-art measuring methods, and this means that blood pressure is a vital sign (Staessen et al. 2000). High blood pressure (or hypertension) increases the risk of cardiac arrest, heart failure, and stroke, and its measurement is used as an important vital sign. Blood pressure can be categorised as normal, elevated, or stage 1 or stage 2 high blood pressure: Normal blood pressure is a systolic pressure of less than 120, and a diastolic pressure of less than 80, which is generally recorded as 120/80. Elevated blood pressure is systolic pressure with a range of 120 to 129, and diastolic pressure of less than 80. Stage I hypertension: Systolic blood pressure (BP) range 130–139 or diastolic BP range 80–89 mm Hg; Stage II hypertension: Systolic BP >= 140 or diastolic BP >= 90 mm Hg. Pulse oximetry, though not usually considered as a vital sign, can be a very important measure to ascertain an individual's health status, and hence it is called the fifth vital sign (Mower et al. 1998).

Experiments to determine the use of pulse oximetry as a vital sign have been conducted in the past, for example, in an emergency in geriatric assessments using pulse oximetry to measure the oxygen saturation in geriatric patients, which has led to improved diagnosis and treatment. Gas measurements in blood provide critical information regarding the oxygenation, ventilation, and acid-base concentration in blood; however, these measurements are not frequent.

It is well known that oxygenation can change very quickly, and in the absence of continuous oxygenation measurements, these changes may go undetected until it is too late. Pulse oximeters measure the blood oxygen saturation continuously and non-invasively using SpO2 (Mower et al. 1998) sensors. The blood-oxygen saturation indicates the haemoglobin concentration, due to the haemoglobin affinity to oxygen in the arterial blood, which becomes saturated with oxygen. In healthy adults, the saturation range can vary from 94% to 100%. The SpO2 sensor has a pair of light-emitting diodes (LEDs) and a photodiode on a probe element that is clipped to the patient's body (usually a fingertip or an earlobe). The red LED has wavelength of 660 nm, the other is an infrared element with wavelength of 910 nm. Absorptions on each wavelength differs significantly with changes in oxygenated and de-oxygenated concentrations of blood; therefore, from the differences in absorption due to red and infrared light, the oxy/deoxyhemoglobin ratio can be calculated. As the amount of blood in the capillaries depends on the actual blood pressure on the capillary wall (due to heartbeats), the heartbeat rate can be measured as well with the pulse oximeter.

2.8.1 Injury severity and trauma scoring for survival prediction using physiological parameters

The scoring measures, such as the NEWS, the GCS, the RTS, the TRISS, the SAPS II/III, and Ps have been successfully used to identify high health risks in patients that have suffered injury and trauma, and who have been admitted to ICU (Champion et al. 1989; Moore et al. 2006; Schluter 2011; G. B. Smith et al. 2013). The trauma scores used in this research, and the physiological parameters involved, have been presented in table 5.1 for comparison. In the case of emergency, it would be a great advantage if the early warning scores could be calculated in time, and if the healthcare units could be made aware of these scores as soon as possible, to prepare for emergency, even before the patient arrives.

NEWS, RTS, and TRISS scoring schemes used in the research: The NEWS score is based on an aggregate scoring system in which a score is calculated using physiological measurements, recorded in a routine check-up in a hospital or under pre-hospital settings. Six simple physiological parameters that are used for NEWS calculations are the respiration rate, the oxygen saturation, the systolic blood pressure, the pulse rate, the level of consciousness or confusion, and the body temperature. In the case that the patient is in a confused state of mind or disoriented, where the patient may respond to the questions, but is confused, a score of 3 or 4 is assigned to the GCS scale (Teasdale and Jennet 2019; Teasdale and Jennett 1974). The normal GCS score equals 5 for a verbal response. NEWS scoring takes the GCS score into consideration, and in the case of trauma, the GCS scores can be very low, which can affect the NEWS scoring. A score is allocated to each measured parameter, with the magnitude reflecting how the parameter varies from the normal values. These act as weights for each measured parameter. Two additional points are added for people requiring supplemental oxygen to maintain oxygen saturation in blood. There is also an AVPU score (Alert, Voice, Pain, Unresponsive) that can be added to the calculation, depending on the alertness of the patient.

The interpretation of the NEWS score (G. B. Smith et al. 2013): A low score (NEWS 1–4) would ideally require assessment by a competent registered nurse who would further decide how often clinical monitoring would be required, and whether the case should be referred to the next level of diagnosis. A medium score (i.e., NEWS of 5–6 or a RED score) would prompt an urgent review by a clinician that was skilled with the relevant competencies for the assessment of the kind of illness that the patient is suffering from, which would usually be a ward-based doctor or an acute team nurse, who would further assess the patient's health, and if required, would refer the patient to the critical care team. A RED score refers to an extreme condition in one of the physiological parameter (e.g., a score of 3 on the NEWS chart in any one physiological parameter). A high NEWS score (NEWS ≥ 7) should prompt an emergency assessment by a critical care staff with critical-care skills and competencies, and in such cases, the patient has to be transferred to higher critical care settings for diagnosis and treatment.

The use of physiologic scoring systems for identifying high-risk patients for mortality detection has been considered using the Acute Physiology and Chronic Health Evaluation II (APACHE II) and Simplified Acute Physiologic

Score (SAPS II) (Aminiahidashti et al. 2017) models and they are currently used in a large number of hospitals worldwide. Although these scores are not very exact or perfect, they do enable the estimation of the health status of a patient who has had a recent episode of trauma or a similar condition.

Patients brought to the accident and emergency wards may have suffered multiple injuries, in which case the Injury Severity Score (ISS) (S. Baker 2018; Beverland and Rutherford 1983) is used to assess the trauma levels. Such patients who have been injured may have one or multiple injuries, and the ISS (S. P. Baker et al. 1974) is an anatomical scoring method that provides estimates and measures of the overall severity of injured patients. All injuries are assigned an Abbreviated Injury Scale (AIS) (Garthe, States, and Mango 1999) score, and the codes of injuries have been derived from an internationally recognised and accepted dictionary that describes over 2000 injuries and ranges from 1 (minor injury) to 6 (an extreme life-threatening injury). Patients with multiple injuries are scored by adding the squares of the three injuries with the highest AIS scores in predetermined regions of the body and in the order of the severity of injuries. The ISS score can range from 1 to 75, and a score of 75 represents an extreme condition. The maximum score is 75 (25 + 25 + 25), as the maximum severity is 5 for each anatomical part. By convention, a patient with an AIS 6 in one body region is given an ISS of 75. The injury severity score is non-linear, and scores of 9 and 16 are common, while scores of 14 and 22 unusual. The AIS grades are 0—no injury, 1—minor, 2—moderate, 3—severe (not life-threatening), 4—severe (life-threatening, survival probable), 5—severe (critical, survival uncertain), 6—maximal, possibly fatal.

ISS $>$ 15 has been associated with a mortality of 10%. The advantage of using ISS is that it uses anatomical areas of injury to help in formulating a prediction of survival, though at the same time it is difficult to calculate this during the initial evaluation when the patient arrives at the emergency ward, and during resuscitation. In addition, it is difficult to predict the outcomes for patients with a severe single body area injury, though the New Injury Severity Score (NISS), which takes the three highest scores regardless of anatomic area, overcomes this deficit (Linn 1995; Stevenson et al. 2001; I. Y. Whitaker, Gennari, and A. L. Whitaker 2003). The injury severity scoring can be classified as the following:

1. Physiologic: RTS, APACHE, Emergency Trauma Score
2. Anatomical: AIS, ISS, NISS
3. Combined: TRISS, A Severity Characterisation of Trauma (ASCOT), the International Classification of Diseases Injury Severity Score (ICISS)

The restricted hardware device used in the research study presented in this thesis can calculate the early warning scores and injury severity scores in real-time, when the individual has had an episode of trauma. The NEWS, RTS, and TRISS (Schluter 2011) models have been considered in this research presented in table 5.1. In the Trauma Analysis chapter 5, these scores have been calculated and discussed, along with the severity levels that are associated with these scores. The statistical scores associated with these scores have been compared, and the analytical results have been presented in table 5.2. The correlation and regression scores between the NEWS and RTS scores have been studied and are later discussed 5.6. The measurements of the physiological parameters associated with these trauma scores have been measured in real-time, and the scores have been calculated and presented in real-time.

In the calculation of injury severity, the TRISS score remained the most commonly used tool for benchmarking trauma fatality outcome. The survival prediction power of TRISS could be substantially improved by re-classifying the measured physiological parameters and altering the coefficients for the environmental conditions, the demographics or the situations (e.g., combat) (Barnard et al. 2017; Penn-Barwell, Bishop, and Midwinter 2018). Despite some variations in the scoring mechanism in TRISS, due to the influence of demographics and environmental conditions on the patients, it remains a widely used model (Skaga, Eken, and Sovik 2018). Anatomic injury, age, injury mechanism and pre-injury comorbidity are well-founded predictors of trauma outcome and for calculating the TRISS score. Statistical prediction models may have some inaccuracies, though these may be due to inaccurate calibration and inaccuracy due to applications of these models with influence on the environmental conditions.

Early warning scores have largely been used in cardiac emergencies, as these patients, along with other fatal injuries, require medical attention and lead to the emergent incident response. Recognising the early signs of clinical deterioration of patients is thought to improve patient treatment outcomes. The Early Warning System (EWS) scores and the impact of EWS (Alam et al. 2014; Gary B Smith et al. 2013) outcomes were studied on the 48 hr. mortality rate for respiratory failure and cardiac arrest patients (Riordan et al. 2009). It was found that the early warning system scores performed well for predicting cardiac arrest and death within 48 hr. For ailments like cardiac arrests, early warning scoring mechanisms become relevant and applicable as these patients may enter trauma at any time, and healthcare service providers need to prepare ahead of time with readiness to attend to this trauma.

For patients admitted to ICU and facing deterioration of health, physiological parameters such as pulse rate, blood pressure, temperature, and respiratory rate could be used to assess mortality, and serious adverse events (SAEs) such as cardiac arrest could be prevented. The EWS is a scoring system which assists with the detection of physiological changes, and it may help to identify patients who are at risk of further deterioration (Gary B Smith et al. 2013). In cardiac ailments, reduced heart rate (HR) is an established predictor of trauma and further mortality. However, the relationship between the predictors and trauma scoring is poorly understood, hence it becomes important to establish the relationship between heart rate variability and trauma scores (Achten and Jeukendrup 2003; Liddell et al. 2016).

The importance of using injury severity, co-morbidity, and prediction-of-survival scores becomes paramount in military operations when troops who engaged in combat may require medical attention. The situation aggravates when the location of the troops is not known and a soldier requires medical attention if the time frame of the arrival to the base camp is uncertain. In such cases, predicting survival and the measures related to injury severity scores become very important, and the wearable vital signs and physiological measurement kits that can calculate and perform further analysis becomes a very crucial instrument.

The TRISS methodology has been used in both the UK and US Military trauma registries. The method relies on dividing the casualties according to their survival probability (penetrating (Ps_Penetrating) or blunt (Ps_blunt)), though the use different weighing mechanisms based on experiences in combat-related environments. The UK Military Joint Theatre Trauma Registry (JTTR) and the US Military use the same scoring mechanism with some variations in coefficients for soldiers who have been injured in explosions (Barnard et al. 2017). This study aimed to use the UK Military JTTR to calculate new TRISS coefficients for contemporary battlefield casualties who were injured by either gunshot or explosive mechanisms. The secondary aim of this study was to apply the revised TRISS coefficients to examine the survival trends of UK casualties from recent military conflicts. Such systems and early warning scoring kits can be very useful to forces who are deployed in combat zones where the scores can be calculated in real-time in the event of an emergency (Mackenzie and Sutcliffe 2000). The composite sensor kit in this research enables the measurement of physiological parameters that can determine the injury and trauma scores.

These studies mentioned above emphasise the importance of using trauma scores in predicting the mortality and in calculating the probability of survival in injury and trauma situations.

2.8.2 Tables for trauma scoring

In the absence of a real trauma patient, the MIMIC database was used to calculate the trauma scores and it was used to calculate the survival prediction. Since the trauma scores were calculated using the vital signs (Numerics) and physiological parameters, it could be hypothesised that there may be a relationship between the trauma scores, the related physiological parameters and the prediction of survival. Statistical analysis was performed to derive the significance values for this relationship (Domingues et al. 2015).

Once the relationship between the trauma and physiological parameter variables was confirmed, the readings from composite sensors could be used to calculate trauma scores and the prediction of survival in real time. This is imperative for patients who are under continuous monitoring for chronic illnesses, as they may suffer from episodes of trauma at any time. In order to perform multi-parameter analysis using parameters like heart rate, pulse rate, temperature, oxygen saturation, and respiratory rate sensor readings from multiple sensors were gathered, and trauma related scores were calculated. Initially, NEWS (G. Smith 2017) calculations were performed using the following variables and range of values according to table 2.7:

1. Respiratory Rate (breaths per minute) score
2. PPG (%) score
3. Any Supplemental Oxygen score (Yes/No)
4. Temperature in °C (°F) scale
5. Systolic BP score
6. HR (beats per minute) score
7. AVPU score

In a real patient, the Heart Rate and Respiratory Rate (RespR) would be derived from the ECG and the PPG sensor would provide an oxygen saturation reading. It was assumed that ‘No’ supplemental oxygen was provided, as the kit would be worn in non-hospitalised conditions. All the scores required to calculate the NEWS score (G. Smith 2017), could be obtained by the physiological parameters captured by the CHM sensor kit. Following the NEWS score, the RTS was calculated using additional parameters. The RTS (Champion et al. 1989; Champion 2018) is the most widely used prehospital field triage tool, and it was calculated using the variables: The GCS score, the systolic blood pressure score, and the respiratory rate score. RTS requires the Glasgow Coma Scale (GCS) scores (Teasdale and Jennet 2019; Teasdale and Jennett 1974), table 2.9 and table 2.8. The GCS scores quantifies the severity of injuries using eye/verbal/motor responses, and response values listed in the table were used:

The GCS score is indicative of how critically ill a patient is. The trauma scores are merely an indication of deterioration and are suggestive of critical care readiness to a decision support, though should not replace first-hand clinical presentation and diagnosis by an expert. The clinical management decisions with regards to critical illness should not be based solely on the GCS score in the acute setting. If there is a rapid waxing and waning in GCS scores then intubation should be considered in the context of the patient's overall clinical picture.

NEWS calculations with physiological parameters showing a range of values							
Respiratory Rate		Oxygen Saturations		Temperature		Systolic Blood Pressure	
≤8	+3	≤91%	+3	≤35°C / 95°F	+3	<90	+3
9-11	+1	92-93%	+2	35.1-36°C / 95.1-96.8°F	+1	91-100	+2
12-20	0	94-95%	+1	36.1-38°C / 96.9-100.4°F	0	101-110	+1
21-24	+2	≥96%	0	38.1-39°C / 100.5-102.2°F	+1	111-219	0
≥25	+3			≥39.1 °C / 102.3°F	+2	≥220	+3
Any Supplemental Oxygen:				No = 0, Yes = +2			
AVPU Score (Alert, Voice, Pain, Unresponsive)				A = 0 V, P or U = +3			
Calculations: NEWS score = Respiratory Rate score + Oxygen Saturation (%) score + Supplemental Oxygen score + Systolic BP score + Temperature scale + Heart Rate score + AVPU score							
Interpretation: A low score (NEWS 1–4) requires a competent registered nurse to decide if a next level clinical monitoring or an escalation of clinical care is required. A medium score (i.e. NEWS of 5–6) requires an urgent review by a competent clinician, skilled in the assessment of acute illness – to assess whether escalation to a critical-care team is required. A high score (NEWS ≥7) should prompt immediate emergency assessment by a critical care team with critical-care competencies and usually transfer of the patient to a higher dependency care area such as the ICU. (G. Smith 2017)							

Table 2.7: NEWS calculations and interpretation

GCS calculations with reference values		
Best Eye Response (values: 0 - 5)	Best Verbal Response (values: 0 - 5)	Best Motor Response (values: 0 - 6)
4—Spontaneous 3—To speech 2—To pain 1 – No eye opening 0 – Not assessable	5—Oriented 4—Confused conversation 3—Inappropriate words 2—Incomprehensible sounds 1 – No verbal response 0 – Not assessable	6—Obeys command 5—Localizes pain 4—Normal withdrawal (flexion) 3—Abnormal withdrawal (flexion): decorticate 2—Abnormal withdrawal (extension): de-cerebrate 1 – No motor response 0 – None (flaccid)
Calculations: GCS = Eye opening (E) + Verbal response (V) + Motor response (M) = 4 E.g. E1V1M2 E1: No eye opening, V1: No verbal response, M2: Abnormal withdrawal (extension)		
Interpretation: The trauma patients with a GCS of less than 15 require close attention and reassessment. A rapidly declining GCS is concerning and may require immediate critical care intervention. Conversely, a GCS of 15 or more should not be taken as an indication that a patient is not critically ill. If an individual is having a trauma episode with a score of GCS less than or equal to 8 and there is clinical concern of further deterioration based on exam or imaging findings, then intubation can be considered. (Teasdale and Jennet 2019)		

Table 2.8: GCS calculations and interpretation

Following the NEWS and RTS scores, the Injury Severity Score (ISS) (S. Baker 2018) had to be calculated according to table 2.10. ISS is the first scoring system to be based on anatomic criteria, which defines the injury severity for comparative purposes. It standardises severity of traumatic injury based on worst injury of 6 body systems.

Trauma is measured using the TRauma and Injury Severity Score (TRISS) (Boyd, Tolson, and Copes 1987; Schluter 2011; Nedea 2017) scores calculated using ISS and RTS scores according to table 2.11. An important aspect of measuring trauma is to calculate the probability of survival. The Ps scores are measured as Ps blunt or Ps penetrating. Ps blunt indicates the probability of survival if the patient has suffered internal injuries. Ps penetrating scores

<table>
<tr><td colspan="4">RTS calculations with reference values:</td></tr>
<tr><td colspan="4">Physiological parameters required: Systolic BP, Respiratory Rate and the GCS values according to the following reference table. The GCS Value, the SBP Value and the RR Value would be assigned the numerical values depending on the GCS, Systolic Blood Pressure and the Respiratory Rate</td></tr>
<tr><td>Numerical Value Assigned</td><td>Glasgow Coma Scale</td><td>Systolic Blood Pressure</td><td>Respiratory Rate</td></tr>
<tr><td>4</td><td>13-15</td><td>>89</td><td>10-29</td></tr>
<tr><td>3</td><td>9-12</td><td>76-89</td><td>>29</td></tr>
<tr><td>2</td><td>6-8</td><td>50-75</td><td>6-9</td></tr>
<tr><td>1</td><td>4-5</td><td>1-49</td><td>1-5</td></tr>
<tr><td colspan="4">Calculations:
RTS = (0.9368 * GCS Value) + (0.7326 * SBP Value) + (0.2908 * RR Value)</td></tr>
<tr><td colspan="4">Interpretation: A lower RTS score indicates a higher severity. RTS < 4 was proposed for transfer to a critical care trauma center. An RTS score of 1 is indicative of ‘Almost Dead’ or ‘No Chance of Survival’</td></tr>
<tr><td colspan="4">If (RTS >= 12) Severity RTS = 4
Else if (RTS == 11) Severity RTS = 3
Else if (RTS > 3 && RTS <=10) Severity RTS = 2
Else if (RTS <= 3) Severity RTS = 1
(Champion 2018)</td></tr>
</table>

Table 2.9: RTS calculations and interpretation

indicate the patient has suffered injuries which has resulted in blood loss; e.g. Ps penetrating would mean that a person has fallen and has bruises; for example, a soldier wounded in war. Ps scores, along with TRISS scores give an indication of how serious the injuries have been. A similar experiment has been performed in the past, with logistic regression analyses being performed using 412 cases with scores on all severity measures. A trauma injury severity score of more than 11.13 indicated more than a 95% probability of survival (Barnard et al. 2017; Penn-Barwell, Bishop, and Midwinter 2018). The TRISS score provides an estimate of Ps blunt and Ps penetrating trauma scores based on the patient's age, RTS, and ISS results. It is possible to modify TRISS scores depending on the situation, the environmental conditions, and the sample population under consideration, by altering the TRISS coefficients. (Alencar Domingues et al. 2018)

There are severity levels associated with NEWS and the RTS scores, e.g., an RTS of less than 3 would mean that the probability of survival of the patient

Calculating ISS score with AIS score values for organs in various body regions.		
Organs affected	Abbreviated Injury Scale (AIS) Score	
Head, Face, Chest, Abdomen, Pelvis or External	No injury	0
	Minor	1
	Moderate	2
	Serious	3
	Severe	4
	Critical	5
	Un-survivable	6
Calculations:If the 3 most severe injuries in the body are A, B, and C, then $ISS = A^2 + B^2 + C^2$		
If a patient has an AIS of 6 in any body system, they are automatically assigned an ISS of 75. (S. Baker 2018)		

Table 2.10: ISS calculations and interpretation

is almost nil, or that the patient is already dead. The RTS and NEWS scores, along with probability of survival scores can be transmitted to the healthcare service provider in real-time using commonly available telemetry communication media, and the healthcare service providers can use these scores to ascertain the extent of injuries and/or trauma, and they can get ready with their emergency procedures. Such a mechanism can save valuable time whilst the patient is being taken to the emergency ward. If the Ps scores start falling below 4 or start approaching 0, alarms could be raised, indicating an emergency. These scores could also be transmitted wirelessly over the Internet to the healthcare service provider. In the absence of human subjects under trauma or severe injury, MIMIC II Numerics records were used to demonstrate the function of the composite sensor kit. Statistical analysis of the NEWS and RTS scores, along with the probability of the survival scores, showed that the NEWS and the RTS scores were correlated, as shown in the results section. In addition, the severity of injuries and the resulting health status using NEWS and the RTS scores were calculated using the vital signs as parameters. Vital signs were used as individual and independent variables, and NEWS and the RTS values were dependent variables, as were the Ps blunt and Ps penetrating scores.

Calculating TRISS scores using ISS and RTS scores		
	Blunt	Penetrating
b0	-0.4499	-2.5355
b1	0.8085	0.9934
b2	-0.0835	-0.0651
b3	-1.7430	-1.1360
AgeIndex is 0 if the patient is below 54 years of age or 1 if 55 years and over		
Calculations: The TRISS determines the Ps score of a patient from the ISS and RTS using the following formulae: $Ps = 1/(1 + e^{b})$, where, $b = b0 + b1(RTS) + b2(ISS) + b3(Age)$ and, the coefficients b0 $= -0.4499$, b1 $= 0.8085$, b2 $= -0.0835$, and b3 $= -1.7430$ for Ps (blunt), assuming that the patient has suffered no external injury. (Nedea 2017)		

Table 2.11: TRISS calculations using ISS and RTS scores and interpretation

2.9 Integration of EHR with injury and trauma scores

Injuries and disease can be classified according to the International Classification of Diseases (ICD) classification codes, and it can be used with clinical classification codes like the Systematized Nomenclature of Medicine-Clinical Terms (SNOMED-CT) (Richesson, Andrews, and Krischer 2006), and Logical Observation Identifiers Names and Codes (LOINC) (Bodenreider, Cornet, and Vreeman 2018; Forrey et al. 1996). Injury can be described in two ways using ICD-10: the external cause of injury and the nature of the injury. As an example of ICD coding, if death and the causes of death for a particular patient have to be coded according to ICD-10, then the external cause of injury and the nature of Injury have to be determined (Fingerhut and Warner 2006). The External Cause codes describe the mechanism or the cause of the injury (e.g., motor vehicle crash), and the manner or intent of the injury (e.g., unintentional). The Nature of Injury codes describe the body region or the site of the injury (e.g., hip) and the diagnosis (e.g., fracture) (*Injury Data and Resources - ICD Injury Matrices* 2015) The ICD injury matrices are frameworks that are designed to organise ICD-coded injury data into meaningful groupings that are agreed upon by the global medical community. The matrices were developed specifically to facilitate national and international comparability in the presentation of injury statistics (Fingerhut and Warner 2006).

Once the early warning and trauma scores have been calculated, the EHR with the public healthcare service provider can be updated using ICD and SNOMED/LOINC classification codes using Health Level 7 (HL7) standards. FHIR is an HL7 standard that provides interoperability specifications for web services and EHR databases (Westra et al. 2018).

A very important application for wearable IoT healthcare monitoring devices is the ability to locate the individual when the trauma-related events take place. With the availability of low-cost wearable GPS and Global System for Mobile Communication/General Packet Radio Service (GSM/GPRS) receivers, which can be embedded into the wearable kits, such a provision can made available. The GPS receiver can provide the location-specific information, and the composite sensor can provide the physiological information and trauma scores. This composite payload can be transmitted to the healthcare service provider and can enable them to get ready for an emergency. It can also help the ambulance critical care team can get ready for the emergency procedures while they are on their way to the incident location. Several GPS/GNSS systems already exist in mobile service vans tracking systems; e.g., an efficient vehicle tracking system has been implemented for tracking the movement of vehicles using a smartphone application with a micro-controller interfaced with GPS/GNSS technology to track the location in real-time. The vehicle tracking system uses the GPS module to obtain geographic coordinates at regular time intervals. The system also uses Google Maps Application Programming Interface (API) to display the vehicle on the map in the smartphone application, and it can estimate the distance and time for the vehicle to arrive at a given destination (Lee, Tewolde, and Kwon 2014).

2.9.1 Integration with EHR and location awareness

Integrating Trauma and Injury Scores with Electronic Health Records. The calculation of trauma and injury scores may not be adequate to address the emergency response, and the trauma information should be transmitted to the healthcare repository in real-time, and the incidence response should be generated by the sensor kit itself. The problem, however, is that the description of the injury has to conform to a standard coding system that is recognised by the healthcare service provider's information systems; e.g., if the processed heart rate readings from the ECG sensors identify arrhythmia, then this event has to be logged into the EHR records according to a standard coding system. The methods section 6.5 of the chapter Electronics Health Records Interoperability describes the standard coding scheme and a sandbox server that conforms to the FHIR standards that are accepted worldwide. In the methods chapter on trauma analysis, a FHIR server implementation has been discussed and a sample observation of the RTS trauma score has been shown encapsulated in XML file format.

Location Awareness to Trigger a Real-Time Incident Response

In order to implement a prompt and real-time incident response, the use GPS/GNSS and Geographical Information Systems (GIS) tools were required to locate the nearest healthcare service provider. One such tool is the Quantum GIS (QGIS), which is an open-source software that can align and map geographical maps to GPS coordinates. In the Methods section it was used to create layers of information covering a geographical area; e.g., an area with contours for plains at same altitude, or areas in a map that have the same demographic information about healthcare centres in vicinity. This information was modelled as layers, and it was overlaid over the GPS coordinates. The tool can be used to load road and rail route information into the environment, and it can be used to identify the shortest path between two points in a network based on either distance or time (Albrecht 2007). Various filtering mechanisms have been used to overcome the problems related to noise using stationary wavelet transforms, a Chebyshev second-order filter, and a Savitzky-Golay filter for signal conditioning. The algorithms were implemented in MATLAB and could be ported to the embedded hardware. Comprehensive trauma scoring could be performed in real-time, and the scores could be uploaded to the FHIR servers if required. The location awareness built into the kit using GPS modules could be used to locate the nearest healthcare centre, and a shortest path could be calculated to reach the destination.

Chapter 3

Materials

3.1 Health Monitoring kit for real-time signal acquisition

The Composite Health Monitoring (CHM) kit, as shown in figure 3.1, consisted of an ECG, PPG sensors, a GPS module and a 3-Axis accelerometer interfaced with a Texas Instruments AM335x based Beaglebone Black (BBB) small board computer running Debian Linux 7.9. The SciPy and Scikit-Learn packages along with MATLAB Embedded Coder Hardware Support packages support Debian Linux 7.9 to interact with BBB for General Purpose Input Output (GPIO) and serial communication. The software libraries were used to acquire signals in real time from human subject and denoise and filter the signal according to MITDB format. As mentioned earlier Arduino Micro clocked at 16 MHz was interfaced with the PPG and the ECG analogue front-end AD8233 from Analog Devices Inc. directly. The Arduino sampled the ECG and PPG sensor with a sampling frequency of 1 kHz. The raw ECG signal acquired from human subject has noise due to motion artefacts and baseline wandering. The noisy signal was filtered using a Chebyshev Type II filter order = 2, sampling frequency = 1 KHz, with a passband (Wp) of between 1 Hz and 100 Hz, and a stopband (Ws) of between 0.5 Hz to 100 Hz. The signal was further smoothed using a Savitzky–Golay filter with order = 3 and frame length = 101. The MITDB arrhythmia records in digitised form have three files '*dat*' file containing the

digitised waveform '*atr*' or '*qrs*' file containing the annotations that describe the file '*hea*' file containing the information related to digitisation of the record, it is also called the header file. The header file for each record contains fields that describe the Analogue to Digital Conversion (ADC) used to digitise it. These fields include the signal type (such as ECG, ABP, or SpO2), the physical units of the original analogue signal (such as mV, mmHg, or degrees Celsius, the gain, the baseline (the sample value that would correspond to a physical value of zero for that particular record, which is often but not always the centre of the ADC range. It may even lie outside of the ADC range), the *adczero* (the sample value at the centre of the ADC range, which is 0 for ADC at 0 origin and a non-zero value for ADC offset), and the number of bits of ADC precision (most of the PhysioBank records were sampled at 12 bit resolution). These values specified for the digitisation of a particular record help in determination parameters of the analogue to digital conversion process which may help to convert between digital to analogue and analogue to digital formats if required. These parameters provide raw ADC units which were helpful in signal filtering, baseline-correction and further conversion between digital and analogue formats.
The CHM kit captured signals in real time from the following sensor modules, as shown in the figure 3.1 containing following modules.

1. ECG Sensor module

2. PPG (SpO2) sensor module

3. GPS module

ECG sensor breakout board based on an Analog Devices AD8232 The AD8232 analogue front end was used to measure the electrical bio-potential activity of the heart through electrodes attached (glued/taped) to the skin. The ECG sensor board was interfaced with a Texas Instruments AM335x-based Beaglebone Black (BBB) through GPIO ports. The AD8233 is an integrated signal conditioning block for bad potential measurement applications. It can acquire, amplify and filter potential signals in noisy conditions which are present in ECG signals due to motion or electrode misplacement. It can be easily interfaced

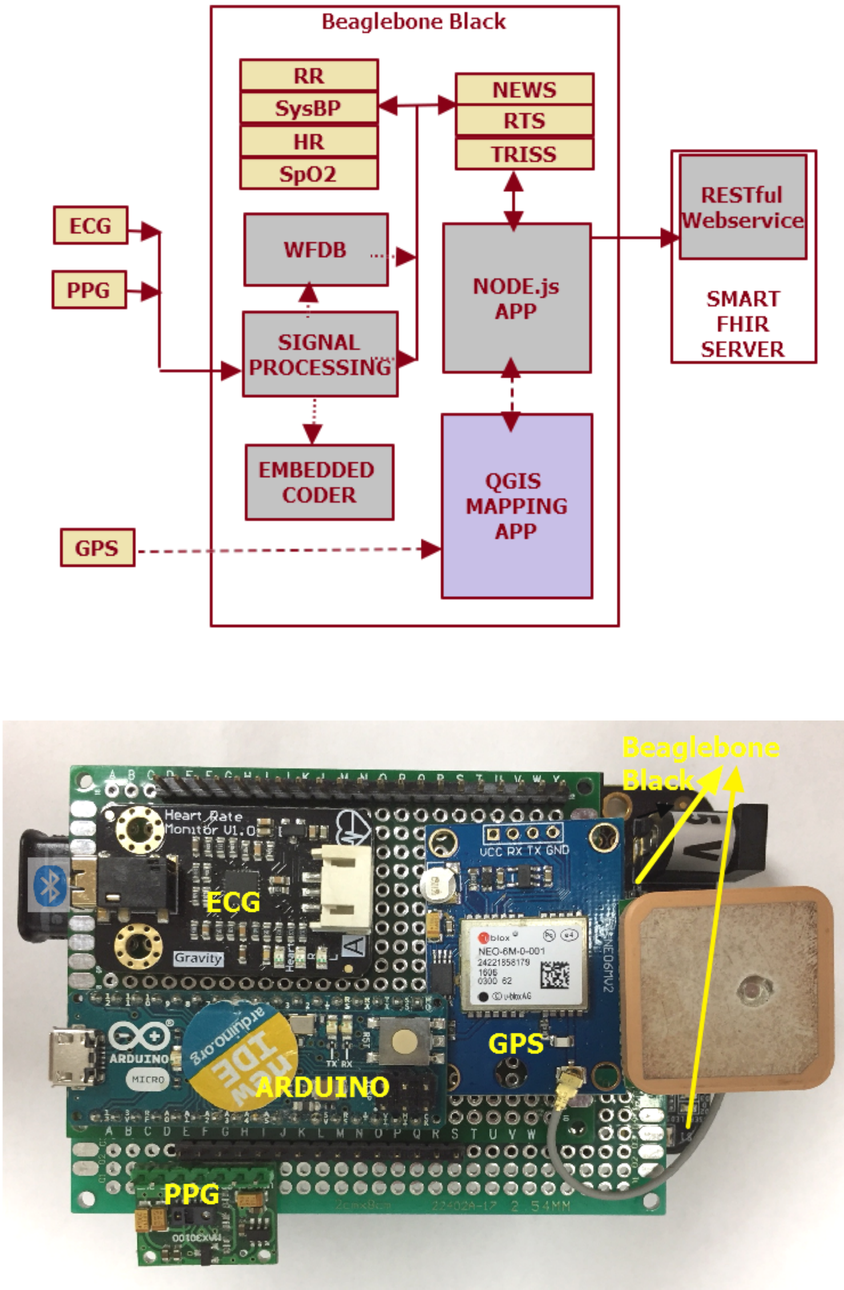

Figure 3.1: The CHM kit block diagram showing all the data acquisition, signal processing, and computing components. Figure also showing the ECG sensor, SpO2, and the GPS/GNSS (positioning) sensor boards, to capture vital signs from human subjects. Breathing rate (BR) or the respiratory rate (RR) are key physiological parameters that are used in calculating trauma scores, and they are still widely measured by counting the breaths manually. The PTT was used to estimate the RR from the electrocardiogram (ECG) and pulse-oximetry (Photoplethysmogram, PPG) signals. These RR non-invasive methods of RR estimation are applicable in both healthcare and fitness monitoring (George B. Moody, 1985)

with an analogue to digital converter on a microcontroller to acquire bio-potential signals. It has a high pass filter for eliminating motion artefacts and filter is tightly coupled with instrumentation amplifier for large gain and high pass filtering in a single stage. Using proper electronic design with active and passive components, the cut-off frequency for the internal filter could be set for a suitable application. To improve the common mode rejection of the line frequencies and undesired interference, a right leg drive (RLD) amplifier has also been provided. The important feature of AD8233 is the fast restore function that reduces the duration of long settling tails of high pass filters. If there is an abrupt signal change due to a leads off condition (when the silver-chloride - AgCl electrode patch comes off), the AD8233 automatically adjusts to a higher filter cut-off, which helps quick recovery and enables acquisition of accurate measurements. The DFRobot Gravity heart rate monitor sensor (*Heart Rate Monitor Sensor DFRobot* 2017) that embeds the AD8233 chip was used to acquire ECG samples from human subject in real time. The sensor was interfaced with Arduino micro analogue pin A1. The timer task interrupt service routine was set to capture the ECG samples at 1 kHz sampling frequency. The ECG signal acquisition block is the same as described in the chapter of ECG signal analysis. The steps involved in ECG signal acquisition, signal filtering, signal conditioning and signal smoothing are similar as well.

The PPG (SpO2) sensor module hosted a MAX30101 high-sensitivity pulse oximeter from Maxim Integrated. It was designed to run on either 3.3 V or 5 V power supply, and it communicated with BBB over an Inter-Integrated Circuit (I2C) interface. The MAX30101-based board included internal LEDs, photo-detectors, and optical elements, and it could remove noise by low ambient light rejection. The MAX30101 integrated red, green, and IR (infrared) LED drivers to modulate the LED pulses for SpO2 and heart rate measurements. As a principle, it is known that the oxygen-saturated blood absorbs light differently than unsaturated blood. Pulse oximeters measure the oxygen saturation, giving an indication of the percentage of haemoglobin concentration in blood that is saturated with oxygen. In a healthy adult, these readings can range from 94% to 100%. Since oxygen-saturated blood absorbs more infrared light than red light, and unsaturated blood absorbs the opposite, the SpO2 readings are calculated

by the comparison of the amount of absorption of these two types of light, as quantified by the current generated by the photo-detectors.
The GPS breakout board hosts the u-blox NEO-6 series GPS module and interacts with the BBB through the serial interface.

3.1.1 Location Awareness Additions to the Wearable Sensor Kit Using the GIS Application and the GPS Module

A very important application for any wearable IoT healthcare monitoring kit is to be able to locate the individual when the trauma related events take place. With the availability of low cost wearable GPS/GNSS, or the GSM/GPRS receivers, the location awareness could be embedded in the kit itself (Lee, Tewolde, and Kwon 2014). The GPS receiver could provide location-specific information, and the composite sensor could provide physiological information and trauma scores. This composite payload could be transmitted to the healthcare service provider, which could enable them to get ready for emergency. With the pre-loaded GIS information, related to the rail and road routes and the traffic conditions, the shortest path/route between current location and the nearest healthcare centre could be calculated using QGIS network analysis tools.

The 'u-blox' NEO-6M GPS receiver and positioning engine was used to acquire position-specific information from GPS satellites. The power save mode (PSM) allows for a reduction in system power consumption by switching between acquisitions and tracking mechanisms. The GPS position is obtained using a mechanism called 'triangulation' (GPS.js, 2018). The format of incoming data from the GPS satellite is specified by the National Marine Electronics Association (NMEA) definitions, and each complete line of transmission is called a 'sentence', and multiple sentence data is called a 'transmit'. Some of the sentences are: GLL—latitude/longitude data, GSA—overall satellite data, ZDA—date and time, WPL—waypoint location information, XTE—measured cross track error, RMB—recommended navigation data for GPS, GSV—detailed satellite data amongst others. Each one of these abbreviated sentences has specific information related to the location. As characters (sentences) arrive from in the GPS receiver, these are buffered, and the parser will detect when a complete sentence has been provided, and the sentence gets broken down into its respective elements to retrieve the required values such as position coordinates. The kind of information that can be extracted from the parser depends on the GPS/GNSS receiver module. Almost all GPS/GNSS modules on the market support basic sentences, which are GGA (GPS Fix Data), RMC (Recommended Minimum Data), GSA (Overall Satellite data), GSV (Detailed Satellite data), GLL (Latitude/Longitude data), and VTG (Vector Track and Speed over the Ground). These are the standard structures that are commonly used in an application, and most of the information related to location, speed, direction, time, and navigation could be retrieved. It is also possible to use the GPS coordinates to gather all the terrestrial and demographic information using an open-source library like RTKLIB (Takasu 2011). The GPS information only provides the location coordinates, though these have to be mapped and aligned according to the geographical mapping system. RTKLIB OSM is an open source GNSS toolkit for performing precise positioning. It was possible to determine the position, using a GNSS receiver. The software supports all major satellite constellations (GPS, GLONASS, Galileo, and others) and it uses standard file exchange formats. The toolkit can be used on Windows and Linux platforms. A number of GPS receivers provided raw measurements (carrier phase and code pseudo range), which were compatible with RTKLIB (Tomoji Takasu and Yasuda 2009). The library was then used to calculate precise positioning to centimeter-level accuracy positioning. The most affordable were the single frequency receivers. The dual frequency receivers were more expensive, but they had higher accuracy, especially for baselines that were longer than about 50 km; the advantage was much less pronounced in sub-km baselines.

The GPS coordinate information, along with the GIS mapping tools, was used to locate the nearest healthcare service provider. The following steps were carried out to achieve this: The road graph plugin in QGIS was used for this task to load road layers for a geographical area in UK. Using the coordinates of the healthcare service providers in the nearby area, these were overlaid as layers. The start point layer became the current GPS coordinates and the end-point layers were the coordinates to the nearby healthcare service providers. Then, using the network analysis tool in QGIS, the shortest path to the nearest healthcare service provider was calculated, and the center information was retrieved. The shortest route to the center was traced according to the road graph-mapping layer.

The GIS data was provided by Geofabrik (*Geofabrik OpenStreetMap data for region: Essex* 2018). The GPS/GNSS-based current position location, and the network analysis tool were used to calculate the shortest path between the current location and an end-point, which could potentially be a healthcare center. For calculating the shortest path from within an application, the following steps were carried out:

1. To match geographical maps with GPS coordinates;
2. To generate a heatmap of the roads traveled, based on GPS track recordings;
3. To download road map data from an online repository of shapefiles and transform it into a network of roads;
4. To store the road network in a database;
5. To generate own records of journeys using a GPS tracking device log of the route traversed;
6. To implement a map-matching algorithm to match GPS track recordings to an existing road network using shapefiles.

Matching GPS data against a map: A GPS receiver/logger captures a series of latitude and longitude coordinates over time and traces the path of someone moving from place to place. The GPS coordinates are recorded and stored according to the person's movements. Commonly available GPS devices enable the recording of a journey that is taken on foot or by a vehicle, by recording a series of coordinates. The GPS device does not know which roads on the route map were followed during the journey. Map matching is the process for taking a GPS recording of the coordinates that are followed during a journey, and matching

it against a database of roads on road map to identify the set of roads that were used on a particular journey.
For the map-matching task, three artefacts were required:

1. An accurate GPS track recording of the journey containing a log of GPS coordinates which would identify the roads that were followed on the journey.

2. An accurate database of road maps mapped to global geographical coordinates.

3. A suitable algorithm to match the GPS coordinates against the road map database.

For the current task using GPS coordinates, a road map and a suitable algorithm, the heatmap of commonly used roads to reach a potential healthcare center, was generated.
A set of road map data in shapefile format was downloaded from OpenStreetMap (OSM) (*Recording GPS tracks - OpenStreetMap Wiki* 2018), and converted into a network of directed road segments. A collection of GPS traces for the journey from the start location to an end location was generated using OSM and GPS traces utility online, which could identify the commonly traveled roads. The traces are normally exported as GPS Exchange Format (GPX) file. A GPS heatmap based on commonly used roads from a start point to an end-point, and captured by GPS devices and available on OSM GPS traces was generated. OSM is a widely used source of GIS/GPS data, and for road map data, www.geofabrik.de was used to download the relevant files in 'osm' format. In order to calculate the shortest path between two points, the starting and ending points were to be selected, and the shortest available path between those two points would be automatically calculated and suggested in real time. The track data was made persistent in a SpatiaLite database, and the Basemap was a GeoTIFF raster image downloaded from OSM. Along with track data and Basemap layers, additional layers to display the temporary information on top of the map were created. The temporary information was: the currently selected starting point obtained by current GPS coordinates from the GPS/GNSS receiver device. The end-point

selected, which was the location of the healthcare center. The shortest available path between the two points traced using line geometry.

Obtaining the Basemap: The GeoTIFF raster image downloaded from OSM was passed through the GDAL utility in QGIS, which aligns the raster image and makes corrections according to GPS coordinates, to generate a basemap that can be used in an application. Alternatively, the GeoJSON utility could be used to obtain maps from GPS coordinates.

Defining the map layers: A separate map layer was created for each of the following: Basemap, Track, Start Point, End Point, shortest path. The Basemap layer was overlaid with the track layer stored in the SpatiaLite database. The map layers could also display additional attribute information e.g., healthcare centre information stored in the database.

Defining the map renderers: Appropriate symbols and renderers from QGIS were used to draw the vector data onto the map. The Start Point and End Point actions allowed the user to set the start- and end-points in order to calculate the shortest path between these two points.

To calculate Find Shortest Path action: The QGIS network analysis library was used to perform the actual calculation to find the shortest path between the start- and the end-points. The shortest path algorithm was run on the tracklayer in the memory-based map layers (Start Point and End Point).

3.1.2 Shortest Route Calculation Using GNSS/GIS Algorithms

Calculating the shortest distance between two points is a very common spatial problem related to Geographical Information Systems (Albrecht 2007), which was solved using the Network Analysis tool in QGIS (*Network Analysis* 2016). The Road Graph plugin of QGIS with network analysis algorithms was used to calculate the shortest path distance or time, by calculating the cumulative cost between two points in a network. The plugin provided a measure of the cumulative cost based on the length between two nodes of a network. The measurements took into consideration the first case, when the speed limit was the same for all the roads (the edges of our network) or the second case, when the speed limit differs for some selected roads. The "Roads" and "Routes" information was downloaded from Geofabrik (*Geofabrik OpenStreetMap data for region: Essex* 2018) repository in the form of shapefiles. The shortest path algorithm in Figure 6 showed that a distance of 4.15 km could be covered in 0.6 hr at 40 km/hr.

3.1.3 FHIR application for the CHM kit

Physiological parameters such as heart rate, oxygen saturation, and pulse rate can be modelled according to HL7 FHIR specifications as observations, and the events of trauma could be modelled as 'assessment scales'. The assessment scales, scoring systems, or indexes are observations with specific characteristics. They have severity-points calculations that can make a quantitative statement on the severity and prognosis of a disease or injury. The scores in FHIR context are used to convert 'soft' observations into 'hard' data and evidence. Typically, assessment scales combine the individual values into a total score, which can be calculated for a reference population. The assessment scale can either be a single value, it can consist of several dozen values, which can be calculated using a complex mathematical calculation or a statistical technique. According to the SNOMED-CT classification, TRISS is an assessment scale with SCTID: 273886002; and RTS has a SCTID: 273885003 (*SNOMED International Browser* 2018). The entire context of the patient, observations of physiological parameters, and assessment scales can be encapsulated as a resource bundle and can be uploaded to the FHIR sandbox server using RESTful Web-services, as shown in code listing 3.1.

```
// Create a FHIR Observation object.
Observation observ= new Observation();
    // Assign a randomly generated Universal ID (UUID).
     observ.setId(uuid)
    // Set the Observation code according to a Coding System
    // Coding System refers to RTS trauma score in SNOMED CT
    observ.getCode()
        .addCoding()
        .setSystem("http://snomed.info/sct")
```

```
        .setCode("273885003")
        .setDisplay("RTS Trauma Assessment")
    observ.setValue(new QuantityDt()
          .setValue(3)
    // Set the Date and Time stamp for the observation
    observ.setIssued(
      new InstantDt("2017-05-05T15:30:10+01:00"))
```

Listing 3.1: FHIR-specific code to encapsulate an observation of RTS trauma score that can be uploaded as a Resource Bundle in XML or JSON format to the FHIR Server sandbox

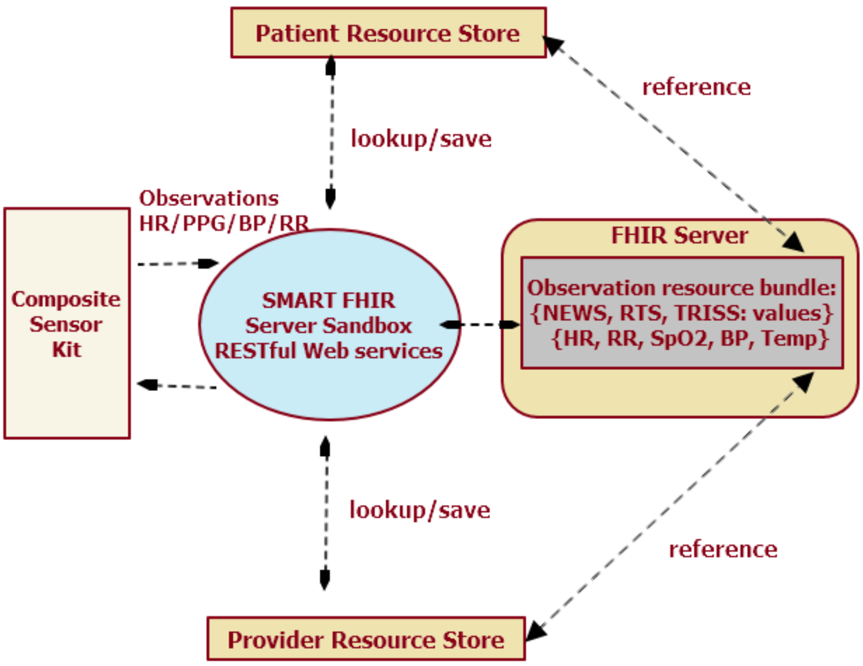

Figure 3.2: SMART FHIR server architecture showing the RESTful Web services that could be accessed from an embedded system hardware (Beaglebone Black).

In order to demonstrate the real-time integration and interoperability of the sensor kit and EHR, a FHIR sandbox was developed, which hosted the EHR functionality and the trauma episodes were modelled as FHIR resources of 'bundles', 'observations' and 'assessment scales'. The readings from the sensor kit were encapsulated as observations, and trauma scores were encapsulated as 'assessment scales' according to FHIR specifications. SMART on FHIR

(Mandel et al. 2016) is a well-known interoperability project with the distinctive goal of developing a platform to enable interoperability between the healthcare application and the FHIR servers, as shown in figure 3.2. The project was called Substitutable Medical Applications and Reusable Technologies (SMART), and it adopted web standards application programming interface transport, authentication/authorisation, user interface, and standard medically coded data. The system helped specify a clinical description of an ailment in a patient. SMART FHIR provides an interoperable interface to develop web services to integrate end user application with the FHIR servers. A HAPI FHIR (Agnew 2016) client server application based on RESTful Web-services was developed that could encapsulate the trauma resource bundle and upload to HAPI FHIR JPA server. A detailed description of the HAPI FHIR client server application has been detailed in chapter EHR interoperability sections 6.4 and 6.5.

3.2 Arrhythmia datasets

To perform an extensive data analysis of ECG samples and to identify patterns of abnormalities present in an ECG waveform, an ECG dataset containing adequate number of samples representing arrhythmia was required, especially the early warning arrhythmia types containing beat waveforms related to PACs and PVCs. Traditionally, ECG waveforms are read in a 10-second period. According to Einthoven's triangle (Crawford and Doherty 2012), as explained in the Literature Review subsection 2.1.1 and Cardio-physiology, Limb Leads I, II and III are used as standard limb leads and very commonly used in wearable kits with three or five electrodes. The three Einthoven bipolar limb leads are determined by the pairwise potential differences between electrodes placed on the Left Arm (LA), Right Arm (RA), and Left Leg (LL). The Lead II is the potential difference between LL and RA. Out of these three leads, the Lead II is widely used as it provides significant electrical signal strength for better signal acquisition. It also produces high amplitude normal QRS complexes in most human subjects. Also, in long term ECG recordings, physical activity causes significant interference in these limb leads. To circumvent this problem, the modified leads were used and the term “modified leads” suggest that the electrode placement on torso are in positions chosen such that the signal closely match the Limb Leads signals. Such a modification is possible because the cardiac electrical field produces time-varying dipole approximation that is generally sufficient to produce same projections with minor changes in positions in the placement of the electrodes along the same axis. The wearable kit described in this chapter uses Limb Lead II for ECG signal acquisition.

Several ECG datasets hosted by the American Heart Association (AHA) and PhysioNet were considered for the research study. In addition ECG dataset samples related to cardiac arrhythmia, software routine libraries to query these datasets were also required to extract physiological parameters and clinical information from the dataset. As the ECG waveform records would be electronically examined using software algorithms, digitisation information was also required to convert signals from raw analogue samples to a digitised format compatible with the dataset.

3.3 MITDB arrhythmia dataset

The MITDB dataset from MIT BIH arrhythmia database maintained by PhysioNet considered for this research study has ECG samples gathered from lead II (ML2 according to MITDB) and V2. The ML2 and the V2 signals are the ECG signals to refer to the electrode placements on the human body. Since the recordings in the dataset were digitised at 360 samples per second at 11 bit resolution, the real-time ECG acquisition described in the subsection 4.5.2 had to sample the ECG readings and digitise the samples using the same sampling frequency, to conform to the MITDB data conversion format for further analysis. Within 11 bit resolution over +/-5 mV range, the sampling value range from 0 to 2047 could be obtained. The MITDB dataset contains signals that were originally filtered using anti-aliasing filter with the pass-band of 0.1 to 100 Hz and notch filter 60 Hz, which was achieved using common digital signal processing libraries in SciPy and MATLAB, which are commonly used in signal processing related

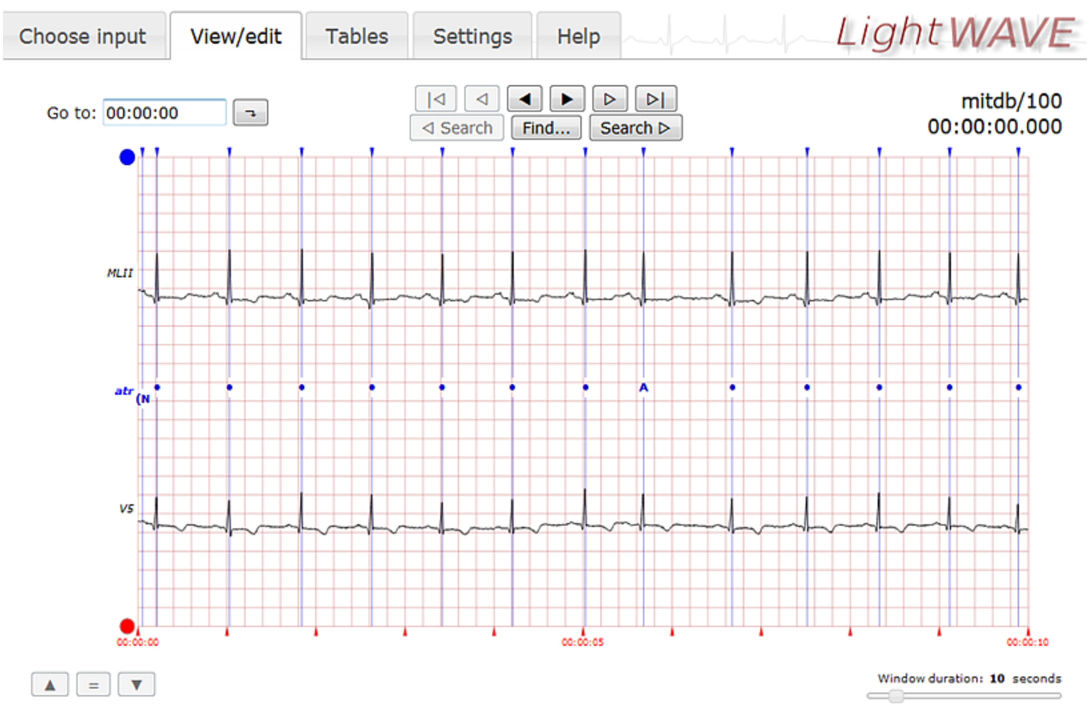

Figure 3.3: The PhysioNet LightWAVE applications showing ECG signals and annotations in an MITDB record. Source: https://PhysioNet.org/lightwave/

research. Since the MITDB database maintainers have already provided the sampling frequency and filter specifications, the same specifications were used for signal acquisition and filtering of ECG signals from human subjects as described in section 4.5 on signal acquisition.

The MITDB Arrhythmia database considered for this research study has 48 patient records of ECG waveforms with all the possible variations of arrhythmia that could be found in a human subject suffering from abnormal heart rhythm conditions. Each record in the MITDB dataset has been manually annotated by physicians and cardiologists identifying events of abnormal heart function. Annotations are labelled at each point in the waveform at specific locations where certain abnormalities were found at those locations. All the ECG recordings have annotations that indicate time of occurrence of the normal and abnormal beats for each heartbeat, also called as beat-by-beat annotations. These limitations could be observed by using tools like LightWAVE provided by PhysioNet. The normal beats appearing as 'blue' coloured dots labelled as 'art' in the LightWAVE plot are shown in figure 3.3.

The beat type annotations are the locations in an ECG signal with clinical and physiological significance indicating normal sinus rhythm or an abnormality found in signal at a particular location. For example, the N indicates the normal beats and V,A,L,R annotations indicate abnormalities found in an ECG signal at corresponding locations. As shown in table 3.1, the non-beat annotation types provide structural information and morphological significance, e.g. the start '(' and stop ')' points in a heartbeat waveform for each of the PR, QRS, ST segments and p, t annotations indicate the peak of P and T waves respectively. To perform extensive data analysis on ECG samples from all the MITDB records, adequate number of samples were required for each of the beat annotation types. As discussed in the literature review section 2.2, premature ventricular complexes and premature atrial beats along with left and right Branch bundle blocks are an indicator of fatal arrhythmia that may occur if not treated in time. To identify these abnormalities, ECG samples in the datasets should have these beat annotations. Having examined the records using the LightWAVE tool it was found that these beat annotations were present in ample quantity in the MITDB records.

The most common beat annotations found in the ECG of all the MITDB records are:	
N	Normal beat
L	Left bundle branch block beat
R	Right bundle branch block beat
V	Premature Ventricular Contraction
A	Premature Atrial Beats
The non-beat type of annotations are as follows:	
(	Waveform onset
)	Waveform end
p	Peak of P-wave
t	Peak of T-wave

Table 3.1: The common beat and non-beat type annotations for ECG signals in PhysioNet MITDB records

Each of the successive annotations is equivalent to RR-interval, and each RR-interval is made up of approximately 250 samples. On average each annotation covers about 360 samples and a single record is approximately 650,000 samples.

The data was obtained by downloading the `ATR, DAT, HEA` files for each record from the PhysioNet website for MITDB dataset. Source:

http://PhysioNet.org/physiobank/database/mitdb/.

Each record consists of at least three files i.e. the ATR, DAT, HEA files. The ATR files are binary files that consist of all the beat and non-beat annotations at particular positions in a signal for each of the MITDB records. The DAT files consist of the binary digitised samples of a signal of the record. Each sample in MIT-BIH record is represented by a 16-bit two's complement amplitude stored as least significant byte first. Any unused high-order bits are sign-extended from the most significant bit. This format is known as Format 16. It is also the format that the freshly acquired signal would have to be converted to, in order to conform to MITDB record format. The HEA files are short text files that describe the contents of associated signal files. The header information consists of the sampling rate, age gender and the medication related information for a particular patient.

3.3.1 PhysioNet WFDB library

PhysioNet also provides PhysioToolkit (Silva and G. B. Moody 2014; Ary L Goldberger et al. 2000) which is a library of software for physiologic signal processing and analysis and detection of physiologically significant events within the signals using statistics and quantitative analysis, digital signal processing and nonlinear dynamics. It is also used for interactive display and characterisation of signals, creation of new databases, and simulation of physiologic and other signals. The focus of this research study was on the extraction of 'hidden' information from biomedical signals, such that information that may have diagnostic value in medicine could be obtained and transformed into mathematical domain for further analysis. The WaveForm DataBase (WFDB) library (G. Moody 2019) provided by PhysioNet was used to extract features from the MITDB dataset.

The PhysioToolkit provides the WFDB (WaveForm DataBase) software package which is used for viewing analysing and creating records for physiologic signals. The WFDB software package has three components:

- WFDB library which is an application program interface to access PhysioNet data sets.

- WFDB routines or applications are online tools or C/C++ subroutines/functions for signal processing and automated analysis.

- WAVE is a software for viewing annotation analysis of signals.

The following primitives were used extensively in chapters 4 and 5 for extracting features from MITDB and MIMIC Numerics datasets.

- `rdsamp` reads ECG signal files for the specified record and outputs the samples as decimal numbers. `rdsamp` starts at the beginning of the record and outputs all samples line by line containing the sample number and samples from each signal, beginning with channel 0, separated by tabs.

- `wrsamp` reads text input (e.g. comma separated file) and outputs the specified columns in WFDB signal file Format-16, either to the standard output or to a disk file. Format-16 sample is represented by a 16-bit two's complement amplitude stored as least significant byte first. Any unused high-order bits of the sample are sign-extended from the most significant bit.

- `gqrs` attempts to locate QRS complexes in an ECG signal in the specified record. The output of gqrs is an annotation file (with annotator extension *qrs*) in which all detected peaks are labelled normal 'N'. The fields of each annotation indicate: (a) the detection pass (0 or 1) during which the QRS complex was detected, (b) the signal number on which it was detected, and (c) the peak amplitude of the annotation detector filter during the QRS complex.

- `rdann` reads the annotation file specified by record, and outputs a text format, one annotation per line. The output contains (from left to right) the timestamp of the annotation as hours, minutes, seconds and milliseconds or sample number where the difference between two consecutive samples is (0.00277 corresponding to 360 Hz as most of the datasets, especially MITDB sampled at 360 Hz.); a mnemonic for the annotation type `(, ), p, N, V, A, N, L, R` corresponding to the annotations in the ECG signal.

- `ecgpuwave` analyses an ECG signal from the specified record, detects the QRS complexes and locates the start and end locations of the P, QRS, and T sub-waves. The output of ecgpuwave is a standard WFDB-format annotation file associated with the specified annotator e.g. *qrs* and *epu* in chapters 4 and 5. This annotation file can be converted into text format using `rdann`.

- `ann2rr` is typically used to obtain list of RR-intervals from ECG annotation file e.g. *qrs* file. By default, the intervals are listed in units of sample intervals (corresponding to 360Hz for MITDB records) to determine the sampling frequency of the input record if necessary.

3.4 MIMIC Numerics dataset

The Multi-parameter Intelligent Monitoring in Intensive Care (MIMIC) Numerics database(Ary L Goldberger et al. 2000), maintained by Physionet and used for trauma analysis in chapter 5 is a collection of 121 records that contain periodic measurements of physiologic vital signs variables obtained from bedside Intensive Care Unit (ICU) monitors. The database is called Numerics (Ary L Goldberger et al. 2000) because these measurements typically appear in numeric form on the ICU bedside monitors. The physiologic parameters are the heart rate, blood pressure (mean, systolic, diastolic), respiration rate, oxygen saturation. The records vary in length from about an hour to more than 77 hours; most are about 35-40 hours in length. The total length of the records is approximately 4658 hours. The physiological parameters were sampled at sampling interval of 1.024 seconds. The records contain patient status alarms which refer to the events that required medical intervention or observation for example observation of heart rate, blood pressure exceeding preset limits. The records also contain monitoring condition alarms which refer to the events that interfered with the function of the monitor for example device malfunction or signal saturation. The MIMIC Numerics database has records for the clinical classes of respiratory failure, congestive heart failure/pulmonary edema, myocardial infarction/cardiogenic shock, post-operative health conditions.

From these clinical classes the trauma situations of patients related to respiratory failure, congestive heart failure, and myocardial infarction, may have occurred in the absence of bedside or ambulatory health monitoring devices. These trauma conditions could be life-threatening and require immediate medical attention and critical care and in such cases where medical attention is required from the time the trauma situation occurred, up to the time these patients were examined by critical care or triage experts, the vital signs and physiological parameters required close monitoring. In such life threatening situations automated trauma scoring and prediction of survival estimation becomes essential for the critical care team to assess the patient's health.

Initially, however, the CHM kit was trained on an existing vital signs database such as MIMIC Numerics which enabled to perform trauma scores and prediction survival tasks. For the purpose of analysis only the physiologic parameter readings were required. The trauma scoring and prediction of survival algorithm, section 5.3 was developed for the MIMIC Numerics database and later tested on freshly captured ECG and PPG samples.

The fresh ECG and PPG signals were filtered and then converted to a format that was recognised by the WFDB routines (Daniel J Scott et al. 2013b; Silva and G. B. Moody 2014). The WFDB library was installed on BBB, and software utilities from the library were used to convert the ECG waveforms to a WFDB format. The MIMIC II Waveform Database is one of the two MIMIC II Databases. The waveform database contained several thousands of records of time series that have been digitised using physiological waveforms and simultaneously recorded Numerics (vital signs) signals of physiologic measurements. Some records also contain alarm annotations and signal quality indexes. The waveforms could be visualised online or by using a WAVE toolkit (Vest et al. 2018) . PhysioNet is a widely used resource for complex physiologic signals, which was created for the 'Research Resources' of the National Institutes of Health (NIH), to instigate the study of cardiovascular and other complex biomedical signals. WFDB is a major component in the PhysioToolkit, and it has about 75 applications for signal processing and automated analysis (Saeed et al. 2011). For the current research experiment and data analysis however, the MIMIC II waveform and

Numerics database was used. The database contained physiologic signals and vital signs in a time series format that were captured from patient monitors for tens of thousands of ICU patients. Data were collected from a variety of ICU admissions varying from (medical, surgical, coronary care, and neonatal) related admissions. The MIMIC II Clinical Database contains clinical data from bedside monitors, and written notes taken by doctors and nurses. The MIMIC II Waveform Database included records of high-resolution physiologic waveforms and minute-by-minute numeric (vital signs) time series (trends) of physiologic measurements. Waveform Database records were matched to the corresponding clinical database (Vest et al. 2018; Pirracchio 2016). The recorded waveforms and Numerics (vital signs) included ECG signals, and often included Arterial Blood Pressure (ABP) waveforms, fingertip PPG signals, and respiration rate signals depending on the patient condition that was being monitored. Numerics (vital signs + physiological signals) typically included heart and respiration rates, SpO2, and systolic, mean, and diastolic blood pressures. The recording lengths also vary from a few days in, to several weeks long. Waveform signals in MIMIC II/III were captured at 125 samples/second and consisted of ECG, PPG, RESP (Respiratory Rate), and SysBP (Systolic Blood Pressure) signals (Saeed et al. 2011; Pirracchio 2016), amongst others. For calculating the trauma and injury severity scores, Heart Rate (HR), Respiratory Rate (RR), Systolic Blood Pressure (SysBP), Oxygen Saturation (SpO2) values were used. In the next section a method to acquire vital signs from ECG and PPG signals captured from human subject is described, which includes the method to convert the samples to WFDB format such that the samples could be passed through the WFDB routines, which require the samples to be sampled at a particular sampling frequency and gain and should be within signal amplitude threshold.

3.5 Scikit-Learn machine learning package

The trained models were persisted using the method *pickle.dumps()* in the Scikit-Learn package *'pickle'*. This method dumped the persistence version of the classifier model as a binary file that could be recognised by Scikit-Learn. The file was copied to BBB which already had Python and Scikit-Learn installed on it. The Python program running on BBB could load the persisted model using the method *pickle.loads().* Once the model was loaded in the memory, it could be used for classification tasks on the fresh test ECG waveforms using the *predict()* method of that particular classifier. By using the *pickle* package the classifier was not required to be trained again on a different target machine, especially if the target device is a resource constrained like BBB, with less memory and processing power as compared to a desktop.

The feature vectors were extracted from the fresh ECG signal over a 10 seconds interval as it is a common practice with standard ECG signal acquisition in clinical environment. A single ECG strip is 10 seconds in duration. As the classifier model was already trained and persisted, it could be loaded back in the memory using the *pickle.loads(file)* function in the pickle package. The classification task was performed using the *predict* method on the classifier. The classification accuracy was analysed using *metrics.accuracy_score, metrics.confusion_matrix* and *classification-report* from *sklearn.metrics* package.

Classifier = pickle.loads(file)

Classifier.predict(feature_vectors)

Chapter 4

ECG Analysis and Arrhythmia Detection

4.1 Introduction

A very important aspect of personalised healthcare is to monitor an individual's health using wearable biomedical devices continuously and essentially to analyse and if possible to predict potential health hazards ahead of time. The prediction aspect embedded in the system helps in avoiding delays in providing timely medical treatment, even before an individual reaches a critical condition.

This chapter focuses on early signs cardiac arrhythmia detection and classification using the ECG samples obtained from a wearable 3-lead ECG kit. Also, the state-of-the-art research shows extensive use of Heart Rate Variability (HRV) analysis for arrhythmia classification, which depends largely on the morphology of the ECG waveforms and the sensitivity of the ECG equipment, induces errors in classification. The wearable 3-lead ECG kits are susceptible to calibration and measurement errors, so the accuracy of classification has to be dealt with at the machine learning phase. The clinical application of HRV analysis and effectiveness in its adoption are still a matter of research and the results tend to vary across age, gender, medications, health status, and physiological variations, among others (Voss et al. 2015). Furthermore, outliers due to spurious ectopy and motion artefact can have major effects on computed HRV values, especially as seen in elderly population with varying supra-ventricular rhythm. HRV analysis is based on the RR-intervals of the waveform, so the analysis can only provide time and frequency domain measures of the waveforms, however the subtle differences in the waveforms as observed in the normal sinus rhythm and Premature Atrial Comtractions (PAC), due to overlapping P-wave and QRS complex, do not produce significant time/frequency variations to provide a clear classification boundary between PACs, PVCs and normal sinus rhythm. With an aim to detect early warning to arrhythmia, the objective during this research study was to identify beats containing PACs and PVCs and separate these from the normal beat waveforms. The differentiating factor between the PACs, Premature Ventricular Contractions (PVC) from the normal sinus rhythm was the PR-interval portion of the waveform and the abnormal QRS complex. So, in addition to RR-interval other features had to be identified which could increase the accuracy of classification. As an ECG waveform is a power signal, power spectral analysis provided the Power Spectral Density (PSD) measures of the sub-waves in the ECG waveform, which provided the required features along with RR-intervals to improve the arrhythmia classification accuracy into the two early signs arrhythmia classes (PVCs and PACs), which was the key hypothesis during the research experiments described in this chapter. To derive these spectral estimates a unique feature engineering algorithm was developed during this research study and is presented in this chapter. The algorithm implements a finite state machine that takes as input the start and stop locations of the P-wave, QRS-wave and the T-wave and the respective peak locations of these sub-waves and calculates their power spectral densities. The P-waves, PR-intervals and QRS complexes were considered and the power spectral densities of these sub-waves were included in the feature vector that was used for arrhythmia classification. Once the power spectral densities were included as a feature vector, the accuracy of classification increased to 97% with the PSD of PR-interval alone, contributed in excess of 35% of total feature importance. The consolidated feature extraction algorithm was used to extract the following features: *PR_Interval, PR_PSD (PR-Interval Power Spectral Density), QRS_Interval, QRS_PSD (QRS_Interval Power Spectral Density), RR_Interval, PowerSpectralDensity (PQRST waveform Power Spectral Density),* *SignalToNoiseRatio*. The class labels were the annotation set AnnotationType:V, A, N with V representing PVCs, A representing PACs and N representing normal sinus rhythm.

As the heart-rate depends on RR-interval, these two were found to be negatively correlated (Pearson) amongst themselves ($r = -0.359$, $p < 0.001$) and $F (2, 24187) = 1125.58$, $p < 001$ $R2 = 8.5\%$, table 4.2. From each of the 48 records in MITDB database about 650,000 (pre-filtered and denoised) samples per record were used to train the classifiers to classify a heartbeat sample as belonging to a category label (AnnotationType) of an abnormal beat annotation. The MITDB dataset had adequate number of samples to enable classification between four major annotation types V,A,L,R representing PVC, PAC, left branch bundle block, right branch bundle block respectively, so the initial classification task involved classification for these abnormal annotation types only. The feature vector for V,A,L,R classification consisted of feature set: age, gender, RR-Interval, ECG signal value mV. From the experiments performed using several classifiers, k-Nearest Neighbours *(k-NN)* classifiers yielded 99.4% accuracy. The feature extraction algorithm extracted features for 24,190 annotations representing the abnormal V,A,L,R annotation types. Due to the disproportionate number of abnormal annotation types, which were approximately 81 abnormal beats per 100,000 beats, the dataset had imbalance in classification labels. The problems related to dataset imbalance was solved using the SMOTE (Synthetic Minority Oversampling Technique) imbalance reduction technique as the A-type and V-type annotations were only 5% and 25% of total annotation count. As the A-type and V-type annotations represented early signs arrhythmia, these two were considered for classification purpose along with the normal N-type annotation. Considering the dataset imbalance and spectral components of PR-Interval and QRS complex a consolidate feature extraction algorithm was used to extract the features. A classification model was developed using *GridSearchCV* and *RandomForestClassifier* with balanced-accuracy scoring, 500 estimators and *StratifiedKFold* cross validation with 5 splits and a 'balanced' class-weight as parameters. An overall classification accuracy score of 97% was observed. The precision accuracy for classification of both V-type and A-type annotations was

100% and for N-type annotation the precision accuracy was 91%. The recall scores were 90%, 100% and 100% for A, V and N type annotations. As the aim of the research was to implement the early signs arrhythmia detection algorithm on a wearable device, the freshly captured ECG samples had to be filtered, denoised and baseline corrected using *Chebyshev* 2nd order and *Savitzky-Golay* filter. An extended feature extraction algorithm was used for signal conditioning and for extracting features from the samples collected in real time using the wearable ECG kit. As the classification algorithm trained on the ECG samples from MITDB dataset was to be used on the real-time ECG samples, these had to be converted in accordance with the MITDB dataset digitisation format using *WRSAMP* utility found in the WFDB software library provided by PhysioNet. The *WRSAMP* routine, takes the raw ECG sample along with gain and scaling factor as an input and converts it to MITDB compatible sample, represented by a 16-bit two's complement amplitude stored least significant byte first.

4.2 Methods: Feature extraction and data analysis for MITDB records

The Class 1 MITDB waveform database is considered the gold standard in ECG analysis and is widely used, referenced and more importantly it is manually annotated by medics and is quite reliable as there are samples of various types of arrhythmia, that are representative of an arrhythmia type, found in patients suffering from heart related conditions. In order to classify arrhythmic beats, MITDB waveform records were used to prepare datasets to train classifiers. The most essential aspect of data analysis is feature extraction and selection following which the models are usually trained.

4.2.1 Feature extraction using WFDB for V,A,L,R arrhythmia types

In order to extract features from the ECG waveforms the WFDB library was extensively used initially to achieve the following functions:

- To select the database records and to open and read signal files
- To set the input sampling frequency and the input/output read/write modes
- To read annotations of the signals for further analysis.
- To carry out time and frequency conversions and to carry out calibration of signals.

The problems related to HRV analysis were that there was significant attenuation in high-frequency ECG signals as in the case of tachycardia and abnormal beat rhythms. As an alternative, frequency domain spectrum analysis using *Lomb* periodogram was performed, and the spectral density was used as a feature (Silva and G. B. Moody 2014). The Heart rate variability (HRV) (Achten and Jeukendrup 2003) has been widely applied in basic and clinical research studies, however, due to the side-effects of effects of age, gender, drugs, health-status measures among others, it is prone to erroneous calculations, especially for real-time arrhythmia detection. Furthermore, outliers due to ectopy and motion artefacts can have major effects on computed HRV values. As an alternative to HRV analysis, frequency domain analysis of signals, especially containing the abnormal heartbeats, was conducted separately for each arrhythmia type used in this research as a precursor to more fatal arrhythmia. Features were extracted for each abnormal heartbeat that indicated an arrhythmia type. As the annotation symbols represented each of the arrhythmia types in the MITDB records, the feature vectors were extracted for these four annotation type symbols: V (Premature Ventricular Contraction: PVC), A (Atrial Premature Beat: APB), L (Left bundle branch block beat: LBBB) and R (Right bundle branch block beat: RBBB) (Ary L Goldberger et al. 2000; G. B. Moody and Mark 2001). In addition to these abnormal annotation type symbols, the MITDB database records are annotated with N annotation type at locations where normal heartbeats were found. The V-type and the A-type annotations do occur in ECG recordings of healthy human subjects as well and can go unnoticed without showing any symptoms (Katritsis, Siontis, and A. J. Camm 2013; Russo 2015). It may take as many as three consecutive PVCs before a ventricular tachycardia is detected or confirmed (Lerma and Glass 2016; Russo 2015) and frequent APBs may lead to atrial fibrillation over a period of time (E. Burns 2018; Di Marco et al. 2014; German et al. 2016). Similarly, LBBB and RBBB may lead to 1st or 2nd-degree heart block. Similar argument could be made for A-type annotation which refers to Premature Atrial Complexes (PAC) and though it can go undetected without showing any symptoms, it may lead to atrial fibrillation.

For all the records, the feature vectors that attributed to abnormal heart rhythm were identified. The important features were: Age, Gender, the ECG signal amplitude for each sample (millivolts), RR-Interval (inter-beat interval in milliseconds) in ECG recording. These features were used for classifying four annotation types V,A,L,R (G. B. Moody and Mark 2001). Initially, the classification tasks only focused on classifying abnormal annotation types V,A,L,R into their respective class labels (Walinjkar and Woods 2017a). For each record in MITDB there are files with the following extensions: `dat, atr, hea, qrs`. E.g. for record number 100, MITDB provides files such as 100.dat containing digitised samples, 100.atr file containing locations of annotations, 100.hea file containing information about the record file (ECG leads used, sampling frequency, age, gender, and medications). Initially, the 'RDSAMP' (READ SAMPLES) utility was used to convert the samples to WFDB compatible format in MATLAB (Silva and G. B. Moody 2014). This utility could read all the samples within a record with the default sampling frequency of 360 Hz. Approximately 650,000 samples per record were read as sample values in millivolts against sample timestamps expressed as sample numbers where sampling interval between two consecutive samples was 0.00277 seconds (1/360 Hz). *RDSAMP* returned sample numbers (tmSamples) and signal value (sigmV) in mV.

```
[tmSamples,sigmV]=rdsamp(recordNumber)
```

Normal beats were removed from the samples and only the abnormal beat annotations were read by the `'RDANN'` (READ ANNOTATIONS) utility in WFDB library. The default annotation file with 'atr' extension corresponding to the MITDB record was used to locate the annotations. This annotation file contained information about the annotation locations within the waveform. The function returned annotation locations as sample numbers for annotation types V,A,L,R and sub-types. The annotation types are an indicator of abnormal events within an ECG waveform. The annotation sub-types point to locations that provide more information about the waveform at a particular instance in time. e.g. the symbols '(' and ')' indicate the start and stop locations of P-wave, QRS wave or the T-wave. For values of `ann = {V| A | L | R}`, all the annotations and their locations in the waveform for these abnormal arrhythmia types could be obtained.

```
[annotationtype,annotationsubtype]=rdann(recordNumber,'atr', ann)
```

For each annotation-type with value N, which corresponded to the QRS peak locations, the `ANN2RR` (ANNOTATION to RR Interval) utility was used to extract the duration between two consecutive R peaks within an ECG waveform. The function took 'atr' file as the annotator and returned the RR-interval at a particular sample number location corresponding to annotation-type N. The RR-intervals by were obtained in terms of number of samples (rrIntervalInSamples) which were multiplied by 0.00277 seconds to obtain RR-Intervals in milliseconds (rrTmSampleNumber).

```
[rrIntervalInSamples,rrTmSampleNumber]=ann2rr(recordNumber,'atr')
```

The normal annotation type expressed as 'N' was not considered for analysis as it contributed to dataset imbalance and noise as the number of normal waveforms exceeded any of the abnormal annotation types by a very large quantity. The abnormal ECG waveforms corresponding to annotation types V,A,L,R have their own properties (e.g. Regularity, P-waves present/absent, QRS interval Heart-rate) that could be used to identify these abnormalities as shown in table 4.1. These properties corresponding to the annotation types are shown in a tabular form. It could have been possible to separate the normal beats from abnormal beats based on the normal range of values of these properties alone. As these properties of the abnormal annotation types, especially V, A, N annotation types, had subtle variations, additional properties had to be measured and extracted using spectral analysis methods. E.g. The A-type and the N-type waves are similar in morphology though the T-wave and the P-wave in two consecutive heartbeats overlap and there is no fixed time duration to identify and ascertain this duration, so instead of time domain analysis frequency domain analysis was required. For classifying heartbeats into abnormal types only, the N-type annotations were not considered. In all 24,190 samples were extracted for the annotation types V,A,L,R . (Walinjkar and Woods 2017a; Walinjkar and Woods 2017b)

V,A,L,R sample quantities : The following quantities of V,A,L,R annotations were found in the entire MITDB dataset when `RDANN` was executed on all the records in the MITDB dataset:

- Premature Ventricular Contractions (PVC): 9130
- Premature Atrial Contractions (PAC): 1546
- Left Branch Bundle Block (LBBB): 7075
- Right Branch Bundle Block (RBBB): 6259

In clinical practice, heart-rate is measured in beats per minute (bpm) and is mostly computed by extrapolation. In HRV analysis, however, heart-rate is modelled as as a quasi-continuous signal, and the RR-interval series is used to obtain samples of that signal at frequent intervals the reciprocal of each interval in minutes is used to calculate the instantaneous heart-rate. To determine whether the extracted features adequately represented the classification labels, it was essential to determine whether they independently contributed to the classification. The heart-rate and the RR-interval were negatively correlated (Pearson - parametric) to each other ($r = -0.359$, $p < 0.001$), figure, 4.2, with a low degree of regression $F(2, 24187) = 1125.58$, $p < .001$ $R^2 = 8.5\%$. The RR-intervals and heart-rate followed a normal distribution in the dataset, so either of these two could be chosen as one of the primary features. As heart-rate depended on RR-interval, the RR-interval was chosen as one of the primary features.

4.2.2 Data analysis for classification of V,A,L,R arrhythmia types

In this subsection classification models that could accurately classify the samples as V,A,L,R annotation types has been presented. The objective of the machine learning based data analysis was to train a machine learning model on datasets comprising of V,A,L,R annotation types, such that, when a fresh set

ECG waveform clinical properties					
Annotation types	Normal sinus rhythm	Premature ventricular complex	Premature atrial contractions	Left bundle branch block	Right bundle branch block
Annotation symbols as represented in MITDB database	N	V	A	L	R
Regularity	Regular	Irregular	Irregular	Irregular	Irregular
P-waves	Present	Absent	Present though premature and may distort previous T-wave	Present	Present
PR interval	0.12 to 0.20 seconds	Zero seconds	0.12 to 0.20 seconds	0.12 to 0.20 seconds	0.12 to 0.20 seconds
QRS interval	Less than 0.12 seconds	Greater than 0.12 seconds wide and bizarre	Less than 0.12 seconds	Greater than 0.12 seconds though inverted QRS complex.	Greater than 0.12 seconds though biphasic with inverted T-wave
Heart-rate	60 to 100 bpm	60 to 100 bpm though depends on the underlying sinus rhythm	60 to 100 bpm frequently higher though depends on the underlying sinus rhythm	60 to 100 bpm though depends on the underlying sinus rhythm	60 to 100 bpm though depends on the underlying sinus rhythm

Table 4.1: ECG waveform clinical properties with their normal value range

Correlation RR-Interval, HeartRate			
		HeartRate	RR-Interval
HeartRate	Pearson Correlation	1	-.359**
	Sig. (2-tailed)		.000
	N	24190	24190
RR-Interval	Pearson Correlation	-.359**	1
	Sig. (2-tailed)	.000	
	N	24190	24190
**. Correlation is significant at the 0.01 level (2-tailed).			

Regression Summary - RR-Interval, HeartRate								
R	R Square	Adjusted R Square	Std. Error of the Estimate	Change Statistics				
				R Square Change	F Change	df1	df2	Sig. F Change
.292[a]	.085	.085	1.143	.085	1125.587	2	24187	.000
a. Predictors: (Constant), RR-Interval, HeartRate								
b. Dependent Variable: AnnotationType								

ANOVA[a]						
Model		Sum of Squares	df	Mean Square	F	Sig.
1	Regression	2942.851	2	1471.425	1125.587	.000[b]
	Residual	31618.500	24187	1.307		
	Total	34561.351	24189			
a. Dependent Variable: AnnotationType						
b. Predictors: (Constant), RR-Interval, HeartRate, F(2, 24187) = 1125.58, p < .001, $R^2 = 8.5\%$						

Table 4.2: Correlation and Regression scores between RR-Interval and HeartRate

of test ECG samples were input to an algorithm, it could detect the abnormal annotation types. The problem was essentially a supervised learning task as the response variable, *AnnotationType*, was a categorical variable with class labels V,A,L,R and the samples had to be classified into one of these class labels (Walinjkar and Woods 2017a). A multi-class supervised learning classification model was used with the feature set: {*age, gender, RR-Interval, signalValue*} with distribution shown in table 4.3.

The samples distribution of extracted features in 24,190 samples for abnormal V,A,L,R annotation types in MITDB records				
Age Int16	Gender Categorical	RR-Interval Double	SignalValue Double	AnnotationType Categorical
Min 23 Median 64 Max 89	0 Male 1 Female	Min 90 Median 288 Max 2114	Min -3.955 Median 1.03 Max 3.635	1 6638 2 2443 3 7091 4 8018

Table 4.3: Samples distribution descriptive statistics for V,A,L,R type annotations

4.2.2.1 Supervised-learning classification models for V,A,L,R annotations

For initial exploratory analysis using supervised learning classification models, only the abnormal annotation types V,A,L,R were considered. The normal beats annotation represented by the annotation type symbol N was not considered as the proportion of abnormal V,A,L,R type annotations to the normal N type annotations in the MITDB records in total, was in the order of: 24,190 / (650,000 x 48) which is approximately 81 abnormal beats per 100,000 beats. The feature extraction algorithm could identify 24,190 samples in the entire MITDB dataset that had V,A,L,R annotation types. The disproportionate samples quantity presented a problem of dataset imbalance which was solved using Scikit-Learn imbalance reduction method presented in later subsection 4.3.3. For the purpose of classifying samples into V,A,L,R annotation types, only abnormal beat samples were considered and the normal N type annotations were filtered. The most important features were the RR-interval along with *signalValue* and the *AnnotationType* was one-hot-encoded from a categorical variable type into four class labels.

The classification learner application in MATLAB was used to train the samples considering all the four features as predictors and parameters shown in table 4.4. Due to the sparsely scattered nature of the predictors, k-Nearest Neighbours (*k-NN*) classifier was chosen. The parameters used for *k-NN* classifiers to enhance the performance of the classifier provided in table 4.4. A total of 24,190 samples in all of the 48 records in MITDB database were used to train the classifiers to classify a heartbeat sample as belonging to a category (or label) of an abnormal beat type.

The supervised learning classifiers used with corresponding parameter values used in MATLAB classification learner	
Feature vector: Age, Gender, RR-interval, signalValue	
Class labels: V,A,L,R	
Bagged Trees classifier Ensemble method: Bag Learner Type: Decision tree Number of learners: 30 10-fold cross-validation	Weighted k-NN classifier Number of neighbours: 10 Distance metric: Euclidean Weight: Squared inverse Standardised data: true 10-fold cross-validation

Table 4.4: Supervised-learning classifiers for training samples to classify V,A,L,R annotations

4.2.2.2 Results: Supervised-learning classification of V,A,L,R annotations types

The k-NN classifier and bagged tree classifier produced higher percentage of overall accuracy in classifying the test samples in all the four types of arrhythmia as shown in figure 4.1 and 4.2 confusion matrix. As the tree based models tend to have overfitting, especially near the hyper-planes for densely populated samples, 10 fold cross-validation was used in MATLAB Classification Learner which produced 97.8% and 98.5% overall classification accuracy for *k-NN* and *Ensemble Bagged Tree* classifiers, respectively. The dataset did not contain a large number of features, however features like age, gender produced a bias in the classifier towards a certain age group, as the maximum number of patients in the dataset happened to be in a higher age group. As RR-interval was the single most important feature used in the list of predictors, and only 48 records were available within a certain age group, the classification model may have biased towards identifying a record rather than the classification of arrhythmia.

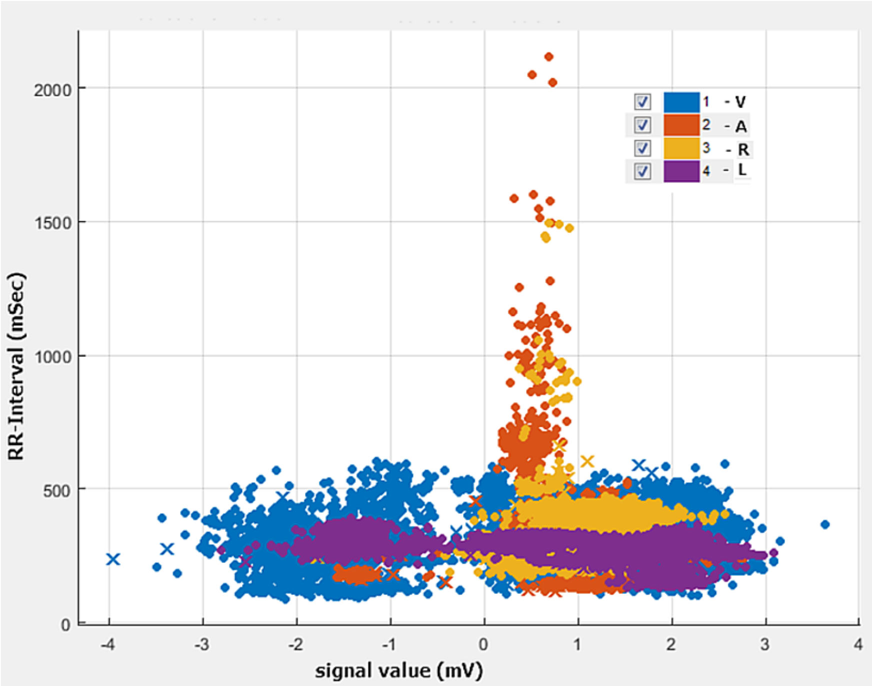

Figure 4.1: k-NN with Number of neighbours: 10; Distance metric: Euclidean; Distance weight: Squared inverse; Accuracy of 97.8% for classifying 4 annotation types of Arrhythmia in MITDB database. Ensemble Bagged Tree classifier produced classification accuracy of 98.5%. The MATLAB classification learner was set to cross-validate at 10-fold cross-validation

4.2.2.3 Methods: Neural-network classification for V,A,L,R annotation types

It was argued that the *k-NN* classifier and the bagged tree based classifiers produced overfitted models, so a neural-network pattern recognition model was also developed. The neural networks are very good at solving pattern recognition problems and are not prone to overfitting as the number of neurons and their weights can be altered in the hidden layer. They are also good at solving problems where complex decision boundary decisions have to be made. The two-layer feed forward neural-network, with one hidden layer, can learn any input-output relationship given enough neurons in the hidden layer. In order to test the dataset and extracted features and to discover patterns in the ECG samples for all the four types of arrhythmia neural-networks pattern recognition models were developed. Similar experiments have been performed in the past where patterns of ECG recordings were analysed in order to extract patterns using artificial neural-network models, and QRS wave

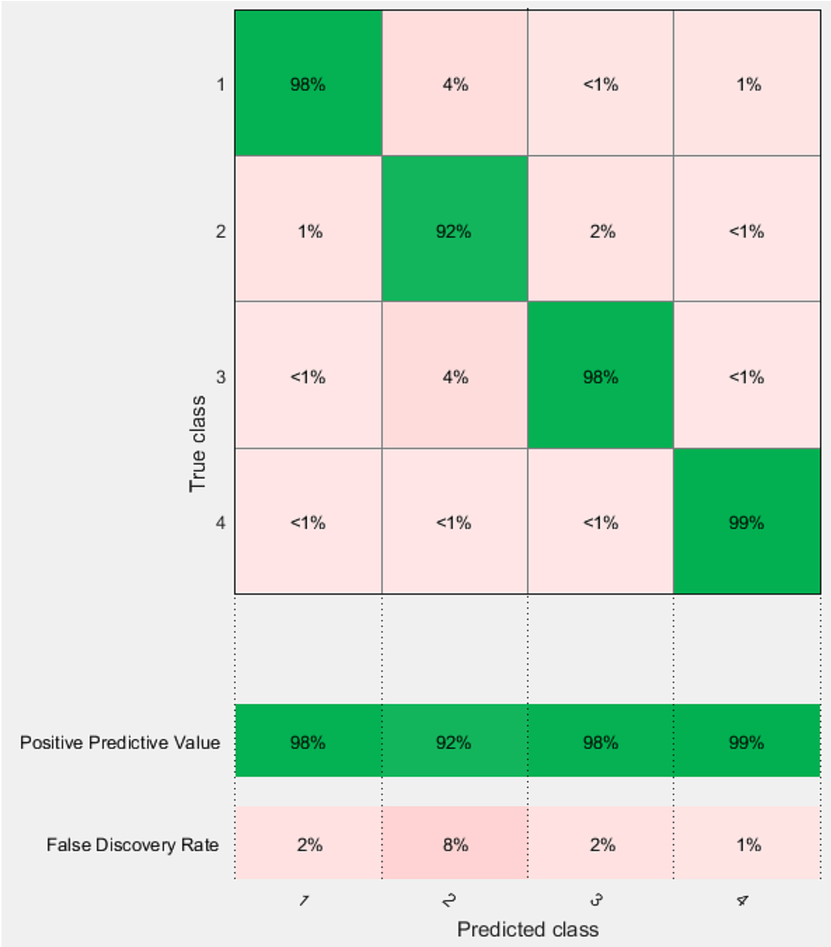

Figure 4.2: Confusion matrix for k-NN classifier model for classifying from a total of 24190 samples across all 47 MITDB records where all the feature vector elements (age, gender, signalValue, RR-Interval,) were used for V=1, A=2, R=3, L=4 class label type of annotations.

characteristics of abnormal beats were compared with normal beats to classify and predict arrhythmia (Adams and Choi 2012; El-Khafif and El-Brawany 2013). Similar techniques exist which use multi-layer feed-forward perceptron models to analyse the waveform for prediction and analysis (Adams and Choi 2012). The MATLAB Neural Net Pattern Recognition model with 25 hidden neurons and Levenberg-Marquardt (back-propagation) training algorithm was used to train the model on the dataset. Different combinations of training-validation-test (70-15-15) %, (60-20-20) % and (60-25-15) % data split percentage were experimented with to generate cross-entropy and classification percentage error. E.g. For (70-15-15)% combination, the input vectors and target vectors were randomly divided into three sets as follows: 70% used for training, 15% used to validate whether the network was generalising and if necessary to stop training before overfitting occurred and 15% used for a completely independent test of network generalisation. The cross-entropy error to evaluate network performance of the neural-network was obtained. The cross entropy error calculated a network performance score given observed and expected outputs, with optional performance weights and other hyper-parameters. The model penalised outputs that were extremely inaccurate, with very little penalty for fairly correct classifications; minimising cross-entropy error and leading to good classifiers. For optimally performing neural-network pattern recognition models, with cross-entropy error of less than 10 and classification errors of less than 2.1% were obtained for several combinations of training-validation-test split as shown in table 4.5. Confusion matrices for the neural-network pattern recognition classification tasks are provided in subsection 4.2.2.4

MATLAB Neural Net Pattern Recognition for V,A,L,R classification with different combinations of Training-Validation-Test data percentages.			
Type of Neural Network	**Number of Hidden Nodes**	**Percentage (%) Training-Validation-Test data**	**Mean-squared error (MSE) and Regression R for test data.**
Neural Net Pattern Recognition	25	70-15-15	Cross-Entropy Error for test data: 7.6 Percent Error: 1.2
	25	60-20-20	Cross-Entropy Error for test data: 9.9 and Percent Error: 2.1
	25	60-15-25	Cross-Entropy Error for test data: 8.7 and Percent Error: 1.7

Table 4.5: Neural-Network Pattern Recognition results for V,A,L,R annotations

4.2.2.4 Results: Neural-network classification for V,A,L,R annotation types

Confusion matrices for neural-network pattern recognition in MATLAB with the three combinations of data split, as described in section 4.2.2.3 are as shown in figure 4.3 and 4.4. Classification accuracy scores of 96.7%, 95.7% and 96.7% were obtained for combinations of training-validation-test (70-15-15) %, (60-20-20) % and (60-25-15) splits respectively.

Figure 4.3: Confusion matrices for MATLAB Neural Net Pattern Recognition yielded 1.3%, 2.5% and 1.7% classification error for training, validation, test data sets in following configuration: (70%,15%,15%), (60%,20%,20%) and (60%,15%,25% split - continued in figure 4.4). Scaled Conjugate Gradient back-propagation algorithm was used as available default in MATLAB pattern recognition tool with the neuron network depth set to 25.

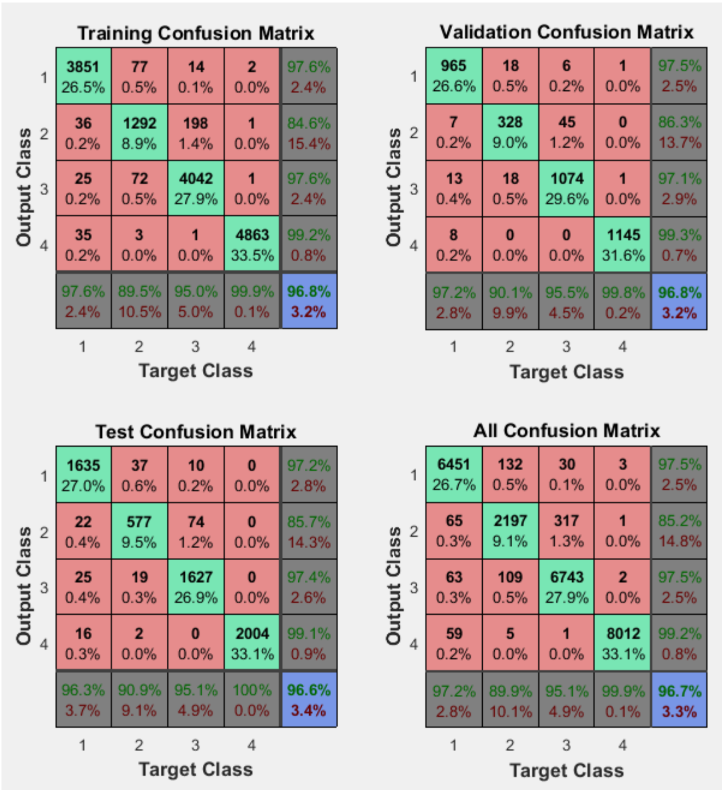

Figure 4.4: Confusion matrices for MATLAB Neural Net Pattern Recognition continued for (60%,15%,25%) split. Scaled Conjugate Gradient back-propagation algorithm was used as available default in MATLAB pattern recognition tool with the neuron network depth set to 25.

4.2.3 V,A,L,R classification problems when N-type annotations considered

Having performed supervised learning based classification using k-NN and neural-network pattern recognition with a higher level of overall accuracy, the effectiveness of using classification models could be ascertained, however these models could not be used in real-time ECG samples classification and cardiac arrhythmia detection and classification as the N-type annotations which represented the normal type samples were not considered in this classification task. In the real time cardiac arrhythmia detection and classification scenario, the ECG samples captured from the human subject would be a mixture of normal and abnormal type of heartbeats. Also, since features such as age and gender were used for classification along with RR-interval, the models could be biased in classifying MITDB records rather than generalising to classify any random V,A,L,R dataset. So a classification model that can generalise and that has been trained on a mixture of all types of normal and abnormal beats was required to perform the classification task in real-time. Also as the research study focused on premature arrhythmia the left and the right branch bundle blocks were not considered for further data analysis tasks.

To briefly examine how a classification model would perform under a mixture of samples of V, A, N annotation types a *GridSearchCV* with *RandomForestClassifier* classification was performed to obtain a classification report with precision, recall, f1-score metrics in Scikit-Learn, shown in table 4.6. The *GridSearchCV* best parameters used were criterion=gini, max_depth=8, max_features=auto, number of estimators=200, class_weight=balanced and 10-fold cross-validation. Although it could be observed that the overall accuracy of 93% was obtained, the classification accuracy of A-type annotation was less than 40%. This was largely due to the imbalance in the dataset where the abnormal samples were only 81 per 100,000 samples. Even amongst the abnormal types i.e. the V-type and the A-type annotations, the V-type annotations samples were more than five times in number.

An alternate feature extraction model was therefore required which could extract more appropriate features that would enable an accurate classification. In

	precision	recall	f1-score	support
A	0.39	0.63	0.48	640
N	0.99	0.93	0.96	7909
V	0.91	0.94	0.93	2963
avg / total	0.93	0.91	0.92	11512

Table 4.6: Less accurate classification due to dataset imbalance when N-type annotation included

order to identify features to enable accurate classification, a more detailed study of the ECG signal was carried out, especially considering the V-type and A-type annotations. The V, A, N type signals had peculiar waveform characteristics. The QRS width and the absence of PR interval in the V type waveforms differentiates it from other waveform types. Similarly, there is an overlap in two consecutive waves in an A-type abnormality. These clinical differences manifest in the ECG waveforms for the respective annotation types and features could be extracted which would enable an accurate differentiation in these annotation types and may enable accurate classification. In the next subsections spectral analysis of ECG waveforms has been illustrated followed by a consolidated feature extraction algorithm that could extract more meaningful and accurate features. Similar experiments have been conducted in the past such: frequency domain analysis and Fourier Transform (Lin 2008) methods to classify abnormal beats based on the morphology, though the method doesn't provide any classifier models with prediction accuracy scores. (Surda et al. 2007) have recognised the fact that due to irregularity in ECG signals, which may contain normal or abnormal beats, the spectral components in a signal can vary, though can be modelled to provide measures to characterise the signal.

4.3 Methods: Spectral Analysis of V, A, N annotation types

If a single normal heartbeat waveform is examined, with a clinical perspective, it consists of the P-wave, the QRS complex and the T-wave and compare the normal sinus rhythm with the abnormal waveforms a noticeable difference could be found. From the clinical literature concerning premature ventricular contractions, i.e. the V-type annotations, the QRS width of this type of abnormality is wider than the other abnormal annotations. The PR interval may or may not be present. So the PR interval and the QRS interval could be considered as important features in classification tasks. The problem however is that these two features depend on the morphology of the waveforms and since there is a lot of additive noise in the ECG waveforms collected from the human subject using a three lead ECG kit, the correctness and the accuracy of PR and QRS intervals could not guarantee an accurate classification.

Alternate measures were required that could be used reliably as features to train the classification model. There are only subtle and minor variations between the abnormal annotation types (V,A,L,R). Hence, if only the clinical properties such as regularity, PR interval, QRS interval and RR interval were considered it would have been difficult to classify between abnormal annotation types or even to differentiate between normal and abnormal annotation types. In order to facilitate this differentiation signal processing approach was chosen and signal properties were extracted. If an ECG signal is closely examined with signal processing perspective, considering the time and frequency properties of the ECG signal, it can be observed that despite being a signal that repeats in pattern, there is an element of randomness, especially with signals with events related to arrhythmia. The signal pattern of P-wave-QRS wave-T-wave may repeat, though in time domain the inter-beat intervals show variations (Surda et al. 2007). These variations exaggerate when abnormal events occur. It was difficult to determine the periodicity of the ECG waveform, especially when V,A,L,R types of abnormalities occurred. An alternate method was therefore adopted to represent features like the PR interval, QRS interval and the power in the signal in frequency domain. Properties such as auto-correlation within the same signal or cross correlation between two signals with same annotation type could have been used, however, the correlation and covariance matrices would only provide coefficients and residual factors explaining the degree to which the signals exhibit randomness. It would have been difficult then to obtain a definitive value to express randomness as a feature value when the abnormal heartbeat occurred. This problem of ineffective representation using correlation and covariance matrices was due to the time domain representation of the signal. In order to circumvent the problem of representation, frequency domain analysis of the abnormal heartbeat was performed. In the frequency domain, the power spectrum of each abnormal heartbeat type was derived, which was followed by the spectral analysis of the abnormal heartbeat, using *periodogram* and *spectrograms* associated with the abnormal heartbeat. It was observed that a unique value could be calculated to express the power spectral density in a signal with abnormal heartbeat. There was a power spectrum associated with each of the four types of arrhythmia, figure 4.5. E.g. the figure 4.5 showing the samples plot along with the power spectrum associated with the V-type annotation (PVC). The power spectrum was generated using MATLAB routine *spectrogram* with a Hamming window (Harris 1987) of one segment and segment length containing total number of samples in the signal. A Lomb-Scargle *periodogram* (Delane et al. 2016) was generated for the V-type annotation normalised by scaling the variance of the sample values by a factor of two with normalised power spread from 10dB to -30dB, produced due to dominant frequencies over the wide QRS complex and absence of P-wave in V-type annotation. The spectrogram showed strong spectral densities (35dB and higher) between samples 40 and 60, due to a wider QRS complex. Also, due to absence of PR interval, less or no spectral densities from samples 10 to 25 were observed.

4.3.1 Power spectrum computations

ECG a power or an energy signal : ECG signal waveforms, either normal or abnormal, are continuous over a given window of observation and possess infinite energy over that window, such signals are called power signals. A window of observation could be tens of seconds as in an ECG strip or a lifetime, during which it is assumed the signal never dies. For power signals, power is expressed only as average power and for such signals Fourier transform may not exist as they may not have a finite integral, so a single measure of power cannot be obtained

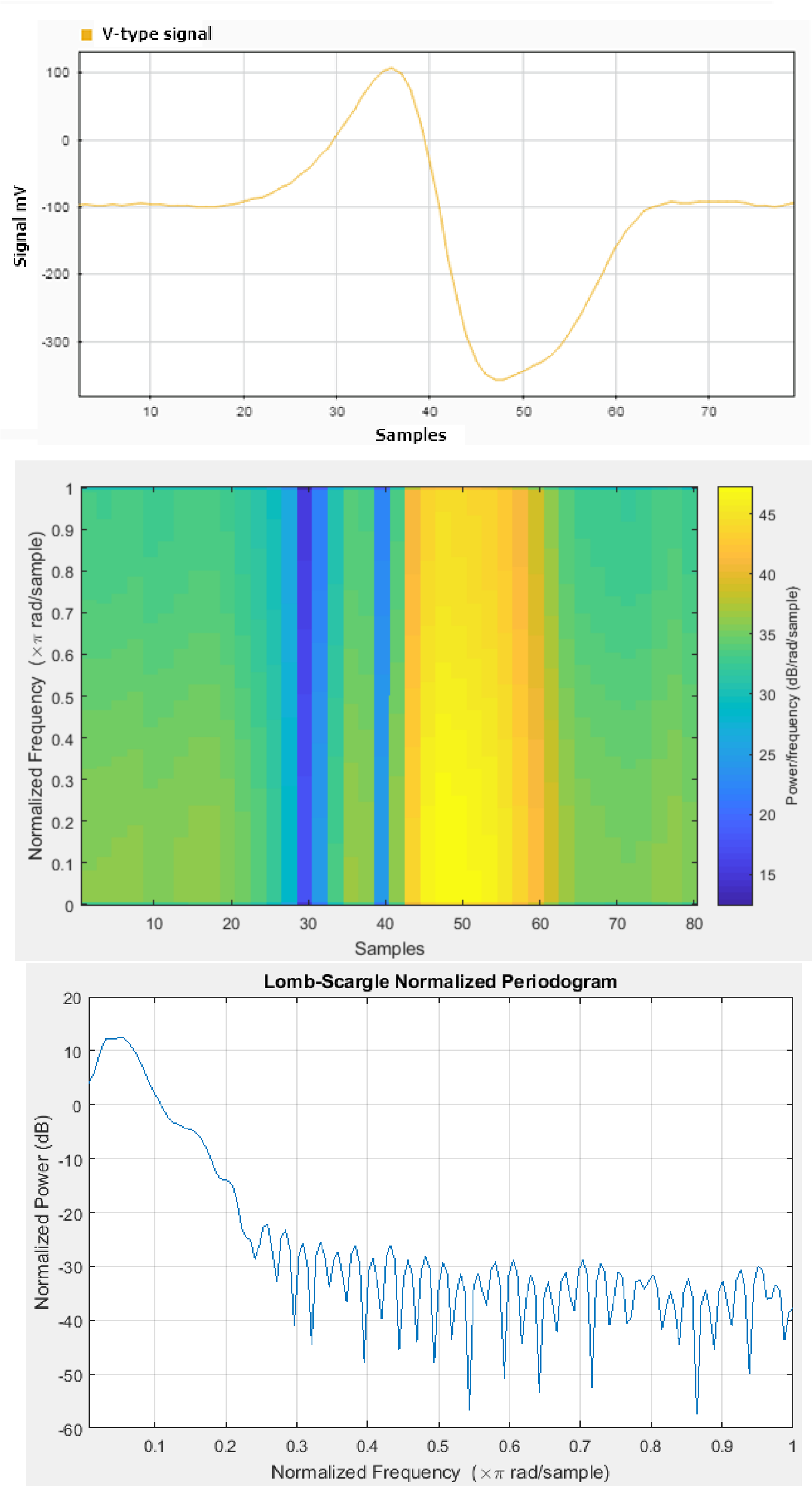

Figure 4.5: Power spectrum content in a single QRS complex in a single V-type heartbeat in an ECG waveform

and spectral densities of the power signal have to be considered instead.

$$Average\ power\ \ (Pa)\,of\ \ signal\ x\,(t):\ \ 0 < Pa < \ \infty$$

$$\begin{aligned} Average\ power\ (continuous,\ time:\ T)\ Pa &= \lim_{T\to\infty}\frac{1}{2T}\int_{-T}^{T}|x\,(t)\,|^{2}dt \\ Average\ power\ \ (discrete,\ length:\ N)\,Pa &= \lim_{N\to\infty}\frac{1}{2N+1}\sum_{n=-N}^{n=N}|x[n]|^{2} \end{aligned} \tag{4.1}$$

Non-stationary nature: The ECG signals regardless of their annotation types are non-stationary signals as their statistical properties vary with time, i.e. statistical measures e.g. mean, variance and deviation of all the samples in a single heartbeat change over time and no two heartbeats have the same values for these statistical measures (Paithane and Bormane 2014).

Auto-correlation: Auto-correlation is a measure of correlation of a signal with its own delayed instance, expressed as function of delay. For non-stationary signals however, the auto-correlation property of the signal could not be calculated as the expected value $E\{X\,(t)\}$ of the signal at a given point in time will not be equal to the original value of the signal $x(t)$ (with Fourier transform $X\,(t)$) displaced by '*k'* intervals.

$$\begin{aligned} For\ an\ ECG\ signal\ x\,(t)\ \ with\ discrete\ equivalent\ x\,[n] \\ E\,\{X\,(t)\}\ \ \neq\ \ \langle x(t+k)\rangle \\ E\,\{X\,(n)\,X(n+k)\}\ \ \neq\ \ \langle x\,(n)\ \ x(n+k)\rangle \end{aligned} \tag{4.2}$$

It then followed that instead of using auto-correlation and average power as features, the power spectral density could adequately represent the annotation types and could be used as a feature. The '*power spectral density is a vector of coefficients* of power spectrum of the signal, so '*bandpower*' was calculated which took PSD coefficients as input and produced a measure of band power in the signal, which was used as a feature value.

Also, in order to emphasise the advantage of using power spectral density as compared to using the QRS intervals in time domain, the bandpower values associated with the power spectrum of some ECG heartbeat samples were calculated. The comparison of PSD estimates against corresponding QRS intervals for V-type and N-type signals is presented in figures 4.6a and 4.6b. It was observed that despite minor or no variations in QRS intervals there were significant variations in corresponding bandpower values equation 4.3.

$$E.g.\ Let\ QRS_N\ and\ QRS_V\ be\ QRS\ intervals\ for\ N-type\ and\ V-type\ signals\ with\ Bandpowers\ BP_N\ and\ BP_V\ respectively.$$

$$\begin{aligned} QRS_N &= \{36,\ 36\} \overset{<corresponds\ to>}{\Longrightarrow} \text{Band Power}\ \ BP_N = \{-0.75983,\ -0.46278\} \\ QRS_V &= \{64,\ 63\} \overset{<corresponds\ to>}{\Longrightarrow} \text{Band Power}\ \ BP_V = \{2.0481,\ -0.36251\} \end{aligned} \tag{4.3}$$

The Welch periodogram (Welch 1967) is a Fast Fourier Transform based computing method used for estimating power spectra in a signal and is carried out by dividing the time-domain signal into successive blocks, forming the *periodogram* for each block, and averaging over these blocks. For calculations used in *pwelch* method to compute power spectral density in an ECG signal:
Divide the available sample sequence of p overlapping sample sequences of D samples each, shifting S samples between consecutive segments. If original sequence is x[k] the pth segment can be expressed as:

$$x_p[n] = x[pS + n] \tag{4.4}$$

Apply the data window w[n] to each segment:

$$Y_p[n] = w[n]x_p[n]p = 0, 1, ..., p - 1 \tag{4.5}$$

The Hamming window, also called a tapering function, is a smoothing function used to rectify discontinuities at the beginning and end of the sampled signal (Harris 1987)The Hamming window function $w(n)$ series considered with N samples:

$$w(n) = 0.54 - 0.46 \cos \frac{2\pi n}{N-1} \tag{4.6}$$

Compute the discrete frequency sample spectrum for each of the p windowed segments.

$$S_p[m] = \frac{T}{UD}|Y_p[m]|^2 \tag{4.7}$$

where,

$$U = \sum_{n=0}^{p-1} |w[n]|^2$$

Compute the arithmetic average of the p different sample spectra at each frequency:

$$S_w[m] = \frac{1}{p}\sum_{p=0}^{p-1} S_p[m], \text{where m} = 0, 1, ..., D-1 \tag{4.8}$$

Root-Mean-Square level of a vector x[n] is:

$$\begin{gathered} X_{RMS} = \sqrt{\frac{1}{N}\sum_{n=1}^{N} |x_n|^2} \\ Bandpower = |X_{RMS}|^2 \end{gathered} \tag{4.9}$$

A generic periodogram could only generate power spectrum of a waveform, though could not generate consistent power estimates for a non-stationary process like an ECG. A modified Welch's technique was used instead to reduce the variance of the periodogram by breaking the time series into segments. No overlaps were considered as it was a single heartbeat under consideration. The Welch's method computed a modified periodogram for a single Hamming window and segment length containing all the samples in the V-type or the N-type heartbeat, to produce the PSD estimates. The *pwelch* function in MATLAB signal processing toolbox returned the power spectral density (PSD) estimate, '*pxx*', of the input signal sample.

$$\begin{aligned} [pxx, fn] &= pwelch(samplesVtype, Hamming(samplesVtype)) \\ bandpower &= 10log_{10}(bandpower(pxx, fn) \end{aligned} \tag{4.10}$$

The reduced time interval between two consecutive RR intervals, due to premature atrial ectopic beat is an indicator of premature atrial contraction. The P-wave, in this case, could be distorted as compared to the normal P-wave in a heartbeat and frequently occurring premature atrial contractions may increase heart rate as the R peaks occur more frequently in a given time-frame. Hence, the factors RR interval, presence or absence of P-wave and its distortion were an important indicator of premature atrial contractions and were used as features at the data analysis stage. The RR interval has been widely used in HRV analysis (Peltola 2012) in bedside monitors and wearable ECG kits, though due to the variability and complex non-linear dynamics of HRV analysis, it has been found difficult to identify patterns corresponding to particular heart arrhythmia. Although HRV analysis has been used to identify presence or absence of heart arrhythmia, it has been difficult to classify the types of heart arrhythmia solely based on HRV analysis.

4.3.2 Methods: A novel feature extraction algorithm using spectral analysis and finite state machines

The ECGPUWAVE utility from WFDB library was extensively used to determine the time intervals for the P-wave, the QRS interval and the T wave. The ECGPUWAVE utility takes a QRS detector annotator file (*'qrs' annotator – GQRS or SQRS annotators from MITDB)* as input which has already annotated an ECG signal with the locations of the QRS peaks. The utility then returns an annotation file with extension *'epu',* containing the locations of the onset and end locations of the P, QRS and T wavelets. The utility uses the sub annotation type symbols to denote these locations, shown in table 4.7. So the P-wave interval would be the interval in the symbols sequence *(p).* Similar sequence could be obtained for the QRS and the T wavelets. According to the sampling frequency for MITDB records: 1 interval = 0.00277 seconds. So the time interval for the P-wave denoted by the symbols sequence *(p)* with *'n'* interval, equals *n * 0.00277 seconds.* Similarly the time interval for QRS and T-wavelets could be obtained.

For calculating the differentiating factor between the N-type and the A-type annotation waveforms, figure 4.7a and 4.7b, instead of considering the PR

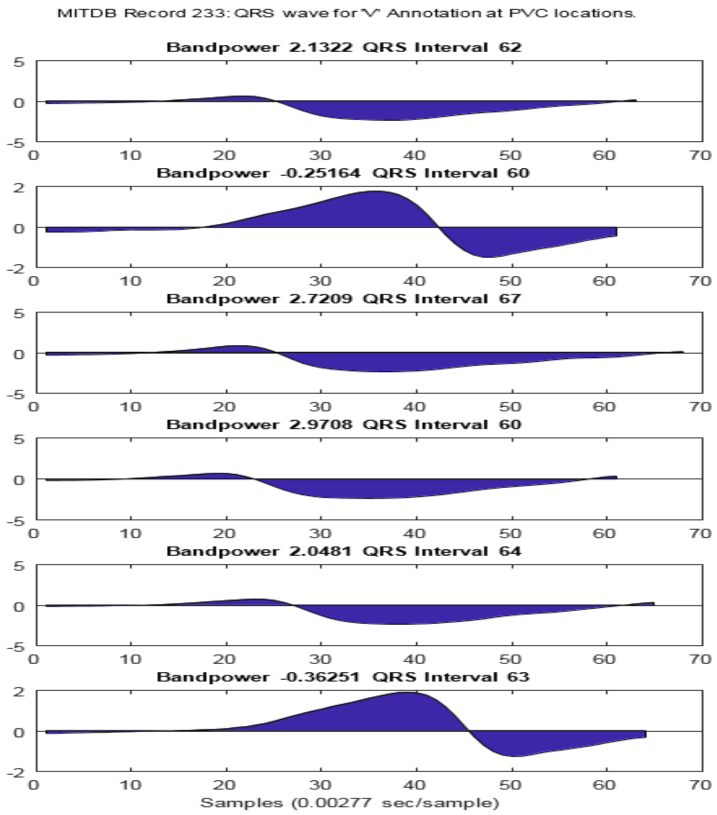

(a) V-type annotation.

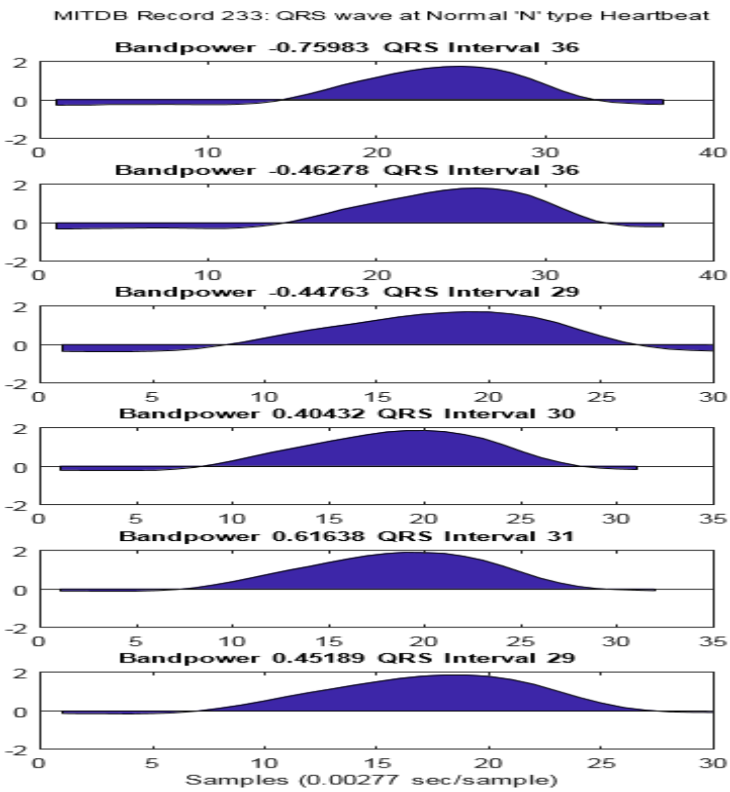

(b) N-type annotation.

Figure 4.6: Power spectral density and bandpower in a QRS wave in normal N type and an abnormal V type annotation in an ECG wave in an MITDB sample record.

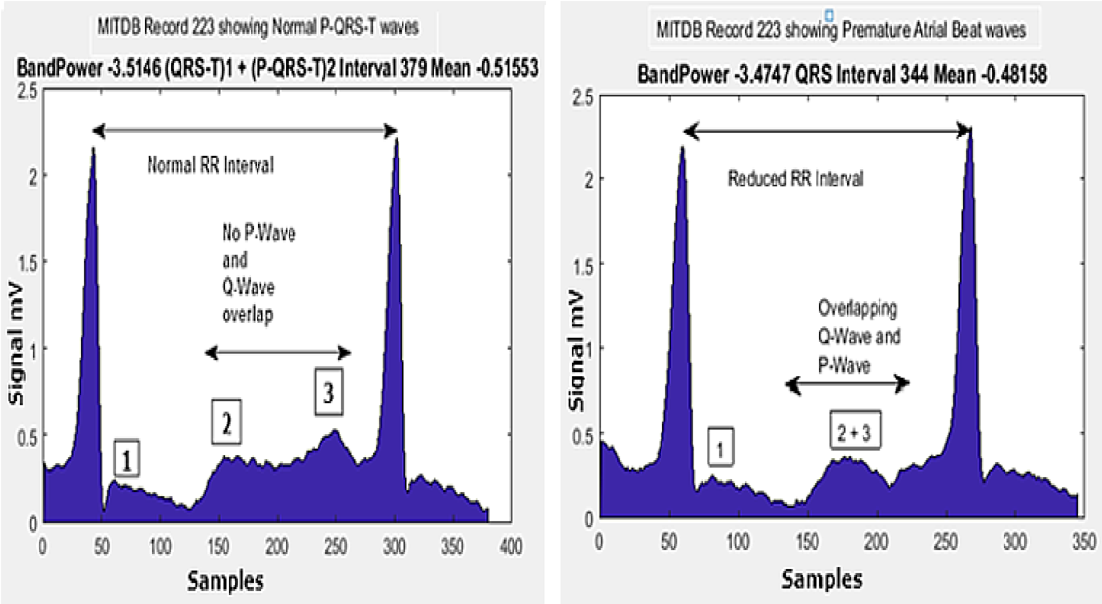

(a) N-type annotation.

(b) A-type annotation.

Figure 4.7: Power spectral density content in an abnormal A-type annotation, with Q-wave and P-wave overlap, as compared to N-type annotation in an MITDB record

interval (*i.e.* the P-wave duration) the T-wave sequence *"(t)"* was added to the P-wave sequence of *"(p)"* resulting into a sequence of the form *"(t) (p)"* or *"(t p)"* or a string consisting of a combination of *(, t, p,)* annotation sub-type symbols showing an overlap between the P-wave and the T-wave. It should be noted that the T-wave from the preceding heartbeat and the P-wave from the following heartbeat were considered to detect the PR interval of the A-type annotation and to ascertain whether there has been an overlap between the P-wave and T-wave of these two consecutive heartbeats. The total time interval for the *"t"* and the *"p"* annotation sub-types provided the required and the extended PR interval for the A-type annotation. Considering the spectral contents of the V, A, N type annotations and the ECGPUWAVE annotations and the locations of the beat and non-beat type annotations a consolidated feature extraction algorithm was proposed as shown in algorithm 4.1.

Each MITDB record has files with extensions: dat (binary signal), atr (annotation locations), hea (record information), qrs (QRS peaks locations)

The algorithm required to pre-process the MITDB records using WFDB library routines to output intermediate file with extension *epu* and also to extract

The non-beat type sub annotations at their respective locations in a P-QRS-T wave in an ECG signal		
P-wave	p	(p)
T wave	t	(t)
QRS wave	N	(N)

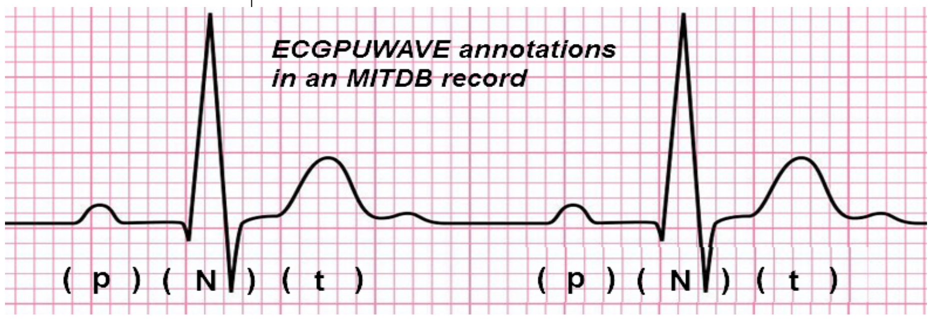

Table 4.7: The non-beat type *ECGPUWAVE* annotations at their respective locations in a P-QRS-T wave in an ECG signal

RR-interval information. The *epu* file contained the start and stop locations of the P-wave, QRS complex and the T-wave.

ECGPUWAVE routine provided by WFDB analysed the ECG signal from the specified record, detecting the QRS complexes and locating the beginning, peak, and end of the P, QRS, and T waveforms. The output of ECGPUWAVE was written as a standard WFDB-format annotation file associated with the specified annotation extension *epu*. The routine took the signal *dat* file and a *qrs* file as input and generated the *epu* file. The QRS detector in the routine was based on the Pan and Tompkins (Pan and Tompkins 1985) algorithm which used the *qrs* annotation file provided by MITDB. The GQRS routine provided by WFDB could have been used as well, however it would have produced the same *qrs* annotator.

E.g. `ECGPUWAVE (recordNumber, epu)` outputs `recordNumber.epu` file containing annotations according to table 4.7 and their locations at various sampling intervals starting from zero.

RDSAMP routine provided by WFDB read the MITDB record signal file (*.dat extension*) for the specified record and generated the samples as decimal numbers on the standard output. The *RDSAMP* routine starts at the beginning of the record and prints all samples containing the sample number (tm) and sample values (signal) beginning with channel zero. In this experiment only the MLII

(Modified Limb II) channel was chosen corresponding to channel zero.

E.g. `[signal, tm] = RDSAMP(recordNumber)` returns sample values and sample number starting from zero.

*RDANN*routine provided by WFDB read the annotation file (e.g. *epu, qrs, atr* files) specified by record or the routine call statement, and generated a plain text translation to the standard output, one annotation per line. The output contained (from left to right) the time of the annotation in sample number corresponding to the timestamp of the annotation; a mnemonic for the annotation type (V, A, N) and the auxiliary information string, if any. E.g. `[atrannsamplenums, atranntype] = RDANN (recordNumber,'atr')` returns the sample number *atrannsamplenums* at the *atranntype annotation* type (V, A, N) locations. The annotations in *atr* file could be all possible annotations found in the MITDB records e.g. V, A, L, R, N, AFib etc., though the annotations in *epu* file could locate: '(', ')', 'p', 'N', 't' annotations as shown in table 4.7. For the purpose of the experiment the V, A, N locations in *atr* file coincided with the N location in the *epu* file; this was due to *ECGPUWAVE* which annotated the V, A, N locations with N annotation corresponding to the QRS peak, regardless of normal (N) beat or PVC (V) or PAC (A) type beats.

ANN2RR routine provided by WFDB extracted a list of RR-intervals, in plain text format, from the specified annotation file (e.g. *atr, qrs* files). The intervals were listed in units of sample intervals (sample interval of 0.00277 sec = 360 Hz sampling frequency)

4.3.2.1 The Finite State Machines (FSM) for V, A, N annotations

The FSMs for V, A, N annotation types are shown in figure 4.8. Each FSM shows the input annotation string that is acceptable by corresponding state machine and is based on the symbols listed in table 4.7. Every FSM is made up of a tuple

$$F = \{\Sigma, Q, q_0, F, \Delta\}$$

where Σ is a set of symbols of an input string, Q is a set of states that the machine would transition on receiving an input symbol, q_0 S is the initial start state S of the machine, F is the set of final states that the machine might end-up when the input string is entirely processed and Δ is the transition function between the Q states on processing the input symbols Σ. The FSMs for the V-type and the A-type annotations are variants of the N-type state machine. The V-type state machine does not have the *'p'* state as there is no P-wave in the V-type arrhythmia and the state R in N-type state machine is replaced by *R'* in the V-type state machine to denote a wide QRS complex, an abnormal QRS sub-wave. The A-type state machine looks similar to the N-type state machine, though due to the overlap of the *'p'* and the *'t'* sub-waves in consecutive heartbeats, additional transitions, especially the premature *'p'* input symbol appear in the transition shown from the T state to the A state of the FSM. The state machines were implemented within the feature extraction algorithm presented in the next subsection 4.3.2.2. The P, R, T states correspond to the P-wave, QRS wave and T-wave. The S state is the initial state which accepts the input string from Σ set of input strings. The V, A, N states correspond to the final states when the FSMs accept the input annotation strings to represent the arrhythmia types. The FSM models are presented in expressions 4.11, 4.12 and 4.13.

N-type FSM model:

$$\begin{aligned} &\text{Input symbols} \\ &\Sigma = \{(,), p, n, t\} \\ \text{Start state S, Transition states P, R, T and Final state N}& \\ &Q = \{S, P, R, T, N\} \\ \text{Initial state S}& \\ &q_o = \{S\} \\ \text{Final state N - Normal beat}& \\ &F = \{N\} \\ \text{Transition function between Q and } \Sigma \text{ to Q states}& \\ &\Delta = Q * \Sigma \rightarrow Q \end{aligned} \tag{4.11}$$

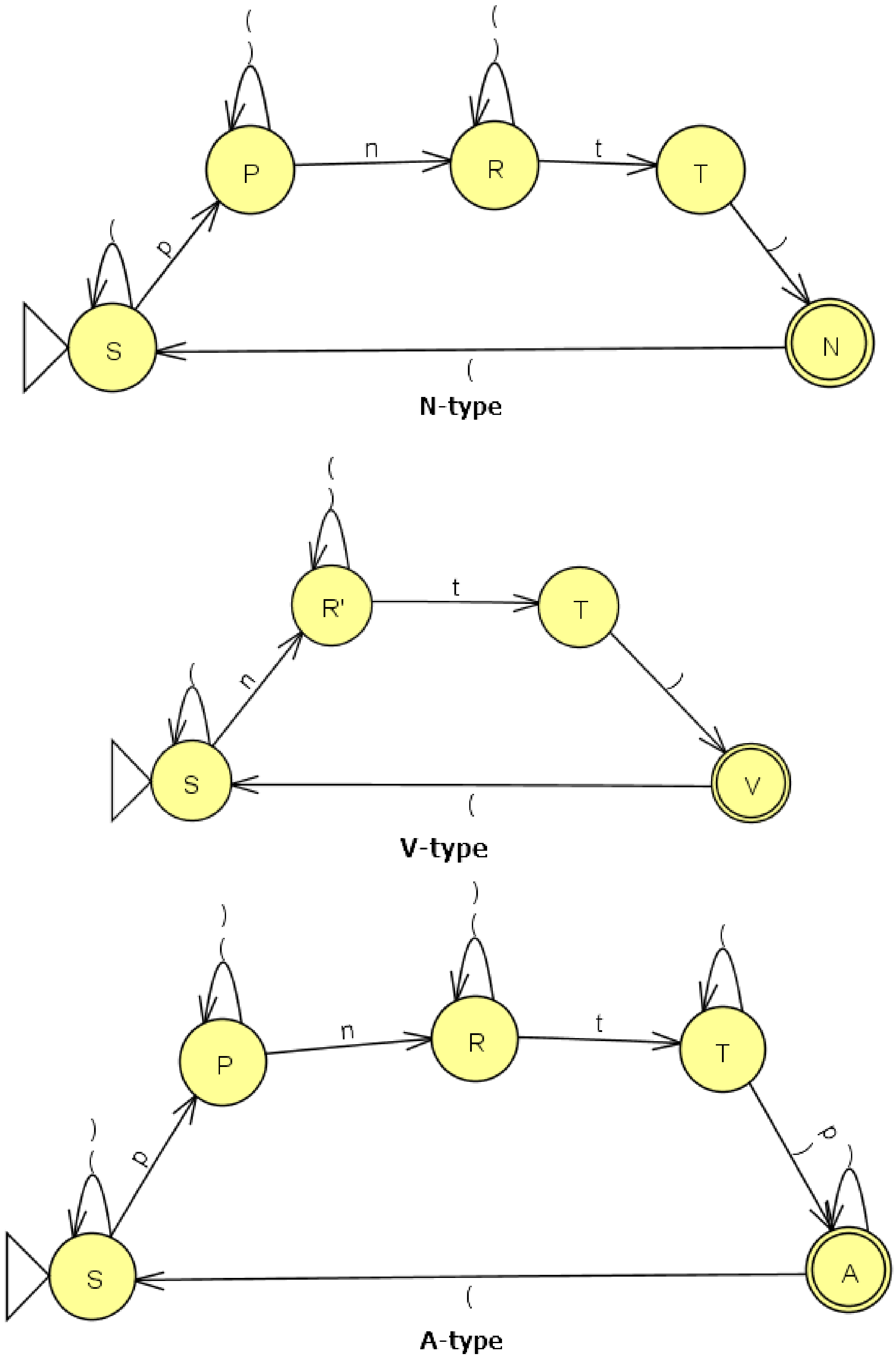

Figure 4.8: Finite State Machines for V, A, N annotation types

V-type FSM model:

$$
\begin{aligned}
&\text{Input symbols}\\
&\Sigma = \{(,), n, t\}\\
&\text{Start state S, Transition states R', T (no P state present)}\\
&\text{and Final state V}\\
&Q = \{S, R', T, V\}\\
&\text{Initial state S}\\
&q_o = \{S\}\\
&\text{Final state V - V-type arrhythmia}\\
&F = \{V\}\\
&\text{Transition function between Q and } \Sigma \text{ to Q states}\\
&\Delta = Q * \Sigma \to Q
\end{aligned}
\tag{4.12}
$$

A-type FSM model:

$$
\begin{aligned}
&\text{Input symbols}\\
&\Sigma = \{(,), p, n, t\}\\
&\text{Start state S, Transition states P, R, T}\\
&\text{and Final state A}\\
&Q = \{S, P, R, T, A\}\\
&\text{Initial state S}\\
&q_o = \{S\}\\
&\text{Final state A, A-type arrhythmia}\\
&F = \{A\}\\
&\text{Transition function between Q and } \Sigma \text{ to Q states}\\
&\Delta = Q * \Sigma \to Q
\end{aligned}
\tag{4.13}
$$

4.3.2.2 Consolidated feature extraction algorithm for V,A,N annotations

A consolidated feature extraction algorithm is presented in this subsection based on the theory presented in the this subsection 4.3.2 and paragraph 4.3.2.1 considering the annotation sub-type sequence symbols `‘(‘`, `‘)’`, `‘p’`, `‘N’`, `‘t’`. The algorithm is a finite state machine implemented as a sub-routine that calls actions based on the input sequence symbol when an ECG signal with annotated sub-types is parsed by the algorithm. The state machines represented by 4.12, 4.12 and 4.11 were implemented in the algorithm. The feature vector generated from the feature extraction algorithm was as follows:
{*PR_Interval, PR_PSD, QRS_Interval, QRS_PSD, RR_Interval, PowerSpectralDensity, SignalToNoiseRatio*}
The classification target variable with possible values (V, A, N) was: {*AnnotationType*}

Algorithm 4.1 Algorithm for extracting features from MITDB records for arrhythmia classification

---

function WELCHSPECTRUM(`x[n]`)
  $W[n]$ = `Array[n]`, $Y[n]$ = `Array[n]`
  $S[n]$ = `Array[n]`, $S_w[n]$ = `Array[n]`
  N = length(`x[n]`)
  $W[n]$= 0.54 + 0.46.cos(2πn/(N-1)) ▷ /*Hamming window length N*/
  $Y[n] = W[n]$ `x[n]`
  U = $\sum W[n]^2$
▷ /* D = Number of Overlapping samples*/
  D = 1
▷ /* P = Three segments: P-wave, QRS and T-wave one sample apart*/
  P = 3
▷ /* 1/T : 1/360 Hz sampling frequency */
  T= 0.00277
  m = N - D
  $S[m]$ = T/UD ($\sum Y[m]^2$)
  $S_w[m]$ = 1/P ($\sum S[m]$)
  return $S_w[m]$
end function

function BANDPOWER($S_w[n]$)
  N = length($S_w[n]$)
  $bandpower$ = 1/N ($\sum S_w[n]^2$)
  $bandPowerdB$ = 10.$\log_{10}$ ($bandpower$)
  return $bandPowerdB$
end function

function SIGNALNOISERATIO($S_w[n]$)
  N = length($S_w[n]$)
  snr = 10.$\log_{10}$ ($S_w[n]^2$)
  return snr
end function

procedure EXTRACTFEATURESMITDB
  $mitdbrecordsVAN$ = record[1:47]
  for $recordNumber$ = 1: length($mitdbrecordsVAN$) **do**
▷ /*generates epu annotations file for each record containing : (, p, N, t and) annotations*/
    `ECGPUWAVE (recordNumber, 'epu')`
  end for

Algorithm 4.1 Algorithm for extracting features from MITDB records for arrhythmia classification (continued)

```
    for recordNumber = 1: length(mitdbrecordsVAN) do
        [signal, tm]=RDSAMP(recordNumber)    ▷ /*tm = sample number*/
        ML2signal = signal[:,1]
        totalsamples = length(tm);   ▷ /*atranntype takes values (V, A, N)*/
        [atrannsamplenums, atranntype] = RDANN(recordNumber,'atr');
  ▷ /*epuAnnotType takes values: (, p, N, t, ) with corresponding sample number
  epuAnnotSampNumbers at the annotation location*/
        [epuAnnotSampNumbers, epuAnnotType] =
                        RDANN (recordNumber, 'epu')
  ▷ /*rrIntervals at corresponding sample locations annotated in atr file*/
        [rrIntervals, rrSampleNumbers] = ANN2RR($recordNumber$,'atr')

        [rrIntervalAndSampleNumbers] = [rrIntervals rrSampleNumbers]
  ▷ /*features initialised*/
        featureAnnotationType = 'N'; featurePRinterval = 0;
        featureQRSinterval = 0;
        featureRRinterval = 0;
        featurePowerSpectralDensity = 0;
        featureSNR = 0; featurePRpsd =0; featureQRSpsd =0;
                                  ▷ /*Iterate all epu annotations: (,), p, N, t */
        for iEPUannot = 0 : length(epuAnnotSampNumbers) - 1 do
            if epuAnnotType(iEPUannot) == 'N') then
  ▷ /*sample number at N-type annotation enter R-state of the state machine */
                epusampnum = epuAnnotSampNumbers(iEPUannot);
  ▷ /*iterate all atr annotations (V, A, N)*/
                for iATRann = 1 : length(atrannsamplenums) - 1 do
  ▷ /*check if atr annotations and epu annotations coincide*/
                    if (atrannsamplenums(iATRann) >=
                     epuAnnotSampNumbers(iEPUannot - 1))
                     &&
                     (atrannsamplenums(iATRann) <=
                     epuAnnotSampNumbers(iEPUannot + 1)) then
  ▷ /*Assign the featureAnnotationType values V or A or N */
                        featureAnnotationType = atranntype(iATRann);
                        break For loop;
                    end if
                end for
  ▷ /*calculate featurePRinterval and featureQRSinterval*/
                k = iEPUannot - 1;
  ▷ /*iterate epu annotations to locate start/end of P-wave, QRS wave and
  T-wave for input string (p)(N)(p) to the Finite State Machine (FSM)*/
                while epuAnnotType(k) != 'N' do
  ▷ /*check if P-wave precedes QRS peak - enter P-state of the FSM*/
                    if epuAnnotType(k) == 'p' then
  ▷ /* Locate the PR segment on either side of the P-wave peak*/
```

Algorithm 4.1 Algorithm for extracting features from MITDB records for arrhythmia classification (continued)

```
                prsamplefrom = epuAnnotSampNumbers(k - 1);
                prsampleto = epuAnnotSampNumbers(k + 1);
                featurePRinterval = prsampleto - prsamplefrom;   ▷ /*featurePRinterval*/
                X_p[n] = prsamplefrom:prsampleto
                [psd1] = Cal WelchSpectrum(X_s[n]);
                featurePRpsd = Call BandPower(psd1);
 ▷ /* locate QRS interval segment on either side of QRS peak - enter R-state of the finite state machine*/
                qrssamplefrom = epuAnnotSampNumbers(iEPUannot - 1);
                qrssampleto = epuAnnotSampNumbers(iEPUannot + 2);
 ▷ /* featureQRSinterval*/
                featureQRSinterval = qrssampleto - qrssamplefrom;
                X_q[n] = qrssamplefrom:qrssampleto
                [psd2] = Call WelchSpectrum (X_q[n] );
                featureQRSpsd = Call BandPower(psd2));
                break While loop;
 ▷ /* check if P-wave absent in which case T-wave from previous beat precedes QRS peak - enter R-state and then the T-state */

            else if epuAnnotType(k) == 't' then
 ▷ /* featurePRinterval set to zero if P-wave absent*/
                featurePRinterval = 0;
                featurePRpsd = 0;
 ▷ /*QRS interval when P-wave absent, has wide QRS complex */
                qrssamplefrom = epuAnnotSampNumbers(iEPUannot - 1);
                qrssampleto = epuAnnotSampNumbers(iEPUannot + 2);
                featureQRSinterval = qrssampleto - qrssamplefrom;
                X_q[n] = qrssamplefrom:qrssampleto;
                [psd3] = Call WelchSpectrum (X_q[n]);
                featureQRSpsd = Call BandPower(psd3));
                break While loop;
            end if
            k = k - 1;
            if k == 0 then
                break While loop;
            end if
        end while
```

Algorithm 4.1 Algorithm for extracting features from MITDB records for arrhythmia classification (continued)

```
90:             for iRRann = 0 : length(rrSampleNumber) - 1 do        ▷ /* calculate featureRRinterval*/
                ▷ /*check if RR-interval sample numbers coincide with epu sample numbers*/
91:                 if (rrSampleNumber(iRRann) >=
92:                   epuAnnotSampNumbers(iEPUannot - 1))
93:                   &&
94:                   (rrSampleNumber(iRRann) <=
95:                   epuAnnotSampNumbers(iEPUannot + 1)) then
96:                     featureRRinterval = rrIintervals(iRRann); Refer line 38
97:                     break For loop
98:                 end if
99:             end for                       ▷ /* for iRRann iteration ends*/
                ▷ calculate Signal-Noise-Ratio and Power Spectral Density
100:            samplespsdsnrfrom = epuAnnotSampNumbers(iEPUannot - 4);
101:            samplespsdsnrto = epuAnnotSampNumbers(iEPUannot + 4);
102:            X_snr[n] = samplespsdsnrfrom: samplespsdsnrto
103:            [psd4] = Call WelchSpectrum (X_snr[n]);
104:            featurePowerSpectralDensity = Call BandPower(psd4));

105:            S_snr[n] = samplespsdsnrfrom:samplespsdsnrto
106:            featureSNR = Call SignalNoiseRatio(S_snr[n]) ;
107:        end if                        ▷ /*end if iEPUannot == 'N' */
108:        featureAnnotationType = atranntype(iEPUannot);
109:        if featureAnnotationType not in ('V','A','N') then
110:            iEPUannot ++ ;                ▷ /*next iteration */
111:        end if
112:        newSampleRow = [featureAnnotationType,
113:            featurePRinterval, featurePRpsd,
114:            featureQRSinterval,
115:            featureQRSpsd, featureRRinterval,
116:            featurePowerSpectralDensity, featureSNR]
117:     end for                      ▷ /*end for all iEPUannot annotations */
118:   end for                        ▷ /* end iterating all MITDB records*/
119: end procedure
```

4.3.3 Methods: Data analysis pipeline for V, A, N classification

The Python Scikit Learn toolkit with Anaconda distribution was used for the following data analysis steps. The Python Pandas data frames were used to import the tables containing the target and predictor variables. The *AnnotationType* variable being the target variable. As there were three classes for target variables, with annotation types V, A, N, one-hot encoding was performed to obtain a binary denotation of the annotation types. Data analysis steps for machine learning based classification were as follows:

The Data analysis pipeline:

- Step 1: Since the scale of the feature values in the feature vectors affected the bias and the variance of the classifier, the feature vectors had to be scaled and normalised accordingly. The Scikit *StandardScaler* could have been used on the data such that its distribution would have a mean value 0 and standard deviation of 1. *StandardScaler* works well when normalisation is required where all the features are scaled within a normalised range of values e.g. {-1, +1} though more than normalisation, since the predictor variables had outliers with RR-intervals in excess of 1.1 sec, PR-intervals in excess of 300 ms and QRS intervals greater than 190 ms, standardisation to remove outliers was required. *RobustScaler* based standardisation was performed so that the outliers would have no effect on the classification tasks by using *quantile_range* between (15, 85) and scaling set to true. The *RobustScaler* removed the outliers and limited the QRS PSD and PR PSD in the following ranges: (-15, 10) and (-15, 15) dB respectively as shown in figure 4.9

- Step 2: Having performed robust scaling, since some features attributed to the least amount of variance only the first 'k' best features were considered for a classification task. *SelectKBest* feature selector was used to identify first six features *(k=6)* that attributed to maximum variance in the feature values, figure 4.10. The selector uses the *f_classif* scoring function which is essentially the Analysis Of Variance (ANOVA) F-value score.

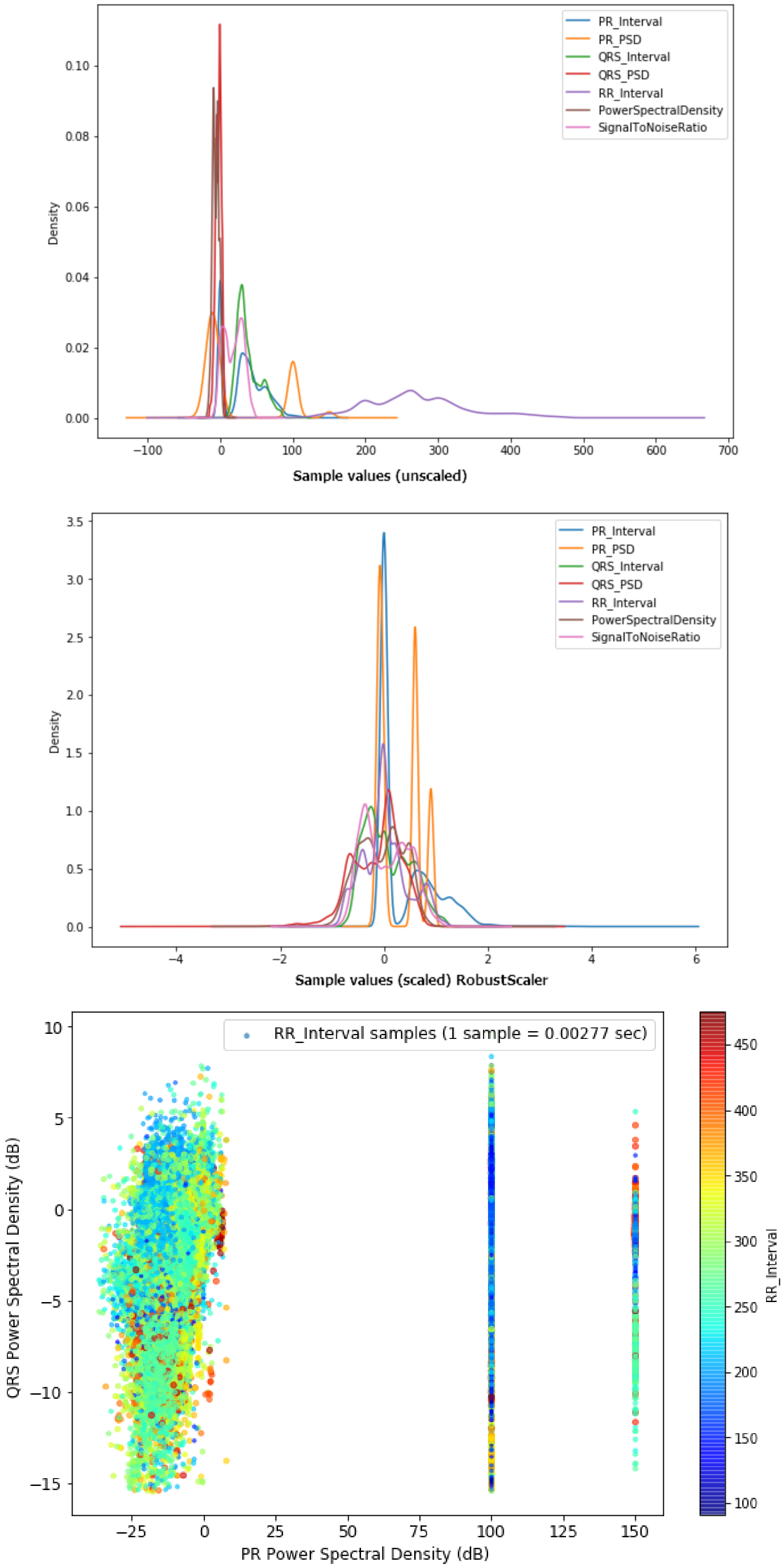

Figure 4.9: Standard and Robust scalers distribution and scatter plot of QRS vs PR intervals power spectral densities over RR-Interval

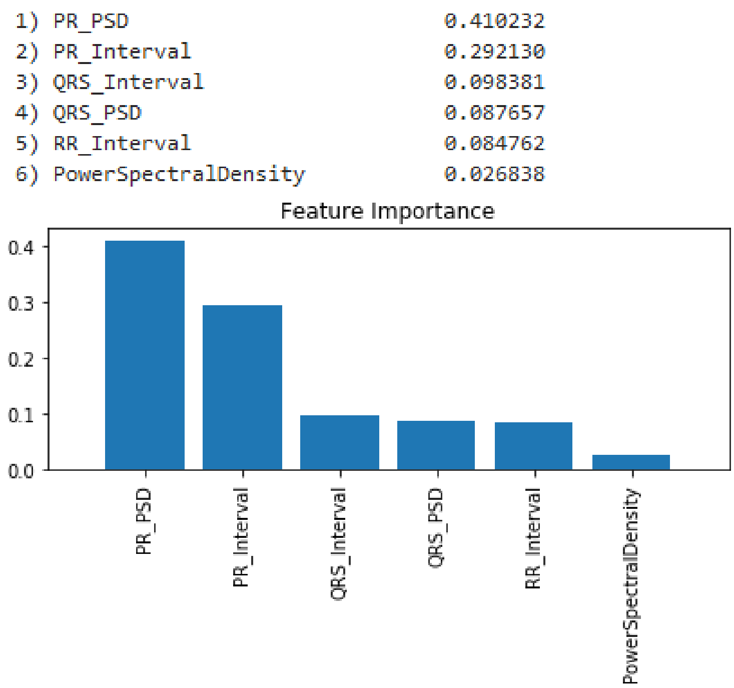

Figure 4.10: Feature importance after extended feature extraction algorithm considering power spectral densities and using *RandomForestClassifier*

- Step 3: A *RandomForestClassifier* with 500 estimators (number of trees in the forest), and ‘balanced’ class weight was used only to determine feature importance (not for classification task). The “balanced” mode uses the values of the features to automatically adjust weights inversely proportional to class frequencies in the input data. Due to the novel feature extraction algorithm which considered power spectral densities instead of intervals, the PR_PSD (power spectral density of PR-interval) alone contributed to the maximum variance (41%) in the input dataset. The QRS_PSD (power spectral density of QRS-interval) was almost as important as the QRS-interval. Despite PR-interval being most important features in any ECG classification task to differentiate between PVC, PAC and Normal sinus rhythm, its power spectral density turned out to be more important feature to differentiate between these arrhythmia types.

- Step 4: Dataset imbalance removal: The target response class variable *AnnotationType*, had the following distribution from a total of 38371 samples: A 2132, N 26362, V 9877. Considering a 70-30% training-test dataset split, the training set was 24,941 samples and validation-test set was 13,430 samples. In order to eliminate or at least reduce the imbalance of the dataset, over and under sampling along with regularisation techniques were applied to the dataset. There were several techniques available, like adding more samples to the less represented class, resampling, using penalised models, using a variety of performance metrics and generating synthetic samples or by using a combination of these techniques. It was not possible is to add more samples for the A-type annotation, as the entire MITDB database had no more than 2132 samples. The N-type annotation had the maximum number of samples. A complete oversampling of the underrepresented class variable or under sampling of most-represented class variable may have been possible, though these may have introduced synthetic values to just one of these class types. As a solution and to impart balance between under an oversampling the Synthetic Minority Oversampling Technique (SMOTE) type balancing was performed. The SMOTE balancing technique not only oversamples the underrepresented class but it also under samples the overrepresented class. The *fit_sample*() transformed the feature set to $\{\textit{Training Set}\} = \{\ \textit{51405}\}$ from an original $\{\textit{Training Set}\} = \{\ \textit{24941}\}$ samples.

- Step 5: Classification based on SMOTE balancing: Initially, *LogisticRegression* with *Lasso* regularisation was attempted by setting the penalty attribute to '*penalty=l1*'. The Lasso technique was used as it shrinks the less important feature's coefficient to zero thus, removing or at least eliminating the effect of less important features altogether.

  ```
  LogisticRegression(penalty='l1', multi_class = 'ovr', solver =
  'liblinear')
  ```

  The *multi_class = 'ovr'* option was set for multiclass classification using *One-vs-Rest* classifier and a 'liblinear' solver was chosen as it is most suitable for multiclass classification for *LogisticRegression* models. Even with SMOTE type balancing and *Lasso* regularisation the *LogisticRegression* model with *GridSearchCV cross* validation showed an overall *balanced_accuracy* score of 90%, table 4.8 using 10-fold cross validation.

Hyper-parameters:

`C = [0.1, 10, 100, 1000, 10000]`

`Gamma = [0.001, 0.0001]`

`Scoring = 'balanced_accuracy'`

`Cross validation (cv) = 10`

It was observed that the precision, recall, f1-score metrics showed significant improvement from the previous classification after SMOTE balancing was performed as shown in table 4.8 . The classification accuracy for A-type annotation increased from 39% to 87% after SMOTE balancing was performed; the A-type annotation beats being the most underrepresented response class type in the entire dataset.

Comparison of accuracy scores before and after SMOTE balancing

	precision	recall	f1-score
A	0.39	0.63	0.48
N	0.99	0.93	0.96
V	0.91	0.94	0.93
total	0.93	0.91	0.92

	precision	recall	f1-score
A	0.87	0.84	0.85
N	0.90	0.94	0.92
V	0.93	0.92	0.93
micro avg	0.90	0.90	0.90
macro avg	0.90	0.90	0.90
weighted avg	0.90	0.90	0.90

Table 4.8: Comparison of classification accuracy scores before and after SMOTE balancing using *LogisticRegression*

A *'balanced_accuracy'* score seemed more appropriate instead of just the 'accuracy' scoring, as it would take into consideration the class imbalance of the feature dataset. This was largely due to the linear separation due to the *LogisticRegression* models.

- Step 6: *LogisticRegression* works well with linear classifications, however, it may not be the most appropriate model for nonlinear feature sets. As the feature importance calculations were already performed in Step3, a classification model based of feature importance was chosen with the *RandomForestClassifier* which was used, in this step, as a classifier along with *GridSearchCV* to perform a hyper-parameter tuning, table 4.9. In addition, *StratifiedKFold* with 5 splits was used for cross validation (*cross_val_score*) with *balanced_accuracy* scoring, which increased the overall *balanced_accuracy* for all the target response class variables and for the A-type response class variable to more than 95%.

A similar experiment was performed using *KNeighborsClassifier (k-NN)* with *k=5* and an overall *balanced_accuracy* of more than 95% was obtained. Both *RandomForestClassifier* and *k-NN* are prone to overfitting. In order to circumvent the problem of overfitting, cross validation with *StratifiedKFold* and *balance_accuracy* scoring was used. Rather than relying only on the precision accuracy score, the scores such as *balanced_accuracy, recall, f1-score metrics* were obtained as a classification report. The *Scikit Learn cross_val_score* cross validation was used on training as well as test data sets with *StratifiedKFold* cross validation with 5 splits which made sure that all the classes were equally represented in the cross validation process.

4.4 Results: Data analysis pipeline for V,A,N classification

On executing the data analysis pipeline from section 4.3.3 an overall classification accuracy score of 97% was observed. The training and the test accuracy scores were more than 97% and the prediction accuracy score was more than 96%. The precision accuracy for classification of V-type and the A-type annotations was 100% and for N-type annotation the precision accuracy was 91% as shown in table 4.9.

The *k-NN* classifier and the *RandomForestClassifier* are known to be quick learners and are quite accurate when the data is skewed. Having reduced the dataset imbalance and as the classification models could obtain classification accuracy of more than 97%. In previous experiments, due to dataset imbalance it wasn't possible to obtain higher accuracy of classification, especially for the A-type annotation. As could be observed in the feature importance table obtained earlier using *RandomForestClassifier*, the classification models could obtain 90% precision recall in classifying the A-type annotation which was the most under-represented class type before SMOTE imbalance reduction.

GridSearchCV and RandomForestClassifier based classification parameters and results	

Parameter grid for GridSearchCV	{
	'n_estimators': [200, 500],
	'max_features': ['auto'],
	'max_depth' : [4,8],
	'criterion' :['gini'],
	'n_jobs':[2]
	}

RandomForestClassifier	n_estimators=500 class_weight="balanced"
GridSearchCV	estimator= RandomForestClassifier scoring='balanced_accuracy'
Cross validation using *cross_val_score* and *StratifiedKFold* validation	scoring='balanced_accuracy', cv=StratifiedKFold(n_splits=5)
GridSearchCV RandomForestClassifier best params: {'criterion': 'gini', 'max_depth': 8, 'max_features': 'auto', 'n_estimators': 200	
Results: GridSearchCV RandomForestClassifier training accuracy: 0.974 +/- 0.001 GridSearchCV RandomForestClassifier test accuracy: 0.974 +/- 0.001 GridSearchCV RandomForestClassifier Prediction Accuracy: 0.967378346158	

GridSearchCV RandomForestClassifier classification report

	precision	recall	f1-score	support
A	1.00	0.90	0.95	9227
N	0.91	1.00	0.95	9227
V	1.00	1.00	1.00	9227
micro avg	0.97	0.97	0.97	27681
macro avg	0.97	0.97	0.97	27681
weighted avg	0.97	0.97	0.97	27681

Table 4.9: *GridSearchCV* and *RandomForestClassifier* based classification parameters and classification report following SMOTE imbalance reduction for V, A, N annotation types using the features extracted from the consolidated feature extraction algorithm.

The classification model was persisted in binary format using the Scikit-Learn package, section 3.5, and deployed on the target device for prediction. In the following section signal acquisition and conditioning of fresh ECG samples have been discussed. The denoised and filtered ECG samples were converted to a recognisable MITDB format as described in section 4.5.3. It was this MITDB compatible signal that was provided as an input to the classification model persisted on the target device. The model could then classify between the V, A, N annotation types in real time. As the research focused on implementing the classification and prediction of arrhythmia on the wearable resource constrained device, it was essential that the trained model could be ported and persisted to the target device to only make predictions without having to train the classifier model on the training set again on the resource constrained device. As the classification model could be ported and executed on the target device, the feature-set *fitting* and *transformation* methods, which normally required greater processing power and had larger memory requirements, were not required to be executed on the target device, nor were any of the regularisation, dataset balancing or cross validation tasks performed again on the target device. Since the model was already trained, tested and cross-validated, it performed its classification tasks on the target device with optimal accuracy, section 4.7 . In order to perform the classification tasks on the test ECG waveforms, feature vectors had to be extracted from ECG signals captured in real time, using the same feature extraction algorithm that was used to extract features from the MITDB arrhythmia database. In order to run the feature extraction algorithm on the test ECG waveforms, these test ECG waveforms had to be converted to a WFDB compatible records and prior to that the signal had to be filtered and denoised. The method of real time signal acquisition is presented in the next subsection 4.5 with the details of the signal processing algorithms and input output parameters.

4.5 Methods: ECG signal acquisition from human subject

The objective of the research study was to detect arrhythmia type in real-time and in order to facilitate monitoring cardiac health, the samples had to be collected from human subjects in real-time and regardless of position and motion and over longer duration. The raw ECG signal acquired from the human subject is a very noisy waveform. This is due to the bio-electric interference, muscular contraction and environmental conditions. The waveforms also has problems related baseline wander and noise due to motion and bio-electric interference. The baseline wander is a problem in waveforms where the signals stray from their baseline with an upward or a downward trend due to electrical interference. The signals, therefore, had to be denoised and filtered in real-time using appropriate signal processing algorithms on a resource constrained device like the Beaglebone Black (BBB). Initially, however, the raw ECG signal was studied and analysed to derive an appropriate filtering mechanism and to identify filter parameters and subsequent signal conditioning methods were implemented to generate a resulting ECG waveform that was denoised and was WFDB compliant. The general idea was to denoise and detrend the signal abnormalities and yet preserve the features of the ECG signal by minimising the modifications to the morphological structure of the signal.

4.5.1 ECG signal filtering, denoising and wavelet analysis

In order to analyse the raw ECG signal, MATLAB was used for signal processing. The raw samples were captured at 1 KHz 12 bit resolution with Arduino Micro and the samples were normalised and extended to 2n samples. Eventually the samples had to be digitised according to a format acceptable by MITDB database such that the WFDB routines in MATLAB could be used on these sampled waveforms. The 3-lead ECG kits samples noisy due to bio-electric interference of the external environmental conditions, the body posture and motion. The signal was normalised and denoised using MATLAB with the parameters shown in table 4.10:

Chebyshev II second order filter was used in MATLAB with a sampling frequency of 1 KHz, followed by zero-offset signal conditioning and removing the baseline wandering. For further baseline wandering correction and for signal smoothing Savitzky-Golay filter with order N=3 and frame length of 11 was applied to smooth the signal without destroying the original signal properties in digital format. The detrended signal is just the baseline corrected signal subtracted from the original ECG signal, figure 4.11 and table 4.10. The Chebyshev filter has a steep roll-off and is good at removing high-frequency noise and Savitzky-Golay filters (AlMahamdy & Riley, 2014) are optimal filters such that they minimise the least-squares error in fitting a polynomial to frames of noisy data, hence were chosen as most appropriate choice for the task. A relatively denoised signal was obtained, figure 4.11 after Chebyshev and Savitzky-Golay filtering, though a detrended and baseline corrected signal was required which would conform to MITDB WFDB requirements, such that when WFDB routines like *RDANN, WRANN, and ANN2RR* were used these could read and write the annotations and generate annotations files for the denoised and detrended signal. (Walinjkar and Woods 2017b; Walinjkar 2018a)

Chebyshev II and Savitzky-Golay filter parameters for freshly captured ECG signal.
Chebyshev II, second order filter parameters : E.g. *cheb2ord in MATLAB*; Sampling Frequency (Fs) 1 KHz Nyquist Frequency (Fn) = Fs/2 Passband Frequency (Normalised) (Ws) = [1.1 100]/Fn; Stopband Frequency (Normalised) (Wp) = [0.1 101]/Fn; Passband Ripple (dB) Rp = 1; Stopband Ripple (dB) Rs = 150;
Savitzky-Golay filter parameters for signal smoothing: Filter-order=3 and Frame-length=11 E.g. *sgolayfilt in MATLAB*
ECGSignal[n] = Array[n] (ECG samples of length 'n') BaselineCorrectedSignal[n] = sgolayfilt(ECGSignal[n], 3, 11) DetrendedSignal[n] = ECGSignal[n] - BaselineCorrectedSignal[n]

Table 4.10: Chebyshev II and Savitzky-Golay filter parameters for denoising and conditioning of fresh ECG signal acquired from human subject.

4.5.2 Results: ECG Signal processing on resource constrained device in real-time

Although a detrended and denoised ECG waveform was obtained using Chebyshev and Savitzky-Golay filters and wavelet analysis in a desktop environment with four core processor and 12GB system memory, the same method had to be implemented on a resource constrained device such as the BBB with ARM Cortex-A9 processor and 1 GB system memory; the analysis had to be performed on the raw ECG signal acquired from human subject in real time.

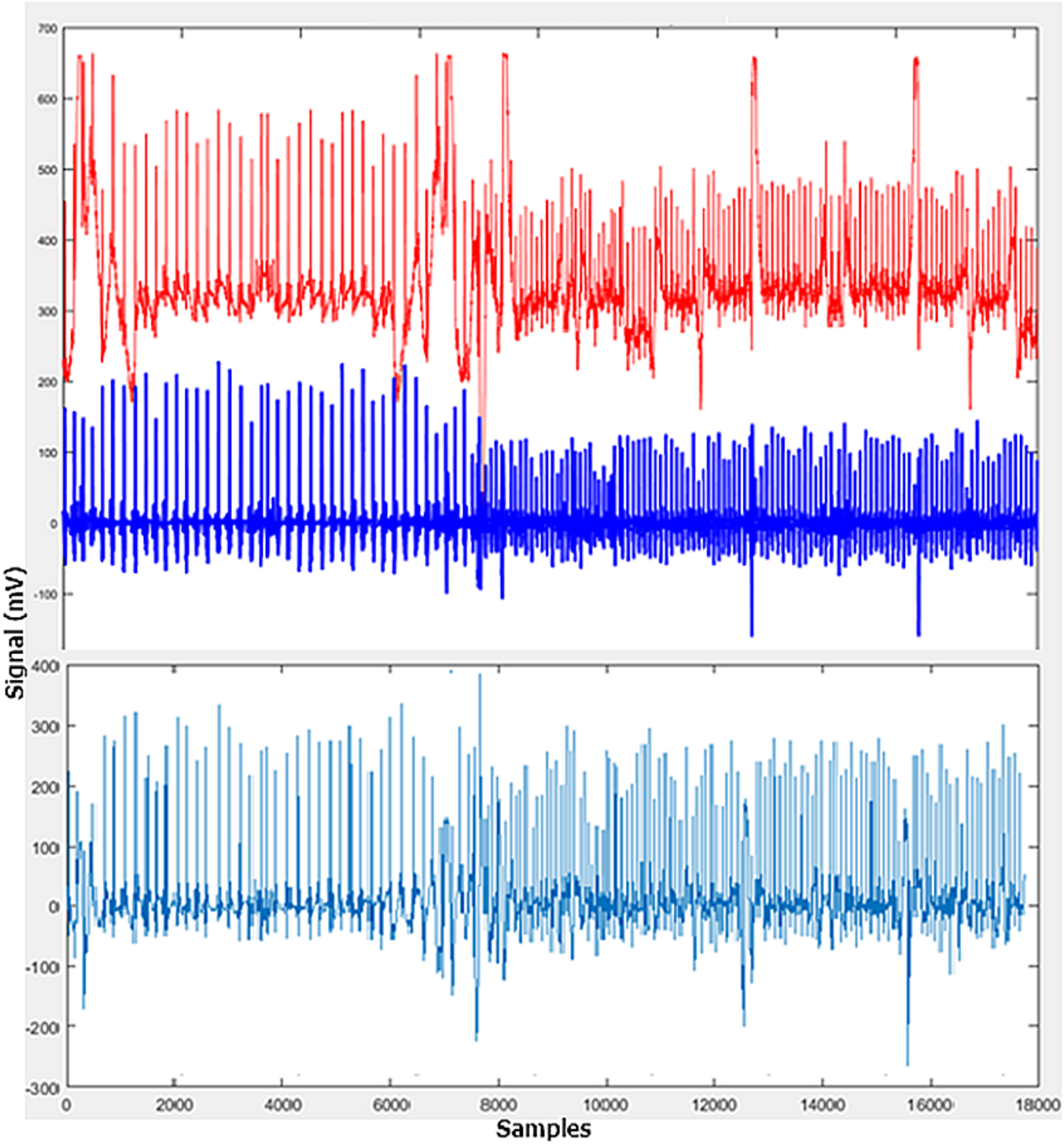

Figure 4.11: The raw ECG signal obtained from human subject after denoising, filtering and baseline correction using Chebyshev 2nd order and Savitzky-Golay filter

The discrete wavelet transform version of PyWavelet *'pywt.Wavelet('sym4')'* was used to obtain 'Symlet 4' wavelet which was used to identify the P-QRS-T sequence in an ECG signal, figure 4.12. The *pywt.wavedec* method was used for multilevel decomposition of the ECG signal and the *pywt.waverec* method was used for reconstruction of the filtered signal, figure 4.13. Although the wavelets in the ECG signal could be identified, these could not be effectively filtered and more importantly these could not be effectively baseline-corrected, so the entire signal filtering had to be performed using Chebyshev and Savitzky-Golay filter (AlMahamdy and Riley 2014).

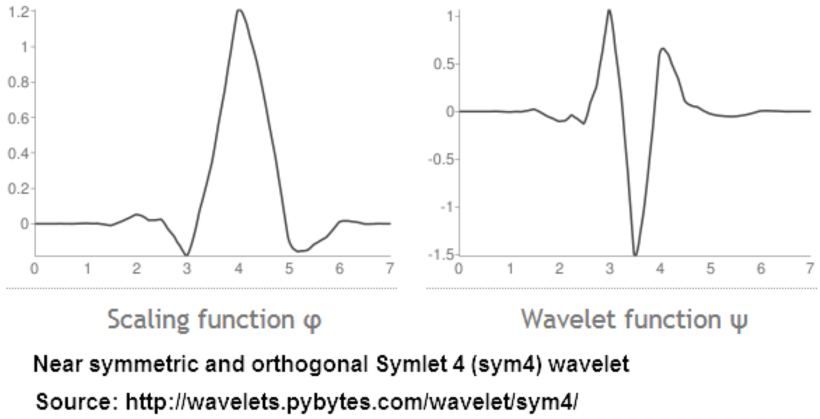

Figure 4.12: A Symlet 4 wavelet in PyWavelet toolbox in Python equivalent to MODWT in MATLAB

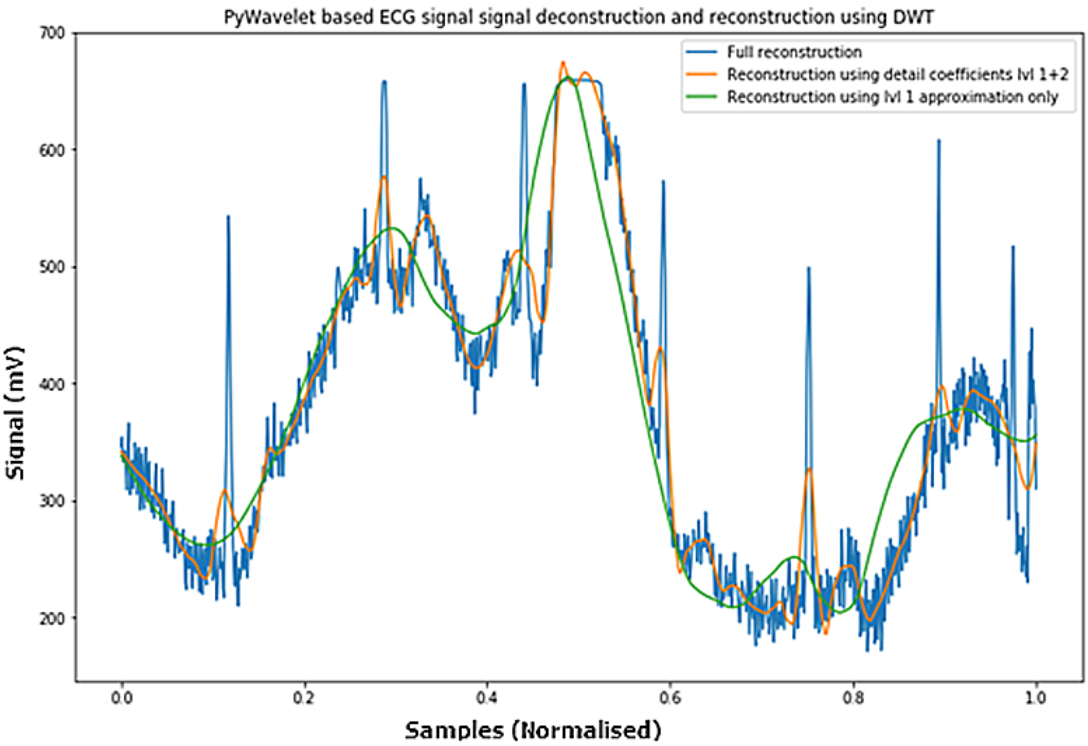

Figure 4.13: Signal reconstruction of a noisy ECG signal using Discrete Wavelet Transform utility pywt.wavedec in PyWavelet toolbox

The Chebyshev II and Savitzky-Golay filters were designed with parameters in table 4.11 and the *filtfilt()* method was used for phase correction. The noisiest portion of the signal is shown in the figure 4.14, after filtering, signal conditioning and baseline correction.

Having designed the required filters, the signals had to be captured from the ECG sensor interfaced with Arduino micro. The Arduino was in turn interfaced with BBB to the serial port at 115200 baud, parity: none, start and stop bits: none. The signals were captured from human subject in real time where each of the ECG sample was of the format '*E: <ECG Sample>*' and the PPG signal was of the format '*P: <PPG Sample>*'. The Python program running on the BBB received the samples over the serial port and resampled the signal at 1 KHz. The BBB has a 16 bit resolution analogue to digital converter. The signal was then passed through the filters that had been designed followed by the baseline correction, which essentially removed the baseline wander. Once the signal was filtered, it had to be converted to an appropriate WFDB format such that the WFDB routines could be executed on the samples to obtain the feature vectors that would then become the test data sets. These test feature sets would then be passed through the classification models already trained generated from the previous data analysis tasks. The models that were trained in the data analysis tasks, were persisted on a resource constrained device which could be reloaded in the memory to perform classification tasks on the freshly acquired ECG waveforms. In order to perform the classification tasks on the freshly acquired ECG waveforms, feature vectors had to be extracted from these filtered ECG waveforms, using the same feature extraction algorithm that was used to extract features from the MITDB arrhythmia database. In order to run the feature extraction algorithm on the test ECG waveforms, these test ECG waveforms had to be converted to a WFDB compatible records.

An effectively denoised baseline corrected signal could be obtained in MATLAB using discrete wavelet transform, however this task was performed in a desktop environment with a powerful processor and adequate memory to perform the compute intensive tasks. In the real time ECG signal acquisition and processing however, the same task had to be performed on a resource constrained IoT device like the Beaglebone black. The SciPy Python, PyWavelet toolbox was used with 'Symlet 4' wavelet which could help in the construction and reconstruction of the ECG signal with adequate filtering, though could not eliminate the baseline wander. The same combination of Chebyshev II 2^{nd} order filter and Savitzky-Golay filter was used in SciPy Python with minor variations in the parameters as compared to the MATLAB version as shown in table 4.11. A normalised, filtered, denoised and baseline corrected signal was obtained as shown in the figure 4.14.

Filter parameters for resource constrained device Texas Instruments Beaglebone black.
A Chebyshev II band stop filter was designed with following parameters: Bandstop: Passband wp = [0.2, 0.7], Stopband ws = [0.3, 0.6] The maximum loss in the passband: 5(dB) The minimum attenuation in the stopband: 60 (dB).
The Savitzky-Golay filter parameters for a resource constrained device : Window_length: 101 It is the length of the filter window (i.e. the number of coefficients). Filter_order: 3 It is the order of the polynomial used to fit the samples.
ECGSignal[n] = Array[n] (ECG signal of length 'n') Sig_cheby2_filtered[n] = signal.filtfilt(ECGSignal[n]) Y_savitzky_golay[n] = signal.savgol_filter(Sig_cheby2_filtered[n]) BaselineCorrected = Sig_cheby2_filtered[n] - Y_savitzky_golay[n] (*The baseline correction is merely a difference between the Chebyshev II and Savitzky-Golay filtered signal*)

Table 4.11: Chebyshev II second order filter and Savitzky-Golay filter parameters for resource constrained device Texas Instruments Beaglebone black.

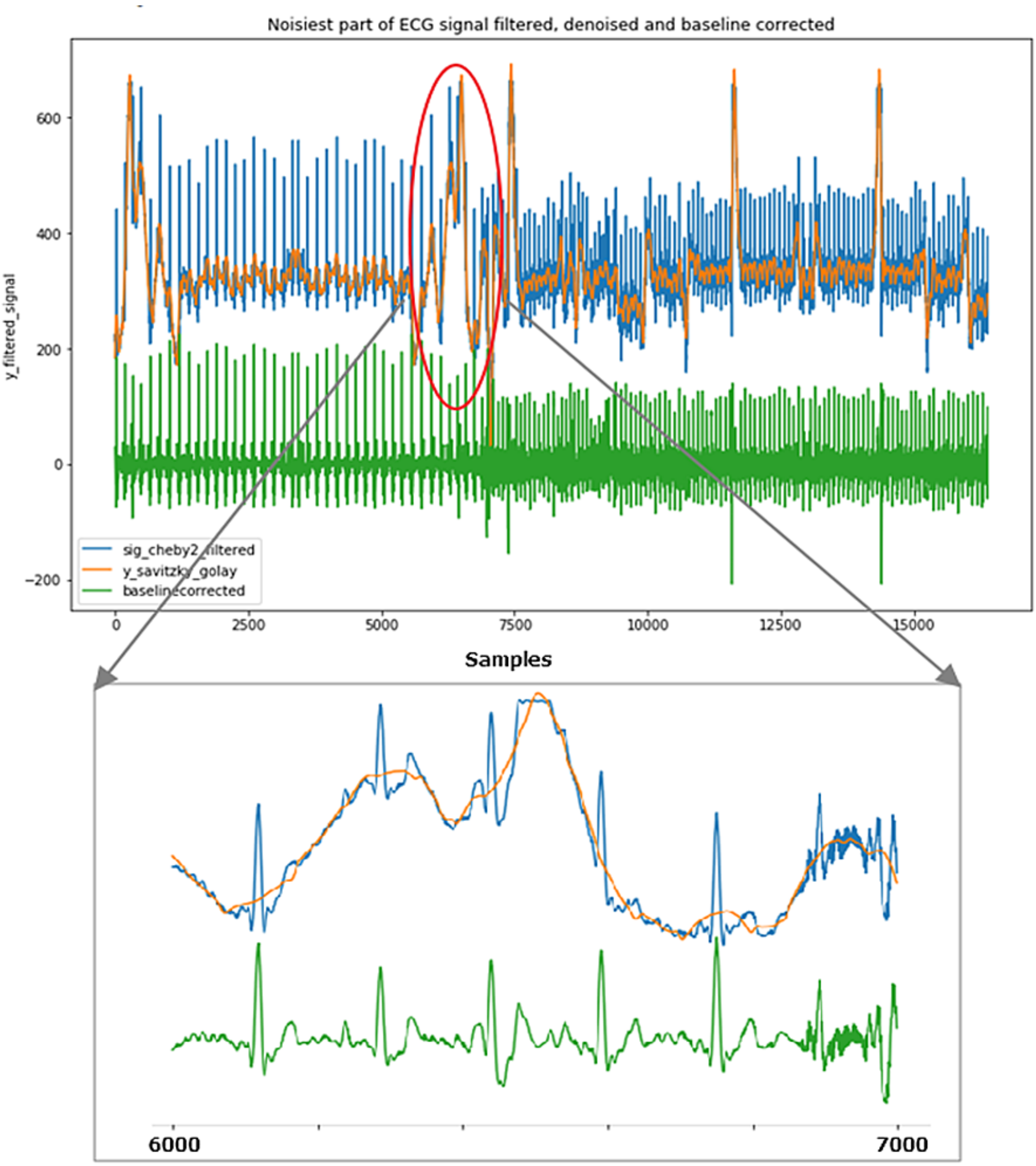

Figure 4.14: Filter parameters for Chebyshev II second order filter and Savitzky-Golay filter implemented in SciPy Python for denoising, conditioning and baseline correction on Beaglebone black.

4.5.3 Methods: ECG signal conversion to WFDB format

The steps for ECG signal conversion to WFDB compatible record were as follows:

The samples from the ECG and PPG sensor were acquired by Arduino Micro clocked at 16MHz and transmitted to BBB over the serial port at 115200 baud and received by BBB using the Adafruit GPIO library for BBB with a sampling frequency of 1 KHz. The ECG signals were resampled at 360 Hz similar to the sampling frequency of the records in MITDB arrhythmia database. The signal had to be resampled and filtered using Chebyshev II and Savitzky-Golay filters as explained in section 4.5.2, in order to obtain an ECG signal that could be converted to a record compatible to the MITDB database. This step had to be performed as the WFDB routines that were used to extract features from MITDB records, could be used for freshly acquired ECG signal as well as used in the pre-processing stage of algorithm 4.2. Also, the classification model that was trained on MITDB record would then execute the prediction task on this converted and WFDB compatible signal. The inter-sample interval between two consecutive samples in the MITDB record was 0.00277 seconds (1/360 Hz)

The *'wrsamp -F 360 -G 1000 –i <denoised_ecg_samples_file>'* command from WFDB was used to convert these samples to a WFDB-compatible record where '1000' was the gain. The WFDB record conversion sampling frequency is 360 Hz, which was different from the data acquisition sampling frequency of 1 KHz. It is a common clinical practice that the ECG strips are analysed in batches of 10 second intervals, as each ECG strip is 10 seconds in duration.

The '*gqrs -r ecg_samples_file -m 1.5'* command was used to obtain the QRS complexes from the samples. The threshold was set to 1.5 millivolts, and a *qrs* annotation file was generated. The QRS annotations are the locations in the ECG waveforms where the QRS peaks occur. This '*qrs'* annotation file would be used by the other WFDB routines to extract features.

The *'rdann -a qrs -r ecg_samples_file'* command, which uses the '*qrs'* annotation file, was used to detect the R-peaks in the ECG waveform.

The *'ann2rr –a qrs –r ecg_samples_file'* command, which uses the '*qrs'* annotation file, was used to detect the RR intervals between consecutive QRS peaks in the ECG signals. The RR interval is one of the important features in the feature extraction model.

The '*ecgpuwave –a qrs –r ecg_samples_file –o epu*' command, which uses the '*qrs*' annotation file, was used to generate another annotation file with '*epu*' extension. This annotation file contained the locations of the start '(', stop ')' , P-wave 'p', QRS complex 'N' and T-wave 't' sub annotation type locations in the fresh ECG signal.

The '*rdann -a epu -r ecg_samples_file -p <annotation_subtype>*' command, which used the '*epu*' annotation file from the previous *ecgpuwave* command, was used to locate the annotation subtypes 'p' and 't' which are essentially P-wave and T waves with their onset and stop boundaries, the N type annotation being the QRS wave. The *'rdann'* command was executed thrice for detecting the locations of P-wave, T-wave, QRS complex and their start and stop locations. The command generated a file for each of these annotation types and sub-types each containing a column of sample numbers which represented the locations of P-wave, T-wave and the QRS complex along with their start and stop positions.

4.6 Methods: Feature extraction and V,A,N classification on restricted device

A feature extraction algorithm 4.2 similar to algorithm 4.1 was developed, though this algorithm contained the WFDB format conversion pipeline described in section 4.5.3 which used WFDB routines to convert ECG samples acquired in real-time to a record compatible with WFDB and MITDB arrhythmia database. As the model trained on MITDB database would predict on the freshly acquired test signal, it was required that the signal was MITDB compatible. The classifier model was persisted and deployed on a restricted target device described in sections 3.1 and 3.5.

Algorithm 4.2 Real-time feature extraction algorithm for a resource constrained device

procedure ECGPREPROCESSOR
    `WRSAMP -F 360 -G 1000 -i ecgSamples.txt -o dat`
    ▷ The routine generated the WFDB compatible ecgSamples.dat file
    `GQRS -r ecgSamples.dat -m 1.5`
    ▷ The routine generated the ecgSamples.qrs file containing the locations for QRS peaks as compared to Algorithm 4.1 where the atr annotation file was used to extract feature annotations to train V, A, N classifier.

    $[qrsannsamplenums, qrsanntype]$ = `RDANN -r ecgSamples -a qrs`
    ▷ The routine read the QRS peaks annotations from the qrs file, *qrsanntype* took value N as compared to Algorithm 4.1 where the values were V, A, N
    $[rrintervals, rrsamplenumbers]$ = `ANN2RR -a qrs -r ecgSamples`
    ▷ The routine calculated the RR intervals from the qrs annotation file
    $[rrintervalsandsampnums] = [rrintervals\ rrsamplenumbers]$
    `ECGPUWAVE -a qrs -r ecgSamples -o epu`
    ▷ The routine generated the annotations file with extension epu containing the locations of (,), N, p, t annotations from the corresponding qrs file.
    $[epuAnnotSampNumbers, epuAnnotType]$ =
        `RDANN -a epu -r ecgSamples -p (, ), N, p, t`
    ▷ The routine read the epu annotations file to return $[epuAnnotSampNumbers, epuAnnotType]$ corresponding to the (, p, N, t,) annotations. **return** $[epuAnnotSampNumbers, epuAnnotType]$
end procedure

procedure FEATUREEXTRACTIONREALTIME $[epuAnnotSampNumbers, epuAnnotType]$ = `Call ECGPreprocessor`
    ▷ /*features initialised*/
    $featurePRinterval = 0$; $featurePRpsd$ =0;
    $featureQRSinterval = 0$; $featureQRSpsd$ =0;
    $featureRRinterval = 0$;
    $featurePowerSpectralDensity = 0$;
    $featureSNR = 0$;
    ▷ /*Iterate all `epu` annotations: (,), p, N, t */
    for $iEPUannot = 0$: length($epuAnnotSampNumbers$) - 1 **do**
        if $epuAnnotType(iEPUannot)$ == 'N') **then**
    ▷ /*sample number at N-type annotation */
            $epusampnum = epuAnnotSampNumbers(iEPUannot)$;
    ▷ /*iterate all atr annotations (V, A, N)*/
            for $iQRSann = 1$: length($qrsannsamplenums$) - 1 **do**
    ▷ /*iterate all N-type annotations obtained from `qrs` annotator file only to obtain N-type annotation locations, as compared to Algorithm 4.1 where the class labels were obtained using the `atr` annotation file*/

Algorithm 4.2 Real-time feature extraction algorithm for a resource constrained device (continued)

if $(qrsannsamplenums(iQRSann) >=$
$epuAnnotSampNumbers(iEPUannot$ - 1))
&&
$(qrsannsamplenums(iQRSann) <=$
$epuAnnotSampNumbers(iEPUannot + 1))$ **then**

▷ /*iterate all N-type annotations and if `epu` annotations and `qrs` annotations do not match break the loop and proceed to next `epu` N-type annotation. In Algorithm 4.1 *FeatureAnnotationType* class label was assigned a value from (V, A, N). As this algorithm only generated feature vector samples, $featureAnnotationType$ was not required */

break For loop;
end if
end for

▷ /*calculate $featurePRinterval$ and $featureQRSinterval$*/

$k = iEPUannot$ - 1;

▷ /*iterate epu annotations to locate start/end of P-wave and T-wave*/

while $epuAnnotType(k)$!= 'N' **do**

▷ /*check if P-wave precedes QRS peak*/

if $epuAnnotType(k) ==$ 'p' **then**

▷ /* locate the PR segment on either side of the P-wave peak. WelchSpectrum and BandPower routines from Algorithm 4.1 */

$prsamplefrom = epuAnnotSampNumbers(k$ - 1);
$prsampleto = epuAnnotSampNumbers(k + 1);$
$featurePRinterval = prsampleto$ - $prsamplefrom$; ▷ /*featurePRinterval*/
$X_p[n] = prsamplefrom{:}prsampleto$
$[psd1] =$ `Cal WelchSpectrum`$(X_s[n])$;
$featurePRpsd =$ `Call BandPower`$(psd1)$;

▷ /* locate QRS interval segment on either side of QRS peak*/

$qrssamplefrom = epuAnnotSampNumbers(iEPUannot$ - 1);
$qrssampleto = epuAnnotSampNumbers(iEPUannot + 2);$

▷ /* featureQRSinterval*/

$featureQRSinterval = qrssampleto$ - $qrssamplefrom$;
$X_q[n] = qrssamplefrom{:}qrssampleto$
$[psd2] =$ `Call WelchSpectrum` $(X_q[n])$;
$featureQRSpsd =$ `Call BandPower`$(psd2)$);
break While loop;

▷ /*Check if P-wave absent in which case T-wave from previous beat precedes QRS peak */

else if $epuAnnotType(k) ==$ 't' **then**

▷ /* featurePRinterval set to zero if P-wave absent*/

$featurePRinterval = 0$;

Algorithm 4.2 Real-time feature extraction algorithm for a resource constrained device (continued)

```
48:                 featurePRpsd = 0;
 ▷ /* locate QRS interval when P-wave absent*/
49:                 qrssamplefrom = epuAnnotSampNumbers(iEPUannot -
 1);
50:                 qrssampleto = epuAnnotSampNumbers(iEPUannot + 2);
51:                 featureQRSinterval = qrssampleto - qrssamplefrom;
52:                 X_q[n] = qrssamplefrom:qrssampleto;
53:                 [psd3] = Call WelchSpectrum (X_q[n]);
54:                 featureQRSpsd =  Call BandPower(psd3));
55:                 break While loop;
56:             end if
57:             k = k - 1;
58:             if  thenk == 0
59:                 break While loop;
60:             end if
61:         end while
62:         for iRRann = 0 : length(rrSampleNumber) - 1 do ▷ /* calculate
 featureRRinterval*/
 ▷ /*check if RR-interval sample numbers coincide with epu sample numbers*/
63:             if (rrSampleNumber(iRRann) >=
64:                 epuAnnotSampNumbers(iEPUannot - 1))
65:                 &&
66:                 (rrSampleNumber(iRRann) <=
67:                 epuAnnotSampNumbers(iEPUannot + 1)) then
68:                 featureRRinterval = rrIintervals(iRRann); Refer line 5
69:                 break For loop
70:             end if
71:         end for                        ▷ /* for iRRann iteration ends*/
 ▷ /*calculate Signal-Noise-Ratio and Power Spectral Density over the entire
 heartbeat*/
72:         samplespsdsnrfrom = epuAnnotSampNumbers(iEPUannot - 4);
73:         samplespsdsnrto = epuAnnotSampNumbers(iEPUannot + 4);
74:         X_snr[n] = samplespsdsnrfrom: samplespsdsnrto
75:         [psd4] = Call WelchSpectrum (X_snr[n]);
76:         featurePowerSpectralDensity =  Call BandPower(psd4));

77:         S_snr[n] = samplespsdsnrfrom:samplespsdsnrto
78:         featureSNR = Call SignalNoiseRatio(S_snr[n]) ;
79:     end if                             ▷ /*iEPUannot == N ends */
80:     newSampleRow = [featurePRinterval, featurePRpsd,
81:         featureQRSinterval,
82:         featureQRSpsd, featureRRinterval,
83:         featurePowerSpectralDensity, featureSNR]
84:   end for                              ▷ /*iEPUannot iteration ends*/
85: end procedure
```

The feature vectors generated were according to the following tuple: {*PR_Interval, PR_PSD, QRS_Interval, QRS_PSD, RR_Interval, Heart rate, PowerSpectralDensity, SignalToNoiseRatio*} where,
PR_Interval: PR interval in a heartbeat waveform
PR_PSD: the power spectral density in the PR interval
QRS_Interval: the QRS duration in the QRS complex
QRS_PSD: the power spectral density in the QRS complex
RR_Interval: the RR-interval at a given location in the waveform
PowerSpectralDensity: the power spectral density of the entire P QRS T wave
SignalToNoiseRatio: the signal-to-noise ratio of the entire P QRS T wave.
Target class variables: V, A, N annotations representing PACs, PVCs and Normal sinus rhythm

Having obtained the filtered signal it could be passed through the feature extraction algorithm implemented using WFDB routines and ported and deployed to the Beaglebone black. The algorithm used WFDB routines along with power spectral estimation methods in SciPy package to obtain the features from the test ECG signal acquired from human subject in real time. It was this ECG signal (converted to an MITDB compatible record) that was used by the classification model that was persisted on the Beaglebone black. The model could then classify between the V, A, N annotation types in real-time. The Algorithm 4.2 could extract WFDB compatible features, though only N-type annotations could be tested when used for healthy patients. A clinical trial would be required to test the algorithm on patients who are known to be suffering from cardiac arrhythmia to extract V-type and A-type annotations. Due to the scope of the research and limitations related to running clinical trials, the algorithm was tested only on an existing MITDB record *MITDB/223* which was completely omitted from the training and test samples set. The record was chosen as it contained both the V-type and A-type annotations and the samples from the records were read into a test `ecgSamples.txt` text file and passed through algorithm 4.2 followed by the classifier model that was serialised and stored on the resource constrained

Beaglebone Black device.

4.7 Results: Real-time V,A,N classification on restricted device

The record *MITDB/223* that was completely omitted from the training phase was used as the test record to test the data analysis pipeline on the target device. The record contained 2029 N-type, 72 A-type and 473 V-type annotations (total 2574 samples). The statistical distribution of the record is shown in figure 4.15 and as could be seen throughout the MITDB records, the A-type samples occurred in extremely smaller quantities as compared to the V-type and the N-type annotations. The data analysis pipeline, based on subsection 4.3.3, that was persisted and copied to the target device, produced an overall classification accuracy of over 91% and the precision, recall and f1-scores were 100%, 73% and 84% respectively for the most under-represented class of A-type annotations, figure 4.16

	PR_Interval	PR_PSD	QRS_Interval	QRS_PSD	RR_Interval	PowerSpectralDensity	SignalToNoiseRatio
count	2573.000000	2573.000000	2573.000000	2573.000000	2573.000000	2573.000000	2573.000000
mean	39.481928	9.193155	34.056743	-4.098382	238.183832	-8.956229	20.010243
std	25.047190	49.032044	13.553444	3.246442	40.509777	3.166314	12.318828
min	0.000000	-36.240800	10.000000	-24.778500	114.000000	-21.164500	-12.059800
25%	25.000000	-16.932900	26.000000	-5.632600	219.000000	-10.866100	7.547700
50%	43.000000	-13.217700	31.000000	-4.613800	234.000000	-9.764400	24.382800
75%	52.000000	-7.943600	39.000000	-3.450200	259.000000	-8.124800	28.993500
max	123.000000	150.000000	85.000000	6.885800	478.000000	3.875100	51.751800

Figure 4.15: Descriptive statistics for samples obtained from human subjects in real-time for feature vector extracted using Algorithm 4.2

Serialised Classifier Scikit-learn Pickle - classification report

	precision	recall	f1-score	support
A	1.00	0.73	0.84	2029
N	0.79	1.00	0.88	2029
V	1.00	1.00	1.00	2029
micro avg	0.91	0.91	0.91	6087
macro avg	0.93	0.91	0.91	6087
weighted avg	0.93	0.91	0.91	6087

Figure 4.16: Arrhythmia classification (V, A, N) on a resource constrained device for samples obtained from human subjects in real-time for feature vector extracted using Algorithm 4.2

4.8 Discussion: Early warning arrhythmia detection and signal processing

The main objective of the research study was to detect, identify and classify early warning ECG signs in real-time using a wearable device and upload the abnormal observations along with trauma information to an EHR database using standard coding schemes. Such a provision would avoid delays in providing timely medical treatment, even before an individual reaches a critical condition. Certain devices like the Holter monitor and the AliveCor ECG monitoring kit, mentioned in the literature, can perform long-term monitoring, though these kids cannot detect early warning arrhythmia. The AliveCor uses HRV analysis and adaptive regression based techniques to detect atrial fibrillation which is a much fatal arrhythmia condition. The aim of the research study was to detect and identify early stage arrhythmia given fresh test ECG samples acquired from human subject in real time. The main problem solved in this research study is the real-time detection, identification and classification of test ECG samples into early warning arrhythmia annotation types similar to those found in the MITDB arrhythmia database. In the arrhythmia detection methods mentioned in the literature and also in the WFDB library that is widely in this and other research studies mentioned in the literature, it was the real-time arrhythmia annotator component that was missing. After investigating the research problem, it was found that annotating a fresh ECG signal by classifying it into normal and abnormal annotation types and sub-types, was not a computational task that could be solved by linear logic or statistical methods. Even though the statistical measures of waveform characteristics change over waveform belonging to the same type, patterns of the waveform remained the same. The machine learning approach was therefore chosen initially to train the models on a widely used MITDB arrhythmia database and then present the model with fresh test ECG samples.

4.8.1 ECG Arrhythmia detection and classification

After studying the ECG signal it was observed that the signal is non-linear and random so despite having same pattern, the waveform characteristics and their statistical measures differ even in the same type of waveform, belonging to normal or abnormal sub-types. Due to the randomness in the signal and intermittent nature of the V and the A type annotations, regression based prediction and adaptive auto-regressive models could not produce accurate classification results, especially when the model is presented with a fresh test ECG signal. So supervised classification and pattern recognition methods seemed like a more appropriate choice. By the successful implementation of the V,A,L,R classifier with a classification accuracy of more than 97% using supervised learning and cross-entropy of less than 10 and best-case classification percent error on test-set of 1.2% (dataset split - 70-15-15%) and worst case classification percent error on test set of 2.1% (dataset split – 60-20-20%), the hypothesis that supervised classification and neural network pattern recognition algorithms could be successfully trained on features extracted from the dataset of ECG records with abnormal annotation types, could be accepted. As the Scikit-Learn classification models could be persisted and ported to a wearable and resource constrained IoT device, the classification models could be executed on fresh ECG samples obtained from a human subject in real-time. The QRS detection is an important aspect in ECG analysis and techniques such as K-Means, PCA (Principal Component Analysis), K-Nearest Neighbours (K-NN) and Artificial Neural Network (ANN) have been successfully used in the past yielding over 99% classification accuracy (Adams and Choi 2012; El-Khafif and El-Brawany 2013).

The drawback with some of these was that these models tend to accept test data in large samples and perform analysis on entire dataset in a single execution cycle instead of beat-by-beat samples in real-time on multi-core machines adequate system memory. Although, this may help to develop analytical models, they remain isolated from monitoring equipment and could not be be used in real-time monitoring in order to generate alarms and alerts related to arrhythmia in real time. In methods section an illustration to overcome this limitation has been demonstrated by combining the data acquisition with machine learning servers in real time. By transmitting the JSON (JavaScript Object Notation) encapsulated ECG readings in real time to the server that is already trained on ECG data from MITDB the analytical server performs the analyses and classification tasks. There also exists a high degree of correlation between Heart Rate Variability (HRV) and arrhythmia and HRV has been used in the past to detect sudden cardiac deaths (Ebrahimzadeh, Pooyan, and Bijar 2014). Techniques such as k-Nearest Neighbours (k-NN) and Multilayer Perceptron Neural Network (MLP) (Ebrahimzadeh, Pooyan, and Bijar 2014) have been previously used with some success to predict sudden cardiac deaths with a high degree of accuracy (about 99.73%, 95%. .96.52%) The problem however is that HRV analysis depends on the morphology of the ECG waveform and QRS detection, which depends on the accuracy of the ECG equipment and accurate 12-lead ECG equipment may not be portable and certainly not wearable. The same feature extraction algorithm and machine learning models developed in methods section could be used with other databases from PhysioNet e.g. the Creighton University ventricular tachycardia database, MIT-BIH atrial fibrillation database and Holter database which are records of patients who suffered sudden cardiac death during recordings and can be used for ECG pattern recognition of extreme conditions. Other techniques exist which use multi-layer feed-forward perceptron models to analyse the waveform for prediction and analysis (Adams and Choi 2012). Many of these and other techniques consider the morphological structure of the ECG waveform where RR interval values were commonly used for comparative analysis. However, the morphological structure of the QRS waveform and past pattern from the individual's own waveform to use for a comparison to detect abnormal from normal waveform had presented challenges related to adaptive and auto-regressive analysis.

Despite of the accurate classification algorithms, practical arrhythmia classification in real-time was not possible due to size and processing power constraints related to the IoT device and the requirement of the accurate 12-lead ECG equipment and also due to the non-real time batch processing nature of the algorithms, which taken together are not portable or wearable. The feature extraction method illustrated in this research study, without completely relying on the morphology of ECG waveforms, produced almost as accurate results as produced by machine learning and feature extraction models that relied on HRV analysis. Furthermore, HRV analysis is susceptible to be influenced by the age and gender specific information (Voss et al. 2015) physical state of the individual like running, climbing and dormant and sleeping states (Padulo et al. 2013). The problem with V,A,L,R arrhythmia classification, mentioned earlier, was that it did not consider the N-type arrhythmia annotations. In theory the N-type heartbeat and the A-type heartbeat appeared very similar in structure and morphology; the difference being that with A-type abnormality the two consecutive heartbeats overlap showing a very subtle difference between the N-type and the A-type annotation beats, which were very difficult to capture using basic feature vectors that considered Heart-rate and RR interval in V,A,L,R arrhythmia classification. The inclusion of PR interval in the extended feature extraction algorithm that considered spectral components in the ECG waveform, produced accurate measures for spectral characteristics of the ECG waveform and its sub portions: the P-wave, QRS wave and the T-wave. The spectral characteristics - power spectral density, bandpower and signal to noise ratio, that were used as feature values enabled accurate classification. The PR interval and its power spectral density turned out to be an essential feature which amongst themselves contributed to 65% (37% PR_PSD and 28% PR interval) of explained variance as ascertained by feature importance values derived using *RandomForestClassifier*. There was a large imbalance in the dataset where the abnormal samples were only 81 per 100,000 normal samples. Even amongst the abnormal types i.e. the V-type and the A-type annotations, the V-type annotations samples were 10 times the A-type annotations, which would result into only 39% classification accuracy for the A type annotation. After SMOTE balancing, a One-vs-Rest LogisticRegression with Lasso regularisation with L1 penalty and a 'liblinear' solver, balanced_accuracy score for the A type annotation classification alone increased from 39% to 87%. With GridSearchCV and *RandomForestClassifier* and *StratifiedKFold,* with 5 splits*,* cross validation in Scikit-Learn, following SMOTE balancing, the accuracy of classifying the A-type annotation increased to 100% and overall prediction accuracy increased to more than 97%. The *StratifiedKFold* cross validation helped to minimise overfitting. Prior to the novel feature extraction algorithm based on spectral analysis and data analysis using imbalance reduction, the classification models were not able to produce accurate results due to subtle differences in the V, A, N type annotations. After having established the feature importance and by choosing PR_PSD, PR interval, QRS_PSD, QRS interval and RR Interval as top five features out of the total 8, which explained 95% of total explained variance, the classification accuracy increased to more than 97%. The major factor contributing to higher classification accuracy was the spectral analysis study of the ECG signal and its sub-portions. In the absence of power spectral density measure of the sub portions of the ECG wave, e.g. P-wave and the T-wave of the once the heartbeats, the PR interval duration itself would not contribute to the variance in the predictor feature variable. It was confounding that the PR interval remaining same the power spectral density could be different. The trained models could be persisted and deployed on a restricted hardware (CHM kit 3.1) using Scikit-Learn *pickle* package.

By combining the real-time data acquisition, signal processing and arrhythmia classification, the early stage arrhythmia classifier could analyse and classify arrhythmia continuously in real time and could raise appropriate alarms. With the further integration with electronic health records and other ubiquitous platforms, the method could be extended to monitor and to respond to emergencies related to health monitoring of individuals while they remain engaged in day to day activities (Nguyen et al. 2017).

4.8.2 ECG signal acquisition and an extended feature extraction algorithm

The problems associated with ECG signal acquisition have always been related to electrical interference, body motion and its effect on the waveform that manifests as baseline wander. The raw ECG signal is noisy and the ECG waveform characteristics such as PR interval, QRS interval and the RR interval could not be accurately calculated from this noisy signal. If the signal was not appropriately filtered and conditioned, these errors would have manifested as approximation errors and could have affected further analysis. The 3 lead ECG sensor AD8233 from Analog Devices interfaced with Arduino Micro and Beaglebone black could effectively sample the ECG signals at 1 kHz and 10 bit ADC resolution. The samples acquired by Beaglebone black over the serial port contained ECG, PPG signals and the ECG signals were separated and resampled at 360 Hz to be converted to an appropriate WFDB format. The signal was de-noised and filtered and errors due to motion artefacts were minimised using appropriate filtering techniques and baseline wander corrections. The Chebyshev II 2^{nd} order filter along with Savitzky-Golay filter (window length 101 and order 3) were effective in noise removal and baseline correction. These filters could be effectively implemented using SciPy on Beaglebone black with Debian Linux 7.9 and could filter the noisiest portion in the ECG signal. The WFDB routines *WRSAMP, GQRS, ANN2RR, TACH* and *ECGPUWAVE* were very effective in converting the filtered ECG samples into an MITDB compatible record that could be used for feature extraction. The advantage of converting the ECG signal to an MITDB compatible record was that all the routines in the WFDB library could be used on this converted ECG signal the characteristics of the ECG signal. The WFDB routines, along with reading and writing annotations related to QRS locations and start and stop positions of P-wave, QRS wave, T-wave, can also extract physiological parameters such as ECG derived respiration rate, power spectral density, heart rate, arterial blood pressure amongst others. The extended feature extraction algorithm that extracted power spectral densities related to

PR interval, QRS wave and the signal-to-noise ratio in a heartbeat belonging to normal or abnormal type, significantly increased the classification accuracy, even for the underrepresented abnormal A-type annotation.

The limitation of the MITDB dataset was that, not more than 38,371 samples could be obtained for the V, A, N type annotations out of which only 2132 represented the A-type annotations. So the SMOTE balancing technique had to be applied to the feature set, which introduces synthetic samples while over-sampling the underrepresented response variables and under-sampling the over-represented response variables. This introduction of synthetic samples may increase the classification accuracy though the model may not respond as intended when presented with fresh ECG test samples. This limitation could be overcome if an extended dataset with adequate samples, which represented all response class type variables could be obtained. The same feature extraction algorithm could be used to extract relevant features from an extended dataset with adequate samples. Due to the non-linearity in the feature vector space and their non-standard distribution a clear decision boundary could not be obtained using linear models like the Support Vector Machines and Logistic Regression. To avoid overfitting Lasso regularisation technique was used with LogisticRegression which showed a balanced accuracy score of 90% and less for the underrepresented A-type annotation. Lasso, Ridge, Elasticnet regularisation techniques could have been used, though due to non-linearity in the feature vector space, these could not be effectively used in the classification models. The biggest advantage of Chebyshev filters is a steeper roll-off at cut-off frequency, though have problems related to passband ripple and ringing effect. Although signal denoising was performed effectively even in the noisiest portion of the signal, motion artefacts introduced due to different states of body motion such as walking or running and sleeping states were not adequately characterised and may require approximation of errors handling using adaptive filters and 3-axis accelerometer. Although these complex classification tasks have been implemented on an IoT device, the power requirement if a concern for 24/7 operation of such a device, especially in cases like detection of PVC and PAC beat annotations, which could appear less than 30 times in 24 hours or even a week, so energy harvesting techniques could be used to manage power consumption.

4.9 Summary: Early warning arrhythmia detection and classification

With an aim to recognise the abnormal patterns in long-term ECG monitoring, the chapter initially described the experiments that were performed using data analysis pipelines for V,A,L,R classification. A preliminary feature extraction algorithm for the MITDB MIT-BIH arrhythmia database has been described giving consideration to the digital format of the records along with the annotations related to the normal and abnormal heart beats that were used in ECG analysis to detect cardiac arrhythmia. The PhysioNet Waveform Database (WFDB) library which provided software routines to query and analyse the MITDB records using these annotations, was used for feature extraction. Currently, there exists no software library in literature that could take an ECG recording in real-time, extract features and annotate the beat samples as belonging to a certain arrhythmia class types. The methods of feature extraction using WFDB routines is presented to determine the effectiveness of using *k-Nearest Neighbours (k-NN)* and *RandomForestClassifier* models and pattern recognition for arrhythmia detection. Initial exploratory analysis was performed on the MITDB records using a reduced feature set (Age, Gender, RR-Interval, signal value (mV)) and class labels containing only the abnormal beat rhythms V,A,L,R representing PVCs, PACs, Left Branch Bundle Blocks (LBBB) and Right Branch Bundle Blocks (RBBB) as adequate number of samples for these arrhythmia types were found in MITDB dataset. The data analysis for V,A,L,R classification is presented in the subsection 4.2.2 Once the effectiveness of using machine learning classification models was established a detailed feature extraction algorithm was developed by extracting features from physiological parameters of the ECG waveform. As was argued that an ECG signal is a non-stationary signal, the statistical properties of the signal could vary over time. Also, no two normal heartbeats or abnormal heartbeats could belonging to the same class type can have the same waveform, so it was difficult to obtain feature values that were consistent in describing and classifying the waveform into a specific arrhythmia type 4.2.3. This problem was resolved by performing wavelet and spectral analysis over the sub-wave portions of the ECG waveform. The methods of spectral analysis of an ECG wave belonging to a class type and it's comparative analysis to differentiate between class types are presented in section on spectral analysis section 4.3. The data analysis section 4.3.3 describes in detail the pipelines used for features transformation (standardisation, normalisation, scaling and dataset imbalance removal) used in data analysis preprocessing tasks prior to generating and fine-tuning the classification models. The rationale behind using a particular supervised learning classification model has also been discussed to explain the choice of a particular model. The results obtained from the data analysis using the classification models are presented in detail in results section using classification report containing accuracy, precision, recall and f1-scores. The classification models were serialised and deployed on a wearable target device, so that the classification of arrhythmia types could be done in real-time in-situ. In the ECG signal acquisition and processing section 4.5 the method of signal acquisition is described, followed by detailed signal processing techniques for signal denoising, filtering and conditioning. The freshly acquired ECG signal is noisy due to electrical interference and motion artefacts, several filtering techniques and wavelet transforms are described along with the rationale of using these techniques. The signal filters were developed in MATLAB signal processing and wavelet toolboxes initially, to model the filter parameters, though since the filter was deployed on the wearable target device a SciPy model was developed using the parameters similar to the MATLAB models. The detailed specification of the digital filter is presented in the filter design subsections 4.5.1 and 4.5.2 Once the ECG samples were filtered, they were digitised according to MITDB compatible data format so that the classification models trained on MITDB dataset could be used on the ECG samples captured in real-time. In order to achieve this task, the WFDB routines were used to transform fresh ECG samples to digitised MITDB format, subsection 4.5.3. A digitisation pipeline along with the feature extraction pipeline provided a unique method of achieving the real-time ECG signal acquisition, transformation and extraction objectives in real-time signal acquisition phase, presented in 4.6 subsection. An extended feature algorithm was developed and is presented as Algorithm 4.2 to achieve the real-time feature extraction pipeline.

Chapter 5

Trauma Analysis

5.1 Introduction

The fatal cardiac arrhythmia can lead to emergencies and trauma conditions, and at any time and location and whilst the individuals remain engaged in their day-to-day activities. As the objective of the research study was to predict early signs of arrhythmia and to produce early warning signs and to predict survival, a reliable trauma scoring measure or measures were required to ascertain patient's health status when an emergency occurred. The vital signs (Holcomb et al. 2005; Lockwood, Conroy-Hiller, and Page 2004) and certain physiological parameters could help in calculating trauma scores to indicate the trauma condition of the patient. In order to perform trauma scoring a health monitoring kit was required to perform arrhythmia classification and trauma analysis simultaneously in real-time. The challenges in performing trauma scoring tasks were that bedside monitors and equipment in hospitalised settings are normally used in trauma scoring and some vital signs such as the respiratory rate and the blood pressure, are normally obtained using clinical instruments such as the Spirometer and the Sphygmomanometer, which are not wearable. Also, trained staff is normally required to attend triage emergencies to interpret the vital signs and to manually calculate and interpret the trauma scores. In the absence of direct measurements, these measures had to be calculated and approximated so that all the vital signs became available for calculations. A solution has been proposed in this chapter to acquire and calculate intermediate vital signs and intermediate trauma scores from ECG and Photoplethysmogram (PPG) signals (Dinh, Luu, and Cao 2017) using the MITDB WFDB libraries (Ary L Goldberger et al. 2000) and signal processing techniques on a wearable resource constrained device. A PPG is an optically obtained plethysmogram that can be used to detect blood volume changes in the micro-vascular bed of tissue. Furthermore, the arrhythmia and trauma related information had to be integrated with Electronics Health Records (EHR) if a trauma event occurred. In order to make this provision the challenge was to encapsulate the trauma related scores, the vital signs profile and the cardiac arrhythmia related information, along with location information, in a standard format and according to clinical terminology acceptable by EHR globally. The trauma and arrhythmia related information could be transmitted in real time and could be shared across multiple EHR repositories and Decision Support Systems (DSS) worldwide for further consultation with medics having diverse skill-sets and for research.

In this chapter operation of the Composite Health Monitoring (CHM) kit (Walinjkar 2018a) explained in section 3.1 is presented in a form of a unique pipeline for ECG and PPG signal acquisition and processing tasks, followed by machine learning based prediction and classification along with the encapsulation of trauma scores, vital signs profile and location information to be transmitted to EHR servers using standard telemetry protocols. A novel trauma scoring algorithm is also presented in this chapter that could aggregate a combination of trauma scores that could determine the prediction of survival of an individual under trauma condition. To determine the efficacy of this algorithm, it was tested on the MIMIC Numerics dataset, which is essentially a vital signs dataset of patients admitted to the ICU. The National Early Warning Signs (NEWS), Revised Trauma Scores (RTS), and TRauma Injury Severity score (TRISS) and Prediction of Survival (Ps) scores were calculated using the vital signs extracted from the dataset (Champion et al. 1989). The vital signs and physiological parameters are usually obtained in a hospitalised environment or from ambulatory equipment, however, the CHM kit presented in this chapter, could calculate these scores in real-time and could provide trauma and prediction survival scores to the critical care team ahead of emergencies. For trauma scoring, the proposed algorithm could approximate and extract respiratory rate and systolic blood pressure from ECG and PPG signals. The MITDB WaveForm DataBase (WFDB) library 3.3.1 was used to extract vital signs from the MIMIC Numerics dataset. The WFDB library is a collection of primitive routines to extract information from any time-series waveform signal. From the physiological parameters extracted using WFDB routines, along with the Pulse Transit Time (PTT) calculated using the ECG and PPG samples (Dinh, Luu, and Cao 2017), the algorithm was able to approximate the respiratory rate and systolic blood pressure, which were used to calculate the trauma scores.

5.2 Methods: Vital signs and conversion to WFDB format

This section describes a unique pipeline of WFDB routines, which when executed in particular order on ECG and PPG samples produced vital signs and physiological parameters that were used in trauma scoring. The WFDB routines required that the samples were in a particular format as described in the pipeline. The steps for obtaining vital signs from fresh ECG and PPG samples and conversion to WFDB compatible format were as follows:

1. The samples from the ECG and PPG sensor were acquired by Arduino Micro clocked at 16MHz and transmitted to BBB over the serial port at 115200 baud and received by BBB using the Adafruit GPIO library for BBB with a sampling frequency of 1 KHz. (Analogue-to-Digital Converter in Arduino Micro has 10-bit resolution counter) The ECG signals were resampled at 360 Hz similar to the sampling frequency of the records in MITDB arrhythmia database. The signal had to be resampled and filtered using Chebyshev II and Savitzky-Golay filters as explained in previous sections, in order to obtain an ECG signal that could be converted to a record compatible to the MITDB database. This step had to be performed as the WFDB routines that were used to extract features from MITDB records, could be used for freshly acquired ECG signal as well. The inter-sample interval between two consecutive samples in the MITDB record was 0.00277 seconds (360 Hz)

2. The `WRSAMP -F 360 -G 1000 -i ECGPPGSamples.txt -o dat` command from WFDB was used to convert these samples to a WFDB-compatible record where 1000 was the gain. The WFDB record conversion sampling frequency is 360 Hz, which was different from the data acquisition sampling frequency of 1 KHz. The routing generated the *ECGPPGSamples.dat* file containing the WFDB compatible samples. It is a common clinical practice that the ECG strips are analysed in batches of 10 second intervals, as each ECG strip is 10 seconds in duration.

3. The `GQRS -r ECGPPGSamples.dat -m 1.5` command was used to obtain the QRS complexes from the samples. The threshold was set to 1.5 Volts, and a `qrs` annotation file was generated. The QRS annotations are the locations in the ECG waveforms where the QRS peaks occur. This `qrs` annotation file was used by the other WFDB routines to extract features.

4. The `RDANN -r ECGPPGSamples -a qrs` command, which uses the `qrs` annotation file, was used to detect the R-peaks in the ECG waveform. The command generated file containing timestamps (as sample numbers) and R-peak locations at these timestamps.

5. The `TACH -a qrs -r ECGPPGSamples` command, which uses the `qrs` annotation file, was used to detect the instantaneous heart rate in the freshly captured ECG signals. Heart rate was another important physiological parameter in trauma scoring.

6. The `ECGPUWAVE -a qrs -r ECGPPGSamples -o epu` command generated the `epu` annotations file with extension `epu` containing the locations of (,), N, p, t annotations from the corresponding `qrs` file.

7. The `RDANN -a epu -r ECGPPGSamples -p k where k = {(, p, N, t,)}` routine read the epu annotations file to return (, p, N, t,) annotation type/sub-type values with corresponding sample number values at the annotation location corresponding to annotation types/sub-types which were essentially P-wave and T-wave with their onset and stop boundaries and the N-type annotation being the QRS wave. The command was

executed thrice for detecting the locations of P-wave, T-wave, QRS complex and their start and stop locations. The command generated a file for each of these annotation types and sub-types each containing a column of sample numbers which represented the locations of P-wave, T-wave and the QRS complex along with their start and stop positions.

The following additional steps were performed to obtain all the vital signs related information. The two additional physiologic parameters required for vital signs based trauma analysis were the Systolic Blood Pressure (SysBP) and the Respiratory Rate:

(a) The number of samples between an R-peak (i.e. the sample number at the location of N type annotation) and the next available PPG peak was determined, and the time duration corresponding to these samples was calculated, which provided the Pulse Transit Time (PTT) value that was used to determine the systolic blood pressure. At 360 Hz, the WFDB sampling frequency interval between two consecutive samples would be approximately 0.00277 seconds. The systolic blood pressure and the respiratory rate were calculated from the readings from the ECG and PPG sensors using the PTT, the Pulse Arrival Time (PAT), and the Pulse Delay Time (PDT). (Dinh, Luu, and Cao 2017; *Heartisans - How it works* 2017)

(b) The `EDR -r ECGPPGSamples -i ECGPPGSamples -f 0 -t 10` command was used to generate the ECG Derived Respiratory Rate (EDR) samples for 0 to 10 second time frames and corresponding to the `qrs` annotation file. This provided the average respiratory rate over a 10 seconds interval. Traditionally, in a hospitalised or ambulatory patient monitoring situation a Spirometer would be used to obtain respiratory rate. For a wearable kit however, the ECG derived respiratory rate was used instead.

5.2.1 Respiratory Rate and Blood Pressure Calculations

The Respiratory Rate was calculated using the Physionet Waveform

Database (WFDB) library using the EDR routine, and the derived value had a high correlation to the measured values, as found by the authors of the library (Ahmad et al. 2012). Since the ECG waveforms were available, Respiratory Rate was calculated from the ECG waveform itself. Usually, to obtain a respiration signal from an ECG kit, the transthoracic impedance is measured between the ECG electrodes, so the respiration signal is obtained from ECG electrode contacts rather than from the ECG waveform. This method required special-purpose hardware and it was not possible to obtain respiratory rate from a recorded ECG signal. Another method was to obtain the respiratory signal using beat-to-beat variations in RR intervals or their reciprocals, which were primarily due to Respiratory Sinus Arrhythmia (RSA). As this method worked best in younger population, in whom RSA is most pronounced, it could not be used widely as a large number of patients being monitored were an elderly population.

The ECG-Derived Respiration (G. B. Moody, Mark, et al. 1985) technique was based on the observation that the changing ECG electrode position induces transthoracic impedance variations, as the lungs fill and empty. Thus the lead axes vary at different points in the respiratory cycle, and measurement of signals across a cardiac electrical axis showed variations that were correlated with respiration. The EDR could be obtained even if the RSA was absent. The EDR method is an approximation method and not as accurate as Spirometry, however it is effective in the absence of a Spirometer. The WFDB toolkit provided the EDR routine that could extract RR from an ECG signal given a QRS annotation file. The EDR routine is a C program and it was compiled on the BBB with GNU/Unix/Linux target platform.

The Blood Pressure (BP) is also an important vital sign used in trauma scoring, and in the absence of an integrated sensor, there were challenges to measure BP, and to remove motion artefacts. Researchers have tried to overcome these challenges by analysing oscillometric pulses after amplitude modulation and amplification of the ECG signal (S. Kumar and Ayub 2015; Park et al. 2006) The Pulse Transit Time (PTT) feature, which was calculated from ECG and PPG signal, could be used for BP estimation. A prototype was developed and tested, which achieved a mean absolute difference of less than '5' mm Hg for estimating the BP with the reference *Omron BP monitor*. It was assumed that in the absence of Respiratory Rate and BP sensors that could be readily integrated with the composite wearable sensor kit, the estimated values of Respiratory Rate and BP derived from ECG waveforms could be used to calculate the trauma and injury scores. PTT was measured as the time interval between the R-peak in an ECG wave and a characteristic point at predetermined peak of the PPG signal in the same cardiac cycle(Dinh, Luu, and Cao 2017; Park et al. 2006). The PTT was the difference in the timestamps between the R-peak and PPG-peak as shown in figure 5.1. By using PTT, the Systolic Blood Pressure (SysBP) was calculated as follows:

$$\begin{aligned} PTT &= T_{PPGpeak} - T_{Rpeak} \\ SBP &= 4.8008600358 * 10^4 * PTT + 1.308532932 \end{aligned} \tag{5.1}$$

The PTT and SysBP expressions 5.1 are used in the next section for real time trauma scoring and prediction of survival. The section also presents the Algorithm 5.1 for real time data acquisition to obtain physiological parameters from human subjects.

5.3 Methods: Algorithm for trauma scoring and survival prediction

As trauma analysis and scoring was performed on MIMIC Numerics dataset an algorithm (Algorithm 5.1) was proposed to derive physiological parameters from the dataset in order to calculate the intermediate trauma scores that could be used in calculation and approximation of prediction of survival. As the dataset belonged to a category of clinical class admitted to the hospital in ICU ward, the prediction of survival values calculated by the algorithm had to agree with the health status of the patients. In addition, the same algorithm was supposed to extract the same physiological parameters that occur in the MIMIC Numerics dataset. As a wearable IoT device, the CHM kit, was used, which had no Spirometer or Sphygmomanometer, the respiratory rate and systolic blood pressure had to be approximated rather than be measured on the human subject. These extracted parameters were then used in the proposed trauma scoring and prediction of survival algorithm. The WFDB routines were used to extract physiological parameters from the ECG and PPG signals acquired from human subject in real time. The WFDB routines were used after converting the raw ECG and PPG signal to a WFDB compatible record. This task involved resampling and denoising of the signals as recommended by MITDB.

As explained in section 5.2.1, the respiratory rate was obtained using the EDR routine from WFDB toolkit and systolic blood pressure was obtained using PTT that was calculated from ECG and PPG samples. An algorithm had to be developed to calculate all the vital signs and physiological parameters from the ECG and PPG readings from a human subject in real time. As the ECG and PPG samples were gathered with a sampling frequency of 1 kHz, these had to be resampled to convert the samples to a WFDB format. As the entire analysis was to be performed within a 10 seconds interval, after which the next batch of samples became available in a Comma Separated Variables (CSV) file generated after sampling the ECG and PPG signals over a 10 seconds interval and the trauma scoring and prediction of survival scoring was performed every 10 seconds. Also, since the ECG strips are normally read over a 10 second interval by cardiologists, the same convention was followed. The samples transmitted by Arduino Micro to BBB in the CSV string format `E:<ecgsamples>, P:<ppgsamples>, S:<spo2readings>` were parsed to split into the ECG samples, the PPG samples and the SpO2 readings. The SpO2 calculations, were performed on Arduino Micro from the PPG samples gathered from the PPG sensor, before they were transmitted to BBB. The SpO2 calculations implemented on Arduino Micro for MAX30100 PPG sensor used the expressions 5.2 , 5.3 and 5.4 provided by the manufacturer and Oxullo Interscans Ltd.(Oxullo 2019). The infra-red sensor reading `(irVal)` and the red LED reading `(redVal)` from the PPG sensor were used, over $X_{irVal}[n]$ and $X_{redVal}[n]$ samples with 1 KHz sensor sampling frequency.

$$\begin{aligned} InfraRed^2 &= \sum_0^n (X_{irVal}[n])^2 \\ Red^2 &= \sum_0^n (X_{redVal}[n])^2 \\ Ratio^2 &= 100.\frac{\log_e \frac{InfraRed^2}{n}}{\log_e \frac{Red^2}{n}} \end{aligned} \tag{5.2}$$

$$\begin{aligned} if(Ratio^2 > 66) \quad index = Ratio^2 - 66 \\ if(Ratio^2 > 50 \quad \text{and} \quad Ratio^2 < 66) \quad index = Ratio^2 - 50 \end{aligned} \tag{5.3}$$

$$\begin{aligned} spO2LUT[43] = \{&100, 100, 100, 100, 99, 99, 99, 99, 99, 99, 98, 98, 98, 98, \\ &98, 97, 97, 97, 97, 97, 97, 96, 96, 96, 96, 96, 96, 95, 95, \\ &95, 95, 95, 95, 94, 94, 94, 94, 94, 93, 93, 93, 93, 93\} \\ spO2 = spO2LUT&[index] \end{aligned} \tag{5.4}$$

The following WFDB routines were used in Algorithm 5.3 to extract physiological parameters from the ECG signal captured from human subject:

The WRSAMP routine in WFDB toolkit was used to generate the digitised WFDB compatible ECG record file sampled at 360 Hz.

The GQRS routine in WFDB toolkit was used to generate the QRS annotator file with the R peaks locations for the ECG samples gathered.

The FindPeaks routine in Python SciPy package which finds all local maxima by simple comparison of neighbouring values, was used to obtain the PPG peak locations in the PPG samples file.

The RDANN routine in WFDB toolkit was used to detect the R-peaks locations using the QRS annotation file.

The PTT value or a cardiac cycle was determined by calculating the difference between the R-peak and the PPG peak locations in the same cardiac cycle, as shown in figure 5.1. The number of samples between these two peaks locations multiplied by a factor of 0.00277 seconds would obtain the PTT value in

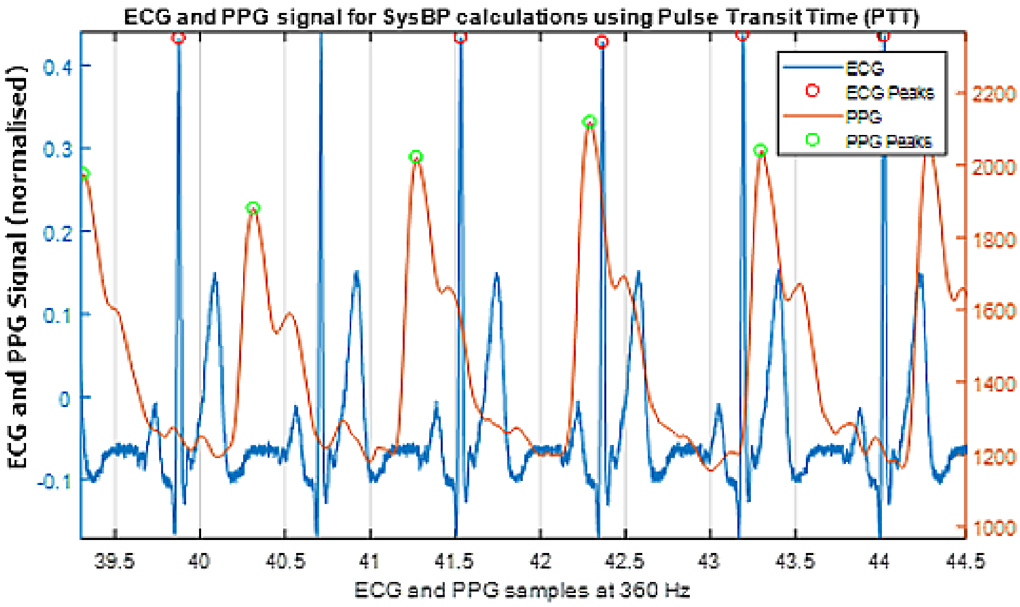

Figure 5.1: ECG and PPG signal for calculating PTT and SysBP

a cardiac cycle. The PTT value was used to calculate the systolic blood pressure.

The PTT value calculated from the ECG and the PPG signals may have contained outliers and noise. A moving average filter with frame length of 3 was used to eliminate the effects of noise, which may have occurred due to noise in ECG and PPG signals. The outliers were eliminated using a Gaussian filter and by providing a filtering condition, e.g. the elimination condition of SysBP > 140. The moving average filter could adequately smooth the data points and provided minimal filtering as shown in figure 5.2.

The TACH routine in WFDB toolkit was used to detect heart rate using the QRS annotation file. The vital signs were thus obtained from a human subject in real time using the PPG and the ECG samples. Depending on whether the samples were obtained from the sensors or from the MIMIC Numerics database, a record tuple was generated for further trauma analysis.

The following steps were carried out on the MIMIC Numerics dataset as no trauma patient was available to demonstrate the trauma scoring in real time:

For the purpose of illustration, considering that the MIMIC Numerics dataset was used, where the patients were admitted to the ICU, GCS score of 4 was assumed. The AVPU score of 3 was assumed as the patient may not be alert and not fully conscious in the ICU. The NEWS score was calculated based

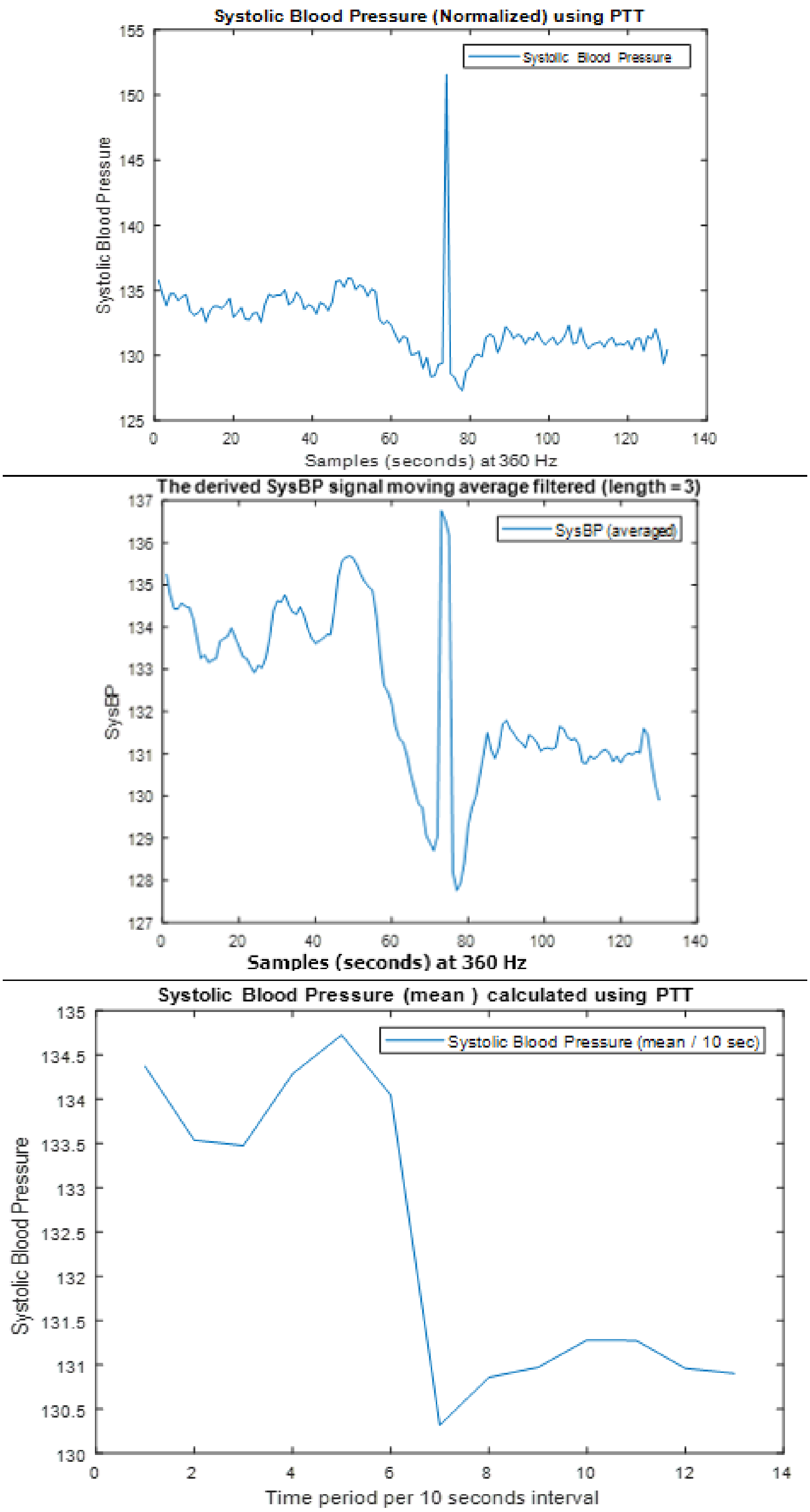

Figure 5.2: Systolic blood pressure (SysBP) (Normalised) calculated using PTT with sample interval 0.00277 (360 Hz) and the expression 5.1. The figure also shows the approximated values using moving average filter

on the NEWS table 2.7 reference values for Respiratory Rate SpO2, supplemental oxygen, temperature, Systolic BP, Heart Rate and alertness AVPU.

The severity levels were associated with the NEWS scores where the severity equals 1 for NEWS if the NEWS ≤ 4, severity equals 2 if $5 \leq$ NEWS ≤ 6 and severity equals 3 if NEWS ≥ 7. The similarity scores could be used to raise alarms and alarms remotely to the critical care team responsible for the patient.

Trauma scores and corresponding physiological parameters.			
	NEWS	**RTS**	**TRISS**
Parameters used	Respiratory Rate Oxygen Saturations Supplemental Oxygen (Y/N) Temperature Systolic Blood Pressure Heart Rate AVPU Score	Glasgow Coma Scale (GCS): Eye + Verbal + Motor response score Systolic BP Respiratory Rate	Uses RTS and ISS ISS: (Anatomical injury scores for Head + Face + Chest + Abdomen injury) Severity of injury
Interpretation	NEWS of 1 to 4: escalation of clinical care NEWS of 5 to 6 or a RED score: escalation to critical care NEWS $\geq$ 7: escalation to critical care with maximum competency	GCS < 15 warrants close attention GCS <8 is of clinical concern RTS $\leq$ 2: critical care situation with less than 15% chance of survival	ISS of 75 and higher is critical with less chance of survival. Ps (blunt or penetrating) values (0 to 1): Values less than 0.15: less chance of survival

Table 5.1: Interpretation of trauma scores and physiological paramters

There were severity levels for the RTS scores as well. If RTS greater than or equal to 12 then the severity score for RTS was assigned a value of 4. Appropriate alerts and alarms could be raised depending on the severity levels according to the reference table values for RTS 2.9.

Following the RTS score, the ISS score was required as for the final trauma score both RTS and ISS scores were required. The AIS scores were assigned based on the severity of injury according to the ISS reference table

2.10. For the MIMIC Numerics data analysis, since the patients were admitted to the ICU, the AIS score of 4 corresponding to injury level `SEVERE` was assumed, resulting in ISS = 48.

Since the trauma was measured using the TRauma and Injury Severity Score (TRISS), all the values pertaining to trauma score were calculated beforehand along with the necessary assumptions according to the RTS, ISS and the TRISS reference table 2.11 and value reference table 5.1. In addition to severe cardiac arrhythmia, the trauma could have also been due to an internal injury or a condition or it could be due to an external injury due to penetration from an external foreign object.

Denoted as blunt or penetrating, the TRISS trauma scores are essentially coefficients calculated using the RTS and ISS scores. These interim scores along with measuring the extent of trauma, are also used in prediction of survival in the individual being monitored and suffering from a traumatic experience. The Probability of Survival (Ps) scores, denoted as Ps_blunt and Ps_penetrating were calculated from these interim scores. A prediction of survival score close to 0 is presumed to indicate certain death and the prediction of survival score close to 1 is indicative of better chances of survival in a critical health situation.

The following algorithm was proposed that could obtain the physiological parameters from human subjects in real time and was used to perform real time trauma calculations.

Algorithm 5.1 Algorithm for extracting physiological parameters from human subject for Trauma Scoring calculations

```
procedure ExtractPhysiologicalParameters(
)                         ▷ /*The timer routing to accept samples in batches of 10 seconds */
    ClinicalClass ← Respiratory_Failure
    File.open(ECGPPGSamples.txt)
    Timer ← 10   seconds
    Timer.start: Call TimerStartRoutine
    On Timer.end: Call TimerEndRoutine
end procedure

procedure TimerStartRoutine
    while Timer ≠ 0 do
        ECGPPGsamplesLine = Serial.readline(ECGPPGsamples)
        csvSamples = parse(ECGPPGsamplesLine, separator = ",")
        ecgSample = csvSamples(E:)
        ppgSample = csvSamples(P:)
        spo2Sample = csvSamples(S:)
        File.writeline(ecgSample + \tab +ppgSample + \tab + spo2Sample + \newline )
    end while
end procedure

procedure TimerEndRoutine
    SysBP_values = Array[]
    SysBPs_samplenumbers = Array[]
    [PPG_peaks, PPG_peakssamplenumbers] =
            SciPy.signal.findpeaks(PPGSamples360Hz, height = 1800)
                                                        ▷ 1800mV threshold for PPG

    SysBP = Call ExtractSystolicBloodPressure(PPG_peaks, PPG_peakssamplenumbers)

    Window = 3
    cumsum, movingavgSysBP = [0], []
    for counter, element = 0 : length(SysBP) - 1 do
        cumsum.append(cumsum[counter-1] + element)
        if counter ≥ Window then
            movingavg = (cumsum[counter] - cumsum[counter-Window])/Window
            movingavgSysBP.append(movingavg)
        end if
    end for
    SysBPs_values = movingavgSysBP                        ▷ corrected SysBP values
    [HeartRate_samplenumbers, HeartRate_samplevalues] =
            TACH -a ECGSamples360Hz.qrs -r ECGSamples.dat
    [RespiratoryRate_samplenumbers, RespiratoryRate_samplevalues] =
            EDR-r ECGSamples.dat -i ECGSamples360Hz.qrs
    File.open(PhysiologicalParameters.txt)
    for i = 0 : length(Rpeaks_samplenumbers do
        if Rpeaks_samplenumbers[i] ==
                SysBPs_samplenumbers[i] == HeartRate_samplenumbers[i] ==
                RespiratoryRate_samplenumbers[i] == Spo2_samplenumbers[i] then
            File.writeline(SysBPs_values[i]+ \tab + HeartRate_samplevalues[i] + \tab +
                RespiratoryRate_samplevalues[i] + \tab + Spo2_samplevalues[i])
        end if
    end for
    Timer.start: Call TimerStartRoutine
end procedure
```

Algorithm 5.2 Algorithm for calculating Systolic Blood Pressure from ECG and PPG readings and Pulse Transit Time (PTT)

procedure EXTRACTSYSTOLICBLOODPRESSURE($R_{peakssamplenumbers}$,$PPG_{peakssamplenumbers}$)
    for (**do**$ecgPeakSampleNumber = 0$: length($R_{peakssamplenumbers}$) - 1)
        for (**do**$ppgPeakSampleNumber = 0$: length($PPG_{peakssamplenumbers}$) - 1)
            if (**then**$ppgPeakSampleNumber > ecgPeakSampleNumber$ && $ppgPeakSampleNumber < ecgPeakSampleNumber + 1$)
                $PTTSampleDiffernce =$ $ppgPeakSampleNumber$ - $ecgPeakSampleNumber$
                $PTT = PTTSampleDiffernce$ * 0.00277
                $SBP =$ `4.8008600358 * 10^4 * PTT + 1.308532932`
                $SysBPs_{values}$.append(SBP)
                $SysBPs_{samplenumbers}$.append($ecgPeakSampleNumber$)
            end if
        end for
    end for
    return $SysBPs_{values}$
end procedure

Algorithm 5.3 Algorithm for Sampling ECG and PPG Signals using WFDB routines

procedure SAMPLEECGPPGWITHWFDBROUTINES
    `WRSAMP -F 360 -G 1000 -I  ECGPPGSamples.txt -o ECGSamples.dat 1 0`
▷ (1 0) indicating only one column with column index = 0 containing ECG samples selected; the other two columns were for PPG and SpO2 readings

    `WRSAMP -F 360 -G 1000 -I  ECGPPGSamples.txt -o PPGSamples.dat 1 1` ▷ (1 1) indicating only one column with column index = 1 containing PPG samples selected
    `WRSAMP -F 360 -G 1000 -I  ECGPPGSamples.txt -o spo2Samples.dat 1 2` ▷ (1 2) indicating only one column with column index = 2 containing spo2 samples selected
    `RDSAMP -r spo2Samples.dat -pS > spo2Samples360Hz.txt`
    $Spo2_sample_numbers$ = Array[]
    $Spo2_sample_values$ = Array[]
    $Spo2sample$ = Array[2]
    File.open(spo2Samples360Hz.txt)
    while ! File.EndOfFile **do**
        $Spo2SampleLine$ = File.readline()
        $Spo2sample$ = parse(Spo2SampleLine, separator = "")
        $Spo2_sample_numbers$.append(Spo2sample[0])
        $Spo2_sample_values$.append(Spo2sample[1])
    end while
    `GQRS -r ECGSamples.dat -o ECGSamples360Hz.qrs  -m 1.5`
    $[R_{peaks}, R_{peakssamplenumbers}]$ = `RDANN -a ECGSamples360Hz.qrs -r ECGSamples.dat`
    `RDSAMP -r PPGSamples.dat > PPGSamples360Hz.txt`
    $PPGSamples360Hz$ = Array[]
    File.open(PPGSamples360Hz.txt)
    while ! File.EndOfFile **do**
        $ppgSample$ = File.readline()
        $PPGSamples360Hz$.append(ppgSample)
    end while
end procedure

5.4 Results: Trauma Analysis

When the Algorithm 5.1 was executed on the MIMIC Numerics database a total of 368,721 samples from eight patients admitted to ICU for the clinical class `Respiratory_Failure` were obtained. It was observed that since the patients were admitted into ICU wards, the NEWS and the RTS scores agreed with their health status as the NEWS and the RTS severity scores less than 4 indicated the patients were under severe trauma. The MIMIC Numerics database, being a critical care database, is widely accepted database of vital signs related analysis. In this chapter however, the Numerics physiological parameters were used for prediction of survival as well. The waveforms for a sample record 033n in MIMIC Numerics dataset is shown in figure 5.3 and the power spectrum of the Respiratory Rate signal associated with the record is shown in figure 5.4.

Once the trauma scores were generated for the MIMIC Numerics database, relationship between NEWS and RTS scores and the prediction of survival scores was determined. Given a set of physiological parameters (heart rate, respiratory rate, blood pressure and oxygen saturation (SpO2)) it was possible to determine which trauma scoring mechanism would be most appropriate for a clinical class of trauma. For illustration, a clinical category of `Respiratory_Failure` was considered for trauma calculations. The NEWS and RTS scores were calculated along with TRISS and Ps scores. In order to determine the degree of correlation between NEWS and RTS scores such that one of these could be used for prediction of survival, correlation analysis was performed between these two feature variables. Although the correlation was derived for clinical class `Respiratory_Failure`, the same task could be performed for other clinical classes such as congestive heart failure and myocardial infarction which are the other two clinical classes represented by the MIMIC Numerics database. The correlation between RTS, NEWS, and the Ps scores was obtained. (Walinjkar 2018a)

As a clinical class where no external injury was considered from the MIMIC Numerics database only the Ps_blunt score was considered for Ps values, with statistical distributions as shown in table 5.2. The NEWS and RTS scores consider different physiological parameters and assumptions with regards to the

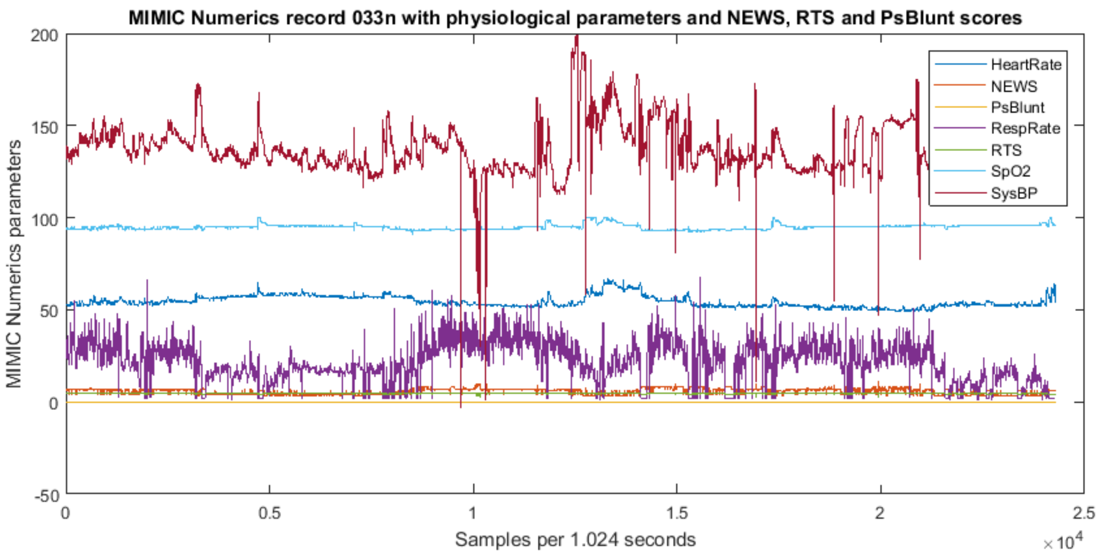

Figure 5.3: MIMIC Numerics record 033n with physiological parameters and NEWS, RTS trauma scores

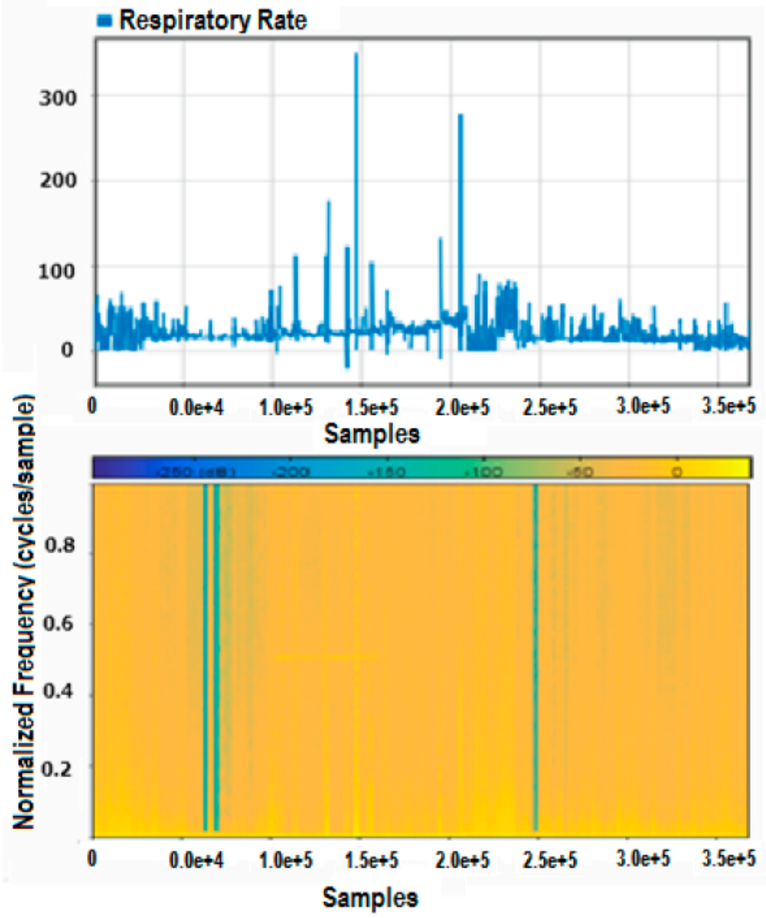

Figure 5.4: The signal waveforms for respiratory rate for Record 033n of the MIMIC Numerics database. Spectral image of the respiratory rate (RR) waveform showing two episodes of respiratory rate failure for Record 033n

patient's health status at a given point in time during the trauma episode. The NEWS score relies mainly on the physiological parameters while the RTS score considers the GCS value involving the sensory response system of an individual.

Descriptive Statistics for Physiological parameters					
	N	Minimum	Maximum	Mean	Std. Deviation
SysBP	368721	-3	360	135.70	26.049
HeartRate	368721	3.85	206.00	63.6646	41.88845
RespiratoryRate	368721	-20	350	20.39	10.448
SpO2	368721	-20	355	77.47	29.424
N (listwise)	368721				
Descriptive Statistics for trauma scores					
	N	Minimum	Maximum	Mean	Std. Deviation
NEWS	368721	3	15	6.88	3.417
RTS	368721	1.9602	5.0304	4.956928	.1815849
PsBlunt	368721	.00979	.40351	.18683	.13184
PsPenetrating	368721	.00777	.34004	.19102	.08811
N (listwise)	368721				

Table 5.2: Descriptive statistics for physiological parameters and trauma scores

The hypothesis to be tested was that given NEWS and the RTS score, will just one of these scores be able to adequately represent the trauma severity and prediction of survival of a patient in trauma situation. It was then required to determine whether there is any correlation between the NEWS and the RTS scores. Also, since Ps score depended on these two scores, how much would the change in either of these two scores affect the Ps scores, so regression analysis was performed for NEWS, RTS and Ps scores. As NEWS is an early warning score, it is normally used to prepare for a trauma situation, while the RTS score provides a measure of the extent of trauma.

Another hypothesis to be tested was that, given the physiological parameters (Heart-rate, Respiratory Rate, SpO2, SysBP), will it be possible to predict the survival of the patient under trauma condition. To test the hypothesis correlational analysis was required between physiological parameters and Ps scores. Also, to what extent would the Ps score change if any of the physiological parameters changed, which required regression analysis between physiological parameters and the Ps scores. The dataset extracted using the algorithm proposed in this chapter with the relevant trauma scores and prediction of survival scores was used with MATLAB and IBM SPSS tools to generate correlation and regression models to discover the relationship between these three scores in trauma analysis. (Walinjkar 2018a)

Correlation: RTS, NEWS and Ps: Would either the RTS or the NEWS score be able to provide measure of trauma for the patient and also predict patient survival?

Assumptions: As RTS and NEWS scores used similar physiological parameters it was assumed that were correlated so either of these would have adequately predicted patient survival. It was assumed that the RTS and the NEWS scores had a strong positive relationship amongst themselves given a trauma condition. A GCS value of 4, corresponding to severe trauma, was assumed as the dataset belonged to patients admitted to the ICU. An AVPU value of 3 was assumed as the patients were in the ICU in an unresponsive state. A clinical class of `Respiratory_Failure` was assumed for 8 human subjects.

Steps: the RTS, NEWS and Ps_blunt scores for all the 8 human subjects were extracted. The descriptive statistics of all the variables were analysed. The Pearson‘s (parametric – assuming normal distribution) correlation coefficients (two-tailed) were calculated for the RTS and NEWS scores, using the bi-variate correlation statistical tool. Linear regression was performed on the NEWS and RTS variables using PS_blunt as the dependent variable to assert predictive capability of NEWS and RTS with regards to prediction of survival.

Correlation: physiological parameters and Ps: Could the physiological parameters SpO2, Heart Rate, Respiratory Rate, systolic Blood Pressure and Age be used to predict patient survival without having to calculate NEWS and RTS? There may be some correlation between the physiological parameters themselves, as some parameters may be interdependent on the others for a particular type of trauma condition.

Assumptions: As a measure for prediction of survival was to be predicted (Ps or

Ps_blunt), regression analysis was required to be performed on the physiological parameters to ascertain the extent of effect the physiological parameters would have on patient survival. Correlational analysis was also performed to figure out relationships amongst the physiological parameters. Age was considered as a factor for regression analysis as a large number of trauma patients, especially, related to respiratory failure and cardiac illnesses belonged to the elderly age group. It was assumed that the physiological parameters may be correlated for a given trauma condition, however, merely having a correlation amongst the parameters may not adequately represent the co-relationship between the parameters (taken collectively) and the dependent variable Ps_blunt. It was therefore assumed that regardless of correlations between the physiological parameters, it was a linear regression analysis that was more important than the correlation. A non-parametric distribution was assumed with the physiological parameters.

Steps: Correlations analysis, table 5.3, was performed on the physiological parameters SysBP, Heart rate, Respiratory Rate, SpO2 and no significant positive co-relationship amongst the parameters was found. Regression analysis was chosen to ascertain predictive capability of physiological parameters. Linear regression analysis was performed on the physiological parameters SpO2, Heart Rate, Respiratory Rate, systolic Blood Pressure and Age with PS_blunt as dependent variable.

Correlations – Physiological parameters						
		SysBP	Heart Rate	Respiratory Rate	SpO2	PsBlunt
SysBP	Pearson Correlation	1	.396**	-.015**	.497**	-.476**
	Sig. (2-tailed)		.000	.000	.000	.000
	N	368721	368721	368721	368721	368721
HeartRate	Pearson Correlation	.396**	1	-.269**	.863**	-.878**
	Sig. (2-tailed)	.000		.000	.000	.000
	N	368721	368721	368721	368721	368721
Respiratory Rate	Pearson Correlation	-.015**	-.269**	1	-.213**	.338**
	Sig. (2-tailed)	.000	.000		.000	.000
	N	368721	368721	368721	368721	368721
SpO2	Pearson Correlation	.497**	.863**	-.213**	1	-.942**
	Sig. (2-tailed)	.000	.000	.000		.000
	N	368721	368721	368721	368721	368721
PsBlunt	Pearson Correlation	-.476**	-.878**	.338**	-.942**	1
	Sig. (2-tailed)	.000	.000	.000	.000	
	N	368721	368721	368721	368721	368721
**. Correlation is significant at the 0.01 level (2-tailed).						

Table 5.3: Correlation between physiological parameters and Probability of Survival

5.5 Results: Relationship of trauma scores with their predictors

In order to validate the hypothesis that there is a correlation between RTS, NEWS, and the Ps blunt or Ps penetrating scores, the statistical analysis had to be performed with an existing dataset. The MIMIC 2 Numerics dataset hosted by PhysioNet was used to perform the statistical analysis. The dataset was cleaned to extract features relevant to the NEWS and the RTS calculations according to patients admitted to the ICU and belonging to a clinical class category `Respiratory_failure`. Once the vital signs samples of all the patients belonging to a clinical category was extracted, columns for each of the vital signs were used for statistical analysis. The analysis was performed on 368,721 samples from eight patients admitted to ICU for the clinical class `Respiratory_failure`. The samples were known to be taken at the interval of 1 second. It was observed that since the patients were admitted into ICU wards, the NEWS and the RTS scores agreed with their health status. The NEWS and the RTS severity scores less than 4 indicated the patients were under severe trauma, and this helped to accept the hypothesis. The MIMIC II (Saeed et al. 2011; Pirracchio 2016; Daniel J. Scott et al. 2013a) database is widely accepted, and some experiments of similar nature have been performed on the dataset, so that it can be used for trauma score calculations. (Walinjkar 2018a)

The vital signs and physiological parameters from PhysioNet and the MIMIC II Numerics (mimicdb/numerics) database were used to calculate NEWS and RTS, and to generate correlation and regression models using the vital signs/physiological parameters for a clinical class of patients with `Respiratory_failure` and admitted to ICU.

NEWS and RTS scores showed no significant correlation ($r = 0.25$, $p < 0.001$) amongst themselves; however together, NEWS and RTS showed significant correlations with Ps (blunt) ($r = 0.70$, $p < 0.001$). RTS and Ps (blunt) scores showed some correlation ($r = 0.63$, $p < 0.001$) and the NEWS score showed significant correlation ($r = 0.79$, $p < 0.001$) with Ps (blunt) scores, as shown in table 5.4.

Regression: Considering the age, heart rate, systolic BP, respiratory rate and SpO2 as predictors to PS_blunt, the predictors showed significant positive R for regression at F (5,368715) = 1098725, $p < 0.001$, total R2 = 93%, as shown in table 5.5.

Both RTS and NEWS that were considered as variables to predict Ps had significant positive relationship with R for regression that was significant at F (2, 368,718) = 442,679.9, $p < 0.001$, total R2 = 70% as shown in table 5.6

There was no significant correlation between NEWS and RTS ($r = 0.25$, $p < 0.001$), which was due to the limitations of the sample space belonging to a particular clinical class. An extensive regression analysis over the entire 'Numerics'

Scores and Correlation Measure		PsBlunt	NEWS	RTS
PsBlunt	Pearson Correlation	1	0.7950 **	0.0630 **
	Sig. (2-tailed)		0.000	0.000
	N	368721	368721	368721
NEWS	Pearson Correlation	0.795 **	1	−0.252 **
	Sig. (2-tailed)	0.000		0.000
	N	368721	368721	368721
RTS	Pearson Correlation	0.063 **	−0.252 **	1
	Sig. (2-tailed)	0.000	0.000	
	N	368721	368721	368721
**Correlation is significant at the 0.01 level (2-tailed).				

Table 5.4: Correlation between RTS, NEWS and PsBlunt scores

Model	R	R Square	Adjusted R Square	Std. Error of the Estimate
1	0.968 [a]	0.937	0.937	0.03306513230
[a] Predictors: (Constant), SpO2, RespiratoryRate, SysBP, HeartRate				

Table 5.5: Regression score between SpO2, RespiratoryRate, SysBP, Heart rate to predict PsBlunt

dataset would be necessary to establish an affirmative correlation between NEWS and RTS scores. There may not be a higher degree of correlation between NEWS and RTS scores themselves, which was due to the sample space considered from a single 'clinical class' for analysis. If the most recent MIMIC II/III Numerics dataset, which contains more than 22,200 records, each record covering 72 hrs, a positive significant relationship between RTS and NEWS could potentially be observed as shown in table 5.6

There was, however, a significant positive relationship between NEWS and PsBlunt (r = 0.79, p = 0.01) and a moderate positive relationship between the RTS and PsBlunt (r = 0.63, p = 0.01). Correlation and regression between Age, Heart rate, SpO2, SysBP and PsBlunt: There were positive significant relationships between Age (r = 0.91, p = 0.01), Heart rate (r = 0.87, p = 0.01), and SpO2 (r = 0.94, p = 0.01) with PsBlunt. There were weak positive relationships between SysBP (r = 0.47, p = 0.01) and Respiratory Rate (r = 0.33, p = 0.01) with PsBlunt.

Parametric Correlations			
		NEWS	RTS
NEWS	Pearson Correlation	1	-.252**
	Sig. (2-tailed)		.000
	N	368721	368721
RTS	Pearson Correlation	-.252**	1
	Sig. (2-tailed)	.000	
	N	368721	368721
**. Correlation is significant at the 0.01 level (2-tailed).			

Regression Model Summary				
Model	R	R Square	Adjusted R Square	Std. Error of the Estimate
1	.840^a	.706	.706	.071489738500000
a. Predictors: (Constant), RTS, NEWS				

ANOVA^a						
Model		Sum of Squares	df	Mean Square	F	Sig.
1	Regression	4524.882	2	2262.441	442679.903	.000^b
	Residual	1884.438	368718	.005		
	Total	6409.319	368720			
a. Dependent Variable: PsBlunt						
b. Predictors: (Constant), RTS, NEWS						

Table 5.6: Correlation and Regression between NEWS and RTS scores

5.6 Methods: Regression model for survival prediction using trauma scores

As the vital signs and the RTS and NEWS scores were significantly correlated to the probability of survival Ps, a regression model was used to determine the prediction efficacy related to the vital signs and trauma scores. So that the regression model generalises and does not cause overfitting, regularisation tasks were performed and ElasticNet model was chosen as the regression model. The ElasticNet regularisation applies both L1-norm and L2-norm regularisation to penalise the coefficients in a regression model. The L1-norm (Lasso regularisation) adds a constraint to the loss-function that penalises the model by the absolute weight coefficients and L2-norm (Ridge regularisation) adds a constraint to the

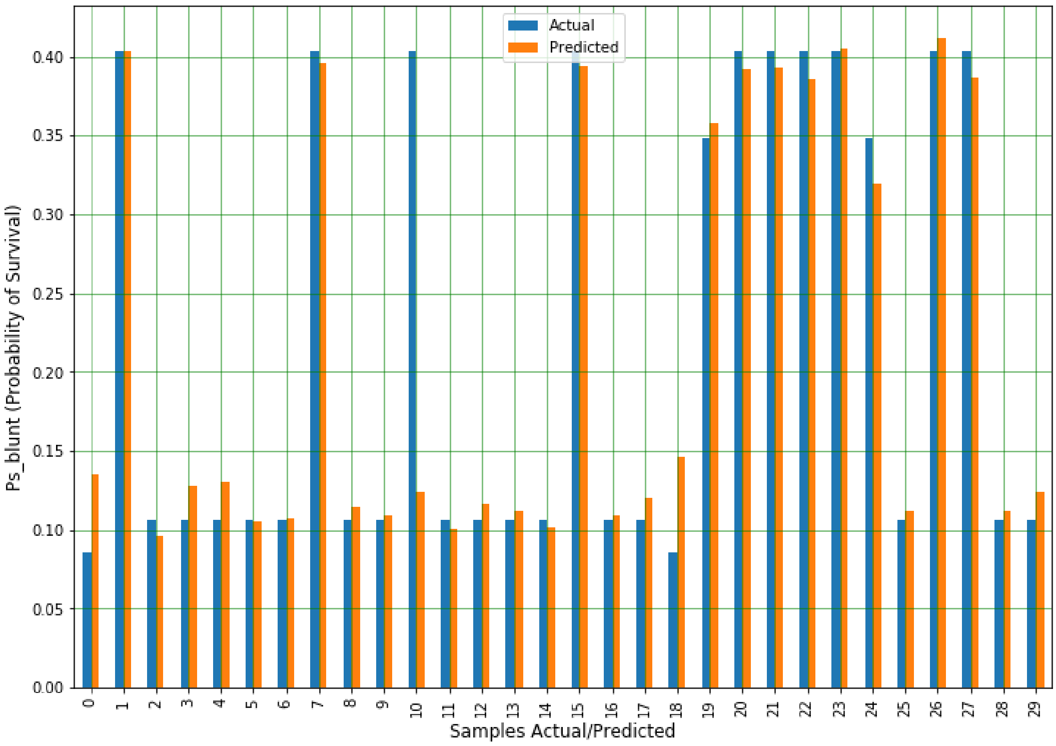

Figure 5.5: Regression chart for Ps_blunt for MIMIC record 033n using trained *ElasticNet* predictor model

loss-function that is a linear function of the squared coefficients. ElasticNetCV model was chosen so that the model could be cross-validated as well to avoid overfitting and to achieve bias-variance trade-off.

Following parameters were chosen for the regression task:

Features variables: 'SysBP','HeartRate','RespRate','SpO2','NEWS','RTS'

Response variable: Ps_blunt

ElasticNetCV alpha values = [0.0001, 0.001, 0.01, 0.1, 0.3, 0.5, 0.7, 1]

Cross-validation value cv = 10 fold

Optimal alpha value returned by cross-validation α *= 0.0001*

	ElasticNetRegressionCoefficient
SysBP	-0.005963
HeartRate	-0.129465
RespRate	0.058491
SpO2	-0.385718
NEWS	0.026419
RTS	0.242047

Figure 5.6: Regression coefficients for *ElasticNet* predictor model

5.7 Results: Probability of survival using trauma scores

The ElasticNetCV regression model produced the following regression scores:

Mean Absolute Error: 0.01447

Mean Squared Error: 0.00106

Root Mean Squared (RMS) Error: 0.0326

The regression model trained on the vital signs extracted from the MIMIC Numerics dataset could predict the Probability of Survival (Ps) with RMS error of less than 3.3% on a test sample MIMIC Numerics record *MIMIC/033n*. A bar-chart showing actual vs predicted values of Ps are shown in figure 5.5 and the ElasticNet regression coefficients are shown in figure 5.6

5.8 Discussion: Real-time trauma analysis using vital signs

The research began with the questions and the hypothesis of being able to calculate trauma scores for patients under trauma, using wearable sensor kits, non-invasively in real time and importantly, under no ambulatory or hospitalisation settings. It was also hypothesised that given the vital signs plus physiological information about the patient and the corresponding trauma scores, the prediction of survival scores could be estimated, which, could help the critical care team at a remote location to prepare for the emergency procedures. To enable such a system to function without key infrastructural changes, location information had to be garnered, and the information payload had to be transmitted in real time and using standard telemetry protocols and clinical coding standards. The four main vital signs like temperature, pulse rate/heart rate, respiration rate (rate of breathing), blood pressure (non-invasive systolic) and oxygen saturation were adequate to calculate the trauma scores and prediction of survival (Clifton et al. 2011; Holcomb et al. 2005; Lockwood, Conroy-Hiller, and Page 2004)

From the results obtained, Chebyshev Type II order 2 passband and Savitzky-Golay filter, turned out to be effective in removing signal noise, motion artefacts, and baseline wandering in ECG and PPG and PPG waveforms, yielding a better signal-to-noise ratio. The respiration rate and blood pressure as vital signs were important physiological parameters, and in the absence of a sensor that can directly and non-invasively measures these parameters, it was found that the ECG-derived measures could be used. Respiratory rate was calculated using the PhysioNet WFDB library using the EDR utility, and the derived value has a high correlation to the measured values, as found by the authors of the library.(G. B. Moody, Mark, et al. 1985) The EDR WFDB routine is a C program and it could be compiled on Beaglebone black target GNU C++ compiler.

Systolic blood pressure, was an important vital sign used in trauma scoring, and in the absence of an integrated sensor; there were challenges in measuring the BP and in removing motion artefacts. The PTT calculations turned out to be very effective in approximating systolic blood pressure using the *findpeaks* methods on ECG and PPG waveforms. Pulse-oximetry, as the fifth vital sign (Mower et al. 1998) was also used in calculating trauma scores, and it was required in trauma calculations and in the prediction of survival assessment. The Oxulllo library for Arduino Micro, discussed earlier in this chapter and in methods chapter, could calculate SpO2 readings non-invasively.

The correlation and regression scores between NEWS, RTS, and Ps scores were studied, and a high degree of regression was observed between the NEWS and RTS, taken together with the Ps. There may not be a higher degree of correlation between the NEWS and RTS themselves, though this may have been due to the limited samples trauma considered from a single 'clinical class' for analysis. A positive significant cor-relationship between RTS and NEWS could potentially be observed, if the most recent MIMIC II/III Numerics dataset, which has more than 22,200 records could be used for regression task.

When an ElasticNet regression model trained on the vital signs extracted from the MIMIC Numerics database was executed on a test sample, it could generalise and predict probability of survival score with a root mean squared error of less than 3.3%, actual vs predicted values of Ps are shown in figure 5.5 and the ElasticNet regression coefficients are shown in figure 5.6.

In the calculations for injury severity scores, TRISS (Boyd, Tolson, and Copes 1987) remains the most commonly used tool for benchmarking trauma fatality outcome. The predictive power of TRISS could be substantially improved by re-classifying the measured parameters, and by altering the coefficients for the sample space belonging to a particular clinical class. The TRISS scores formed the basis for calculation of prediction of survival scores, and for predicting mortality and estimating mortality rate.

Once the early warning and trauma scores were calculated, the EHR with the public health care service provider could be updated using the International Classification of Diseases (ICD) and SNOMED/LOINC (*SNOMED International Browser* 2018; *Injury Data and Resources - ICD Injury Matrices* 2015; Richesson, Andrews, and Krischer 2006) classification coding system using HL7 standards. Fast Health Interoperability Resources FHIR is a HL7 standard that provides interoperability specifications for web services and EHR databases, and by modelling the trauma scores into FHIR 'Observations' and 'Bundles' of information payload the trauma-specific information could be logged into EHR databases for future decision support, and to prepare for emergency procedures ahead of time (Benson and Grieve 2016a; Raths 2014)

It was observed that since the analysis was performed on datasets of patients that were admitted to the ICU wards, the NEWS score, the RTS scores, and the prediction of survival scores agreed with their health status. The NEWS and the RTS severity scores of less than 4 indicated the patients were under severe trauma, and this helped to accept the hypothesis. The MIMIC II Numerics database is a widely accepted database, and the trauma scoring hypothesis could be effectively tested with the datasets in the database as it contained all the vital signs required for calculating trauma scores.

By putting the data acquisition, signal processing tools and techniques along with the trauma scoring and standard clinical coding practices together and by embedding location awareness into the composite healthcare monitoring kit, it could be concluded that a real-time incident response system for trauma related events could be implemented. Such a system would prepare the critical care team in healthcare units to prepare for emergencies well ahead of time, and can reduce the mortality rates for severe injuries and trauma.

5.9 Summary: Trauma analysis

The chapter began with an argument that fatal cardiac arrhythmia episodes can lead to traumatic conditions which may occur any time whilst the individuals being monitored remain engaged in their day-to-day activities. In order to perform trauma analysis wider signs and certain physiological parameters were required. As the CHM kit using this research study could obtain ECG and PPG signals from human subject, the signals had to be used to calculate the intermediate physiological parameters and vital signs. A novel trauma analysis algorithm was developed which used the PhysioNet WFDB library to generate a novel pipeline to extract physiological parameters from the ECG and PPG signals and to convert the signals to an WFDB recognised format.

The major challenge was to calculate blood pressure and respiratory rate using the ECG and PPG signals obtained from human subjects, usually these are obtained using sphygmomanometer and spirometer respectively. The systolic blood pressure was calculated using PTT, which is the time interval between the R-peak in an ECG wave and a pre-determine peak of the PPG wave. The

Respiratory Rate was obtained using WFDB routine called EDR, which provided and approximated measure of the Respiratory Rate.

The algorithm on trauma analysis also calculated the RTS, NEWS, TRISS scores, severity levels and prediction of survival scores associated with a trauma condition, in case of an emergency. The trauma scores along with their associated severity levels, are normally calculated after the patient has been admitted to the hospital under triage conditions, however in doing so, currently, valuable time in providing treatment to the patient is being lost. As the CHM kit could also upload the trauma information to the critical care team from a remote location, the team could prepare in readiness for when the patient arrived at accidents and emergencies. The physiological parameters, the vital signs and various trauma scoring mechanisms were studied and analysed as explained in the Literature Review section 2.8.2.

The MIMIC Numerics database was used to derive correlation between RTS and NEWS trauma scores and to derive correlation between vital signs and probability of survival scores. It was found that, though NEWS and RTS scores were not significantly correlated amongst themselves, individually, they had significant correlation with probability of survival scores. All the vital signs were significantly correlated to the probability of survival scores.

As the objective of developing the trauma analysis algorithm was to be able to predict survival of a patient under trauma condition, a linear regression model was trained on vital signs and trauma scores as predictors. The regression model when used on an isolated record in the MIMIC Numerics database, could predict the probability of survival values with a root mean squared error of 2.5%. The trauma analysis algorithm and the ElasticNet regression model could be easily ported to a restricted hardware such as the BBB to enable real time trauma scoring and survival prediction.

The CHM kit aimed to offer more than the Holter and AliveCor (NICE 2015) monitors in function, with advanced features like early arrhythmia detection and classification, trauma analysis and prediction of survival along with a provision to integrate with the EHR databases.

Chapter 6

Electronic Health Records Interoperability

6.1 Introduction

Electronic Health Records (EHR) is an essential element in human healthcare monitoring these days. As a large amount of data continues being archived and uploaded to healthcare repositories, virtually every second across the globe, vast amount of data mining tasks continue being modelled and modified to extract valuable decision support information. The Health Level 7 (HL7) consortium provides the framework and related standards for the exchange, integration, sharing, and retrieval of electronic health information that supports clinical practice, management and delivery. With the large number of Internet of Things (IoT) health care kits becoming available it has become increasingly difficult to log the real-time patient monitoring information to healthcare repositories. As patients continue being monitored in real-time, it has become essential that the trauma events information such as a stroke or an episode of fatal cardiac arrhythmia be uploaded to the EHR in real-time. Currently available monitoring devices can monitor and analyse an abnormal condition but may not be able to upload these events in real-time. This research study focused on developing real-time interoperability tools and services which could enable wearable IoT devices to interact with an EHR that can provide a standard query and update interface through web-services. As the queries and updates could be performed in real-time a prompt decision support could be obtained in the case of an emergency. The Fast Healthcare Interoperability Resources (FHIR) specification was used to develop the query and update interface and to encode trauma related information in terms of FHIR (Agnew 2016; Braunstein 2018; Raths 2014; Mandel et al. 2016) resources, conceptual and logical models using clinFHIR (Braunstein 2019; Hay 2017) tools. The study did not focus on EHR database modelling as such, rather a novel service model interface to EHR databases based on FHIR standard was researched and developed. This model that could encapsulate the real-time trauma and arrhythmia information, could be reused in any IoT device that required to update the EHR through standard FHIR interfaces. A HAPI FHIR (Agnew 2016) interface was implemented on an IoT device which could upload real-time ECG, PPG and relevant trauma information on a test FHIR server. The HAPI FHIR application code could encapsulate ECG arrhythmia, vital signs and trauma events in a single observation and could upload it to the HAPI FHIR server (Braunstein 2018; Hussain, Langer, and Kohli 2018). Several such observations could be linked to a patient context and could be observed in real time in EHR. The ECG, the PPG, vital signs and trauma events were encoded according to Systematized Nomenclature of Medicine - Clinical Terms (SNOMED-CT) and Logical Observation Identifiers Names and Codes (LOINC) specifications. The alerts and alarms mechanism could assist the emergency response teams at the hospitals to prepare for an emergency well in time. An analogue front-end biomedical device was used for data acquisition and signal processing and the IoT devices were networked over wireless network to upload the events and observations to the FHIR server in real time. The system focussed on ‘preventive care’ to enable timely critical care response.

In this chapter, as referred in publication (Walinjkar 2018b) Appendix A in order to demonstrate that a wearable IoT device could be able to update the EHR records in real time, the hardware and software architecture was extended to accommodate the provision of formatting and encapsulating the ECG analysis and trauma analysis related information in a standard format, such that it could be uploaded to EHR in real-time. Initially, in this chapter, a brief overview of FHIR healthcare interoperability framework has been provided to outline the content and purpose of FHIR resources, models and services that are covered by the FHIR specifications. A brief description of the FHIR resources along with their interrelationships the format of data exchange has been provided. An abstraction of the usability of EHR data across all 5 levels (foundation, implementation, administration, record-keeping and clinical reasoning) has been provided with technical and clinical perspectives. As the research study focused on real time updates, a method of encapsulating health status related information, in standard format, from within the wearable device and using standard telemetry protocol had to be devised. As information being transmitted was of clinical nature, it was encoded using standard coding terminologies using SNOMED CT and LOINC coding systems. In order to demonstrate the use of the coding systems, an overview of SNOMED-CT coding schemes along with interrelationships between clinical codes has been provided. An Oracle Java based FHIR test server and HAPI FHIR client based implementation has been explained. In the methods section a detailed implementation of a HAPI FHIR client has been explained. Before encoding the health status using clinical parameters these had to be modelled using FHIR recording and quotable concepts as FHIR resources, observations and device specific elements. A FHIR modelling tool clinFHIR (Hay 2017) was extensively used for modelling coding concepts and deriving interrelationships between the quotable concepts and medical scenarios. Currently in hospitalised and general practices in NHS UK and several countries across the globe, the cardiac arrhythmia and trauma specific information could only be uploaded in hospitalised or general practice settings, i.e. the primary or the tertiary critical care settings. As the research study aimed at providing real-time solutions in preventive care a provision had to be made within the proposed Composite Health Monitoring (CHM) kit itself to update the EHR as and when emergencies would arise. The usage of clinFHIR tool which modelled codable concepts, resources, and elements, components using scenario modeller, logical modeller and conceptual modelling tools. SNOMED-CT is a coding system that describes clinical concepts, vocabulary, descriptions and inter-relationships between clinical codes. The results and discussions section discusses the advantages of using the FHIR based client application and FHIR modelling tools to develop an IoT-based real-time decision health support system.

6.2 EHR Preview

There are commercially available health monitoring kits for example the Holter ECG kit which is capable of monitoring a patient to record heart's rhythms for 24 to 48 hours during normal human activity (Hughes et al. 2015). The kit however only records the ECG and it does not analyse the heart rhythm to detect heart arrhythmia. The ECG recordings have to be manually analysed by an expert cardiologist. There are several such kits like the Alivecor (Bansal and Joshi 2018) and the Shimmer Sensing kits(A. Burns et al. 2010) which effectively monitor heart conditions though do not upload the traumatic events related information that a patient may have undergone. The system proposed in this research consists of a software implemented on the wearable IoT device which could encapsulate the sample readings in a standard XML or JSON format and could transmit the samples to the analytical server that could upload the FHIR payload to the FHIR server after performing the trauma analysis task in real-time. Attempts have been made in the past to make real time updates to electronic health records using internet client server technologies. To develop such an infrastructure covering the entire state or country could be a complex process and may involve government policy decision making. Even if such an implementation does exist, it may be difficult to integrate an existing system with health records in geographically diverse conditions across the globe, and a standard may be required to bring the management of resources under a single canopy or at least have the resources and services interoperability through standard interfaces. The HL7 (Health Level-7) is a standards agency that develops standards for electronic health resources and FHIR is one such standard that enables electronic health records (EHR) interoperability through web-service interfaces is HL7 FHIR Web services (Raths 2014).

6.3 Overview of FHIR Healthcare Interoperability workflow

FHIR is an emerging standard in healthcare interoperability and it is widely used in tertiary care and hospitalised environments in the presence of critical care staff. The research study focused on applications of early warning cardiac arrhythmia and trauma analysis, it was deemed imperative that the results of data analysis be made applicable to the critical care team ahead of an emergency. For such a system to work efficiently the data analysis results had to be made applicable to the critical care team regardless of time and location of the patient or an individual being monitored. In the literature review chapter is it has been argued that arrhythmia and trauma related episodes often occur when medical help is not available in the vicinity. In such cases the health status related information had to be transmitted to the EHR and the critical care team electronically and in real time using telemetry protocols. A complete workflow of the process from data acquisition to signal conditioning, followed by data analysis and abnormal event classification and further followed by upload of the real time health monitoring information to FHIR server is illustrated in Figure 6.1. A typical situation where such a system could be used would be general practices, care homes, rehabilitation centres and in residences where elderly, disabled and individuals taken ill due to a medical condition have been accommodated and are being monitored. Such a system, due to its wearable nature, can also be used by individuals during their day to day activities. In order for such a system to be effective, the electronic record-keeping algorithms had to be ported and implemented on the proposed IoT CHM kit.

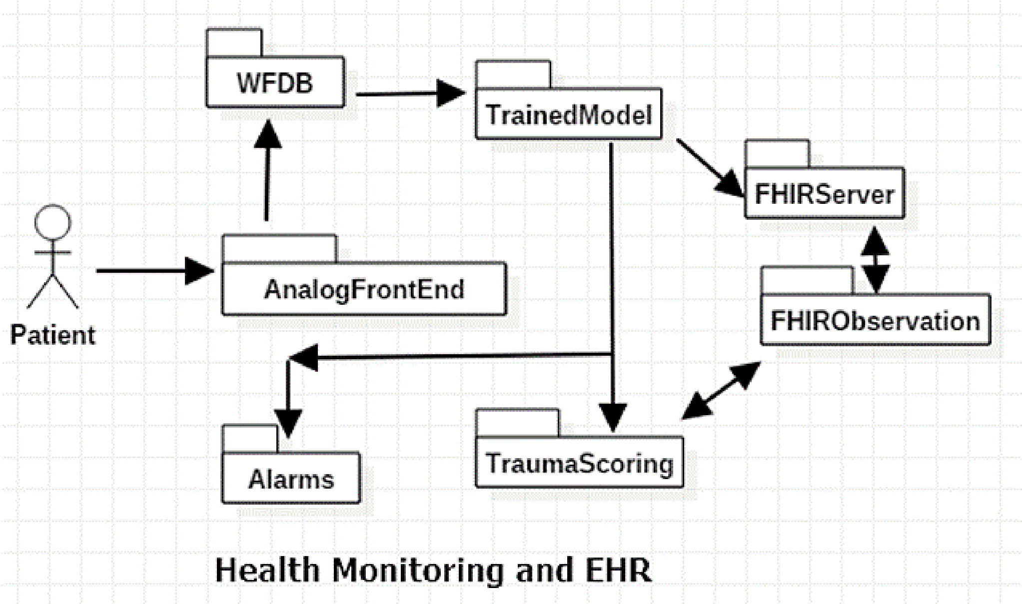

Figure 6.1: Health Monitoring in a typical IoT based wearable kit demonstrating data-acquisition to FHIR observation upload to FHIR Server

6.4 FHIR Interoperability

Fast Healthcare Interoperability Resources (FHIR) defines a set of “Resources” that represent clinical concepts. The resources can be coded and managed in isolation, or aggregated into complex structures and documents which could be archived and queried as and when required. FHIR specifications have been designed for the web; the resources are based on simple XML or (JavaScript Syntax Notation) JSON structures, with an http-based RESTful protocol and each resource is encapsulated and identified by a Uniform Resource Locator (URL). An overall FHIR framework overview(Benson and Grieve 2016b; Benson and Grieve 2016a; Agnew 2016) is shown in table 6.1

6.4.1 FHIR interoperability: A clinical perspective

The FHIR (Mandel et al. 2016) specification was designed to enable the exchange of healthcare-related clinical data and manage public health data and provide data sets for research and was intended to be usable world-wide in a wide variety of contexts, such as in-patient, ambulatory care, acute long-term critical care, community and allied healthcare services. The FHIR specification was chosen to develop software architecture to enable development of interoperable

The FHIR framework overview				
Level I Basic framework	Foundation (data types, extensions and data formats)			
Level II Supporting implementation	Terminology (code system, value set, concept map)	Conformance (structure definition, capability statement)	Security (Security, provenance)	Exchange (RESTful API, messaging services)
Level III Linking to real-world	Administration (Patient, Practitioner, Care team, Device)			
Level IV Record-keeping	Clinical (Allergy, Problem, Procedure, Risk assessment) Diagnostics (Observation, Report, Specimen) Medications (Medication, Request, Dispense, Statement) Workflow (Introduction, Task, Appointment, Schedule) Financial (Claim, Account, Invoice)			
Level V Reasoning healthcare process	Clinical reasoning (Library, Measure, Measurement report)			

Table 6.1: FHIR specification framework across levels of EHR service delivery

solutions using FHIR. The FHIR specification does not attempt to specify good or best clinical practices and does not define workflows or medical pathways for patients or clinicians. In fact it garners existing medical pathways and best practices and device specifications to enable development of digital services to acquire healthcare data to drive research and decision support. In this section only those portions of the specification has been highlighted that are likely to be of an interest to the clinical community.

Resources: From a clinical and enviable perspective, the FHIR resources are the most important elements of the FHIR specification. They could be thought of as the building blocks that reflect different types of clinical and administrative information that can be captured and shared. The resources are templates for individual allergies, prescriptions, referrals, test observations and medical reports. These debits may contain resource instances that may describe patient-related information (health conditions, prescriptions and procedures) as well as administrative information (practitioners, health care service, location). Some resources are infrastructure components that enable record-keeping, pharmacy, medical reports and other allied systems which can form bases for effective clinical decision-making and clinical decision support engines. Each resource template contains a highly-focused and articulated data, though combined with other resource templates, creates a useful clinical record. The resource maps contain information related to the actions that a user (patient, practitioner, ancillary staff) may take e.g. to look up patient records, to make a note in their history or similar such actions.

The resource templates may also have "extensions" to add information to existing resource templates of a particular type. E.g. a "prescription" form might have extension elements added to support tracking of restricted medications depending on allergies of patients. A FHIR resource may not always exist for a patient or a type of medical treatment though due to internal references between the FHIR resources, some information could be calculated.

For the amount of information encapsulated by a FHIR resource, some resources are very broad in terms of the amount of information it may encode, like the all-important Observation resource to encapsulate vital signs, laboratory results, psychological assessments and a variety of other things. FHIR is intended for sharing medical data and visualising only contextual information relevant to the user profiles concerned with the resource. E.g. a plain narrative resource instance containing information such as their phone numbers, their date of birth, their residence address or similar may not be of importance to the practitioner treating the patient, while it may be of relevance to the administrative staff who may want to post referral letters, pathology reports, etc. to the patient's residence.

6.4.2 FHIR interoperability: A developer's perspective

The FHIR resources are exchanged via a RESTful interface, such as active service that can encapsulate relevant information and shared the information across user profiles at remote locations. In this type of RESTful API, the actual interface could be defined by some organisation and different vendors then implement that interface – i.e. provide an actual software that works in the way that the specification describes in order to access and perform tasks on the EHR data to enable decision support. The FHIR RESTful API can enable following actions:

- search: search for existing patient information
- read: read only specific portion of information as allowed or abstracted for a user profile
- create: add new information about the patient related to prescriptions and procedures
- update: add a new page (version) to the contents of a specific folder
- delete: remove a piece of patient information for administrative purposes
- history: review past history of the patient procedures, prescriptions, medications
- transaction: replicate information and shared with multiple user profiles
- operation: perform tasks related to updates, modifications and deletion of the records

6.5 Methods to implement FHIR on IoT devices

Even before the RESTful FHIR client and the server were developed the health status information pertaining to a patient being monitored had to be modelled before being encapsulated according to a resource bundle using FHIR specifications. The clinFHIR tool was used effectively to generate the models to bundle the resources generated from data acquisition, arrhythmia classification, trauma analysis related scores. The CHM kit generates physiological parameters from the data acquisition stage, the ECG and trauma analysis stages along with intermediate results in between these stages. The entire FHIR resource bundle is a composite resource that is output by the CHM kit pertaining to arrhythmia and trauma situation.(Walinjkar 2018b) Such a resource bundle has never been generated in past researches mentioned in the literature review. Currently the FHIR Resources focus only on atomic observations related to ECG such as the

ECG samples and ECG diagnostic reports as examined by an expert cardiologist or a cardiac nurse. Currently the encoding systems such as SNOMED CT or LOINC can encode ECG readings and certain arrhythmia types, though currently no research study exists that is suggestive of encoding early warning arrhythmia and real-time trauma analysis information into a FHIR Resource bundle. In this research not only the ECG readings have been bundled as FHIR Observation, but the early warning arrhythmia such as denoted by the V-type and the A-type arrhythmias, representing the premature ventricular complexes and premature atrial beats respectively, have been encoded and bundled as FHIR Observation. Furthermore, if the cardiac arrhythmia is a fatal kind or if the patient has suffered an accident or has undergone trauma due to a medical health condition, the trauma specific information have also been encoded and bundled as FHIR Resource observations. All the physiological parameters and analytical information generated from the intermediate calculations have been encoded using standard clinical terminologies coding system such as SNOMED-CT and LOINC. Such a wearable system which provides an all-in-one solution from signal acquisition to EHR updates can find application in trauma and triage situations.

6.5.1 FHIR observations encoded according to standard coding systems

The implementation of interoperable component on IoT devices requires modelling FHIR resources, codes and if required codable concepts based on FHIR specifications. As a typical healthcare monitoring kit an analogue front-end device such as the 3-lead ECG sensor was used for data acquisition which in turn was interfaced with their intelligent processor like the Texas Instruments Beaglebone black. The readings obtained from an analogue front-end was de-noised filtered and conditioned to obtain a smooth waveform. In order to classify, detect and separate abnormal signals from the normal ones classification models were developed and trained in existing datasets targeting a particular abnormality. The WFDB was used to extract features from ECG and PPG samples. Once the features were obtained machine learning models were developed to train on a given set of features in order to predict abnormality in test samples. Along with detecting ECG arrhythmia trauma analysis scores were also generated. A JSON (JavaScript Object Notation) structure that encapsulated the sample readings was adopted which passed the samples to the HAPI FHIR test server(Agnew 2016)) to be logged to EHR if anomalies were detected or if the patient's health deteriorated as reflected by the trauma and prediction survival scores. The ECG and PPG samples encapsulated with JSON data structures were transmitted over 10 seconds' intervals to a HAPI FHIR sandbox test server (Agnew 2016) which is a Java implementation of FHIR RESTful Web services. The observation object that encapsulated an instance of observation was coded according to SNOMED-CT coding system as shown in code listing 6.5.1 . An observation object was bundled with information related to an event of abnormal heartbeat or a trauma event with trauma scores and was uploaded to the sandbox test server. The sandbox test server could be a FHIR based data store like GP-Connect from NHS UK (NHS-Digital 2018). Once abnormal beats or waveforms were detected appropriate alarms could be raised and potentially be passed on to the healthcare agency entrusted with the patient care. The FHIR specification on security also supports OAuth authentication and authorisation service which the consumer services can embed in their FHIR servers.

```
Observation getObservationBundle(){
    Observation obsTrauma = new Observation();
        obsTrauma
                .getCode()
                .addCoding()
                .setSystem('http://loinc.org')
                .setCode('74291-6')
                .setDisplay('Trauma Comorbidity');
        obsTrauma.addComponent(new Observation.Component())
                .setValue(
                new QuantityDt()
                        .setValue(Float.parseFloat(
                        arrstrECGDerivedObs[4])))
                .getCode()
                .addCoding()
                .setSystem('http://snomed.org/sct')
```

```
                .setCode('273885003')
                .setDisplay('Revised Trauma Score');
        obsTrauma.addComponent(new Observation.Component())
                .setValue(
                        new QuantityDt()
                              setValue(Float.parseFloat(
                              arrstrECGDerivedObs[5]))
                )
                .getCode()
                .addCoding()
                .setSystem('http://snomed.org/sct')
                .setCode('445416009')
                .setDisplay('Early Warning Score');
        obsTrauma.addComponent(new Observation.Component()).
                setValue(
                        new QuantityDt()
                             .setValue(Float.parseFloat(
                             arrstrECGDerivedObs[6]))
                )
                .getCode()
                .addCoding()
                .setSystem('http://snomed.org/sct')
                .setCode('273886002')
                .setDisplay('Trauma Injury Severity Score');

    return obsTrauma;
}
```

Listing 6.1: Example code to encapsulate a trauma observation

6.6 FHIR Resource modelling using clinFHIR tool

As mentioned earlier the clinFHIR tool was used to model observation resources for the physiological parameters captured and the intermediate results that were generated as a part of analysis tasks. Central to using the clinFHIR tool is the scenario builder, which bills a scenario between interacting FHIR User profiles and FHIR Resources. The scenario builder is an easy-to-use tool that uses graphical interface and graphical models to generate graphical representation of FHIR Resources. In the very least for an example FHIR Appointment resource, the following user profiles and resources could be created using scenario builder. It should be noted that a patient resource created by one organisation may not be similar to the one modelled by another organisation (hospital, healthcare service provider, pharmacy etc.). The FHIR resources and user profiles communicate by exchanging messages, where even if the abstracted data content varies, the operations contracted by RESTful interface remain the same. E.g. the search operation for patient, where the patient information modelled by a general practice would be different from the patient information modelled by another general practice. An example scenario may contain Patient resource who is the subject of the list, the Practitioner resource that created the Patient list, a List of Patient resources and MedicationStatement resources for the individual medications prescribed during individual Appointment resources. An example Patient resource as modelled by clinFHIR tool and the associated JSON structure generated by the tool is shown in figure 6.2. Once the FHIR resources have been modelled and generated in an XML or JSON format they could be exchange between other resources using FHIR Exchange modules and RESTful APIs.

To generate the resource bundle from within the CHM kit following a sequence of events such as cardiac arrhythmia being detected and generation of trauma scores associated with it for a patient resource the following models were generated as shown in figure 6.4.

A Patient resource contained the patient specific information such as name, address, communication contact information etc. For the cardiac arrhythmia related information ECG Observation type and arrhythmia type Observation resources were created.

Following the arrhythmia type detection if a trauma event was generated, a list of vital signs containing the physiological parameters that constitute the vital signs was generated using the List FHIR resource. The vital signs list contained a list of Observations for physiological parameters such as systolic Blood Pressure, Respiratory Rate, Heart rate, SpO2, Temperature. Along with these observations the ECG and the PPG readings at the instance when the arrhythmia and trauma event occurred were also captured as FHIR Observations containing a list of values for a predefined set of intervals.

From the list of observations related to the physiological parameters, an event to calculate trauma scores was generated that created the list of Observations for trauma scores. The trauma scores list of observations contained the RTS, NEWS, TRISS trauma scores that could be used to calculate prediction of survival score in real-time.

The FHIR specification provides a resource classification for medical devices. The CHM kit was modelled as Device resource called composite. The device had a reference to the list of vital signs, a reference to the patient resource, figure 6.3. The patient had a reference to the list of trauma scores there was a direct reference from list of vital signs to the Device resource as the physiological parameters that constituted the vital signs could be directly captured from within the CHM kit.

The clinFHIR tool enables creation of nested resources, where multiple resources and sub- resources can be bundled as a single resource. Each resource could be observed at a lower level of abstraction where relationships between other resources, amongst themselves and also with the main resource could be observed. The composite device resource shown in figure 6.3 has relationships with and references to other resources such as the Patient resource and the List of vital signs resource. An inward directed arrow indicates a resource contained within the main resource e.g. the individual observations such as the PPG readings, the ECG readings, heart rate, arrhythmia type etc. have been shown as being encapsulated within the composite Device resource. The outward directed arrow indicates that only a reference to an external resource has been stored in the current resource. E.g. figure 6.3 shows a reference to the Patient resource from within the Device resource wherein only the resource locator as a reference would be stored in the composite Device resource

Similarly, the List trauma scores resource contains references to the observations pertaining to trauma score calculations for RTS, NEWS and TRISS scores as shown in figure 6.5. As explained earlier that a search query for a

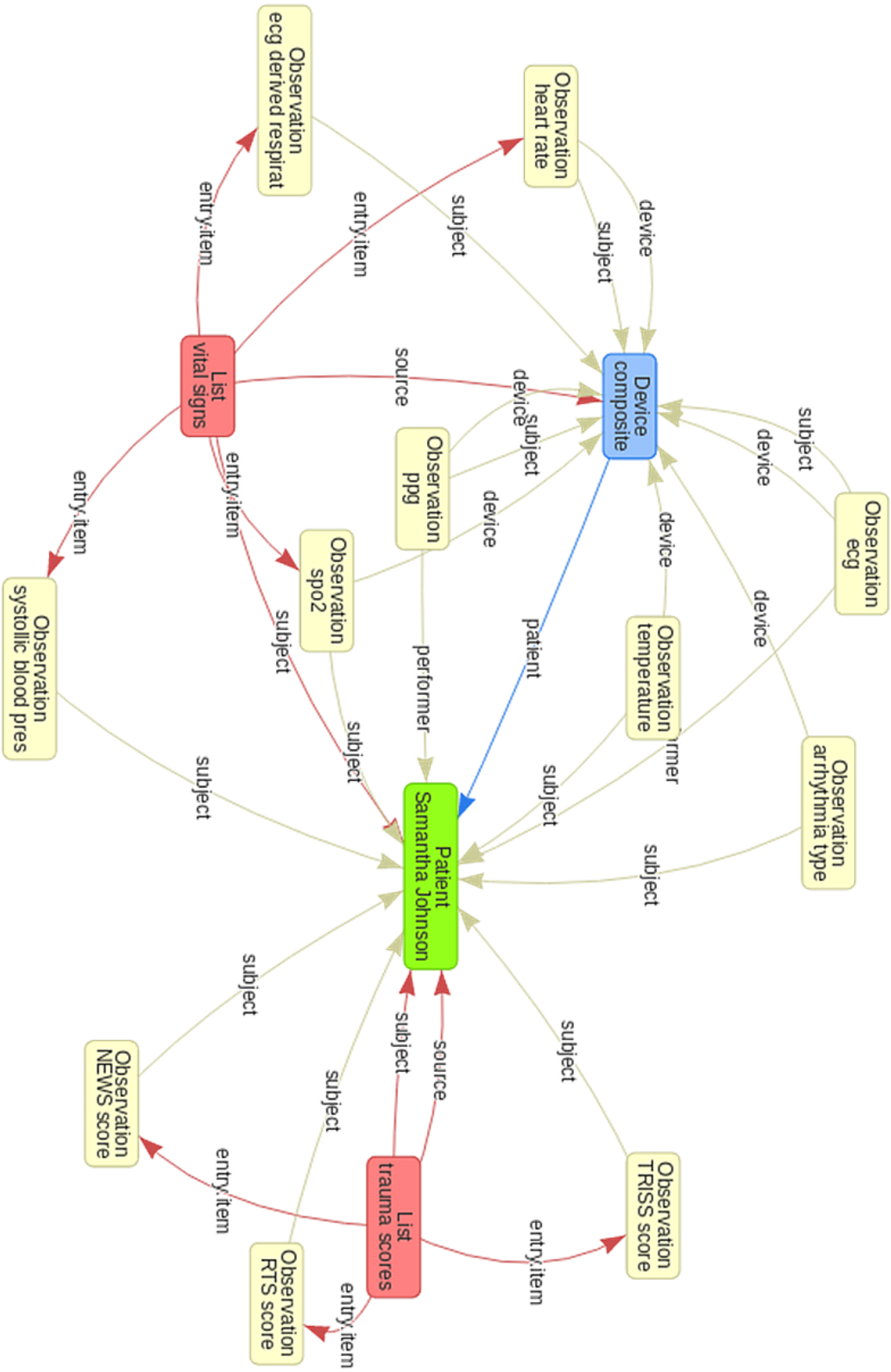

Figure 6.2: FHIR interrelationship between patient, observation, device resources modelled using clinFHIR

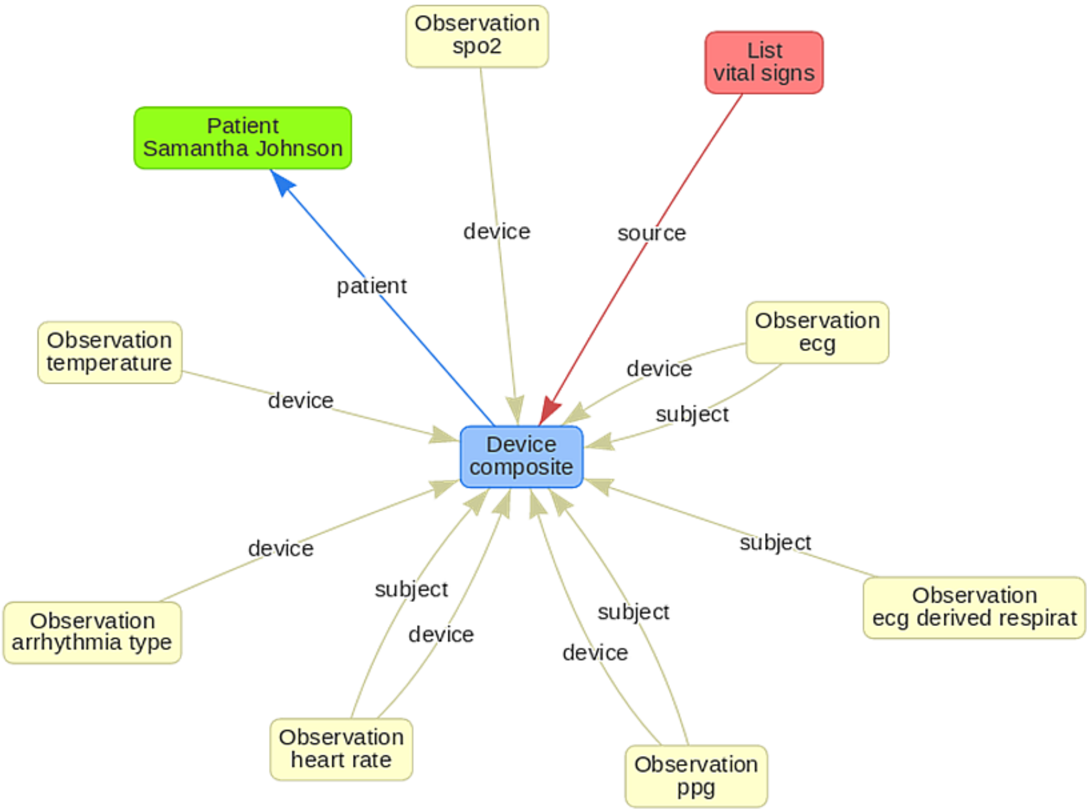

Figure 6.3: clinFHIR model for Device that can capture ECG, PPG readings and can calculate vital signs and provide trauma scores when required

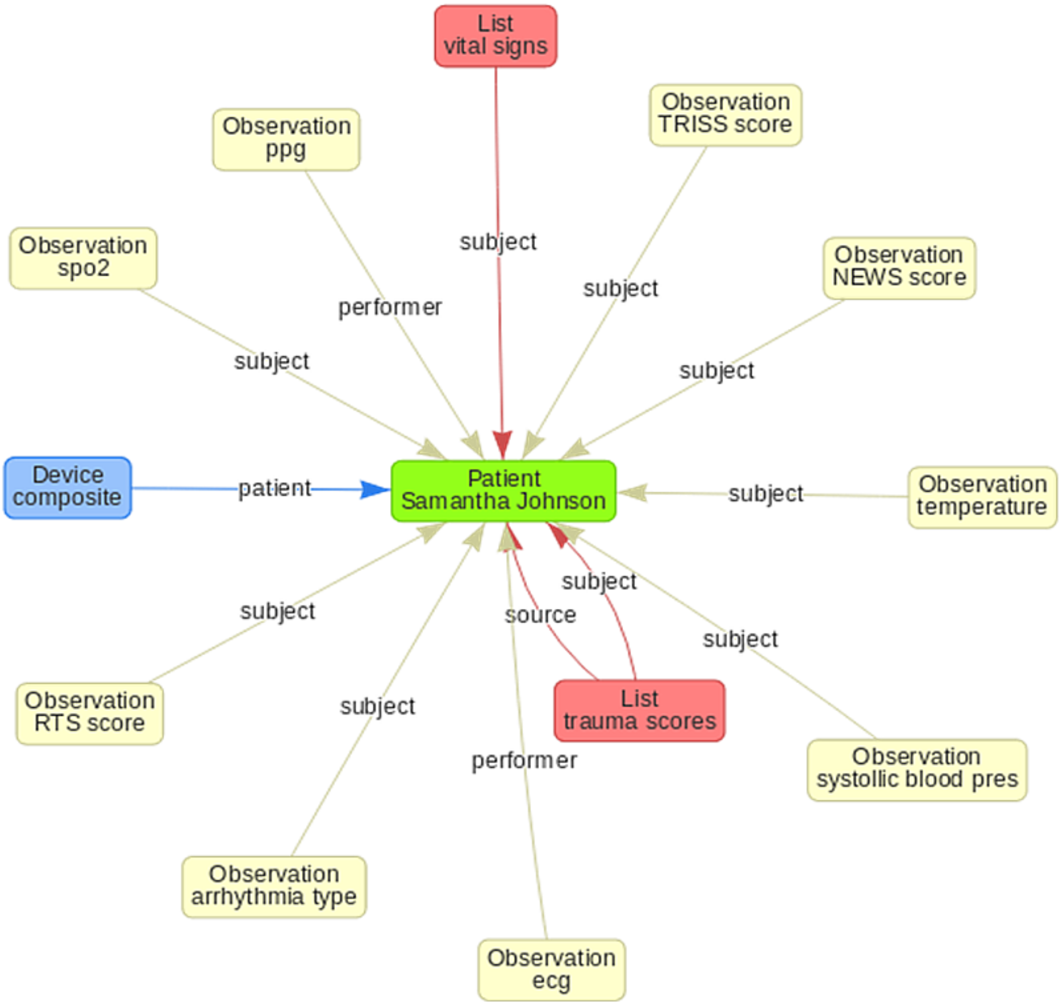

Figure 6.4: A clinFHIR model for Trauma score observation components

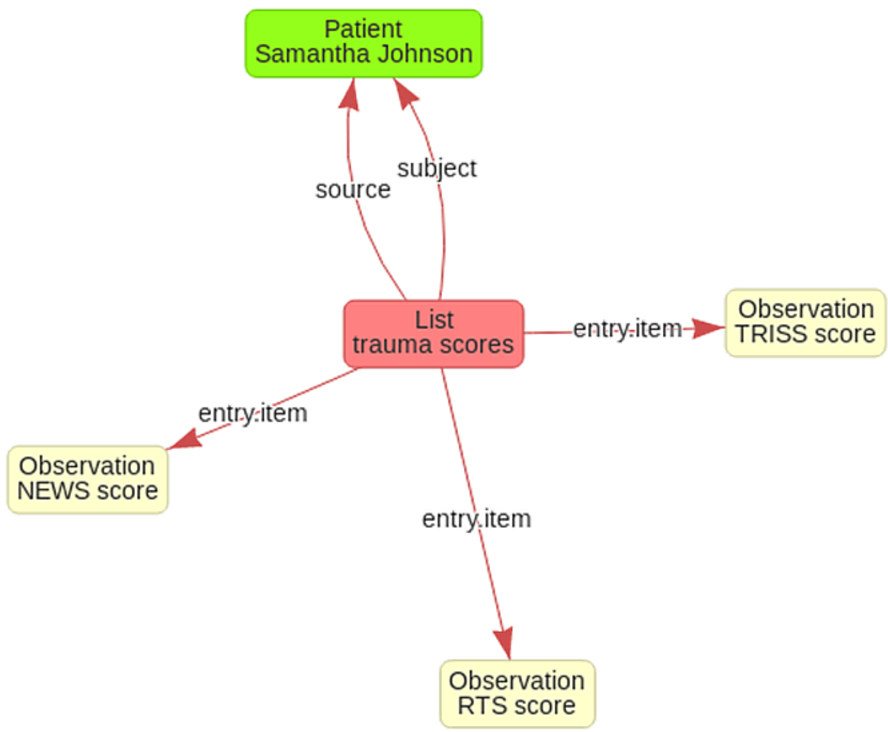

Figure 6.5: clinFHIR model relationship between patient and trauma scores observation

patient resource traverses through all the resources contained within the main resource and also the references to external resources contained within the main resource. E.g. if a read RESTful command is executed on a particular Patient resource using a resource identifier, all the observation bundles contained within the patient resource could be obtained, but also all the other resource bundles such as List trauma scores, Device composite and List vital signs, figure 6.6 can also be read using the read query. The query traverses through all the reference tree structure to acquire information about the resource bundles contained within the resource and also to acquire information related to the resource bundles from their stored references.

If the Patient resource and its relationship with all the bundled Observations and references to List of other observations and the composite Device could be observed, figure 6.4. The clinFHIR can be used as an essential tool to model and observe interrelationships between resources and is a very easy-to-use tool. The tool also helps to allow abstraction and visualisation to only limited level of granularity if constraints have been imposed on a particular resource. E.g. the Administrative staff resource may not have access to information related to

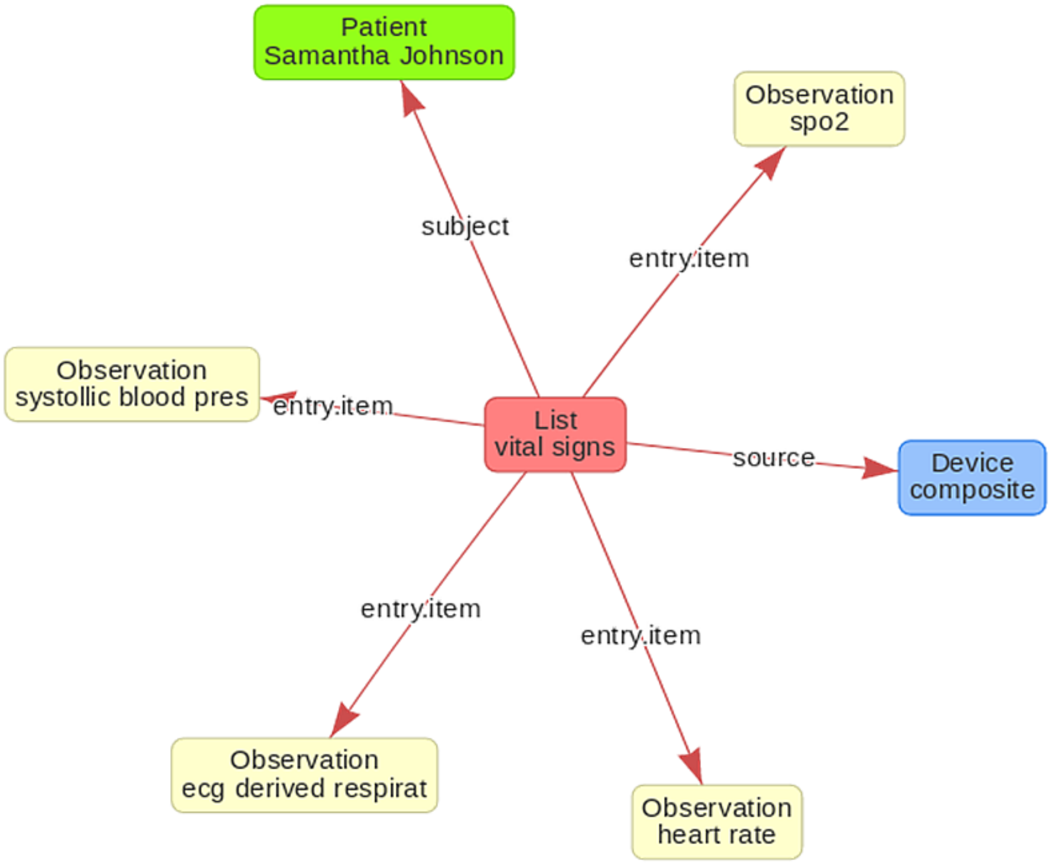

Figure 6.6: A clinFHIR observation resource for vital signs calculated from physiological parameters

Medication resource as it may only be accessible to the Practitioner resource and user profile.

The List vital signs resource in figure 6.6 showing interrelationship between the list of vital signs, the Patient resource and the Device resource. The JSON message generated from clinFHIR tool representing the Patient resource is shown in figure 5.8

6.7 Discussion

One of the objectives of the research study was to develop methods on extracting health status related information and related trauma, if any, in real time and be able to update the EHR repository is using standard protocols and data formats. The major problem associated with such a task was to identify standard telemetry protocols and specifications that have been widely accepted and are currently being used in clinical research and clinical and medical pathways existing within healthcare services worldwide. Although any solution provider can develop bespoke solution for storing and maintaining healthcare, especially public health care data, the data could be used for more productive research purposes only 8 the public health data could be used for research purposes in clinical, research environment. In order to enable sharing of public health data HL7 FHIR specifications has provided a standardised means to access and share suitable information in a controlled manner to enable decision support.

For the purpose of this research study it was not adequate, to only model and encapsulate patient and health status information, as it will required to generate the health status information from within the CHM kit and be able to update the EHR in real-time. The challenge was overcome using the HAPI FHIR client and server RESTful API and a client/server application could be demonstrated from within the CHM kit. The HAPI FHIR client deployed on the CHM kit could create resource bundles pertaining to the physiological parameters acquired from human subject along with the calculated trauma scores could be uploaded to the server if trauma event was detected. The trauma scores and their severity levels could algorithmically detect probability of survival and could raise an event to upload the trauma specific information to FHIR server. The ECG, PPG, Vital Signs and Trauma observations encoded according to a standard coding system (SNOMED-CT or LOINC) would ensure that the FHIR resource bundles could be stored in the EHR in a structured manner for further analysis and research. This system should assist critical care teams to prepare for an emergency ahead of time and may prevent or reduce hazardous situations. The clinFHIR tool turned out to be an effective tool to model FHIR Device and Observation resources. The tool allowed to build a scenario for real time data acquisition and upload of observations. With further consolidation and standardisation of FHIR the same device and observations model could be extended to monitor patients and to upload trauma related information to FHIR serves hosted by public health services in an automated fashion. The device manufacturers can extend the Observation and Device models to encapsulate FHIR resources.

Chapter 7

Conclusions

7.1 Summary

This research study began with an intent to identify and solve problems related to early cardiac arrhythmia detection and classification using a wearable device, which could be worn by an individual regardless of their location and whilst engaged in their day-to-day activities. Cardiac arrhythmia and emergencies associated with accidents and injuries could lead to trauma, so a real-time trauma analysis provision had to be implemented on the wearable health monitoring kit which could assess the trauma severity levels in a patient ahead of an emergency leading to critical care triage situation. The methods chapters *ECG Analysis and Arrhythmia Detection* and *Trauma Analysis* provided solutions and proposed algorithms and devices that solved the problems associated with data acquisition from real human subjects, data analysis in early warning cardiac arrhythmia detection and classification and trauma analysis in real time. These chapters also illustrated the implementation of the algorithms e.g. 4.1, 5.1, 5.3 and the hardware architecture of the wearable monitoring kit with location awareness and electronic health records integration is presented in chapter *Materials* sections 3.1, 3.1.1 and 3.1.3. This chapter presents conclusions drawn from results obtained against aims and objectives as enumerated in the *Aims and Objectives* section in the *Introduction* chapter. The limitations of the results obtained due to tools, techniques and the materials used are also presented.

7.2 Challenges in early warning arrhythmia detection

In the *Introduction* chapter, the current state of art and the problems related to real-time arrhythmia detection were studied and discussed, sections 1.1.1 and 1.3. Although current research in arrhythmia detection illustrates methods and technologies of arrhythmia detection and classification, this has remained confined to machine learning tools and techniques, *Literature Review* section 2.4, which relied on higher compute and memory requirements as compared to the resource constrained IoT devices. The research study presented in this thesis focused on implementing the arrhythmia detection and classification algorithms on a wearable device with restricted hardware. In order to accomplish this task, certain challenges had to be overcome, the most important of which were: training classifier models on arrhythmia datasets, real-time ECG signal acquisition, conditioning and conversion into a format that could be used by the machine learning algorithms that were already trained on a widely used arrhythmia dataset. The real-time constraints associated with the data acquisition and analysis considered in this research study were soft real-time constraints. Having trained the models, these had to be ported to a wearable device implemented on restricted hardware. With regards to the ECG signal acquisition, filtering and signal smoothing had to be performed in real time under noisy conditions as the bio-potential measurement using a wearable device is susceptible to a great degree of noise especially due to external signal interference, muscle movement and motion.

7.3 Challenges in trauma analysis

The *Introduction* chapter sub-section 1.3.2 also mentioned that several cardiac arrhythmia can lead to emergencies and trauma conditions, which need to be monitored and that the emergencies can occur even when the individual being monitored is engaged in day to day activities. A trauma scoring mechanism was required that was widely used in clinical and hospitalised environment and the scoring measures had to be reliable and were required to provide adequate information to ascertain the health status of an individual being monitored. Vital signs and certain physiological parameters were going to provide this information to calculate trauma scores which could be calculated in real-time to produce a measure which could ascertain the extent of trauma and in extreme cases should also be able to provide probability of survival scores. The vital signs required to perform trauma analysis were traditionally obtained from bedside monitors in hospitalised or ambulatory services. Some vital signs such as the respiratory rate and the blood pressure were traditionally obtained using clinical devices such as the spirometer and the sphygmomanometer, which were not easy to use, required calibration, had to be interfaced externally to a measuring device and were not wearable. In the absence of means to directly measure these vital signs, these had to be calculated and approximated so that all the vital signs related information could be produced along with the required physiological parameters that could be used in calculation of trauma scores, section 2.8.2. Technically the challenges were reduced to ECG and the PPG signals analysis in order to extract the intermediate vital signs information using the MITDB WFDB routines and signal filtering/conditioning tools and techniques. For the proposed composite wearable device to be useful to an individual being monitored, the arrhythmia detection and trauma analysis information had to be relayed to the electronic health records where these could be accessed by the general practitioners and the critical care team responsible for the health of the individual. Since the individual being monitored can suffer from a trauma episode regardless of their location, the CHM kit had to be location aware and was supposed to transmit the trauma information in a globally accepted format.

7.4 Contributions against aims and objectives for arrhythmia classification

As discussed in *Literature Review* chapter, section 2.1, the ECG recordings in traditional ECG data acquisition spans over a 10 second interval in a single ECG strip. It was assumed that enough samples covering at least 10 seconds should become available to the arrhythmia classifiers to enable ECG and the trauma analysis tasks presented in this research study. For the samples acquired in real-time, arrhythmia classification tasks were performed on a restricted hardware to classify those arrhythmia types that were a precursor to fatal arrhythmia. To perform these classification tasks, machine learning models were trained on the MIT-BIH MITDB arrhythmia dataset, section 3.3, in order to classify the samples data into the types of arrhythmia that were essentially early warning signs (PACs and PVCs) that may lead to a serious heart condition, section 2.2. In order to train the models feature extraction tasks were carried out using the WFDB routines, section 4.2 and it was argued that though HRV analysis is effective in detecting arrhythmia, it was not the most appropriate technique to detect premature arrhythmia due to their subtle differences in their waveforms and due to maximum reliance of HRV analysis on the morphological structure and heart-rate variance requiring patient monitoring over longer duration. The feature extraction using WFDB routines and data analysis models such as *k-NN* and *RandomForestClassifier* for V,A,L,R arrhythmia classification (Walinjkar and Woods 2017a), presented in sections 4.2.2 and 4.2.2.2 could classify premature arrhythmia with an overall accuracy of more than 97%. Several neural network pattern recognition models with various combinations of training –validation- test data sets were experimented which showed more than 95% overall classification accuracy and it was found that the RR-interval was the most essential feature in V,A,L,R arrhythmia classification task. Although heart-rate could have been used as a feature, since it was found that it was significantly negatively correlated with RR-interval, only RR-interval was considered in the feature vector leading to V,A,L,R classification.

As age and gender were also included as features, the V,A,L,R classification models may have been biased in identifying MITDB records in a certain age group, rather than generalising to classify fresh V,A,L,R samples, these models may only be limited classification tasks for MITDB records, section 4.2.3. The V,A,L,R classification, however, was only aimed at identifying models for arrhythmia classification and to explore the use of WFDB routines extracting features from MITDB datasets. Also, for real time classification of arrhythmia using a wearable device, where the ECG signals could be a mix of normal sinus rhythm and premature arrhythmia, an alternate approach based on spectral analysis (Surda et al. 2007), section 4.3, was chosen as there were subtle differences between the normal sinus rhythm (N-type beats) and premature arrhythmia types (V-type and the A-type). As the power spectral densities were collection of coefficients, bandpower that used the spectral coefficients to estimate power was chosen as feature for each of the sub-waves (P-wave, QRS-wave, T-wave). The power spectral density over sub-waves turned out to be a significant features in V,A,N classification, rather than the interval themselves, as even though there were minor differences in same sub-wave types their bandpower over their respective spectral densities showed significant variance, figure 4.6. The power spectral density over the PR interval alone contributed to more than 35% of feature importance using *RandomForestClassifier*, figure 4.10. A novel feature extraction algorithm based on spectral densities was then developed to extract features from the MITDB records. A unique pre-processing pipeline consisting of WFDB routines *RDSAMP, RDANN and ECGPUWAVE* was used to extract `(,), p, N, t` annotation sub-types from an ECG wave. The finite state machines for each of the V, A, N annotation types, section 4.3.2.1 and figure 4.8, based on annotation sub-type transitions were modelled and were implemented in the novel feature extraction algorithm. The finite state machines ensured that only a unique set of input annotation sub-type sequence be accepted to reach the final state corresponding to each of the V, A, N annotation types. Each sub-type sequence e.g. `'(, p,)'` marked the boundaries of the sub-wave which also helped in determining whether a sub-wave is present or absent and also helped in calculating the spectral densities and bandpower of that sub-wave. The algorithm extracted the relevant features that could be used to differentiate and identify V-type and A-type annotations related to the early warning arrhythmia PVCs and PACs, respectively.

From the nature of the dataset and classification tasks at hands *k-NN* or tree based models e.g. *RandomForestClassifier* seemed like an appropriate choice (Krasteva et al. 2015). A six stage pipeline was developed with a unique pre-processor stage pipeline from section 4.3.3 which produced an overall classification accuracy score of 97%, section 4.4. A dataset imbalance was observed prior to data analysis task with samples for A-type = 2132, N-type = 26362 and for V-type = 9877. After the SMOTE imbalance removal technique the precision accuracy for classification of most under-represented A-type annotation improved to 90% recall score and for N-type annotation the precision accuracy was 91% as shown in table 4.9. As the *k-NN* classifier and the tree based models are susceptible to overfitting, *StratifiedKFold* cross-validation with five splits was performed such that these models could generalised and could be used on the freshly acquired ECG samples. As the data analysis pipeline could be persisted and deployed on the target device to execute the prediction tasks on fresh ECG samples, the training tasks were not required to be executed on the target device, nor were any of the regularisation, dataset balancing or cross validation tasks performed again on the target device. Since the model was already trained, tested and cross-validated, it performed its classification tasks on the target device with overall precision of 91% and A-type classification precision, recall and f1-scores of 100%, 73%, 84% respectively, section 4.7, A-type being the most under-represented annotation type in the MITDB arrhythmia dataset. The test record was the *MITDB/223* record which contained both V-type and A-type annotations and which was completely isolated from training and test data when the classifier was trained.

The ECG signal acquisition phase had to deal with problems related to signal filtering due to body posture, motion and environmental conditions and the signal had to be normalised and denoised using appropriate filtering and signal conditioning techniques on the target device. The Chebyshev and Savitzky-Golay filters were designed (Walinjkar 2018a) to obtain a denoise, detrended and baseline corrected ECG signal from human subject, figure 4.14 section 4.5.2.

As the classification model trained on MITDB dataset that was deployed on a target device would run prediction tasks on freshly acquired signal, these test signals had to be MITDB compatible. A conversion pipeline using WFDB routines 4.5.3 was implemented that would further convert the test ECG signals to WFDB MITDB compatible record. This step ensured that the classifier encountered the same feature values that were used when the model was trained. The classifier when executed the prediction task on this converted signal on target device, produced an overall classification accuracy of over 91%, section 4.7.

This essentially completed the real-time arrhythmia classification workflow from signal acquisition, signal filtering, WFDB format conversion to premature arrhythmia classification, which was the aim of the ECG analysis task at the start of the research study.

7.5 Contributions against aims and objectives for trauma analysis

As discussed in the *Introduction* chapter, section1.3.2 cardiac arrhythmia or severe injury could lead to a trauma situation and the provision was required within the monitoring device to perform trauma scoring tasks in real-time and upload the trauma scores and vital signs to electronic health records in real time. The chapter *Trauma Analysis* focused mainly on solving the problems related to extracting vital signs information (Holcomb et al, 2005) using the CHM kit that performed the signal and data acquisition tasks, followed by machine learning based prediction and classification and encapsulation of trauma scores along with location aware scores transmission to EHR using FHIR Web services. Vital signs MIMIC Numerics database maintained by PhysioNet MITDB (Saeed et al. 2011) was used to extract vital signs related features to calculate the trauma related scores, section 2.8.2: National Early Warning Signs (NEWS), Revised Trauma Scores (RTS), TRauma Injury Severity score (TRISS) and Probability of Survival (Ps) (Boyd, Tolson, and Copes 1987; S. Baker 2018; G. Smith 2017; Champion 2018). These scores are usually calculated using bedside monitoring devices in a hospitalised or ambulatory equipment, though the proposed CHM kit, which is a wearable restricted device, could calculate these scores in real-time and could provide trauma and probability of survival scores to the critical care team in real-time to enable them to prepare for emergencies. In order to achieve this task, the CHM kit had to approximate and extract respiratory rate and systolic blood pressure from ECG and PPG signals, section 5.2.1, which are traditionally captured by spirometer and sphygmomanometer in hospitalised or ambulatory settings. The algorithm to extract vital signs from ECG and PPG signals was tested on the vital signs MIMIC Numerics dataset. The MITDB WFDB library was used to extract vital signs from the MIMIC Numerics dataset. Based on the WFDB routines and the evidence that systolic blood pressure could be approximated using the Pulse Transit Time (PTT) (Ahmad et al. 2012; S. Kumar and Ayub 2015; Dinh, Luu, and Cao 2017) algorithms 5.1, 5.2 could approximate the respiratory rate and systolic blood pressure which along with other physiological parameters were used to calculate the trauma scores.

In the absence of availability of a patient with signs of trauma, the MIMIC Numerics dataset, section 3.4, which contained the vital signs related samples of patients admitted to the ICU, was used to develop and test the effectiveness of the algorithm for trauma scoring and probability of survival. The algorithm on trauma analysis also calculated the severity levels associated with a trauma, which provided the vital information in assessing the critical health status of the patient under a given trauma condition. The trauma scores and their associated severity levels are normally obtained after the patient has been admitted to the hospital under triage conditions. This assessment of trauma only after admitting the patient using bedside monitors and under an expert practitioner's supervision is highly subjective and vital time could be lost in arranging the equipment and staff to handle the emergency. As the CHM kit could calculate the trauma scores in real-time and could provide this information, ahead of time, the critical care team could prepare for emergency response well in time. This provision of assessing the health status in real-time and ahead of an emergency, ubiquitously and regardless of location, makes the CHM kit (an IoT device) an essential tool that could be used in hospitalised and non-hospitalised settings (Duking et al. 2016). The *Trauma Analysis* chapter also focused on deriving relationships between the calculated trauma scores and the dependent probability of survival score, section 5.5. As RTS and NEWS scores were significantly correlated to probability of survival score, one of these could be used in a regression task, section 5.6, to predict the survival score for the patient experiencing trauma.

The chapter *Electronic Health Records Interoperability* focused on developing client-server interface models and data structures to interface with electronic health records using the FHIR protocol and Web-services (Mandel et al. 2016; Agnew 2016). The FHIR Web services was a preferred choice as it has gained substantial prominence in recent years and is currently the most widely used specification for healthcare interoperability. FHIR resource models were created using a FHIR resource modelling tool *clinFHIR* to derive relationships between vital signs and trauma scores, section 6.6. The challenge was then reduced to encapsulating the trauma, physiological parameters according to the FHIR specification and transmitting the payload according to appropriate web-service interfaces implemented using a HAPI FHIR implementation, section 6.5.1.

The CHM kit aimed to offer more than the Holter and AliveCor (Hughes et al. 2015; NICE 2015; Bansal and Joshi 2018), section 1.1.1 monitors in function, with advanced features like early arrhythmia detection and classification, trauma analysis and prediction of survival along with a provision to integrate with the electronic health records.

7.6 Limitations and recommendations

7.6.1 Limitations and recommendations: ECG analysis

The ECG analysis chapter focused on real-time signal acquisition and data analysis. The major limitation of the research study was the absence of clinical-trials of the CHM kit on a patient diagnosed with premature or fatal arrhythmia. Although the premature arrhythmia classifier was tested on a completely isolated MITDB record that was not included in the training and validation of the classifier, it couldn't be tested on a human subject suffering from premature arrhythmia. The signal processing and filtering stage focused on noise removal and baseline wander removal of the freshly acquired ECG signal and obtain a noise free WFDB compatible signal, though motion artefacts related to random motion of the CHM kit according to various degrees of freedom could not be adequately addressed due to absence of datasets that contained both cardiac arrhythmia annotations and motion artefact annotations. Due to unavailability of such a dataset the classifier models couldn't be trained on waveforms that contained both abnormal beats and noise due to motion artefacts. Although there exists a dataset on PhysioNet repository for ECG signals with motion artefacts, the dataset does not contain cardiac arrhythmia related annotations. In addition, the effects of motion artefacts on premature arrhythmia related to motion state E.G.standing running climbing could not be studied due to absence of a dataset annotated with these motion states and arrhythmia annotations.

The preliminary V,A,L,R classification tasks, which focused on identifying machine-learning and neural-network models for arrhythmia classification, considered all 48 records in MITDB dataset for training the classifiers. Although the classifier was cross validated, it was not tested on a record which was not part of the training dataset which may lead to possible contamination of the training – test split of the dataset. As the classifier model included age, gender as features, the model may only be classifying V,A,L,R arrhythmia subjective to the MITDB records and may not have generalised when used on fresh ECG samples. The use of V,A,L,R classification task was only restricted to exploring classification models for V,A,L,R arrhythmia types and was not intended to be used for further analysis in premature cardiac arrhythmia detection and classification. A more elaborate and detailed feature extraction model based on spectral analysis focusing on spectral components of sub waves in an ECG signal was hence developed and implemented as an algorithm, both for MITDB records and for feature extraction from an ECG signal from a human subject.

The V,A,N annotation classifier that was tested on a *MITDB/223* record was completely isolated from the training and test data during the training phase, produced recall and f1-scores of 73% and 84% respectively, though this was due to the lack of adequate number of samples; A-type samples were only 2,132 (5.5%) out of a total of 38,371 samples across all the V,A,N annotations. As the classifier could predict V-type and N-type with overall accuracy of 91%, the accuracy could improve if the classifier was trained with adequate samples for V,A,N type annotations. PhysioNet maintainers now suggest that for further data analysis MIMIC III (Johnson et al. 2016) dataset should be considered, which has more than 22,317 waveform records, although these are in the process of being annotated with annotations related to arrhythmia.

7.6.2 Limitations and recommendations : trauma analysis

Only eight patients belonging to a particular clinical class were considered for trauma analysis; with additional samples, the correlation scores between RTS and NEWS may improve. Also, with additional information related to blood chemistry using portable blood chemistry analysis kits, it would be possible to predict mortality and probability of survival using Simplified Acute Physiology Score (SAPS II) (Aminiahidashti et al. 2017; Pirracchio 2016) scores, which is the more precise score, as it also considers blood chemistry and urine samples. In addition, further research may consider the activity monitoring of the human subject using the accelerometer module, which could give more insights into the effect of activity on the ECG and PPG readings. The MIMIC Numerics records were stored in a format that are similar to the waveform records, but since the sampling rates were far lesser than the MITDB records, the Numerics records could not be used for ECG and trauma analysis both. In this research study two separate models for ECG and trauma analysis were developed, though if a dataset containing both, ECG waveforms and vital signs had become available, a single feature extraction algorithm along with a data analysis pipeline could have performed classification and survival prediction tasks in a single sweep. The Numerics data also contained annotations that were related to the patient alerts and monitoring device-related alerts with other non-periodic data; e.g., electrodes being misplaced or devices being disconnected, etc. Information was available for some of the ICU monitor alerts, in some cases with additional observations that were collected from other equipment sources. The copies of the alarm annotation files containing information about these alerts were linked to both the waveform and the Numerics records. Since MIMIC II database is a combination of the waveform and clinical database, a *QueryBuilder* could be used to link the waveform, the Numerics (vital signs), and the clinical information using a Structured Query Language (SQL) could be queried. MIMIC-II was used for annual PhysioNet/Computing in Cardiology Challenges, including the 2012 Challenge, “Predicting mortality of ICU Patients”. Since the relationship between the risk of mortality in the ICU and the physiological variables depends on the sample space of the dataset, the prediction can be improved by using automated neural networks or data-mining approaches, to predict hospital mortality in ICU patients.

7.7 Future Work

The need for continual and long-term monitoring of the patient under observation has grown in recent years which has led to the growth of wearable health monitoring devices becoming available in open consumer market. The impetus in recent years has been towards having to detect and identify early warning signs pertaining to several health hazards which may cause trauma situations if not treated in time. The accuracy of classification and identification of health conditions, especially cardiac arrhythmia, using long-term monitoring however, depends on the size of the dataset available to train the machine learning and neural-network models. The research study presented in this thesis involved commonly used and standard classification models such as the *k-NN* and *RandomForestClassifier* which are supervised learning models that were trained on datasets with known annotations, e.g. V,A,L,R . Due to limitations in sample size, other more efficient and adaptive techniques could not be used such as the semi-supervised algorithms. In long-term cardiac arrhythmia, monitoring patient's own ECG samples gathered over longer duration could help in identifying anomalies and by annotating anomalies with anomaly detection and signal processing algorithms using wavelet theory. Reinforcement-learning models could then be used to penalise or incentivise decision nodes that could detect and identify an anomaly in the patient's own ECG signal.

With the miniaturisation of IoT devices and analogue front-end devices containing high precision analogue-to-digital converters it has now become possible to capture bio-potential signals with a high degree of accuracy. As the microcontrollers are becoming more powerful, with 32-bit architectures becoming available, adaptive and reinforced machine learning algorithms could be implemented on a microcontroller architectures requiring lesser power consumption as compared to the microprocessor architectures; something quite desirable in a wearable device capable of monitoring 24 x 7. As advanced signal processing libraries are becoming available for microcontroller architectures e.g. CMSIS-DSP and CMSIS-NN (Lai and Suda 2018) for signal processing and neural networks respectively on ARM Cortex-M family of microcontrollers it will become possible to train and annotate bio-potential signals in real time.

Although the research study presented in this thesis focused on cardiac arrhythmia similar techniques could be used in studying other health conditions related to Electroencephalography (EEG), Electromyography (EMG) (Mazzetta et al. 2019) and studies related to Oncology as human body responds by altering its bio-electric potential when it experiences physiological changes and by emitting bio-electric distress signals which manifests in the form of fluctuations in bio-potential on body surface. The combination of features extracted from ECG, EEG and EMG in response to a certain health condition could help in determining physiological response to a certain disease and the stage of the illness related to the disease. Machine-learning and neural-network models could then be trained on these features to detect physiological disorders at an early stage. Although a matter of further study and research bio-potential signal processing can lead to a completely new era of early-stage and early-warning non-invasive detection systems which can prevent health hazards and severe health conditions ahead of time.

References

Welch, Peter (1967). “The use of fast Fourier transform for the estimation of power spectra: a method based on time averaging over short, modified periodograms”. In: *IEEE Transactions on audio and electroacoustics* 15.2, pp. 70–73.

Baker, Susan P et al. (1974). “The injury severity score: a method for describing patients with multiple injuries and evaluating emergency care”. In: *Journal of Trauma and Acute Care Surgery* 14.3, pp. 187–196.

Teasdale, Graham and Bryan Jennett (1974). “Assessment of coma and impaired consciousness: a practical scale”. In: *The Lancet* 304.7872, pp. 81–84.

Beverland, DE and WH Rutherford (1983). “An assessment of the validity of the injury severity score when applied to gunshot wounds”. In: *Injury* 15.1, pp. 19–22.

Moody, George B, Roger G Mark, et al. (1985). “Derivation of respiratory signals from multi-lead ECGs”. In: *Computers in cardiology* 12.1985, pp. 113–116.

Pan, Jiapu and Willis J Tompkins (1985). “A real-time QRS detection algorithm”. In: *IEEE Trans. Biomed. Eng* 32.3, pp. 230–236.

Long, W. B., B. L. Bachulis, and G. D. Hynes (1986). “Accuracy and relationship of mechanisms of injury, trauma score, and injury severity score in identifying major trauma”. In: *Am J Surg* 151.5, pp. 581–4. ISSN: 0002-9610 (Print) 0002-9610.

Boyd, C. R., M. A. Tolson, and W. S. Copes (1987). “Evaluating trauma care: the TRISS method. Trauma Score and the Injury Severity Score”. In: *J Trauma* 27.4, pp. 370–8. ISSN: 0022-5282 (Print) 0022-5282.

Harris, Frederic J. (1987). “Chapter 3 - Multirate FIR Filters for Interpolating and Desampling”. In: *Handbook of Digital Signal Processing*. Ed. by Douglas F. Elliott. San Diego: Academic Press, pp. 173–287. ISBN: 978-0-08-050780-4. DOI: `https://doi.org/10.1016/B978-0-08-050780-4.50008-4`. URL: `http://www.sciencedirect.com/science/article/pii/B9780080507804500084`.

Champion, H. R. et al. (1989). “A revision of the Trauma Score”. In: *J Trauma* 29.5, pp. 623–9. ISSN: 0022-5282. DOI: `10.1097/00005373-198905000-00017`.

Linn, S. (1995). “The injury severity score–importance and uses”. In: *Ann Epidemiol* 5.6, pp. 440–6. ISSN: 1047-2797 (Print) 1047-2797.

Forrey, A. W. et al. (1996). "Logical observation identifier names and codes (LOINC) database: a public use set of codes and names for electronic reporting of clinical laboratory test results". In: *Clin Chem* 42.1, pp. 81–90. ISSN: 0009-9147 (Print) 0009-9147.

Mower, William R et al. (1998). "Pulse oximetry as a fifth vital sign in emergency geriatric assessment". In: *Academic emergency medicine* 5.9, pp. 858–865.

Garthe, E., J. D. States, and N. K. Mango (1999). "Abbreviated injury scale unification: the case for a unified injury system for global use". In: *J Trauma* 47.2, pp. 309–23. ISSN: 0022-5282 (Print) 0022-5282.

Rajskina, M. E. (1999). *Ventricular fibrillation and sudden coronary death*. Developments in cardiovascular medicine. Boston: Kluwer Academic Publishers, xxii, 213 p. ISBN: 0792385705 (alk. paper). URL: `Publisher%20description%20http://www.loc.gov/catdir/enhancements/fy0819/99033619-d.html%20Table%20of%20contents%20only%20http://www.loc.gov/catdir/enhancements/fy0819/99033619-t.html`.

Goldberger, Ary L et al. (2000). "PhysioBank, PhysioToolkit, and PhysioNet: components of a new research resource for complex physiologic signals". In: *Circulation* 101.23, e215–e220.

Mackenzie, R and R Sutcliffe (2000). "Pre-hospital Care: The Trapped Patient". In: *Journal of the Royal Army Medical Corps* 146.1, pp. 39–46. DOI: `10.1136/jramc-146-01-09`. URL: `http://jramc.bmj.com/content/jramc/146/1/39.full.pdf`.

Staessen, J. et al. (2000). "Modern approaches to blood pressure measurement". In: *Occupational and Environmental Medicine* 57.8, pp. 510–520. ISSN: 1351-0711 1470-7926. DOI: `10.1136/oem.57.8.510`. URL: `http://www.ncbi.nlm.nih.gov/pmc/articles/PMC1740006/`.

Hernandez, Alfredo I et al. (2001). "Real-time ECG transmission via Internet for nonclinical applications". In: *IEEE Transactions on information technology in biomedicine* 5.3, pp. 253–257.

Moody, George B and Roger G Mark (2001). "The impact of the MIT-BIH arrhythmia database". In: *IEEE Engineering in Mefdicine and Biology Magazine* 20.3, pp. 45–50.

Stevenson, M. et al. (2001). "An overview of the injury severity score and the new injury severity score". In: *Injury Prevention* 7.1, p. 10. DOI: `10.1136/ip.7.1.10`. URL: `http://injuryprevention.bmj.com/content/7/1/10.abstract`.

Meek, Steve and Francis Morris (2002). "Introduction Leads rate rhythm and cardiac axis". In: *Bmj* 324.7334, pp. 415–418.

Achten, Juul and Asker E. Jeukendrup (2003). "Heart Rate Monitoring". In: *Sports Medicine* 33.7, pp. 517–538. ISSN: 1179-2035. DOI: `10.2165/00007256-`

200333070 - 00004. URL: http://dx.doi.org/10.2165/00007256-200333070-00004.

Whitaker, Iveth Y., Terezinha D. Gennari, and Aristarcho L. Whitaker (2003). "The difference between ISS and NISS in a series of trauma patients in Brazil". In: *Annual proceedings. Association for the Advancement of Automotive Medicine* 47, pp. 301–309. ISSN: 1540-0360. URL: https://www.ncbi.nlm.nih.gov/pubmed/12941232%20https://www.ncbi.nlm.nih.gov/pmc/PMC3217565/.

De Chazal, Philip, Maria O'Dwyer, and Richard B Reilly (2004). "Automatic classification of heartbeats using ECG morphology and heartbeat interval features". In: *IEEE transactions on biomedical engineering* 51.7, pp. 1196–1206.

Lockwood, C., T. Conroy-Hiller, and T. Page (2004). "Vital signs". In: *JBI Libr Syst Rev* 2.6, pp. 1–38. ISSN: 1838-2142 (Print) 1838-2142.

Bowman, Sue E (2005). "Coordination of SNOMED-CT and ICD-10: getting the most out of electronic health record systems". In: *Coordination of SNOMED-CT and ICD-10: Getting the Most out of Electronic Health Record Systems/AHIMA, American Health Information Management Association.*

Holcomb, John B et al. (2005). "Manual vital signs reliably predict need for life saving interventions in trauma patients". In: *Journal of Trauma and Acute Care Surgery* 59.4, pp. 821–829.

Burnham, Robert S., Robert S. McKinley, and Daniel D. Vincent (2006). "Three Types of Skin-Surface Thermometers: A Comparison of Reliability, Validity, and Responsiveness". In: *American Journal of Physical Medicine & Rehabilitation* 85.7, pp. 553–558. ISSN: 0894-9115. DOI: 10.1097/01.phm.0000223232.32653.7f. URL: https://journals.lww.com/ajpmr/Fulltext/2006/07000/Three_Types_of_Skin_Surface_Thermometers__A.1.aspx.

Clifford, Gari D, Francisco Azuaje, Patrick McSharry, et al. (2006). *Advanced methods and tools for ECG data analysis.* Artech house Boston.

Cooke, William H et al. (2006). "Heart period variability in trauma patients may predict mortality and allow remote triage". In: *Aviation, space, and environmental medicine* 77.11, pp. 1107–1112.

Fingerhut, L. A. and M. Warner (2006). "The ICD 10 injury mortality diagnosis matrix". In: *Injury Prevention* 12.1, pp. 24–29. ISSN: 1353-8047. DOI: 10.1136/ip.2005.009076. URL: http://www.ncbi.nlm.nih.gov/pmc/articles/PMC2563502/.

Moore, L. et al. (2006). "Statistical validation of the Glasgow Coma Score". In: *J Trauma* 60.6, 1238–43, discussion 1243–4. ISSN: 0022-5282 (Print) 0022-5282. DOI: 10.1097/01.ta.0000195593.60245.80.

Park, EK et al. (2006). “Continuous measurement of systolic blood pressure using the PTT and other parameters”. In: *2005 IEEE Engineering in Medicine and Biology 27th Annual Conference*. IEEE, pp. 3555–3558.

Richesson, Rachel L, James E Andrews, and Jeffrey P Krischer (2006). “Use of SNOMED CT to represent clinical research data: a semantic characterization of data items on case report forms in vasculitis research”. In: *Journal of the American Medical Informatics Association* 13.5, pp. 536–546.

Albrecht, Jochen (2007). *Key concepts and techniques in GIS*. Sage.

Shouldice, Redmond B, Conor Heneghan, and Philip de Chazal (2007). “Automated detection of paroxysmal atrial fibrillation from inter heartbeat intervals”. In: *2007 29th Annual International Conference of the IEEE Engineering in Medicine and Biology Society*. IEEE, pp. 686–689.

Surda, Jozef et al. (2007). “Spectral properties of ECG signal”. In: *2007 17th International Conference Radioelektronika*. IEEE, pp. 1–5.

Lin, Chia-Hung (2008). “Frequency-domain features for ECG beat discrimination using grey relational analysis-based classifier”. In: *Computers & Mathematics with Applications* 55.4, pp. 680–690.

Kocheril, Abraham G and Ali A Sovari (2009). *Practical Rapid ECG Interpretation (PREI)*. New York, US: Nova Biomedical Books. ISBN: 9781612096674.

Morris, Francis, William Brady, and John Camm (2009). *ABC of Clinical Electrocardiography (2nd Edition)*. Hoboken, NJ, USA: BMJ Books. ISBN: 9781444312492.

Riordan William P., Jr. et al. (2009). “Early Loss of Heart Rate Complexity Predicts Mortality Regardless of Mechanism, Anatomic Location, or Severity of Injury in 2178 Trauma Patients¹”. In: *Journal of Surgical Research* 156.2, pp. 283–289. ISSN: 0022-4804. DOI: `10.1016/j.jss.2009.03.086`. URL: `http://dx.doi.org/10.1016/j.jss.2009.03.086`.

Takasu, Tomoji and Akio Yasuda (2009). “Development of the low-cost RTK-GPS receiver with an open source program package RTKLIB”. In: *International symposium on GPS/GNSS*. International Convention Center Jeju Korea, pp. 4–6.

Baman, T. S. et al. (2010). “Relationship between burden of premature ventricular complexes and left ventricular function”. In: *Heart Rhythm* 7.7, pp. 865–9. ISSN: 1547-5271. DOI: `10.1016/j.hrthm.2010.03.036`.

Banerjee, Swati and Madhuchhanda Mitra (2010). “ECG feature extraction and classification of anteroseptal myocardial infarction and normal subjects using discrete wavelet transform”. In: *2010 International Conference on Systems in Medicine and Biology*. IEEE, pp. 55–60.

Burns, Adrian et al. (2010). "SHIMMER – A wireless sensor platform for noninvasive biomedical research". In: *IEEE Sensors Journal* 10.9, pp. 1527–1534.

Cohen, Todd J. (2010). *A patient's guide to heart rhythm problems.* A Johns Hopkins Press health book. Baltimore Md.: Johns Hopkins University Press, xi, 211 p. ISBN: 9780801897740.

Gomes, Pedro R et al. (2010). "ECG dataacquisition and classification system by using wavelet-domain hidden markov models". In: *2010 Annual International Conference of the IEEE Engineering in Medicine and Biology.* IEEE, pp. 4670–4673.

Taouli, S. A. and F. Bereksi-Reguig (2010). "Noise and baseline wandering suppression of ECG signals by morphological filter". In: *Journal of Medical Engineering & Technology* 34.2, pp. 87–96. ISSN: 0309-1902. DOI: 10.3109/03091900903336886. URL: https://doi.org/10.3109/03091900903336886.

Zadeh, A. E., A. Khazaee, and V. Ranaee (2010). "Classification of the electrocardiogram signals using supervised classifiers and efficient features". In: *Comput Methods Programs Biomed* 99.2, pp. 179–94. ISSN: 0169-2607. DOI: 10.1016/j.cmpb.2010.04.013.

Adochiei, Felix, Ioana Edu, and Narcis Adochiei (2011). "Comparative filtering methods for noisy ECG signals". In: *2011 E-Health and Bioengineering Conference (EHB).* IEEE, pp. 1–4.

Clifton, Lei et al. (2011). "Identification of patient deterioration in vital-sign data using one-class support vector machines". In: *2011 federated conference on computer science and information systems (FedCSIS).* IEEE, pp. 125–131.

Saeed, Mohammed et al. (2011). "Multiparameter Intelligent Monitoring in Intensive Care II (MIMIC II): A public-access intensive care unit database". In: *Critical care medicine* 39.5, pp. 952–960. ISSN: 0090-3493 1530-0293. DOI: 10.1097/CCM.0b013e31820a92c6. URL: http://www.ncbi.nlm.nih.gov/pmc/articles/PMC3124312/.

Schluter, Philip J. (2011). "The Trauma and Injury Severity Score (TRISS) revised". In: *Injury* 42.1, pp. 90–96. ISSN: 0020-1383. DOI: 10.1016/j.injury.2010.08.040. URL: http://dx.doi.org/10.1016/j.injury.2010.08.040.

Smith, Joyce and Rachel Roberts (2011). *Vital Signs for Nurses.* Wiley-Blackwell. ISBN: 9781444341867. URL: https://www.dawsonera.com:443/abstract/9781444341867.

Takasu, T (2011). "RTKLIB: An open source program package for GNSS positioning". In: *Tech. Rep., 2013. Software and documentation.*

Adams, E Roland and Anthony Choi (2012). "Using neural networks to predict cardiac arrhythmias". In: *2012 IEEE International Conference on Systems, Man, and Cybernetics (SMC).* IEEE, pp. 402–407.

Ahmad, Saif et al. (2012). "Electrocardiogram-assisted blood pressure estimation". In: *IEEE Transactions on Biomedical Engineering* 59.3, pp. 608–618.

Crawford, Jacqui and Linda Doherty (2012). *Practical Aspects of ECG Recording.* UK: M&K Publishing. ISBN: 9781905539307.

Gradl, Stefan et al. (2012). "Real-time ECG monitoring and arrhythmia detection using Android-based mobile devices". In: *2012 Annual International Conference of the IEEE Engineering in Medicine and Biology Society.* IEEE, pp. 2452–2455.

Peltola, Mirja A. (2012). "Role of Editing of RR Intervals in the Analysis of Heart Rate Variability". In: *Frontiers in Physiology* 3, p. 148. ISSN: 1664-042X. DOI: 10.3389/fphys.2012.00148. URL: http://www.ncbi.nlm.nih.gov/pmc/articles/PMC3358711/.

Chakroborty, Sandipan (2013). "Accurate Arrhythmia classification using auto-associative neural network". In: *2013 35th Annual International Conference of the IEEE Engineering in Medicine and Biology Society (EMBC).* IEEE, pp. 4247–4250.

Goy, Jean-Jacques et al. (2013). *Electrocardiography (ECG).* Vol. 1. Bentham Science Publishers.

Hart, John (2013). "Association between heart rate variability and manual pulse rate". In: *The Journal of the Canadian Chiropractic Association* 57.3, pp. 243–250. ISSN: 0008-3194 1715-6181. URL: http://www.ncbi.nlm.nih.gov/pmc/articles/PMC3743650/.

Katritsis, Demosthenes G., George C. M. Siontis, and A. John Camm (2013). "Prognostic Significance of Ambulatory ECG Monitoring for Ventricular Arrhythmias". In: *Progress in Cardiovascular Diseases* 56.2, pp. 133–142. ISSN: 0033-0620. DOI: http://dx.doi.org/10.1016/j.pcad.2013.07.005. URL: http://www.sciencedirect.com/science/article/pii/S0033062013001370.

El-Khafif, Sahar H and Mohamed A El-Brawany (2013). "Artificial neural network-based automated ECG signal classifier". In: *ISRN Biomedical Engineering* 2013.

Kumar, R Ganesh and YS Kumaraswamy (2013). "Investigation and classification of ECG beat using input output additional weighted feed forward neural network". In: *2013 International Conference on Signal Processing, Image Processing & Pattern Recognition.* IEEE, pp. 200–205.

Padulo, Johnny et al. (2013). "A paradigm of uphill running". In: *PLoS One* 8.7, e69006.

Scott, Daniel J. et al. (2013a). "Accessing the public MIMIC II intensive care relational database for clinical research". In: *BMC Medical Informatics and*

Decision Making 13, pp. 9–9. ISSN: 1472-6947. DOI: 10.1186/1472-6947-13-9. URL: http://www.ncbi.nlm.nih.gov/pmc/articles/PMC3598967/.

Scott, Daniel J et al. (2013b). "Accessing the public MIMIC-II intensive care relational database for clinical research". In: *BMC medical informatics and decision making* 13.1, p. 9.

Smith, G. B. et al. (2013). "The ability of the National Early Warning Score (NEWS) to discriminate patients at risk of early cardiac arrest, unanticipated intensive care unit admission, and death". In: *Resuscitation* 84.4, pp. 465–70. ISSN: 0300-9572. DOI: 10.1016/j.resuscitation.2012.12.016.

Smith, Gary B et al. (2013). "The ability of the National Early Warning Score (NEWS) to discriminate patients at risk of early cardiac arrest, unanticipated intensive care unit admission, and death". In: *Resuscitation* 84.4, pp. 465–470.

Alam, N. et al. (2014). "The impact of the use of the Early Warning Score (EWS) on patient outcomes: A systematic review". In: *Resuscitation* 85.5, pp. 587–594. ISSN: 0300-9572. DOI: 10.1016/j.resuscitation.2014.01.013. URL: http://dx.doi.org/10.1016/j.resuscitation.2014.01.013.

AlMahamdy, Mohammed and H Bryan Riley (2014). "Performance study of different denoising methods for ECG signals". In: *Procedia Computer Science* 37, pp. 325–332.

BHF (2014). *We Fight for every Heartbeat, Our Strategy to 2020, British Heart Foundation*. Report. British Heart Foundation. URL: https://www.bhf.org.uk/informationsupport/publications/about-bhf/our-strategy-to-2020.

Chakroborty, Sandipan and Meru A Patil (2014). "Real-time arrhythmia classification for large databases". In: *2014 36th Annual International Conference of the IEEE Engineering in Medicine and Biology Society*. IEEE, pp. 1448–1451.

Di Marco, Luigi Yuri et al. (2014). "Recurring patterns of atrial fibrillation in surface ECG predict restoration of sinus rhythm by catheter ablation". In: *Computers in biology and medicine* 54, pp. 172–179.

Ebrahimzadeh, Elias, Mohammad Pooyan, and Ahmad Bijar (2014). "A novel approach to predict sudden cardiac death (SCD) using nonlinear and time-frequency analyses from HRV signals". In: *PloS one* 9.2, e81896.

Krafty, Robert T. et al. (2014). "Nonparametric spectral analysis of heart rate variability through penalized sum of squares". In: *Statistics in medicine* 33.8, pp. 1383–1394. ISSN: 1097-0258 0277-6715. DOI: 10.1002/sim.6038. URL: https://www.ncbi.nlm.nih.gov/pubmed/24254401%20https://www.ncbi.nlm.nih.gov/pmc/PMC3947457/.

Lee, SeokJu, Girma Tewolde, and Jaerock Kwon (2014). "Design and implementation of vehicle tracking system using GPS/GSM/GPRS technology and smartphone application”. In: *2014 IEEE world forum on internet of things (WF-IoT)*. IEEE, pp. 353–358.

Leutheuser, H. et al. (2014). “Comparison of real-time classification systems for arrhythmia detection on Android-based mobile devices”. In: *Conf Proc IEEE Eng Med Biol Soc* 2014, pp. 2690–3. ISSN: 1557-170X (Print) 1557-170x. DOI: 10.1109/embc.2014.6944177.

Li, Qiao, Cadathur Rajagopalan, and Gari D Clifford (2014). “A machine learning approach to multi-level ECG signal quality classification”. In: *Computer methods and programs in biomedicine* 117.3, pp. 435–447.

Paithane, AN and DS Bormane (2014). “Analysis of nonlinear and non-stationary signal to extract the features using Hilbert Huang transform”. In: *2014 IEEE International Conference on Computational Intelligence and Computing Research*. IEEE, pp. 1–4.

Raths, D (2014). “Trend: standards development. Catching FHIR. A new HL7 draft standard may boost web services development in healthcare.” In: *Healthcare informatics: the business magazine for information and communication systems* 31.2, pp. 13–16.

Richer, R. et al. (2014). “Real-Time ECG and EMG Analysis for Biking Using Android-Based Mobile Devices”. In: *2014 11th International Conference on Wearable and Implantable Body Sensor Networks*, pp. 104–108. ISSN: 2376-8886. DOI: 10.1109/BSN.2014.20.

Silva, Ikaro and George B Moody (2014). “An open-source toolbox for analysing and processing physionet databases in matlab and octave”. In: *Journal of open research software* 2.1.

Cornforth, David, F. Herbert Jelinek, and Mika Tarvainen (2015). “A Comparison of Nonlinear Measures for the Detection of Cardiac Autonomic Neuropathy from Heart Rate Variability”. In: *Entropy* 17.3. ISSN: 1099-4300. DOI: 10.3390/e17031425.

Domingues, Cristiane de Alencar et al. (2015). “Performance of Trauma and Injury Severity Score (TRISS) adjustments: an integrative review”. In: *Revista da Escola de Enfermagem da USP* 49.SPE, pp. 138–146.

Ebrahimzadeh, Elias, Mohammad Pooyan, Sahar Jahani, et al. (2015). “ECG signals noise removal: Selection and optimization of the best adaptive filtering algorithm based on various algorithms comparison”. In: *Biomedical Engineering: Applications, Basis and Communications* 27.04, p. 1550038.

Franz, Barbara, Andreas Schuler, and Oliver Krauss (2015). “Applying FHIR in an integrated health monitoring system”. In: *EJBI* 11.2, pp. 51–56.

Hughes, D et al. (2015). “11 Investigating the effectiveness of 1, 3 and 5 day holter monitoring: should it be limited to 24 h”. In: *Heart* 101.Suppl 5, A5–A6.

ISSN: 1355-6037. DOI: 10.1136/heartjnl-2015-308621.11. URL: https://heart.bmj.com/content/101/Suppl_5/A5.3.

Injury Data and Resources - ICD Injury Matrices (Nov. 2015). en-us. URL: https://www.cdc.gov/nchs/injury/injury_matrices.htm. (accessed: 15.07.2018).

Krasteva, Vessela et al. (2015). "Superiority of classification tree versus cluster, fuzzy and discriminant models in a heartbeat classification system". In: *PloS one* 10.10, e0140123.

Kumar, Sarvesh and Shahanaz Ayub (2015). "Estimation of Blood Pressure by Using Electrocardiogram (ECG) and Photo-Plethysmogram (PPG)". In: *2015 Fifth International Conference on Communication Systems and Network Technologies*. IEEE, pp. 521–524.

Merino, Manuel, Isabel Maria Gomez, and Alberto J Molina (2015). "Envelopment filter and K-means for the detection of QRS waveforms in electrocardiogram". In: *Medical engineering & physics* 37.6, pp. 605–609.

NICE (Aug. 2015). *AliveCor Heart Monitor and AliveECG app (Kardia Mobile) for detecting atrial fibrillation*. Report. URL: https://www.nice.org.uk/advice/mib35/chapter/Technology-overview. (accessed: 18.08.2018).

Rodriguez, R et al. (2015). "Feature extraction of electrocardiogram signals by applying adaptive threshold and principal component analysis". In: *Journal of applied research and technology* 13.2, pp. 261–269.

Russo, Andrea M (2015). "PVCs arising from the moderator band: An under-recognized trigger for idiopathic VF?" In: *Heart rhythm* 12.1, pp. 76–77.

Stroobandt, R., S. Serge Barold, and Alfons F. Sinnaeve (2015). *ECG from basics to essentials step by step*. Chichester, West Sussex, UK ; Hoboken, NJ: John Wiley & Sons, Inc., p. ISBN: 9781119066415 (pbk.)

Townsend, Mark et al. (Dec. 2015). *Cardiovascular Disease Statistics 2015*. en. Tech. rep. publisher: British Heart Foundation. London: University of Oxford, BHF. URL: https://www.bhf.org.uk/informationsupport/publications/statistics/cvd-stats-2015. (accessed: 15.07.2018).

Voss, Andreas et al. (2015). "Short term heart rate variability influence of gender and age in healthy subjects". In: *PloS one* 10.3, e0118308.

Agnew, James (2016). *HAPI FHIR - The Open Source FHIR API for Java*. publisher: University Health Network, Toronto, Canada. URL: https://hapifhir.io/ (visited on 04/10/2018).

Benson, Tim and Grahame Grieve (2016a). "Implementing FHIR". In: *Principles of Health Interoperability*. Springer, pp. 397–416.

— (2016b). *Principles of health interoperability: SNOMED CT, HL7 and FHIR*. Springer.

Delane, A. et al. (Aug. 2016). "Lomb algorithm versus fast fourier transform in heart rate variability analyses of pain in premature infants". In: *2016 38th Annual International Conference of the IEEE Engineering in Medicine and Biology Society (EMBC)*, pp. 944–947. DOI: 10.1109/EMBC.2016.7590857.

Duking, Peter et al. (2016). "Comparison of Non-Invasive Individual Monitoring of the Training and Health of Athletes with Commercially Available Wearable Technologies". In: *Frontiers in Physiology* 7, p. 71. ISSN: 1664-042X. DOI: 10.3389/fphys.2016.00071. URL: http://www.ncbi.nlm.nih.gov/pmc/articles/PMC4783417/.

German, David M. et al. (2016). "Atrial Fibrillation Predictors: Importance of the Electrocardiogram". In: *Annals of Noninvasive Electrocardiology* 21.1, pp. 20–29. ISSN: 1542-474X. DOI: 10.1111/anec.12321. URL: http://dx.doi.org/10.1111/anec.12321.

Johnson, Alistair EW et al. (2016). "MIMIC-III, a freely accessible critical care database". In: *Scientific data* 3, p. 160035.

Lerma, C. and L. Glass (2016). "Predicting the risk of sudden cardiac death". In: *J Physiol* 594.9, pp. 2445–58. ISSN: 0022-3751. DOI: 10.1113/jp270535.

Liddell, Belinda J. et al. (2016). "Heart rate variability and the relationship between trauma exposure age, and psychopathology in a post-conflict setting". In: *BMC psychiatry* 16, pp. 133–133. ISSN: 1471-244X. DOI: 10.1186/s12888-016-0850-5. URL: https://www.ncbi.nlm.nih.gov/pubmed/27165346%20https://www.ncbi.nlm.nih.gov/pmc/PMC4862083/.

Luz, Eduardo Jose da S. et al. (2016). "ECG-based heartbeat classification for arrhythmia detection: A survey". In: *Computer Methods and Programs in Biomedicine* 127, pp. 144–164. ISSN: 0169-2607. DOI: http://dx.doi.org/10.1016/j.cmpb.2015.12.008. URL: http://www.sciencedirect.com/science/article/pii/S0169260715003314.

Mandel, Joshua C et al. (2016). "SMART on FHIR: a standards-based, interoperable apps platform for electronic health records". In: *Journal of the American Medical Informatics Association* 23.5, pp. 899–908.

Network Analysis (July 2016). publisher: Quantum GIS. URL: https://docs.qgis.org/2.8/en/docs/training_manual/vector_analysis/network_analysis.html (visited on 03/05/2018).

Pirracchio, Romain (2016). "Mortality prediction in the ICU based on MIMIC-II results from the super ICU learner algorithm (SICULA) project". In: *Secondary Analysis of Electronic Health Records*. Springer, pp. 295–313.

Sbiti-Rohr, Diana et al. (2016). "The National Early Warning Score (NEWS) for outcome prediction in emergency department patients with community-acquired pneumonia: results from a 6-year prospective cohort study". In: *BMJ Open* 6.9. DOI: 10.1136/bmjopen-2015-011021. URL: http://bmjopen.bmj.com/content/bmjopen/6/9/e011021.full.pdf.

Acharya, U. R. et al. (2017). "A deep convolutional neural network model to classify heartbeats". In: *Comput Biol Med* 89, pp. 389–396. ISSN: 0010-4825. DOI: 10.1016/j.compbiomed.2017.08.022.

Aminiahidashti, Hamed et al. (2017). "Comparison of APACHE II and SAPS II Scoring Systems in Prediction of Critically Ill Patients Outcome". In: *Emergency* 5.1, e4. ISSN: 2345-4563 2345-4571. URL: http://www.ncbi.nlm.nih.gov/pmc/articles/PMC5325910/.

Barnard, Ed B. G. et al. (2017). "The outcome of patients in traumatic cardiac arrest presenting to deployed military medical treatment facilities: data from the UK Joint Theatre Trauma Registry". In: *Journal of the Royal Army Medical Corps*. URL: http://jramc.bmj.com/content/early/2017/10/06/jramc-2017-000818.abstract.

Dinh, Anh, Loc Luu, and Thang Cao (2017). "Blood Pressure Measurement Using Finger ECG and Photoplethysmogram for IoT". In: *International Conference on the Development of Biomedical Engineering in Vietnam*. Springer, pp. 83–89.

Halcox, Julian P.J. et al. (2017). "Assessment of Remote Heart Rhythm Sampling Using the AliveCor Heart Monitor to Screen for Atrial Fibrillation". In: *Circulation* 136.19, pp. 1784–1794. DOI: 10.1161/CIRCULATIONAHA.117.030583. eprint: https://ahajournals.org/doi/pdf/10.1161/CIRCULATIONAHA.117.030583. URL: https://ahajournals.org/doi/abs/10.1161/CIRCULATIONAHA.117.030583.

Hay, David (2017). *clinFHIR Launcher*. publisher: Rhapsody Health. URL: http://clinfhir.com/ (visited on 04/10/2017).

Heart Rate Monitor Sensor DFRobot (2017). publisher: DFRobot. URL: https://wiki.dfrobot.com/Heart_Rate_Monitor_Sensor_SKU__SEN0213 (visited on 11/04/2017).

Heartisans - How it works (2017). en. publisher: Heartisans. URL: https://www.heartisans.com/pages/how-it-works (visited on 05/12/2018).

Nedea, Denise (Mar. 2017). *Trauma Injury Severity Score (TRISS) Calculator*. URL: https://www.mdapp.co/trauma-injury-severity-score-triss-calculator-277/. (accessed: 15.07.2018).

Nguyen, Hoa Hong et al. (2017). "A review on IoT healthcare monitoring applications and a vision for transforming sensor data into real-time clinical feedback". In: *2017 IEEE 21st International Conference on Computer Supported Cooperative Work in Design (CSCWD)*. IEEE, pp. 257–262.

NICE (2017). *Surveillance report 2017 Atrial fibrillation management 2014 NICE guideline CG180*. Report. URL: https://www.nice.org.uk/guidance/cg180/evidence. (accessed: 18.08.2018).

NICE-Medtech-Zio (Mar. 2017). *Medtech innovation briefing [MIB101], Zio Service for detecting cardiac arrhythmias*. Report. URL: https://www.nice.org.uk/advice/mib101/chapter/The-technology. (accessed: 18.08.2018).

Oryema, Brian et al. (2017). "Design and implementation of an interoperable messaging system for IoT healthcare services". In: *2017 14th IEEE Annual Consumer Communications & Networking Conference (CCNC)*. IEEE, pp. 45–52.

Smith, Gary (2017). *National Early Warning Score (NEWS)*. en. URL: https://www.mdcalc.com/national-early-warning-score-news-2 (visited on 05/12/2018).

Tu, Hans T et al. (2017). "Smartphone electrographic monitoring for atrial fibrillation in acute ischemic stroke and transient ischemic attack". In: *International Journal of Stroke* 12.7, pp. 786–789. DOI: 10.1177/1747493017696097. URL: http://journals.sagepub.com/doi/abs/10.1177/1747493017696097.

Walinjkar, A. and J. Woods (June 2017a). "ECG classification and prognostic approach towards personalized healthcare". In: *2017 International Conference On Social Media, Wearable And Web Analytics (Social Media)*, pp. 1–8. DOI: 10.1109/SOCIALMEDIA.2017.8057360.

— (Sept. 2017b). "Personalized wearable systems for real-time ECG classification and healthcare interoperability: Real-time ECG classification and FHIR interoperability". In: *2017 Internet Technologies and Applications (ITA)*, pp. 9–14. DOI: 10.1109/ITECHA.2017.8101902.

Alencar Domingues, Cristiane de et al. (2018). "New Trauma and Injury Severity Score (TRISS) adjustments for survival prediction". In: *World journal of emergency surgery* 13.1, p. 12.

Baker, Susan (2018). *Injury Severity Score (ISS)*. en. URL: https://www.mdcalc.com/injury-severity-score-iss (visited on 07/12/2018). (accessed: 12.07.2018).

Bansal, Agam and Rajnish Joshi (2018). "Portable out-of-hospital electrocardiography: A review of current technologies". In: *Journal of arrhythmia* 34.2, pp. 129–138. ISSN: 1880-4276. DOI: 10.1002/joa3.12035. URL: https://www.ncbi.nlm.nih.gov/pubmed/29657588.

Bodenreider, O., R. Cornet, and D. J. Vreeman (2018). "Recent Developments in Clinical Terminologies - SNOMED CT, LOINC, and RxNorm". In: *Yearb Med Inform* 27.1, pp. 129–139. ISSN: 0943-4747. DOI: 10.1055/s-0038-1667077.

Braunstein, M. L. (Nov. 2018). “Healthcare in the Age of Interoperability: The Promise of Fast Healthcare Interoperability Resources”. In: *IEEE Pulse* 9.6, pp. 24–27. DOI: 10.1109/MPUL.2018.2869317.

Burns, Ed (2018). *Atrial Fibrillation*. URL: https://litfl.com/atrial-fibrillation-ecg-library/. (accessed: 11.12.2018).

Champion, H. R. (2018). *Revised Trauma Score*. en. URL: https://www.mdcalc.com/revised-trauma-score. (accessed: 15.07.2018).

Geofabrik OpenStreetMap data for region: Essex (Apr. 2018). publisher: Geofabrik GmBH. URL: http://download.geofabrik.de/europe/great-britain/england/essex.html (visited on 06/17/2018).

Goldberger, Ary L., Zachary D. Goldberger, and Alexei Shvilkin (2018). “Chapter 8 - Ventricular Conduction Disturbances: Bundle Branch Blocks and Related Abnormalities”. In: *Goldberger’s Clinical Electrocardiography (Ninth Edition)*. Ed. by Ary L. Goldberger, Zachary D. Goldberger, and Alexei Shvilkin. Elsevier, pp. 61–72. ISBN: 978-0-323-40169-2. DOI: https://doi.org/10.1016/B978-0-323-40169-2.00008-1. URL: http://www.sciencedirect.com/science/article/pii/B9780323401692000081.

Hussain, Mohannad A, Steve G Langer, and Marc Kohli (2018). “Learning HL7 FHIR Using the HAPI FHIR Server and Its Use in Medical Imaging with the SIIM Dataset”. In: *Journal of digital imaging* 31.3, pp. 334–340.

Lai, Liangzhen and Naveen Suda (2018). “Enabling deep learning at the IoT edge”. In: *Proceedings of the International Conference on Computer-Aided Design*. ACM, p. 135.

Moses, Scott (Oct. 2018). *Premature Ventricular Contraction (PVC)*. URL: https://fpnotebook.com/CV/EKG/PrmtrVntrclrCntrctn.htm. (accessed: 02.10.2018).

NHS (2018). *Arrhythmia*. URL: https://www.nhs.uk/conditions/arrhythmia/. (accessed: 11.12.2018).

NHS-Digital (2018). *GP Connect*. en. publisher: NHS. URL: https://digital.nhs.uk/services/gp-connect (visited on 04/12/2018).

NICE-Medtech-MIB152 (July 2018). *Remote ECG interpretation consultancy services for cardiovascular disease*. Report. URL: https://www.nice.org.uk/advice/mib152/chapter/The-technology. (accessed: 18.08.2018).

Penn-Barwell, Jowan G., Jon R. B. Bishop, and Mark J. Midwinter (2018). “Refining the Trauma and Injury Severity Score (TRISS) to Measure the Performance of the UK Combat Casualty Care System”. In: *Military Medicine*. ISSN: 0026-4075. DOI: 10.1093/milmed/usx039. URL: http://dx.doi.org/10.1093/milmed/usx039.

Recording GPS tracks - OpenStreetMap Wiki (2018). publisher: OpenStreetMap Wiki. URL: https://wiki.openstreetmap.org/w/index.php?title=Recording_GPS_tracks&oldid=1612100 (visited on 06/18/2018).

Skaga, N. O., T. Eken, and S. Sovik (2018). "Validating performance of TRISS, TARN and NORMIT survival prediction models in a Norwegian trauma population". In: *Acta Anaesthesiologica Scandinavica* 62.2, pp. 253–266. ISSN: 0001-5172 1399-6576. DOI: 10.1111/aas.13029. URL: http://www.ncbi.nlm.nih.gov/pmc/articles/PMC5813212/.

SNOMED International Browser (2018). publisher: SNOMED International. URL: https://browser.ihtsdotools.org/ (visited on 09/10/2018).

UCLH-RACPC (2018). *Rapid access chest pain clinic*. URL: https://www.uclh.nhs.uk/OurServices/ServiceA-Z/CARDIACS/RACPC/Pages/Home.aspx. (visited on 11.12.2018).

Vest, Adriana N et al. (2018). "An open source benchmarked toolbox for cardiovascular waveform and interval analysis". In: *Physiological measurement* 39.10, p. 105004.

Walinjkar, A. (2018a). "A Composite and Wearable Sensor Kit for Location-Aware Healthcare Monitoring and Real-Time Trauma Scoring for Survival Prediction". In: *Applied System Innovation* 1.3, p. 35. ISSN: 2571-5577. URL: http://www.mdpi.com/2571-5577/1/3/35.

— (2018b). "FHIR Tools for Healthcare Interoperability". English. In: *Biomedical Journal of Scientific & Technical Research* 9.5, pp. 001–004. ISSN: 2574-1241. DOI: 10.26717/BJSTR.2018.09.001863. URL: https://biomedres.us/fulltexts/BJSTR.MS.ID.001863.php (visited on 10/30/2019).

Westra, B. L. et al. (2018). "Validation and Refinement of a Pain Information Model from EHR Flowsheet Data". In: *Appl Clin Inform* 9.1, pp. 185–198. ISSN: 1869-0327. DOI: 10.1055/s-0038-1636508.

Braunstein, M. L. (July 2019). "Health Care in the Age of Interoperability Part 6: The Future of FHIR". In: *IEEE Pulse* 10.4, pp. 25–27. DOI: 10.1109/MPULS.2019.2922575.

Mazzetta, Ivan et al. (2019). "Wearable Sensors System for an Improved Analysis of Freezing of Gait in Parkinsons Disease Using Electromyography and Inertial Signals". In: *Sensors* 19.4. ISSN: 1424-8220. DOI: 10.3390/s19040948. URL: https://www.mdpi.com/1424-8220/19/4/948.

Moody, George (Mar. 2019). *WFDB Applications Guide*. publisher: Harvard-MIT Division of Health Sciences and Technology. URL: https://www.physionet.org/physiotools/wag/ (visited on 10/15/2019).

Oxullo, Interscans (Mar. 2019). *Oxullo Arduino-MAX30100 library*. original-date: 2016-05-28T17:28:02Z. URL: https://github.com/oxullo/Arduino-MAX30100 (visited on 05/05/2018).

Teasdale, Graham and Bryan Jennet (May 2019). *Glasgow Coma Scale/Score (GCS)*. en. URL: https://www.mdcalc.com/glasgow-coma-scale-score-gcs (visited on 08/12/2018).

Appendices

Appendix A

Biomedical Journal Sci & Tech Research

ISSN 2574-1241

FHIR Tools for Healthcare Interoperability

Walinjkar, Amit

October, 2018

ISSN: 2574-1241
DOI: *10.26717/BJSTR.2018.09.001863*
Amit Walinjkar. Biomed J Sci & Tech Res

BIOMEDICAL Journal of Scientific & Technical Research

Short Communication **Open Access**

FHIR Tools for Healthcare Interoperability

Amit Walinjkar* and John Woods

Faculty of Computer Science and Electronics Engineering, University of Essex, UK

Received: : September 25, 2018; **Published:** : October 10, 2018

***Corresponding author:** Amit Walinjkar, Faculty of Computer Science and Electronics Engineering, University of Essex, Colchester, Essex, UK, Email: *awalin@essex.ac.uk*; *woodjt@essex.ac.uk*

Abstract

Electronic Health Records (EHR) is an essential element in human healthcare monitoring systems these days. As a large amount of data continues being archived and uploaded to healthcare repositories, virtually every second across the globe, vast amount of data mining tasks continue being modelled and modified to extract valuable decision support information. The Health Level 7 (HL7) consortium provides the framework and related standards for the exchange, integration, sharing, and retrieval of electronic health information that supports clinical practice, management and delivery. With the large number of Internet of Things (IoT) health care kits becoming available it has become increasingly difficult to log the real-time patient monitoring information to healthcare repositories. As patients continue being monitored in real-time it has become essential that the trauma events information such as stroke or cardiac arrhythmia be uploaded to the EHR in real-time. Currently available monitoring devices can monitor and analyse an abnormal condition but may not be able to upload these events in real-time. The proposed research focused on developing real-time interoperability tools and services, which can enable wearable IoT devices to interact with the EHR in real-time and can provide real-time decision support.

The Fast Healthcare Interoperability Resources (FHIR) specification was used to develop and encode trauma related information in terms of FHIR resources, conceptual and logical models using clinFHIR tools. A HAPIFHIR application was implemented on an IoT device which could upload real-time ECG, PPG and relevant trauma information on a test FHIR server. The HAPIFHIR application code could encapsulate ECG arrhythmia, vital signs and trauma events in a single observation and could upload it to the HAPIFHIR server. Several such observations could be linked to a patient context and could be observed in real time in EHR. The ECG, the PPG, vital signs and trauma events were encoded according to Systematized Nomenclature of Medicine - Clinical Terms (SNOMED-CT) specifications. The alerts and alarms mechanism could assist the emergency response teams at the hospitals to prepare for an emergency well in time. An analogue front-end biomedical device was used for data acquisition and signal processing and the IoT devices were networked over wireless network to upload the events and observations to the FHIR server in real time. The system focussed on 'preventive care' as the next generation personalized health-care monitoring devices continue becoming available.

Keywords: IoT Healthcare; Trauma analysis; HL7; ECG FHIR; SNOMED-CT FHIR; HAPI FHIR; clinFHIR

Introduction

There are commercially available health monitoring kits for example the Holter ECG kit which are capable of monitoring a patient patient's heart rhythms for 24 to 48 hours during normal human activity [1]. The kit however only records the ECG and it does not analyse the heart rhythm to detect heart arrhythmia. The ECG recordings have to be manually analysed by an expert cardiologist. There are several such kits like the Alivecor and the Shimmer Sensing kits [2,3] which effectively monitor heart conditions though do not upload the traumatic events related information that a patient may have undergone. The system proposed in this research consists of a software implemented on the wearable IoT device which encapsulates the sample ECG readings in a standard XML or JSON format [4] and transmits the samples to the analytical server that uploads the FHIR payload to the FHIR server after performing the trauma analysis. Attempts have been made on previous occasions to make real time updates to electronic health records using internet client server technologies [5], though to develop such an infrastructure is however, a government policy decision rather than an implementation exercise.

HL7 (Health Level-7) is a standards agency that develops standards for electronic health resources and FHIR is one such standard that enables Electronic Health Records (EHR) interoperability through web-service interfaces is [6] HL7 FHIR Web services. An overview of SNOMED-CT coding schemes along with interrelationships between clinical codes has been provided in this paper. An Oracle Java based FHIR test server and HAPIFHIR client based implementation has also been explained. In the methods section a detailed implementation of a HAPIFHIR client has been explained. The usage of clinFHIR tool which models codable concepts, resources, and elements, components using scenario modeller, logical modeller and conceptual modelling tools has been demonstrated. SNOMED CT is a coding system that describes clinical concepts, vocabulary, descriptions and inter-relationships between clinical codes. The results and discussions section discusses the advantages of using the FHIR based client application and FHIR modelling tools to develop an IoT-based real-time decision health support system.

Overview of FHIR Healthcare Interoperability Workflow

Signal Processing, Dataset Preparation and Analysis

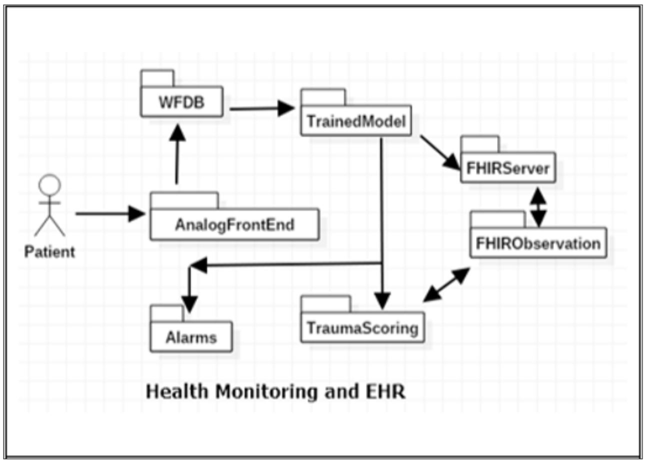

Figure 1: Health Monitoring in a typical IoT based wearable kit demonstrating data-acquisition to FHIR observation upload to FHIR Server.

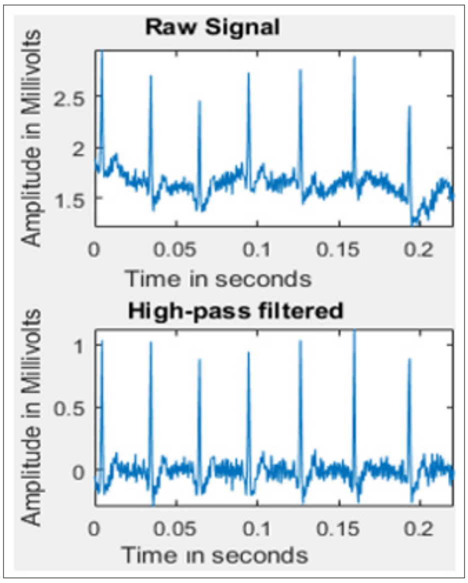

Figure 2: A noisy ECG waveform filtered using digital signal processing algorithms like Chebyshev II order Filter.

A complete workflow of the process from data acquisition to signal conditioning, followed by data analysis and abnormal event classification, further followed by upload of the real time health monitoring information to FHIR server is illustrated in Figure 1. A typical signal processing application involves data acquisition in the form of ECG signal samples being acquired from a human subject. These signals could be acquired from the human subject in noisy conditions where there is bioelectric signal interference and noise due to other electrical components. To remove the noise, signals are filtered using Common filtering techniques using digital filters like Butterworth and Chebyshev filters. There is also noise induced due to motion artefacts, e.g. due to the motion of the patient being monitored and muscular bioelectric signal interference. The filtered waveform extracted from the noisy signal after filtration process is shown in Figure 2. After the signal has been filtered, samples can be acquired to extract features of the waveform for further data analysis. The signals have to be acquired according to Nyquist criteria, where the sampling frequency should be at least half the bandwidth of the signal. The samples prepared are passed to data analysis stage. The data analysis stage typically involves training a machine learning model based on existing waveform data sets.

HL7 FHIR Interoperability

Fast Healthcare Interoperability Resources (FHIR) defines a set of “Resources” that represent clinical concepts. The resources can be coded and managed in isolation or aggregated into complex structures and documents which could be archived and queried as and when required. FHIR has been designed for the web; the resources are based on simple XML or JSON structures, with an http-based RESTful protocol and each resource is encapsulated and identified by a Uniform Resource Locator (URL).

Methods to Implement FHIR on IoT Devices

The implementation of interoperable component on IoT devices requires modelling FHIR resources, codes and if required codable concepts based on FHIR specifications. In a typical healthcare monitoring kit an analogue front-end device such as the 3-lead ECG sensor (Analog Devices AD8233) [7] is used for data acquisition. The data acquisition system is interfaced with their intelligent processor like the Texas Instruments (TI) Cortex A7 processor (TI Beaglebone Black, Texas Instruments, Digi-key, USA). The readings obtained from an analogue front-end was de-noised filtered and conditioned to obtain a smooth waveform. The signal was converted from analogue to digital form and was passed to the intelligent processor like the Beaglebone black. Since the signals and the samples contained noisy elements due to bioelectric interference and external environment conditions they had to be filtered. The signals contained noise frequencies and motion artefacts induced due to the body posture and motion. The samples had to be extensively filtered using filtering mechanisms to remove wandering and motion artefacts [8].

In order to classify, detect and separate abnormal signals from the normal one’s classification models were developed and trained in existing datasets targeting a particular abnormality. In this research, the datasets and software utilities, libraries provided by Physionet Waveform Database (WFDB) were used as shown in Figure 1. The WFDB was used to extract features from ECG and PPG samples. Once the features were obtained machine learning models were developed to train on a given set of features in order to predict abnormality in test samples. A JSON (JavaScript Object Notation) structure that encapsulated the sample readings was adopted which passed the samples to the HAPI (HL7 API) FHIR test server [12] to be logged to EHR if anomalies were detected. The

ECG and PPG samples encapsulated with JSON data structures were transmitted over 10 seconds' intervals to a HAPI FHIR sandbox test server. HAPI FHIR is Java implementation of FHIR and enables development of RESTful Webservices. The observation object that encapsulates an instance of observation was coded according to SNOMED-CT coding system as shown in Figure 3 [10].

```
<Observation xmlns="http://hl7.org/fhir">
        <code>
          <coding>
            <system value="http://loinc.org"/>
            <code value="59408-5"/>
            <display value="PPG Readings 1250 samples"/>
          </coding>
        </code>
        <valueSampledData>
          <period value="125"/>
          <datavalue="10.110.210.310.210.110.310.410.610.710.810.
910.810.610.510.310.110.310.510.410.310.210.2"/>
        </valueSampledData>
</Observation>
      </resource>
      <request>
        <method value="POST"/>
        <url value="obsPPG"/>
      </request>
```

Figure 3: A typical FHIR observation resource showing sampled PPG data with LOINC code 59408-5.

```
Observation obsTrauma = new Observation();
     obsTrauma
          .getCode()
          .addCoding()
          .setSystem("http://loinc.org")
          .setCode("74291-6")
          .setDisplay("Trauma Comorbidity");
     obsTrauma.addComponent(new
Observation.Component()).setValue(
          new QuantityDt()
               .setValue(Float.parseFloat(arrstrECGDerivedObs[4])))
          .getCode()
          .addCoding()
          .setSystem("http://snomed.org/sct")
          .setCode("273885003")
          .setDisplay("Revised Trauma Score");
 obsTrauma.addComponent(new Observation.Component()).
          setValue(
               new QuantityDt()
                    setValue(Float.parseFloat(arrstrECGDerivedObs[5]))
          )
          .getCode()
          .addCoding()
          .setSystem("http://snomed.org/sct")
          .setCode("445416009")
          .setDisplay("Early Warning Score"); //273886002

 obsTrauma.addComponent(new Observation.Component()).
          setValue(
               new QuantityDt()
                    .setValue(Float.parseFloat(arrstrECGDerivedObs[6]))
          )
          .getCode()
          .addCoding()
          .setSystem("http://snomed.org/sct")
          .setCode("273886002")
          .setDisplay("Trauma Injury Severity Score");
```

Figure 4: A Trauma event showing modelled as LOINC code 74291-6 with corresponding SNOMED-CT codes for RTS (273885003), EWS (445416009) and TRISS (273886002) scores.

An observation object could be an event of abnormal signal in ECG waveform or a trauma event with trauma scores such as National Early Warning Signs (NEWS), Revised Trauma Scores (RTS), and Trauma Injury Severity Score (TRISS) [9] as shown in Figure 4. The HAPI FHIR data store could be a FHIR based EHR like GP-Connect/GP-SoC from NHS UK [11]. Once abnormal beats or waveforms were detected appropriate alarms could be raised and potentially be passed on to the health-care agency entrusted with the patient care. The FHIR specification on security also supports OAuth authentication and authorization service which the consumer services can embed in their FHIR servers [13]. The clinFHIR tool [14] was used to model observation resources. The composite IoT device modelled as "Device" resource showing reference to observations like ECG, PPG, blood pressure, heart rate has been shown in Figure 5. The trauma scores calculated from the physiological parameters have been shown in Figures 6 & 7 showing the vital signs being modelled as observations.

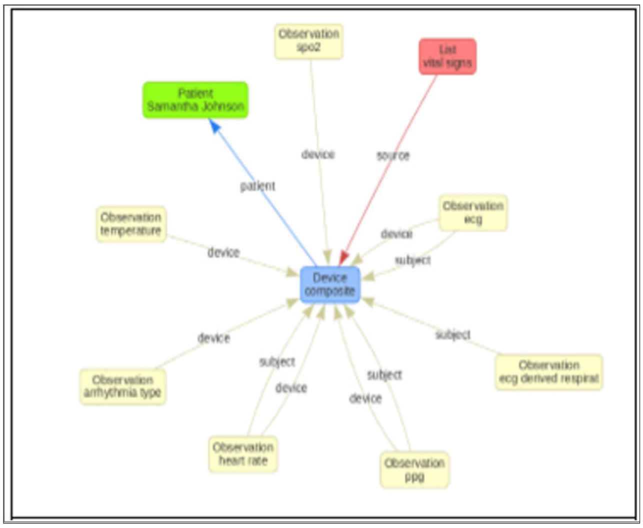

Figure 5: ClinFHIR model for Device that can capture ECG, PPG readings and can calculate vital signs and provide trauma scores when required.

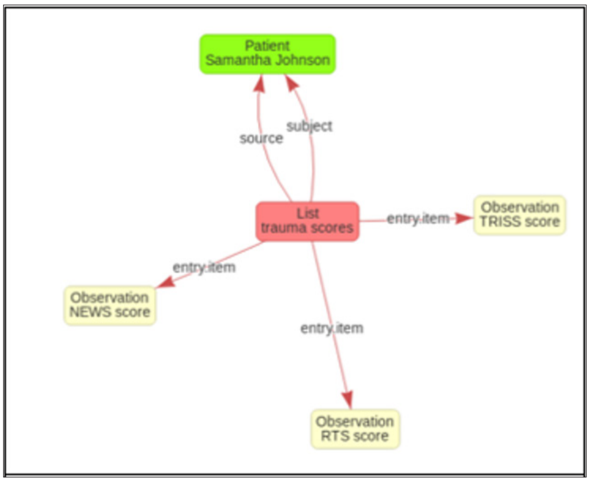

Figure 6: A clinFHIR model for Trauma score observation components.

Cite this article: Amit W, John W. FHIR Tools for Healthcare Interoperability. Biomed J Sci&Tech Res 9(5)-2018. BJSTR. MS.ID.001863. DOI: 10.26717/ BJSTR.2018.09.001863.

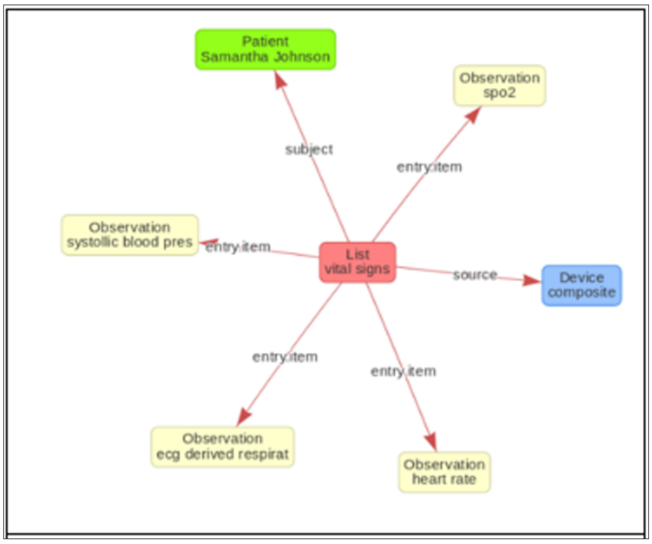

Figure 7: A clinFHIR observation resource for vital signs calculated from physiological parameters.

Conclusions and Discussion

The motivation behind the research was to provide information on how a real-time data acquisition and data analysis system could be integrated with FHIR client to upload the real time events to FHIR cloud server. An implementation of a HAPI-FHIR test server demonstrated the real-time logging of ECG, PPG, Vital Signs and Trauma observations, according to a Standard Coding System (SNOMED-CT or LOINC), to EHR for further analysis by the general practitioners and medics. This system should assist critical care teams to prepare for an emergency ahead of time and may prevent or reduce hazardous situations. The clinFHIR tool turned out to be an effective tool to model FHIR Device and Observation resources. The tool allowed to build a scenario for real time data acquisition and upload of observations. With further consolidation and standardization of FHIR the monitoring device and observations model could be extended to monitor patients regardless of their location or activity, and would enable uploading trauma related information to FHIR serves hosted by public health services in an automated fashion. The device manufacturers can extend the Observation and Device models to encapsulate FHIR resources.

References

1. Douglas L Mann, Douglas P Zipes, Peter Libby, Eugene Braunwald, Robert O Bonow (2015) Braunwald's Heart Disease: A Textbook of Cardiovascular Medicine, (10th Edn.). Elsevier Saunders, USA, p. 1943.
2. Alivecor (2018) Kardiamobile: Peace of mind in your pocket. Leapvault.
3. Shimmer (2018) Individual sensors shimmer.
4. Gackenheimer C (2013) Node.js recipes: A problem-solution approach. Apress, p. 376.
5. Hernández AI, Mora F, Villegas G, Passariello G, Carrault G (2001) Real-time ECG transmission via Internet for nonclinical applications. IEEE Trans Inf Technol Biomed 5(3): 253-257.
6. Mandel JC, Kreda DA, Mandl KD, Kohane IS, Ramoni RB (2016) SMART on FHIR: A standards-based, interoperable apps platform for electronic health records. J Am Med Inform Assoc 23(5): 899-908.
7. Analog Devices (2017) Heart rate monitor for wearable products.
8. Walinjkar A, Woods J (2017) Personalized wearable systems for real-time ECG classification and healthcare interoperability: Real-time ECG classification and FHIR interoperability. Internet Technolo Applic.
9. Walinjkar A (2018) A composite and wearable sensor kit for location-aware healthcare monitoring and real-time trauma scoring for survival prediction. Appl Syst Innov 1(3): 35.
10. Snomed (2017) Code for 3 lead ECG monitoring.
11. NHS Digital (2016) GP System of choice.
12. James A (2018) HAPI FHIR 3.5.0.
13. FHIR (2016) 6.1.0 FHIR Release 3 (STU).
14. Hay D (2017) Hay on FHIR.

ISSN: 2574-1241

DOI: *10.26717/BJSTR.2018.09.001863*

Mete Özkıdık. Biomed J Sci & Tech Res